

NTN®

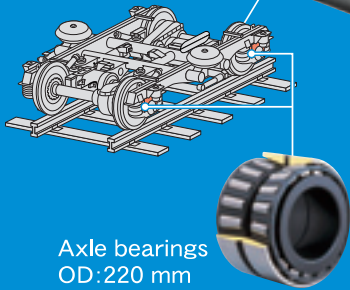
TECHNICAL REVIEW

No.
77

Special Issue;
Efforts for the Environment
December 2009



Essential Elements for Performance



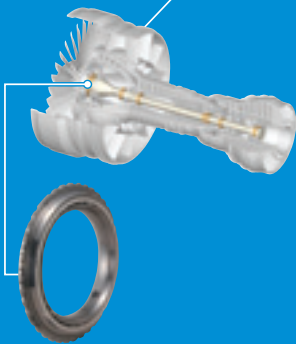
Axle bearings
OD:220 mm



Constant velocity steering joint (CSJ)



Intelligent in-wheel units for EVs



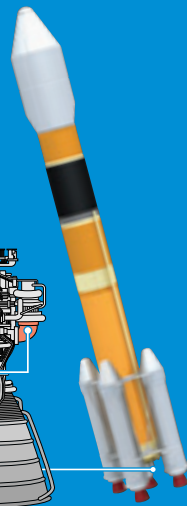
Three-point contact ball bearings
OD:527 mm



Bearings for high speed CT scanner
OD:1,000 mm



Large axle bearings
OD:810 mm



Bearings for turbo pump for rocket engine on H-IIIB rocket
OD:55 mm



Extra large bearings for main shafts
OD:1,580 mm

NTN bearing technologies are filling important roles in diverse fields.

NTN®



TECHNICAL REVIEW

No.77

Special Issue:
Efforts for the Environment

NTN TECHNICAL REVIEW No.77

CONTENTS

Preface

Yoshikazu FUKUMURA 1

● Activity for Reducing Environmental Impact

Initiatives for Environmental Conservation Masakazu HIRATA and Noboru UMEMOTO	2
Approach on Environment by SNR Didier SEPULCHRE DE CONDE and Jean-Hervé BULIT	10

● Environment-responsive Production Engineering

An Approach the Reduction of Environmental Loads in the Material Processing Akira SERA, Hisatsune SAITO, Kenichi NAKANO and Syunsuke MAKINO	18
Improve the Work Environment with Factory Robot Shigeki MATSUSHITA and Genji NAGURA	22

● Environmentally-friendly Products and Technology

Market Trend of Wind Turbine and Bearing Technologies Nobuyuki NINOYU, Souichi YAGI and Tsuyoshi NIWA	28
Eco-friendly Products Development SNR Roulements Siegfried RUHLAND, Ludovic SAUNIER, Cynthia TSEN, Bernard LIATARD and Gérald MIRABEL	34
Actuator for Electromechanical Brake Tatsuya YAMASAKI, Masaaki EGUCHI and Yusuke MAKINO	42
Electric Ball Screw Actuator for Automotive Yoshinori IKEDA and HIRAKAZU YOSHIDA	47
Plastic Bearings of Electric Pump for the Next Generation Cell Norio ITOH and Takuya ISHII	51
Low-torque Roller Lifter Unit Masashi NISHIMURA	56
Hub Bearing for Automobiles for Saving Resources Isao HIRAI	62
V-series Hub Joint Mitsuru UMEKIDA and Yuuichi ASANO	67
Extreme High Load Capacity Tapered Roller Bearings Takashi UENO and Tomoki MATSUSHITA	73
New Spherical Roller Bearings "ULTAGE" Series Type EA and EM Yukihisa TSUMORI	81
Compact Free type Torque Diode Shoji ITOMI	86
Characteristics and Applications of DLC films Kouya OOHIRA	90
Optimized Radius of Roller Large End Face in Tapered Roller Bearings Hiroki FUJIWARA, Takashi TSUJIMOTO and Kazuto YAMAUCHI	96

Round-table talk

Advance and Future of Analysis Technology for Constant Velocity Joints 106

● Our Line of Award Winning Products

"2009 'CHO' MONOZUKURI Innovative Components Awards" Encouragement Award High Capacity Tapered Roller Bearing Takashi UENO	110
"2008 'CHO' MONOZUKURI Innovative Components Awards" Automotive Component Award Constant Velocity Steering Joint (CSJ) Kenta YAMAZAKI	111
"2008 Resource Recycling Technology and Systems" Encouragement Award Development of Briquetting Machine and Accomplishment Recycling System for Steelmaking Dust Shozo GOTO, Ikuo YAMADA and Katsutoshi MURAMATSU	112

Our Line of New Products

114



To the New Issue Featuring Efforts for the Environment

Yoshikazu FUKUMURA
Managing Director

The concentration of greenhouse gases in the atmosphere has increased by about 30% since the onset of the Industrial Revolution. If the emission of greenhouse gases continues at this rate, the rise in temperature is expected to reach almost twice what it was before the Industrial Revolution by the end of the 21st century.

At the end of 2009, the 15th United Nations Climate Change Conference (COP15) was held in Copenhagen where medium and long-term reduction goals were discussed. In every country, efforts are being made to reduce greenhouse gases. Developments in electric cars and other next-generation automobiles, solar and wind power generation, and other new energy fields must also be actively advanced.

Given these circumstances, on July 1, 2009 we established a New Products and Intellectual Property Strategy Department at NTN as a division that keeps future growth in mind. It is responsible for long-term business strategies that emphasize the global environment, energy conservation and resource conservation in the fields of natural energy and electric cars, for example. In addition to utilizing our company's fundamental technologies, this department will promote collaboration between industry, academia and government, as well as with different business fields. The department will also seek to accelerate the development of new products for automobile parts and industrial machinery that meet the requirements of new energy fields, for example.

In our efforts at NTN, we are prioritizing the development of fundamental technologies with the goal of reducing environmental burdens and the development of products that are considerate of the environment in our efforts at NTN.

With the protection of the global environment, the creation of a recycling-based society and the enhancement of environmental management systems as key issues, we are working to raise the levels of our environmental management activities at our production facilities. In particular, we are making great efforts to reduce CO₂ emissions in our industrial activities.

In this publication, we introduce "Activities for reducing Environmental Impacts," "Engineering that is Responsive to the Environment" and "Environmentally-Friendly Products and Technologies" of NTN and SNR, a company that has joined the NTN Group and is headquartered in France. After a roundtable discussion with Dr. Kimata, a former NTN director, we also introduced three developed products that have received prizes in the current and previous fiscal year (two 'CHO' MONODZUKURI Innovative Components Awards and one Resource Recycling Technology and Systems Encouragement Award).

The NTN corporate philosophy is "For New Technology Network: Our contribution to the global community lies in our creation of new technologies and development of new products." In our new "NTN 2010 for The Next Step" medium-term management plan for the next two years from April 2010, we will seek to realize a management core that is not dependent on scale. In order to achieve "harmony with the global environment," we will promote the development of products that are better for the environment and contribute to the sustainable development of society.

Initiatives for Environmental Conservation



Masakazu HIRATA*
Noboru UMEMOTO*

At NTN, we have been conducting our corporate activities based on the NTN Environmental Policy and seeking harmony with the global environment through systematic and continuous initiatives to reduce impacts on the environment. In this article, we introduce our efforts to reduce CO₂ in manufacturing and other efforts for the environment in research and development, as well as in our contributions to society.

At NTN, our entire group is working together to reduce the emissions of CO₂ in order to prevent global warming and decrease the production of waste. Bearings and constant velocity joints, which reduce the amount of energy loss caused by friction, are fundamentally green products. These products are also contributing to the preservation of the environment through their application in fields such as wind power generation, which uses natural energy, and rolling stock, which is a green means of transportation. When we build new factories, we are effectively using natural energy through the incorporation of solar power generation and wind power generation, and adopting manufacturing processes that include environmentally-friendly manufacturing methods that eliminate the use of oil. We are also building more compact production lines and reducing waste through the installation of grinding sludge briquetters. As a result of these efforts, we are establishing factories that are considerate of and good for the global environment.

In ;past publications, we have primarily introduced our new products and technologies. Recently, however, preservation of the global environment and the depletion of petroleum energy resources have become major concerns. For these reasons, businesses are also expected to reduce their emissions of greenhouse gases and adopt activities that are good for the global environment. In this article, we explain NTN's efforts for the environment, focusing on our efforts to reduce CO₂ emissions in particular.

1. Fundamental environmental policies and goals

We have established the NTN Environmental Policy (**Table 1**), making “harmony with the global environment” the top priority of our company, and we are advancing efforts to preserve the environment with the following four policies as guides for our activities.

- i) Develop and sell products that are good for the environment
- ii) Reduce impacts on the environment: work to improve energy efficiency and carefully manage substances that have environmental impacts in every aspect of our business, from manufacturing to distribution and sales, in order to reduce impacts on the environment
- iii) Build comprehensive systems for legal compliance and environmental management
- iv) Contribute to society and protect the natural environment

In order to advance and realize this environmental policy, we have built an environmental management structure for our entire group that is centered on our Companywide Environmental Management Committee. We are setting environmental targets every year for three areas—preserving the global environment, creating a recycling society, and maintaining and improving environmental management systems (**Table 2**), and we are advancing our efforts for the environment as planned.

*Innovation and Intellectual Property Strategy Headquarters Environment Strategy Dept.

Table 1 NTN Environmental Policy

At the NTN group, we make harmony with the global environment our top priority, and we are continuously reducing the impacts on the environment caused by our business activities. We are also striving to constantly contribute to the sustainable development of society.

1. Develop and sell products that are good for the environment

- We will utilize high-precision manufacturing and tribological technologies and develop environmentally-friendly products. By providing these products to society, we will also contribute to promoting energy conservation around the world.

2. Reduce impacts on the environment

- As we strive to help prevent global warming, we will seek to improve energy efficiency in every aspect of our business activities, from the procurement of raw materials, parts and other goods to manufacturing, distribution and sales.
- We will focus on the effective use of resources and strive to reduce waste by thoroughly implementing the 3Rs (reduce, reuse, recycle).
- In addition to comprehensively managing substances with environmental impacts that are used in products and manufacturing processes, we will actively seek to replace chemical substances that are suspected of being harmful with alternative substances, and we will strive to prevent pollution of the environment.

3. Build comprehensive systems for legal compliance and environmental management

- Starting with a foundation of strict compliance with laws and regulations, we will also establish and abide by voluntary standards and in-house regulations that are more stringent in order to respond proactively to the needs of communities and our customers.
- In addition to preparing systems and operation methods for environmental management, by conducting environmental audits we will seek to maintain and improve our environmental management systems. In addition, we will publicize information about the status of our efforts toward the environment and promote communication with the public.
- Through environmental education, internal bulletins and other efforts, we will seek to make every person working at an NTN location aware of our Environmental Policy, and we will seek to increase their awareness of environmental protection.

4. Contribute to society and protect the natural environment

- By actively participating in programs that contribute to local communities and support efforts to protect the natural environment, we will promote interaction with neighboring communities and reduce our environmental impact.

Table 2 Environmental targets in fiscal 2009 and fiscal 2010

	Goal		2009 fiscal year targets	2010 fiscal year targets
Preserving the global environment	Reduction of CO ₂ emissions	Japan	<ul style="list-style-type: none"> ● Total CO₂ emissions: 250,000 tons/year ● CO₂ emissions per basic unit: -8% compared to FY1997 	<ul style="list-style-type: none"> ● Total CO₂ emissions: 317,000 tons/year ● CO₂ emissions per basic unit: -25% compared to FY1997
		Over-seas	<ul style="list-style-type: none"> ● CO₂ emissions per basic unit: +3% compared to FY2006 	<ul style="list-style-type: none"> ● CO₂ emissions per basic unit: -15% compared to FY2006
	Prevention of air, water and soil pollution	Japan	<ul style="list-style-type: none"> ● Conversion from halon to CO₂ fire extinguishers: 70 units (54 unchanged units at the end of FY2009) ● Reduction in the handling of substances subject to the PRTR Law: -38% compared to FY2006 ● Soil testing and purification after the closing of our Takarazuka facility 	<ul style="list-style-type: none"> ● Elimination of all halon fire extinguishers ● Reduction in the handling of substances subject to the PRTR Law: -40% compared to FY2006 ● Compliance with the revised Soil Pollution Countermeasures Law
	Participation in efforts to protect the natural environment	Japan	<ul style="list-style-type: none"> ● Promotion of local revegetation efforts (corporate forest stewardship, etc.) 	—
Creating a recycling organization	Reduction of waste production	Japan	<ul style="list-style-type: none"> ● Advance zero emissions: seek a recycling rate of 99.5% ● Reduce landfill waste to 25 tons/month or less 	<ul style="list-style-type: none"> ● Advance zero emissions: seek a recycling rate of 99.5% ● Reduce landfill waste to 25 tons/month or less
		Over-seas	<ul style="list-style-type: none"> ● Advance zero emissions: seek a recycling rate of 96.3% 	<ul style="list-style-type: none"> ● Achieve zero emissions: seek a recycling rate of 98.3%
	Preservation of resources	Japan	<ul style="list-style-type: none"> ● Weight of purchased paper: -46.2% compared to FY1998 	<ul style="list-style-type: none"> ● Weight of purchased paper: -50% compared to FY1998
			<ul style="list-style-type: none"> ● Reduce styrene foam: -92.4% compared to FY1999 	<ul style="list-style-type: none"> ● Reduce styrene foam: -96.1% compared to FY1999
Maintaining and improving environmental management systems	Internal systems	Japan	<ul style="list-style-type: none"> ● Prepare system for the acquisition of certification at new locations 	<ul style="list-style-type: none"> ● Acquire ISO14001 certification at all locations worldwide
		Over-seas		
	Promote green procurement	Japan	<ul style="list-style-type: none"> ● Enforce thorough compliance with our green procurement standards in our supply chain ● Handle investigations of substances with environmental impacts reliably (begin the application of a REACH-compliant system) ● Advance auditing of substances with environmental impacts (internal auditing, auditing of suppliers) ● Continue inspection of incoming materials 	—
	Promote environmental management in our supply chain	Japan	<ul style="list-style-type: none"> ● Support supplier efforts to obtain ISO14001 and similar certifications: 90% certification rate 	<ul style="list-style-type: none"> ● Certification of all suppliers
	Comply with new laws and regulations	Japan	<ul style="list-style-type: none"> ● Revised Law Concerning the Rational Use of Energy, revised PRTR Law 	—

2. Efforts for the environment in our production activities

The majority of our efforts toward our environmental targets, including preservation of the global environment and creation of a recycling society, occur at our production sites. In this article, we introduce our efforts for the environment in our production activities, focusing on efforts to reduce CO₂ emissions in particular.

2.1 Efforts to reduce CO₂ emissions

At the Third Conference of the Parties (COP3) of the Framework Convention on Climate Change held in 1997, when consensus was reached on numerical CO₂ reduction values for each country, consideration in Japan about efforts for countermeasures against global warming began immediately. The Japanese Federation of Economic Organizations established a voluntary environmental action plan for industry in 1997.

At NTN, we have participated in this voluntary environmental action plan and the CO₂ emissions targets set by the Japan Bearing Industrial Association, which set the target basic unit* for emissions for the 2010 fiscal as 13% less than that of the 1997 fiscal year. We voluntarily set an even higher reduction target of 25 in an effort to further reduce CO₂ emissions.

* The basic unit is the total amount of CO₂ emissions (in tons) per million yen of added value of production.

The first commitment period of the Kyoto Protocol began in 2008, and the importance of setting targets for total CO₂ emissions has increased. The CO₂ emissions for our corporate group have increased yearly, but in March 2008 we added a target for the total emission of CO₂ from our locations in Japan.

The CO₂ generated by our group is the result of our production activities. In order to achieve our target for total emissions, in April 2008 we initiated a CO₂ Reduction Project to investigate the potential to further reduce CO₂ emissions from our factories and initiate efforts to do so. The activities of this project were conducted for one year, and included the acquisition of information about the latest energy conserving technologies and their incorporation, the exchange of information about examples of improved energy conservation and the incorporation of conservation equipment being undertaken at each manufacturing location, as well as the discussion of such implementation plans at other locations. Additionally, we examined the thermal processing furnaces of other companies and invited outside experts to introduce technologies to us. Based on these efforts, we

established a plan to reduce the CO₂ emissions of all our locations by about 20,000 tons, which is equivalent to about 6% of our total emissions in the 2007 fiscal year.

[Changes in the amount of CO₂ emissions and the basic unit]

We can say that the basic unit of CO₂ emissions for our Japanese locations by fiscal year tended to decrease, and our energy efficiency, which affects CO₂ emissions, had been improving annually through 2007. The basic unit for the 2007 fiscal year was 1.46, which was an 18% improvement compared to the 1997 fiscal year, so we achieved our target.

Between the 2003 and 2007 fiscal years, our CO₂ emissions continuously increased each year as we also increased our production volume. However, in the 2008 fiscal year, as a result of the rapid decrease in production from the second half of the fiscal year, the basic unit increased because our energy use did not decline correspondingly with production volume.

Our CO₂ emissions and energy consumption by power source for the 2004 and 2008 fiscal years are shown in **Figs. 2** and **3**, as well as **Table 3**. These illustrations make clear that the majority of our CO₂ emissions are the result of the use of electric power, and that the amount resulting from oil use decreased from the 2004 fiscal year to the 2008 fiscal year. Compared to the 2004 fiscal year, kerosene use decreased, while natural gas use doubled in the 2008 fiscal year (**Table 3**). The use of thermal processing furnaces and other fuel conversion, as well as the replacement of air conditioning equipment, were the causes of this switch from kerosene to natural gas and electricity.

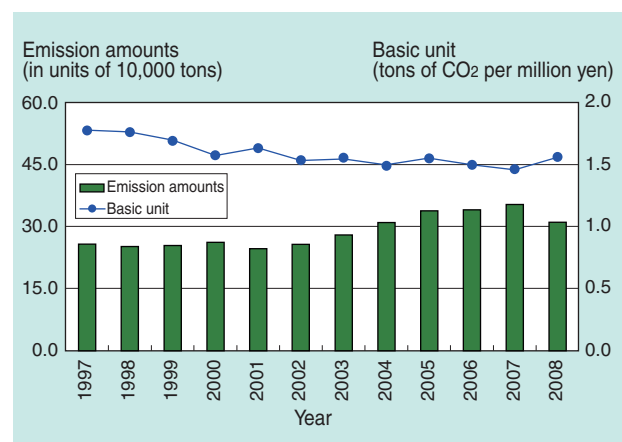


Fig. 1 Change in total CO₂ emissions and CO₂ emissions rate (At operating sites in Japan)

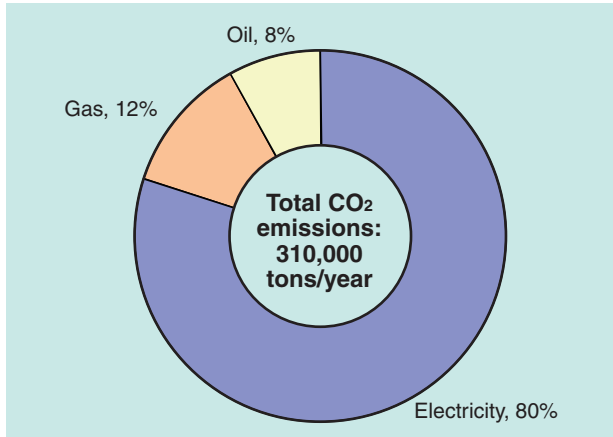


Fig. 2 CO2 emissions by power source (2004)

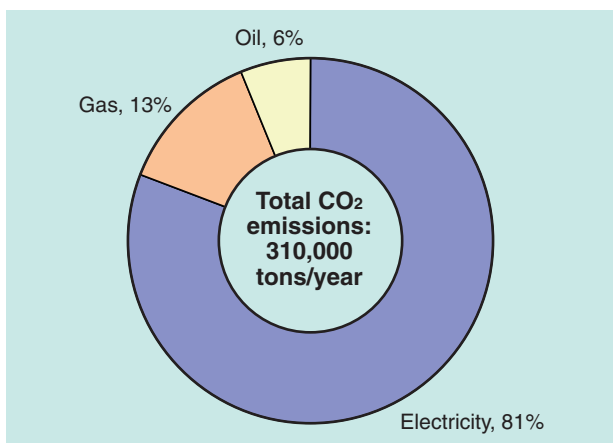


Fig. 3 CO2 emissions by power source (2008)

Table 3 Energy consumption by power source

Type of energy		2004 fiscal year	2008 fiscal year
Electricity (GWh)		510	520
Gas	LPG	7,310	6,810
	Butane (tons) Propane		
	Natural gas (km ³)	3,220	6,330
Oil	Heavy oil (kL)	3,520	2,620
	Kerosene (kL)	4,250	2,590
	Gasoline (kL)	160	160
	Light oil (kL)	130	130

[Efforts to reduce CO2 emissions at production plants]

With the goal of reducing CO2 emissions caused by our production activities, since 2005 we have continuously received energy conservation diagnostics assisted by the New Energy and Industrial Technology Development Organization (NEDO) to receive advice about problem points and proposals for significant reform measures from the perspectives of experts. With this guidance, we have been drafting energy conservation improvement plans.

We will describe examples of energy conservation improvements that we have implemented as a result of these efforts, as well as examples of our own independent efforts.

At our Iwata Works in 2006, in addition to installing in-house power generation equipment, we are also using a pipeline (Fig. 4) to carry the hot water emitted by this equipment to our constant velocity joint factory. Through heat exchange, we are able to heat the facility in the winter, for example, reducing CO2 emissions by about 1,500 tons in a single winter season. We have also been able to reduce the fuel costs from using kerosene boilers.

In 2008, through an energy service company (ESCO), we undertook the replacement of an air compressor with the latest model of turbo compressor (Fig. 5), as well as adopted a system to control the number of units and an intake cooler. We also implemented countermeasures for air pipe leaks and improved air flow. As a result of these efforts, we predict CO2 reductions of 4,000 tons per year starting in the 2009 fiscal year.



Fig. 4 Wastewater pipeline and heat exchanger at Iwata Works



Fig. 5 High-efficiency screw compressor at Iwata Works

At our Kuwana Works, we are advancing the conversion to natural gas as the fuel used for heat treatment facilities. We made the conversion of 22 facilities in 2005, reducing the amount of CO₂ generated due to heat treatment by about 10%. We are continuing this fuel conversion at present.

At our Okayama Works, in 2008, we received a grant from the Ministry of Economy, Trade and Industry (2008 Leading Model Business for the Adoption and Popularization of Load Leveling Equipment). We used this to install a new thermal air-conditioning system (Fig. 6). We also replaced a conventional absorption water cooler and heater that was powered by kerosene with a high-efficiency electric turbo refrigerator. By using these with a thermal storage system that uses electricity late at night, which makes for operation that is even more efficient and as inexpensive as possible, we are able to achieve both CO₂ and cost reductions. By using clathrate hydrate slurry, which is a thermal storage medium that has twice the thermal storage capacity of water, we have increased thermal storage efficiency and reduced energy use in the transportation of the medium. By incorporating this system, we expect to reduce CO₂ emissions by 1,000 tons per year.

In 2008, NTN Kongo Corporation received a grant from the Ministry of the Environment, and installed high-efficiency equipment, including air-conditioning (Fig. 7), lighting, compressors and air blowers at its four factories through an ESCO business. As a part of receiving subsidies for these projects, we joined the Ministry of the Environment's voluntary Domestic Emissions Trading System in the 2009 fiscal year, and we have agreed to a CO₂ reduction target of 3,000 tons per year.

To increase energy conservation in lighting, in 2007 we replaced 185 mercury lamps with high-efficiency metal hydride lamps in the heat treatment plant of our Kuwana Works (Fig. 8), resulting in a reduction of 185 tons of CO₂ per year. At NTN Casting Corp., we installed inverter fluorescent lamps and made other efforts to increase the efficiency of the lighting there. By doing this, we have reduced CO₂ emissions by 690 tons per year. At Hikari Seiki Industry Co., Ltd., in 2007 we replaced all the existing lighting within the factory with inverter fluorescent lamps, which are brighter and better for the environment, resulting in a reduction of the total number of lamps from 520 to 392 and increased efficiency.

At every NTN location, we are also implementing air leak countermeasures (Fig. 9). Through the utilization of leak detectors, we are conducting regular inspections of air pipes for leaks and making improvements as necessary.



Fig. 6 A thermal storage tower for the new air conditioning system installed at Okayama Works



Fig. 7 Turbo refrigerator and cooling tower for the air-conditioning system at NTN Kongo Corporation



Fig. 8 Metal hydride lamps at a heat treatment plant of Kuwana Works



Fig. 9 Check by air leak detector

Through the combination of large-scale energy conservation improvements and small-scale energy conservation activities, we are striving to reduce CO₂ emissions at NTN.

2.2 Waste reduction and resource preservation

In order to reduce waste products, we are seeking to achieve a final target rate of 100% recycling, and we are promoting the recycling of resources. In the 2008 fiscal year, our results were mixed as we achieved a recycling rate in Japan of 99.6%, which is higher than our target of 99%, but we failed to achieve our reduction target overseas. At the same time that we are reducing the production of waste, we are also advancing the development of recycling equipment. In the 2008 fiscal year, the technology for “the development of a briquetting device for dust from iron and steel and the creation of a recycling system” that we developed jointly with Daiwa Steel Corporation, an electric arc furnace manufacturer, received an encouragement award for Resource Recycling Technologies and Systems from the Clean Japan Center, which is a foundation that is affiliated with the Ministry of Economy, Trade and Industry.

2.3 Promotion of green procurement

We have established Green Procurement Standards, and we are striving to protect the environment and improve the environmental performance of our products in cooperation with our business partners. In order to comply fully with regulations and laws related to substances with environmental impacts, including the RoHS and ELV directives and the REACH regulations of the European Union (EU), we have created systems for the analysis of incoming parts and materials, and specialized internal auditing systems for substances with environmental burdens.

The EU’s REACH regulations, which came into effect in June 2007, require manufacturers and importers to register and evaluate the safety of all substances, compounds and chemicals that are known to be emitted from products that are to be used in the EU. At our group, we have prepared a list of 19 chemicals that are included in grease and other products that we export to the EU in amounts of one ton or more annually, and we confirmed that the manufacturers of all the raw materials conducted preliminary registration. 15 substances of very high concern (SVHC), which are substances that are carcinogenic or bioaccumulative, were listed by the European Chemicals Agency in October 2008. Since one of these substances, phthalate ester, has been contained in rubber tools and CVJ boots, our

development divisions, in cooperation with our business partners, are now advancing the development of materials that do not contain this substance.

2.4 Environmental Guidelines for the construction of new factories and structures

We have established guidelines for the construction of new factories and structures in order to contribute to the prevention of global warming by reducing CO₂ emissions and with the goal of reducing energy costs.

[Environmental Guidelines]

- (1) Use solar and wind power generation to provide electricity for offices and kitchens (**Fig. 10**)
- (2) Adopt all-electrical kitchens and EcoCute energy-conserving hot water supply equipment
- (3) For office buildings, plant vegetation on roofs and install film that reflects light and heat on windows
- (4) Ensure that building roofs have heat reflecting paint or two layers
- (5) Use lighting with motion sensors in places where people pass infrequently and there are no safety concerns
- (6) Utilize natural light
- (7) Ensure the use of use stratified (displacement) air-conditioning systems
- (8) Use air-conditioning systems with thermal storage that take advantage of low outdoor temperatures and low electricity costs at night
- (9) Investigate the incorporation of in-house power generation systems that use natural gas and the use of the excess heat generated by such equipment (in cases where heat-use needs are high and natural gas infrastructure is available)
- (10) Prohibit the use of incandescent light bulbs (use inverter florescent lamps and compact fluorescent bulbs)



Fig. 10 Wind power generator at the first factory of NTN Mie Corporation

- (11) Prohibit the use of mercury lamps (adopt the use of high-efficiency metal halide lamps)
- (12) Prohibit the running of vending machines at night (install timers)

3. Efforts for the environment in the development of products

Bearings, constant velocity joints and our other main products make great use of tribological technologies. They serve to reduce friction and wear in rotating parts and the parts that transmit force from rotation. As such, these can be said to be **environmentally-friendly products** or “green” goods. In other articles in this journal, we introduce high-efficiency CVJs and DLCs that are the fruits of our friction reduction technologies, resource-conserving hub bearings that utilize our technologies for designing to conserve resources and other environmental products and technologies.

As indicated in the previous section, the elimination of substances with environmental impacts from our products is an important issue. We have already achieved compliance with the RoHS and ELV directives, so now we will rapidly advance countermeasures for the substances of very high concern (SVHC) defined in the REACH regulations.

In the future, it can be said that the most important issue from the perspective of product development is the extent that we can reduce environmental impact caused by products in their manufacture, use and disposal. From the development stage we will strive to (1) design to suppress the generation of CO₂ in the manufacturing process, (2) design to reduce material loss, (3) reduce the quantity of rare metals used, and (4) decrease energy loss during use (conserve energy). As a part of these efforts, we have begun to promote life cycle assessment (LCA), which is a method of quantitative evaluation. We are currently investigating manufacturing processes, but the next step can be thought to be LCA evaluation of products when they are in use.

4. Efforts to contribute to society

At every NTN location we are promoting efforts to contribute to society in cooperation with local communities.

One such effort is tree-planting. For example, at our Iwata Works, we agreed in July 2008 to join the Shizuoka Mirai No Mori Supporter (supporters of Shizuoka's future forests) system with the Iwata City and Shizuoka Prefecture. In this system, we are undertaking activities at an NTN Kigyo no mori

(corporate forest) where people can interact with nature. At our Okayama Works as well, we signed a Kigyo to kyodo no mori zukuri (public-corporate forest-planting) agreement with Mimasaka City, Okayama Prefecture in August 2008. For five years until March 2013, we are being allowed to borrow about 3.5 hectares of forests owned by the city, and we are advancing efforts to improve the forest there as an NTN Kigyo No Mori. At both of these Works, we have been undertaking efforts to preserve forests in cooperation with local governments until now, but with these agreements, we are further expanding the scale of our activities. These restored forests will provide places of comfort not only for local residents, but they should also allow our employees and their families good opportunities to interact with nature.

5. Conclusion

At NTN we are focusing our abilities on environmental preservation in everything from manufacturing processes to products themselves, including their distribution, use and disposal. When we are building new factories and facilities, we make the incorporation of natural energy, including solar and wind power, a fundamental policy. We are actively incorporating natural energy as one means of reducing CO₂ emissions. In the 2008 fiscal year, we installed 94-kW of solar power generation equipment at our Kuwana Works (Fig. 11) and 62-kW at our Mie Works. So far, we have installed 10 solar power generators, 14 wind power generators and 13 hybrid generators that combine wind and solar power. Together, these generators save the equivalent of 290 tons of CO₂ emissions per year (Fig. 12).

At NTN, our dream is to use the power of the wind and the sun to manufacture bearings, and provide bearings that conserve resources and energy to the greatest extent possible. We will continue our daily efforts to reduce environmental burdens in everything from manufacturing processes to the products themselves, including their distribution, use and disposal.



Fig. 11 Solar power generation system at Kuwana Works

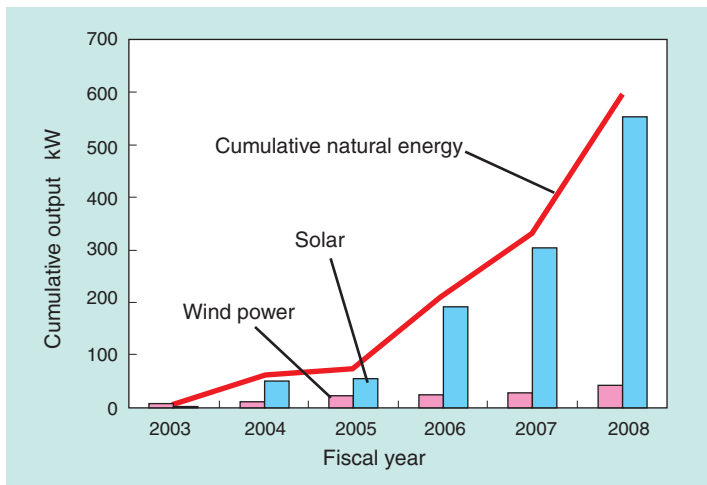


Fig. 12. Natural energy output

Photo of authors



Masakazu HIRATA
Innovation and Intellectual
Property Strategy Headquarters
Environment Strategy Dept.



Noboru UMEMOTO
Innovation and Intellectual
Property Strategy Headquarters
Environment Strategy Dept.

Efforts for the Environment by SNR

Didier SEPULCHRE DE CONDE*
Jean-Hervé BULIT**



When we think about it bearings are present everywhere in our daily lives, from household appliances to aerospace applications not to mention in the automotive market. By reducing the energy needs of many things around us, bearings play a major role in supporting sustainable development. Since 1994, at SNR Roulements, we have integrated environmental concerns into our development. Environmental policy is a major focus for SNR Roulements for not only ecological reasons, but also for economic and image reasons. That is why our environmental policy is being implemented from our head office down to all our workshops and suppliers.

1. EMS of SNR

Since its foundation, SNR has kept an established ISO 14001-complying environmental management system (EMS) for its all operation sites. This EMS is based on a particular portion of the quality management system of SNR commonly applicable to functions and business operations (documentation, education, audit management, etc.).

This EMS is the very basis of the environmental policy of SNR, and SNR wishes to fulfill its environmental objective through continued improvement activities according to the basic principle of PDCA (Plan, Do, Check, Action). The corporate annual guideline of SNR is established according to its environmental policy, guidance for its shareholders, possible environmental impacts resulting from its business activities, new ecology-related legal regulations, and results of internal and external audits. This annual guideline constitutes the basis for planning with all the SNR operation sites, thereby SNR is maintaining follow-up activities for progress and performance of projects by referring to various indices.

Since 1999, all the SNR operation sites have been registered as “multi-sites” defined in ISO 14001, where the latest update took place in 2008.

2. Corporate organization

In SNR, the Environmental Management Division belongs to the Quality Management Department, and is under the directly supervision of the President. **Fig. 1** schematically illustrates the organizational chart of the Environment Management Division of SNR.

In each SNR base within France, a responsible engineer functioning as an environment manager is responsible for smooth operation of EMS in his/her site, by enhancing knowledge about his/her specialty and expanding the scope of his/her role and responsibility.

SNR Annecy Head Office & Plant includes a production plant and research division for bearing products, product and machine test center, including a production engineering division and an engineering service division (including laboratory and precision measurement center). In each division, the “ecology promoter” as a coordinator plays the role of “operation site environment manager”.

In SNR overseas operation sites, the responsibility about environmental issues is assigned to quality managers.

The “Environment Manager in the Head Office” chairs the regular meetings in which environment managers from all the SNR operation sites participate. He/she always checks that the operation and activities about SNR EMS are executed as planned.

*NTN-SNR ROULEMENTS President

**NTN-SNR ROULEMENTS Environment Div. Manager

SNR has developed excellent environmental system tools (environmental database, dedicated environmental analysis software, and ecology-related legal regulations monitoring software), and has been utilizing these tools to support its routine environmental analysis activities and help implement common use of its environmental data by all the operation sites.

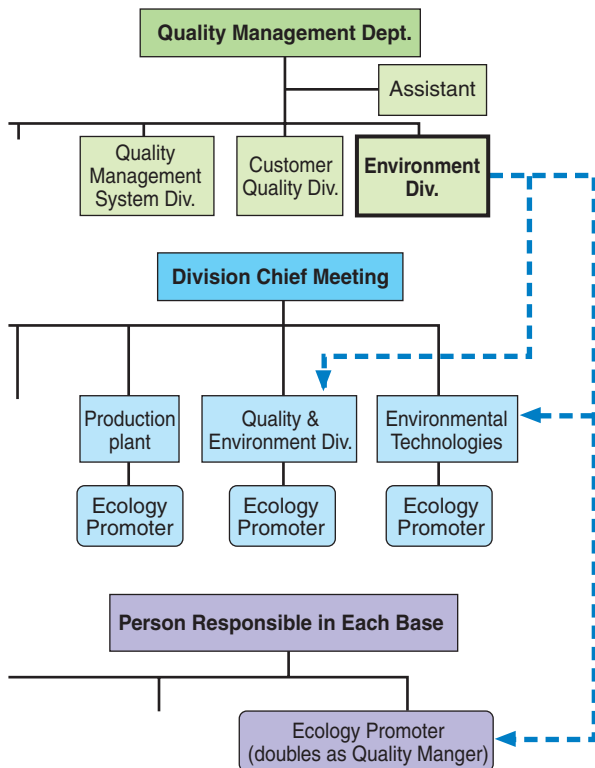


Fig. 1 Organization of SNR Environmental Management Department

3. Production of bearings and resultant environmental impacts

Fig. 2 schematically illustrates factors in bearing production activities that can lead to environmental impacts.

As a result of investigation at each SNR operation site, the following aspects of the bearing production process that may lead to environmental impacts have been identified:

- Energy consumption resulting from production activities and building heating
- Consumption of water and chemical substances used for production process and coolant supply or chilling equipment
- Release of evaporated water and volatile chemical substances into atmosphere
- Solid waste typically occurring from turning and grinding processes
- Wastewater from rinsing machine; waste liquid associated with the production process or process liquid

[Steps in Bearing Production Process]

- (1) Production of bearing rings through forming of blanks (tubes or bars of particular lengths) by machining or press process
- (2) Heat treatment
- (3) Grinding, and super-finishing
- (4) Assembly (bearing ring, rolling elements, and cage)
- (5) Prefilling with grease or fitting of seal, depending on bearing type.

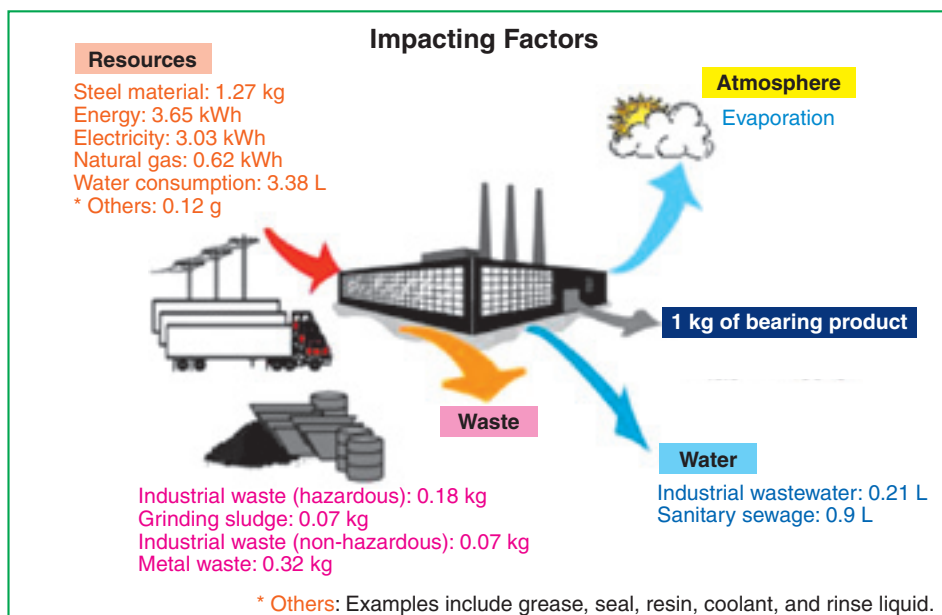


Fig. 2 Environmental impacts

4. Reduction in energy consumption

Typical examples of energy consumption reduction efforts of SNR are as follows:

- (1) An existing conventional air-compressor has been replaced with a high-efficiency screw-type air compressor; the compressed air line is inspected for air leakage at regular intervals (Meythet Plant).
- (2) An exhaust system has been installed in a facility where oil mist of higher concentration was present. During winter in particular, fresh air is supplied to the workplace, thereby significantly improving the environment of the work station. As a result, the overall electricity consumption previously needed for the exhaust system in the entire works as well as boiler gas consumption have been reduced considerably (Meythet Plant).
- (3) Improved employee awareness for reduction in energy on idle or inactive equipment (all SNR plants and offices).
- (4) Two aged fuel-firing boilers have been replaced with one novel gas-firing boiler, thereby improving the environment in the workplace and reducing the energy consumption (Annecy Head Office-Plant).

Fig. 3 shows the type of basic unit for energy consumed for processing in SNR as well as the trend in energy consumption for processing in SNR over

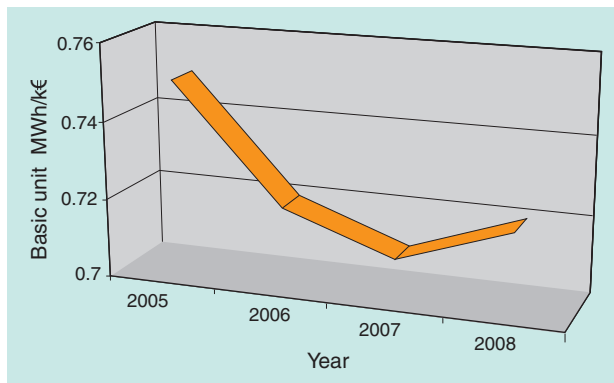


Fig. 3 Energy of processing

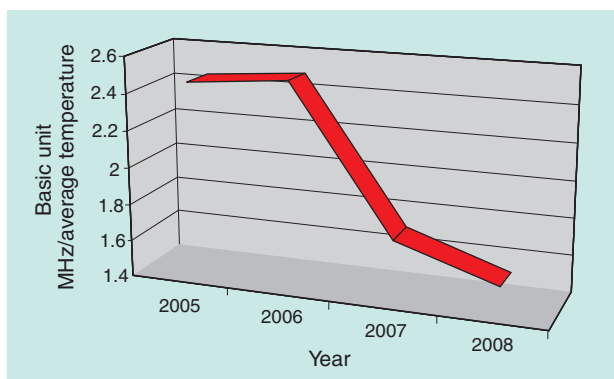


Fig. 4 Energy of heating

past several years. Fig. 4 provides the type of basic unit for energy consumed for building heating at SNR as well as the trend in energy consumption for building heating at SNR over past several years.

5. Reduction in CO₂ emissions

To be able to assess the contribution of SNR's CO₂ emissions reduction efforts to mitigation of greenhouse effect, we have translated the amounts of our energy consumptions in electricity, oil and gas into corresponding "CO₂ emissions".

In terms of CO₂ emissions, the reduction in energies consumed by SNR is equivalent, if its production output remains unchanged, to approximately 3,400 tons reduction in CO₂ emissions. Please note that this reduction is limited only to the SNR operation sites in France. Fig. 5 graphically plots the trend in CO₂ emissions at SNR over past several years.

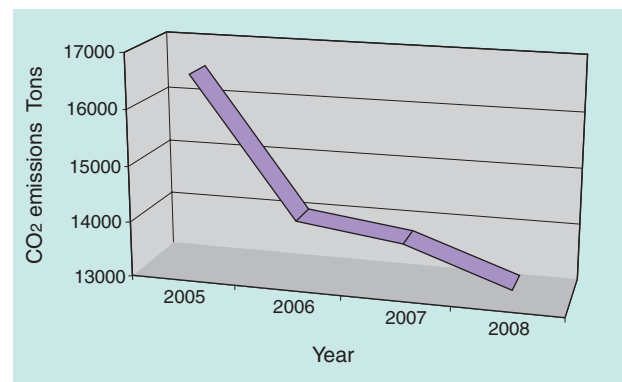


Fig. 5 Discharge of CO₂

6. Reduction in water consumption

Typical efforts so far made by SNR in reducing water consumption are presented below:

- (1) A certain portion of the aged water-cooled salt bath heat-treatment plant has been replaced with a new hardening plant, and for the remaining portion of the existing heat-treatment plant, the rinsing system situated downstream the heat-treatment process has been modified into an overflow design, thereby reducing water consumption (Annecy Plant).
- (2) A new cooling tower has been introduced into the coolant water system for metal working process to help reduce the risk of bleeding bacteria and decreasing water consumption (Meythet Plant).

Fig. 6 illustrates the type of basic unit for water consumption at SNR as well as the trend in water consumption at SNR over past several years.

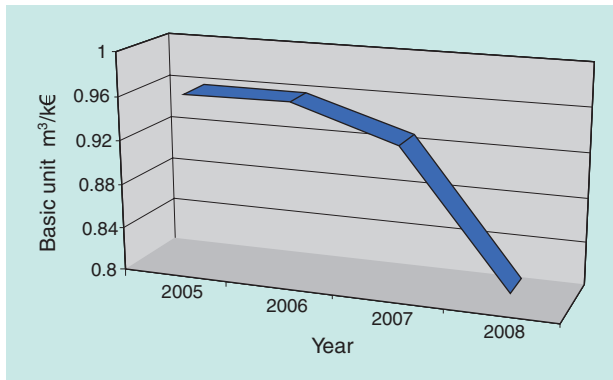


Fig. 6 Consumption of water

7. Reduction in organic compounds emissions into atmosphere

When exposed to sunlight, pollutants such as volatile organic compounds (VOCs) in atmosphere near ground will generate photochemical substances that can adversely affect human health and vegetation. In bearing production processes at SNR, VOCs can typically occur from use of volatile oil, CFC or alcohol employed for rinsing and degreasing of bearing parts.

Some of our efforts for reducing emissions of organic compounds are described below:

- (1) Oil solvent used in final rinsing step within bearing production has been superseded with a less volatile type (at all operation sites of SNR).
- (2) Previously, CFC was used for rinsing bearings before non-destructive inspection. This substance has been superseded with a detergent (Argonay Plant).

Through these efforts, all SNR operation sites within France alone achieved reduction of about 152 tons in terms of VOCs emitted into atmosphere.

Figs. 7 and 8 show the type of basic unit for organic

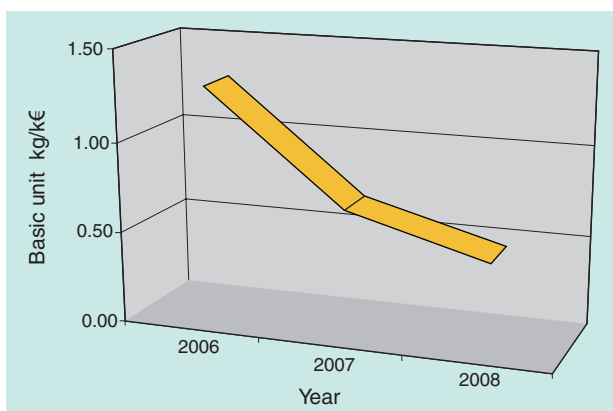


Fig. 7 Organic compound

compounds used at SNR as well as the trend in organic compound emissions into atmosphere at SNR over past several years.

8. Reduction in amount of industrial wastewater

Ordinary municipal wastewater treatment facilities are intended to treat household wastewater, and will not be able to treat all pollutants occurring from industrial wastewater (a pollutant may pass the soil in a wastewater treatment facility and can be released into the environment). To address this problem, it is necessary that wastewater from the production processes at SNR (in particular, the barrel polishing process) is preprocessed within the plant before being released to the nearby municipal wastewater treatment facility). Typical examples of our efforts for reducing emissions of our industrial wastewater to outside facilities are as follows:

- (1) Heavily contaminated rinse water from heat-treatment process is treated in special wastewater treatment equipment rather than being directly released into the municipal wastewater treatment facility (Annecy Plant).
- (2) Previously, wastewater was directly released into a wastewater treatment plant. Now, wastewater having undergone treatment with a high-performance filter is returned to a reservoir and reused. This arrangement positively contributes to reduction in wastewater emission and freshwater consumption (Meythet Plant).

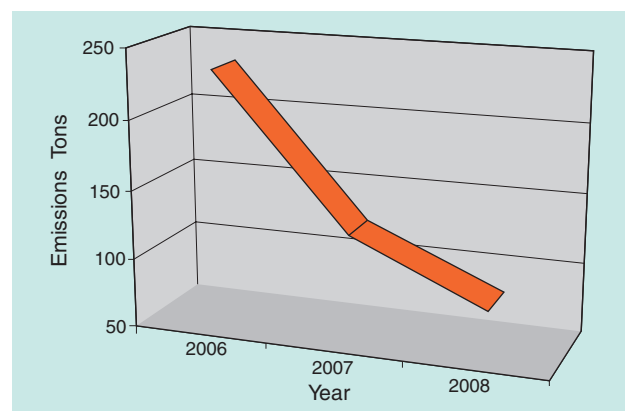


Fig. 8 Emission of organic compound to atmosphere

Fig. 9 illustrates the type of basic unit for reuse of industrial wastewater at SNR as well as the trend in reuse of industrial wastewater at SNR over past several years.

Amount of industrial wastewater can be converted into amount of household wastewater in terms of population (number of residents). Thus, the achievement by efforts of SNR in mitigating environmental impacts in this period through reduction in emissions of wastewater including industrial wastewater is equivalent to reduction of household wastewater consumed by 590 residents.

Currently, the amount of wastewater released from SNR is as small as the amount of household wastewater from only 160 residents. **Fig. 10** illustrates the trend of amount of industrial wastewater from SNR over several years, wherein the amounts of industrial wastewater are shown as converted into the amounts released by residents of ordinary households.

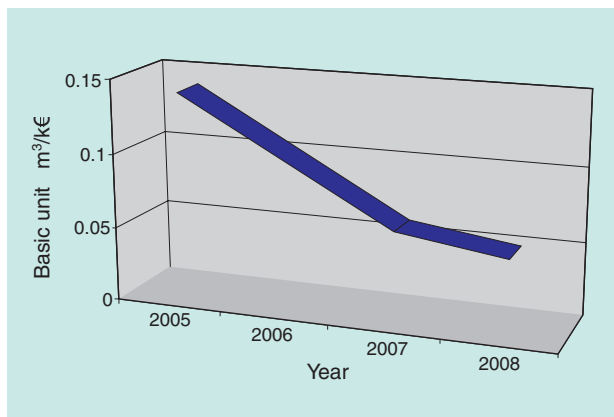


Fig. 9 Reuse of industrial wastewater

9. Management of wastes

Industrial wastes occurring from worksites of production plants can be classified into “non-hazardous wastes” that can be treated together with household wastes; and “hazardous wastes” that must be treated in a special plant. Non-hazardous wastes from industrial processes are more frequently recycled compared to ordinary household wastes. Because this type of wastes typically consists of paper, carton, plastic and glass materials, 90% of them can be recycled. At the same time, SNR has been proceeding with research that will help convert certain hazardous industrial wastes into recyclable-materials. **Figs. 11** and **12** show the amounts of non-hazardous and hazardous industrial wastes occurring from SNR over several years.

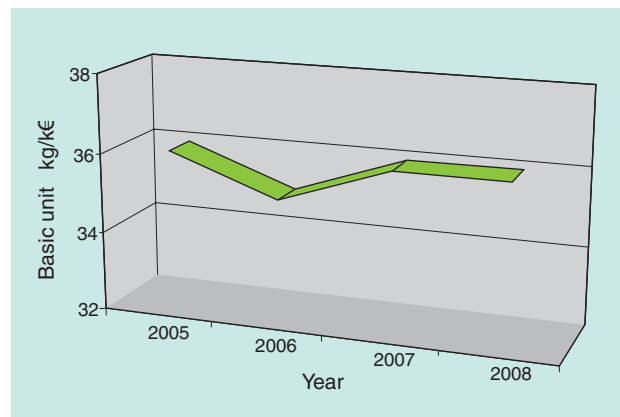


Fig. 11 Innocuous waste

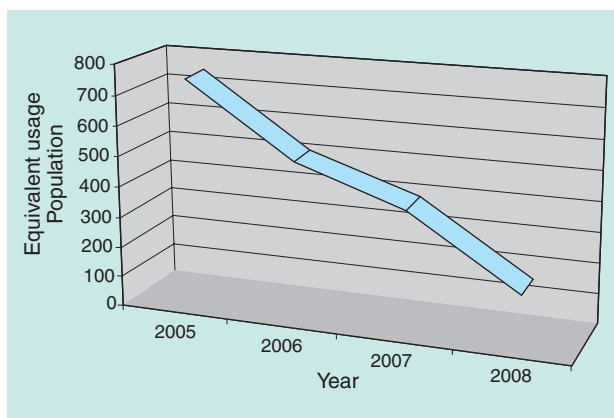


Fig. 10 Conversion to household use (number of people) from industrial use (wastewater)

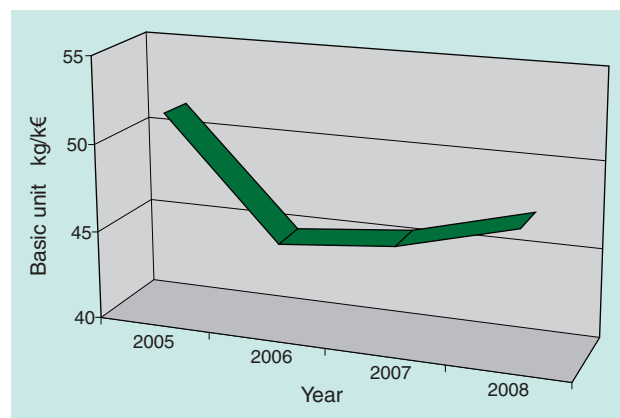


Fig. 12 Harmful waste

10. Ecology-improving technologies of SNR

SNR has long been committed to development and improvement in bearing designs, as well as improvement in bearing product manufacturing processes: each commitment positively contributing to better ecology. Some ecology-improving techniques unique to SNR are summarized below:

[Examples of development and improvement]

- **Improvement in performance of steel material**
Reduction in bearing size helps reduce amount of raw material consumed.
- **Optimization of internal structure**
Reduced friction in bearing helps reduce the energy needed to drive the associated machinery.
- **Improved grease quality**
Reduction in amount of prefilled grease helps reduce amount of chemical substance consumption.
- **Optimized seal performance**
Longer bearing life and reduced grease loss.
- **Compliance with REACH**
SNR assures that it uses the registered chemical substances only.

[Examples of improved production processes]

- Turning process was replaced with forging process: consequently, the amount of metal mass removed from blank has been much reduced.
- Improvement in heat-treatment process has led to mitigated deformation of bearing rings. Consequently, grinding allowance and energy consumption in grinding process have been much reduced.
- Having been supported by CETIM (Centre Technique des industries Mécaniques), SNR has

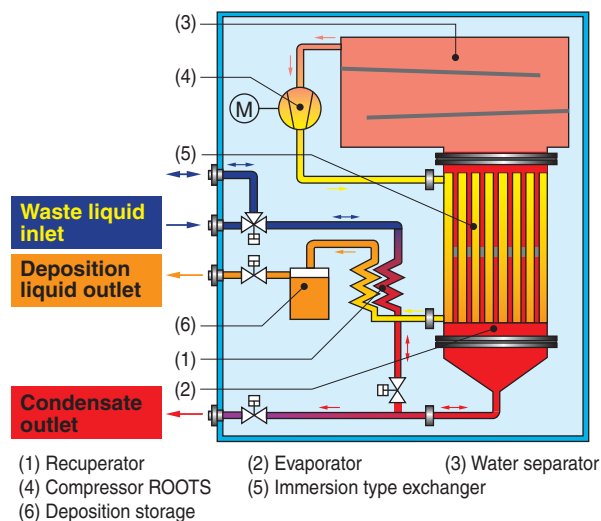


Fig. 13 Principle of VACUDEST

been conducting various surveys about industrial waste.

10.1 Test for steam condenser

Waste liquid essentially comprises water. For this reason, a steam condenser separates water from contaminated liquid through evaporation.

SNR Alès plant has tested an advanced steam condenser. Thanks to the resultant findings, SNR can now calculate data about performance and environmental impacts of a given steam condenser, and has begun assessment of positive effects obtained from a particular steam condenser. Fig. 13 schematically illustrates the operating principle of the steam condenser tested.

10.2 Test for biological purification unit

Waste liquid from a rinsing reservoir contains a very large portion of waste oil. On our biological purification unit, the oil-containing waste liquid is transferred to a biological reactor where the oil content in the liquid is eliminated by bacteria, and then the purified liquid is returned to the rinsing machine. The effectiveness of this demonstration plant has been verified in the SNR Ancey Plant. Fig. 14 shows a schematic illustration of this biological purification unit.

10.3 Grinding sludge briquetting

Sludge occurring from the grinding process contains not only steel powder but also coolant. Thus, this type of sludge is categorized into hazardous wastes. In the SNR Seynod Plant, grinding sludge is divided into coolant and grinding powder, and then the grinding powder portion is compressed into solid briquettes. Being recyclable, these briquettes are reused in a steel manufacturer.

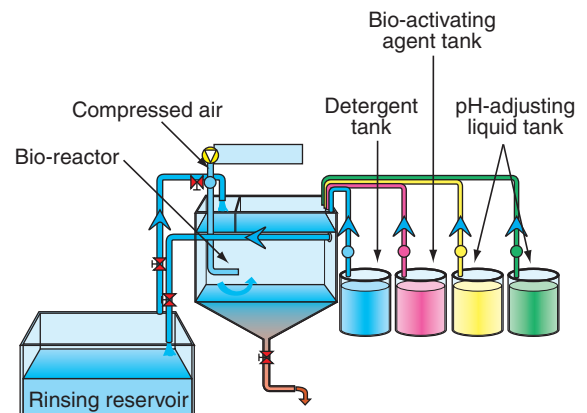


Fig. 14 Biological purification unit

Incorporating an NTN proprietary technology for sludge briquetting (Fig. 15), the process has already been implemented in the SNR's mass-production line. In addition, SNR has been testing techniques for briquetting other sludge types.



Fig. 15 Grinding sludge briquetter

11. Investments into ecology-improving activities

In order to continue its ecology-improving activities, SNR has invested approximately 5 million euro in the 2005-2008 period. Fig. 16 shows a breakdown of the investments by objective for ecological improvement:

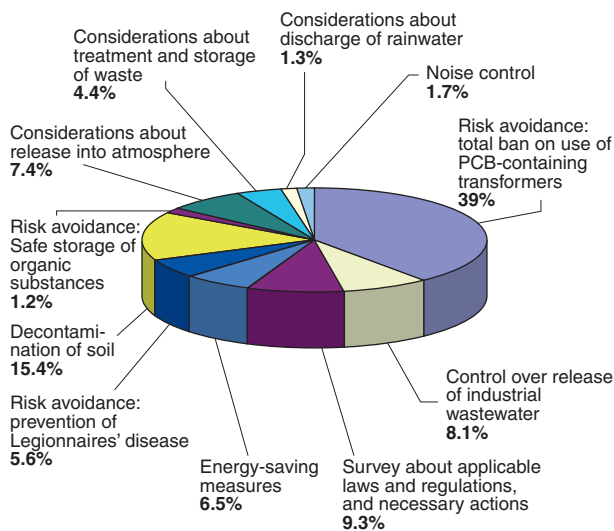


Fig. 16 Investments

12. Promotion for Eco-consciousness

To help the SNR employees become more conscious about their ecology-associated activities, SNR has been keeping a basic eco-education program for its newly hired employees. In particular, SNR provides special eco-education curriculum for its employees working in sites of higher environmental risk within SNR.

SNR is also committed to support of eco-consciousness promoting activities outside SNR. For example, SNR engineers and technicians have been actively presenting ecology-related lectures at universities (Ecole Centrale de Lyon, Polytech Savoie), local science festivals, and ecology-centered special seminars (World Bearing Association (BWA), and ADEME). Fig. 17 shows a picture of an SNR booth at a local exhibition. Also, SNR has been supporting the development of a specialized vehicle for an inter-college eco-run race (vehicles compete for a maximum range run with 1 liter of fuel). Fig. 18 shows a vehicle competing in the eco-run race. This vehicle utilizes SNR-made wheel bearings.



Fig. 17 SNR booth at local exhibition



Fig. 18 Fuel-efficient vehicle with SNR-made wheel bearings at the Shell Eco-Marathon®

13. Conclusion

The achievements in ecology-improving activities described above have resulted from the long years of eco-conscious commitments of SNR employees, and demonstrate that the EMS system of SNR has been beneficial.

Beginning in 1999, all the operation sites of SNR in France, as well as those in Brazil and Romania, have acquired ISO 14001 certification. By closely monitoring its carbon footprint, SNR is making strides to improve its effects on the global environment.

Photo of authors



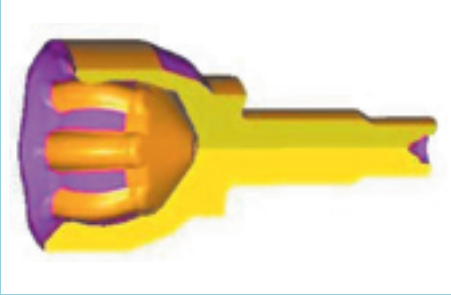
Didier SEPULCHRE DE CONDE
NTN-SNR ROULEMENTS President



Jean-Hervé BULIT
NTN-SNR ROULEMENTS Environment Div. Manager

Efforts for the Reduction of Environmental Impacts in Material Processing

Akira SERA* Hisatsune SAITO*
Kenichi NAKANO* Syunsuke MAKINO*



We developed a forging processing technique that uses a white lubricant to achieve both the reduction of environmental loads and the improvement of the operating environment in the forging process.

We introduce a technology to reduce forging billet weight variation and thea technology that improves yield rate by changing the product shape and the forging process.

1. Use of white lubricant in forging process for constant velocity joint parts

Recently, every manufacturer has been increasingly required to combat the challenge of environmental issues. For example, in the forging process for constant velocity joint parts within Japan’s bearing manufacturers, graphite lubricants (lubricants prepared by dispersing graphite powder into water or mineral oil) have been superseded with white lubricants (water solution primarily comprising organic acid salt and polymer) in an attempt to mitigate environmental impacts and improve working environments in production plants.

Generally, graphite lubricants have been used in the hot forging process because of their better performance in terms of lubricity, die-releasing capability, and die life. However, these lubricants have drawbacks: a work site involving a graphite lubricant can readily get dirty; contaminating oil deriving from a press slide gib may not be readily separated: graphite lubricant mixed with an excessive amount of oil can exhibit deteriorated lubricating performance and needs to be replaced, and the contaminated lubricant will make an industrial waste. To sum up, use of this lubricant type can lead to a heavy environmental impact.

In contrast, white lubricants can help improve work environments in forging process, be readily separated from oil, and readily recovered. Thus, use of this lubricant type can help greatly reduce occurrence of industrial wastes.

Wishing to help conserve the global environment, NTN has been increasing the use of white lubricants. This paper describes its efforts to mitigate environmental impacts through use of white lubricants.

1.1 Features of white lubricants

White lubricants are water-soluble lubricants each essentially comprising of organic acid salt and a polymer. Their features are summarized in **Table 1** below.

Table 1 The characteristic of white lubricants

Lubricant		White lubricant		
		Polymer-based	Carbonic acid-based	Water glass-based
Major components		Alkyl maleate	Phthalate Phosphate Sulfonate	Silicate glass Colloidal silica
Characteristics	Cooling performance	△	×	△
	Drying readiness	△	△	△
	Oil recovering quality	◎	△	△

◎ : Excellent ○ : Good △ : Acceptable × : Poor

NOTE 1) Various white lubricant types are available, including polymer-based, carbonic acid-based, and water glass-based types. Manufacturers of these lubricants have been committed to development, aiming at the optimization of advantages of each lubricant type.

NOTE 2) Aqueous solution of organic acid salt is transparent. After applied to a set of dies and heated to an appropriate temperature, an aqueous solution containing such an organic acid salt will form a whitish lubricant film after its water content has evaporated.

*Production Engineering R&D Center

1.2 Performance of graphite lubricants as compared with that of white lubricants

NTN has compared performance of graphite lubricants with that of white lubricants, in terms of forging-lubrication performance, workability-improving capability, and safety. These results are summarized in **Table 2**. Graphite lubricants excel in forging-lubrication performance. In contrast, white lubricants boast better workability-improving capability and safety. Therefore, so that white lubricants are more commonly used in forging process, their forging-lubrication performance needs to be improved to a level equivalent to that of graphite lubricants.

Table 2 Comparison of capability Graphite with white lubricant

	Function	Graphite lubricant	White lubricant
Forging-lubrication performance	Lubricity, die release property	◎	△
	Die life	◎	△
Workability-improving capability	Working conditions	×	◎
	Die setup, die change	○	○
	Putrefaction resistance	△	◎
	Maintainability against seizure on sliding surfaces and lubricant path	○	△
Safety	Immunity against fire	×	◎

◎ : Excellent ○ : Good △ : Acceptable × : Poor

1.3 Lubrication conditions setup and test result

Any white lubricant exhibits a satisfactory lubricating effect only when it has formed a dry lubricant film. To be able to form an appropriate dry lubricant film, relevant control of die temperature is critical. Therefore, we have studied various working conditions that can help achieve formation of optimal lubricant film and evaluated these conditions.

Fig. 1 shows an example plot of die temperature measurements taken during hot forging processes. First, we have adjusted lubricant application time and

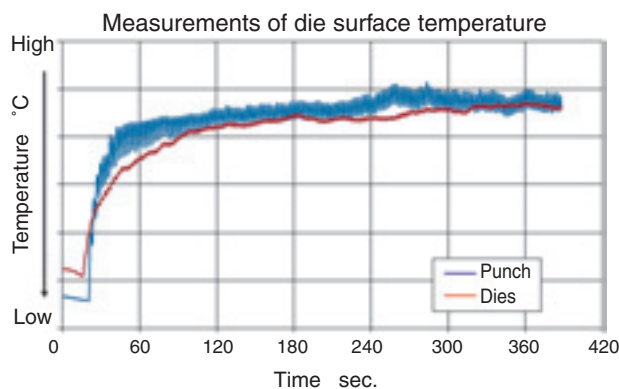


Fig. 1 Example of the result for die temperature check

air blowing time to determine a temperature range where a dry lubricant film readily occurs (**Table 3**). An attempt was then made to quantify necessary lubricating conditions.

Fig. 2 shows a view of lubricant film formed on a punch used to forge an outer race of fixed constant velocity joint.

To be able to determine an optimal set of lubricant film forming conditions, we have first defined conditions about duration and timing for applying lubricant as well as conditions of blowing air. The relevance of these conditions was verified by performing a series of tests on work-pieces being forged. Consequently, we have achieved good results about quality of forging-formed products and extended die life.

As described above, we have adopted a white lubricant in our forging process for NTN constant joint outer race primarily to improve work environments through the selection of an appropriate forging lubricant, control for die temperature, and lubrication conditions. Consequently, we have achieved improvement in work environments. We wish to further extend forging die life and expand a line of applicable bearing numbers and sizes.

Table 3 The film situation by die temperature during the test

Die temperature	State of lubricant film formed on die
Room temperature to low temperature	Water content in lubricant does not evaporate, and the lubricant remains in liquid state.
Low temperature	Water content in lubricant evaporates and a lubricant film is eventually formed; however, this process takes an extended time.
Appropriate temperature	Water content in lubricant evaporates quickly and a lubricant film occurs promptly.
High temperature	Droplets of lubricant rolling on the die surface are repelled from the surface, not being deposited on the die surface to form a lubricant film.



Fig. 2 The film situation of the Punch for the Outer Race Joint

2. Minimization of variation in weight of forging blanks

In order to cope with an increasing rise in raw material prices and help conserve the global environment, demands have been rising for lighter product designs, improved yields with parts that constitute final products, and introduction of near-net-shape forging techniques.

The forging process for constant velocity joint parts begins with a shearing step as illustrated in Fig. 3. Since the shearing is the first step in the entire mass reduction process, it is critical that the blanks being processed have a much more precise weight. Our efforts exercised for this objective are hereunder described.

Incidentally, to be able to minimize variation in the weight of forging blanks, it is necessary to minimize variation in feed length and outside diameter of the steel bar work piece being sheared.

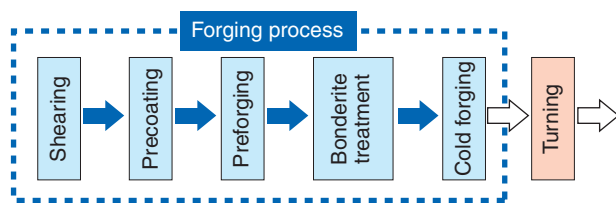


Fig. 3 The Forging process

2.1 Overview of shear press (bar diameter measuring rig) and shear tooling

Fig. 4 schematically illustrates the appearance of our shear press equipped with a bar diameter measuring rig. This machine comprises of the shear press proper, a steel bar feeder, and a bar diameter measuring rig. Before shearing, the bar diameter measuring rig scans the entire area of the steel bar to measure the outside diameter and supplies these measurements to the controller. When a change in the outside diameter is detected, the sizing stopper is shifted accordingly to trigger a weight compensation operation.

Fig. 5 shows the constitution of the shear tooling. The steel bar shearing procedure consists of insertion of the steel bar from the fixed side of the tooling to the sizing stopper, lowering the movable side of the tooling to shear the steel bar, and removing the separate work pieces from the tooling. The separate blanks obtained from shearing are hereunder called “billets”.

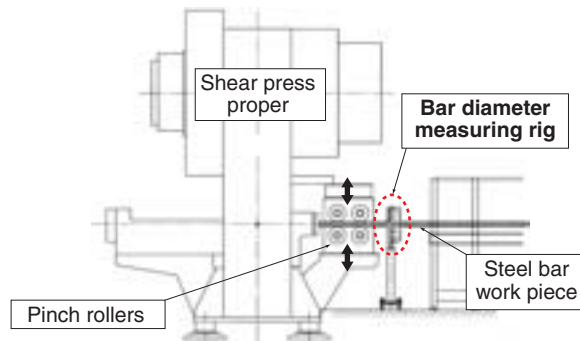


Fig. 4 The outside drawing of a shear press with Feed Forward System of Bar O/D

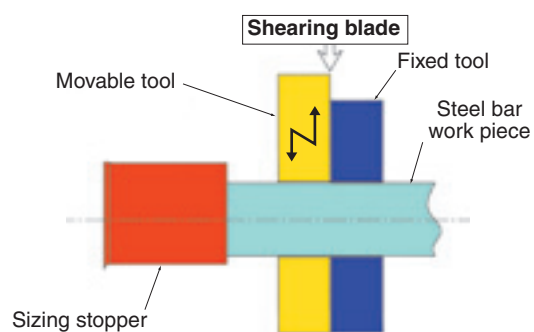


Fig. 5 The image drawing of Shear Tooling

2.2 Countermeasure against variation in billet weight

(1) Countermeasure against variation in entire billet length

(Possible cause) At the beginning of shearing operation, the steel bar was bent by the downward motion of the movable tool. The bar was sheared even though its positioning was, at the time, unstable.

(Remedy) We have modified the form of sizing stopper and shear tooling so that any steel bar is reliably sheared in a stable horizontal position.

(2) Method for correcting variation in steel bar outside diameter

(Cause) The outside diameter can vary even steel bars belong to a same lot (Ex.: if the true diameter of dia. 70 x 100 (nominal) steel bar work piece is 70.1 mm, then the true weight of this work piece will be 11 g greater).

(Remedy) Using the bar diameter measuring rig in Fig. 4, we scanned the entire area of the steel bar work piece to determine the variation in the outside diameter of the steel bar. Then, we determined the deviation in bar diameter relative to the targeted outside diameter and attempted to make weight compensation for the billets by adjusting the length of billets so that the as-obtained billets weigh the same as specimens of targeted outside diameter.

Taking a dia. 69.5 mm steel bar material type as a model, we have investigated currently achievable dimensions and attempted to minimize variation in the entire length and outside diameter with the billets obtained from the steel bar material. Consequently, we have succeeded in limiting the variation in weight of the billets by approximately 60% as shown in Fig. 6.

We, NTN, have been not only attempting to realize lighter bearing designs but also committed to various development works that help mitigate environmental impacts through reduction in the amount of materials used through improvement in machining techniques for our bearing products. One representative example of our commitment is the above-mentioned near-net-shape technique adopted in our forging line, wherein the feed stroke for the steel bar work piece is regulated based on the trend in the measurements obtained from the outside diameter measuring equipment in order to minimize variation in the weight of resultant billets. NTN people in charge of forging technology have been making efforts to develop novel technologies to help realize better ecoconscious manufacturing practices.

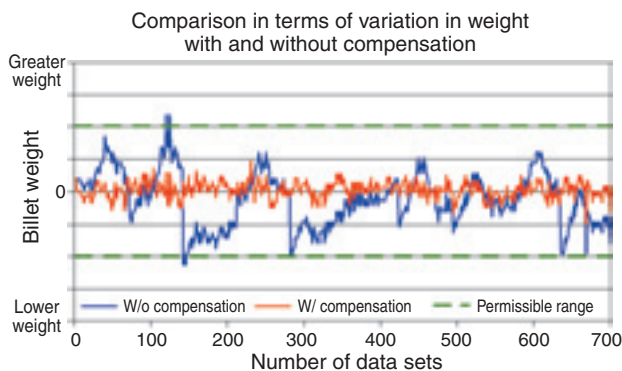


Fig. 6 Weight variation before and after used by Feed Forward System of Bar O/D.

3. Efforts of NTN for improved yield with good constant velocity joint products and reduction in materials used

As a part of our commitment to reduction in environmental impacts, NTN has been challenged with a variety of objectives that include reduction in the amount of materials used in components of NTN products, reduction in the energy consumed during manufacture of these components, and waste reduction. This challenge also applies to the manufacturing of inner races and outer races for NTN constant velocity joint products. To fulfill these requirements, NTN has been involved with efforts for improved yield for constant velocity joint products of

acceptable quality, Typical examples of these efforts include:

- (1) Improved product design that can help delete a machining step for the forged surface while the forged work piece positively satisfies needed functions
- (2) Realization of not only extended die life but also the introduction of near-net-shape techniques by superseding the conventional forging process with a novel forging process (this new forging process technique is realized through introduction of new techniques including a novel analysis technique.)
- (3) Realization of more compact and lighter product designs whose performance is equivalent to that of conventional design, beginning with the review of designs of conventional constant velocity bearing products

Fig. 7 shows some examples of new NTN constant velocity joint products that reflect our efforts in (1) through (3) above. NTN has positively achieved mitigation in its environmental impacts through reduction in material used and alleviation in machining-derived environmental impacts. These contributing techniques include more common use of forging technique to delete certain machining steps including turning, reduction in mass possibly removed by turning, and introduction of more compact and lighter product designs.

We will further remain committed to develop and manufacture ecofriendly bearing products through the development of new techniques aimed at reducing the amount of materials used, mitigating environmental impacts from postforging process, reducing or deleting machining steps, and creating lighter weight product designs by introducing multi-material designs.

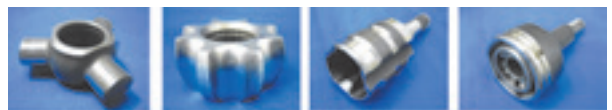


Fig. 7 Variation of Constant Velocity Joint parts

Photo of authors



Akira SERA
Production Engineering
R&D Center

Hisatsune SAITO
Production Engineering
R&D Center

Kenichi NAKAJIMA
Production Engineering
R&D Center

Syunsuke MAKINO
Production Engineering
R&D Center

Improvement of Work Environments with the Use of Factory Robots

Shigeki MATSUSHITA*
Genji NAGURA*



Human sense and experience are necessary for assembling processes. Therefore, automation (mechanization) has been difficult. We used sensor, robot, and simulation technologies, which have made remarkable advances in recent years, and succeeded in improving working environments in the assembly process for constant velocity joints (CVJ).

We introduce this case in this article.

1. Introduction

Constant velocity joints (hereinafter called CVJs) are a major product of NTN and are used in many automobiles as a means of power transmission.

In a typical CVJ assembly process in NTN, 12 to 16 parts are assembled in sequence to form the final product. Fig. 1 schematically illustrates a typical CVJ assembly process.

NTN regards steps ① through ③, which are common to various CVJ types, as the start-up assembly process and steps ④ through ⑥, which can vary depending on the CVJ type processed, as the completion assembly process.

NTN mass-produces a variety of its CVJ products. However, a larger portion of its CVJ assembly is achieved through manual operation because of reasons described below. Thus, these jobs are difficult to execute and pose a heavy burden on the operators.

(1) Unique shapes of CVJ components

Many CVJ components are prone to deformation because of their material and/or shapes, including the rubber boot, resin boot, and ring-shaped boot band made of a thin metal strip.

To be able to automatically install these difficult components, there will be orientation and alignment challenges during component feeding and handling throughout assembly. In conventional practice, position (orientation) of components is visually checked, and components are manually transferred and assembled.

(2) Unique shapes of finished CVJ products

Because each CVJ is designed for a particular function, the individual components of CVJ's and the final products are diverse in shape. Thus, ordinary transfer systems are not readily capable of handling finished CVJ products creating a necessity for human operators to transport these products.

With a larger finished CVJ product weighing approximately 10 kg, and the operators involved will experience heavy physical burden while transferring a work piece from a particular process to a downstream process or while changing the orientation of a work piece.

(3) Precision phase-matching procedure

Many CVJ components (rubber boot, shaft, inner ring, outer ring, etc.) have to be assembled into final products, being fully phase-matched between components.

These components each have unique geometrical features including cut-outs and projections in snap-fit joints and boot receiving joints and these features are used for convenience to achieve an optimal phase-match between components during assembly of CVJ product. The allowance for snap-fit is very small and/or snap-fit joints consist of soft and a hard material components forcing NTN to rely on experienced operators to manually assemble the components and remain conscious of phase matching between components involved.

During manual assembly work of a CVJ product, an operator assembles components into a final product

*Production Engineering R&D Center

while matching phases of the components involved based on visual detection and handling touch. In contrast, to be able to utilize an automatic assembly system for a CVJ product, it is necessary to first detect the phases of all the components involved and relay the data to downstream processes so that the components can be assembled in correct phases.

Creating such a system that produces reliable results poses a great challenge for producing reliable results.

To address the above mentioned challenges, NTN has committed to improving work environments in CVJ assembly facilities by deleting high difficulty and high burden steps. For this purpose, NTN has developed an automated CVJ assembly process incorporating a 6-axis vertical multi-joint robot that is virtually capable of human motions (hereinafter simply called the “robot”).

2. Approaches to automation through use of robot

The objective of the robot-assisted CVJ assembly line recently developed is “the elimination of human activities by automation with robot.” It is intended to mitigate the work load on human operators, and to do so, NTN has executed the following four approaches:

(1) Analysis of work flow

In considering the assembly process involving robots, each manual process step within the whole process has been analyzed and numerically assessed. Based on this obtained knowledge, challenging jobs done by experienced operators have been replaced with automated industrial robots.

(2) Greater scope of applicability

A coordinated operation is performed using of a robot featuring greater degree of freedom of motion while maintaining a simple station for the operator to assist the robot. Consequently, delicate work, which cannot be achieved with a robot alone, is possible, leading to a greater productivity through cooperation.

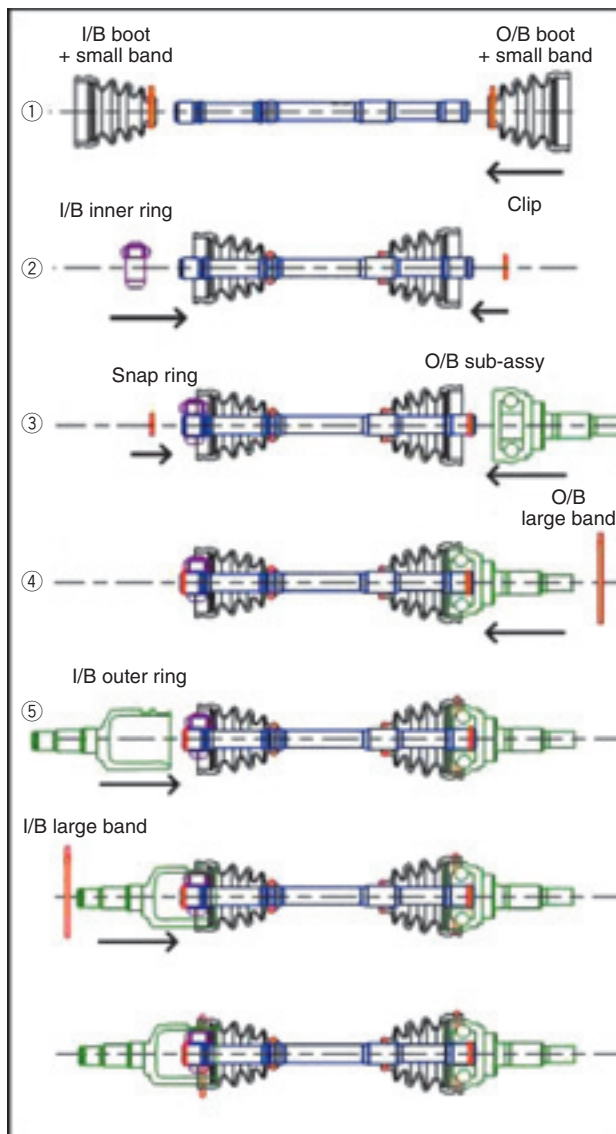
(3) More reliable work piece transfer operation

Through the introduction of a more compact, lighter robot hand as well as optimization for speed and range of robot hand motion, the reliability of robot assisted word has been improved. Consequently, product transfer operation, which was once a largely physical burdening manual process, has now been reduced with robot use.

(4) Numerical control of force-sensitive operation

Where the worker used to do operations by feel or experience, the robots allow for much more controlled operation and gather data during the process as feedback for further engineering.

To help proceed with these approaches, NTN has executed robot motion simulation by gathering loading analysis data from manual operation and using a 3D model. As a result, NTN is now capable of checking equipment layout and potential interference on equipment and running cycle times before equipment installation. Thus, NTN has achieved not only optimal



- | | |
|-----------------------------|---|
| Start-up assembly process | ① Boot and small band are inserted over the shaft. |
| | ② I/B inner ring and O/B clip are fitted. |
| | ③ I/B snap ring and O/B sub-assy are installed. |
| Completion assembly process | ④ OB large band is inserted over the sub-assy. |
| | ⑤ I/B outer ring is inserted, and the boot is fitted. |
| | ⑥ I/B large band is inserted, and both bands are form-fitted. |
| Inspection process | ⑦ Functions and appearance of product are inspected. |

NOTE) "Inboard (I/B)" means the engine-side of CVJ having been installed onto a car body and "outboard (O/B)" means the wheel-side of installed CVJ.

Fig. 1 Standard CVJ assembly processsss

assembly procedure and equipment layout but also a reduction in the development period for this equipment.

Fig. 2 shows a view of the 3D robot motion simulation system.



Fig. 2 Robot simulation

3. Challenges and solutions about automated CVJ assembly process

NTN has identified the following four major challenges with the robot-assisted CVJ assembly process. This section describes these challenges and their corresponding solutions.

- (1) Detection of component orientation
- (2) Automated snap-fitting work for serrated components
- (3) Automated assembly work for difficult-to-handle-shaped components
- (4) Improved efficiency in robot-assisted operation

3.1 Detection of component orientation

To run a problem-free automated assembly, orientation-related data of each component, including position (location), phase, and orientation (front or back), must be correctly sensed.

To address this challenge, NTN has developed a unique intelligent parts feeder capable of correctly orienting/aligning parts. This parts feeder system captures images of CVJ components, makes judgment about position (location), phase, and orientation (front or back) of individual CVJ components based on the captured images and transmits the resultant judgment information to the robot. The system always places individual components arranged in a same orientation into a same location. By this development, reliability in parts transfer with a robot has been much improved, and, at the same time, has eliminated work issues for the operator with respect to aligning parts. **Fig. 3** shows a view of the intelligent parts feeder. **Fig. 4** illustrates a captured image of parts.



Fig. 3 Intelligent parts supply device

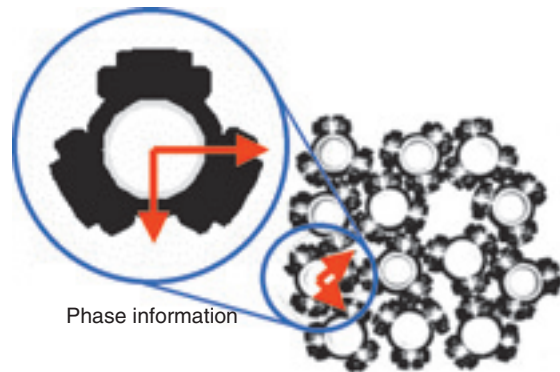


Fig. 4 Tripod and phase information

3.2 Automated snap-fitting work for serrated components

The majority of CVJ components must be assembled with their phases matching. Like many steps in CVJ production, the snap-fitting step for joining serrated components poses a challenge to make automated assembly work for CVJ production possible.

As shown in **Fig. 5**, the outer circumference of both ends of the shaft as well as the inner bore of the inner ring, which receives one end of the shaft, are serrated. Manual phase-matching with the two serrated components is a delicate procedure where mismatch of phases is prone to occur.

To address this issue, NTN has developed two techniques for snap-fitting with these two serrated components, and is applying one technique according to the shape of the components.

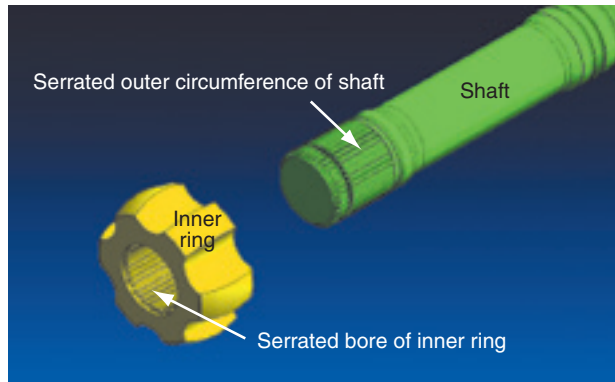


Fig. 5 Serration fitting portion

(1) Exploration-based method

Two serrated components are brought into contact, then, while the state of phase-matching is being explored, they are snap-fitted with each other. A delicate sensor reacting to correct phase-matching between both components sends an electrical signal by another sensor which outputs the signal as an insertion trigger signal.

(2) Measurement-based method

First, the profile of serration on each of both components is measured with a sensor. By referring to the resultant phase information, the serrated shaft end is fitted into the correspondingly serrated bore of inner ring.

3.3 Automated assembly work for difficult-to-handle-shaped components

(1) Boot band insertion work

In this work, the boot band is fit over the outer circumference of a particular small diameter section of rubber boot. Reliability of this operation poses a challenge as two components of very different shape—rubber boot and sheet metal boot band—are joined together.

To address this issue, NTN has invented a unique assembly system in which a guide jig dedicated to band insertion is installed onto an auxiliary station so that the band and rubber boot after undergoing shape correction are joined together.

Because both components are joined together only after correction for shape, this system positively improves reliability and repeatability of the boot band insertion work.

(2) Rubber boot fitting work

In this work, the outer ring is fit into a particular large diameter section of rubber boot. Note that the boot bore and outer ring outer circumference are each uniquely shaped: therefore, successful insertion is

possible only when the phases of both components are correctly matched. In other words, the rubber boot cannot be fitted over the outer ring simply with press-fitting force. Fig. 6 shows the profiles of TJ boot and outer ring—two members that will constitute a joint.

Previously, an experienced NTN operator has been committed to this work, making fine-adjustment efforts based on his/her experience and including information on angle of force and location of pivot point.

Therefore, NTN has analyzed boot fitting motions of its experienced operators to develop numerical data, and has a robot to trace the trajectories of motions of these operators. Consequently, NTN has realized a reliable robot-assisted rubber boot fitting work for its CVJ assembly process.



Fig. 6 Shape of TJ boot bore and outer ring O.D.

(3) Boot band form-fitting work

Through form-fitting, the quick-locking boot band used in NTN's CVJ secures the rubber boot when its retainer is appropriately set. Previously, a delicate form-fitting process was necessary for the boot band made of thin metal strip (this component can readily get deformed); therefore, manual operation was mandatory in order to reliably ensure better quality and productivity.

Fig. 7 shows shapes of the small and large boot bands.

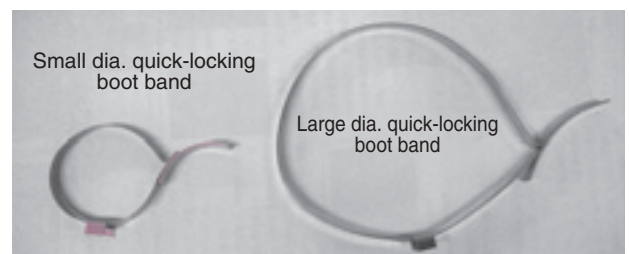


Fig. 7 Shape of one-touch boot band

NTN has attempted to supersede this complicated manual operation with a robot-assisted automated arrangement, and has learned that a special robot hand is necessary and exact tracing of necessary human operators' motions is impossible. Though beginning with the original motions of human operators, NTN has revised/reorganized the necessary motions to develop motions suitable for robot-assisted automation. Consequently, a robot-assisted rubber band fitting operation has been realized which boasts more efficient and reliable operation compared with procedure that could have been achieved by simply tracing human operators' motions.

3.4 Improved efficiency in robot-assisted operation

To be able to fully utilize robot technology in its CVJ assembly process, NTN has developed a unique combined robot hand system.

When an industrial robot system is used for automated production, the robot itself uses a plurality of robot hands that can be changed between. However, this practice of changing hands leads to unavoidable time loss.

To address this problem, NTN has developed a unique combined multi-functional robot hand system. This robot hand system not only combines a plurality of robot hands but also is designed such that each individual hand when active does not interfere with a CVJ component or peripheral equipment. Furthermore, the individual hands are driven by a common single drive, allowing the entire system to be compact and light-weight.

Fig. 8 shows the combined robot hand system that is capable of chucking a boot and a small band at one time.

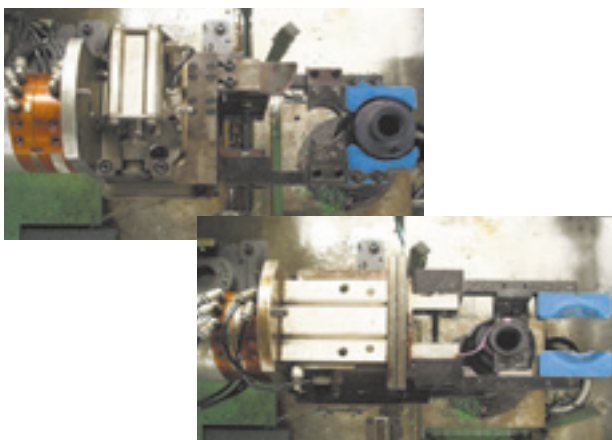


Fig. 8 Operation of combined robot hand (Upper: boot chuck, Lower: small band chuck)

To sum up, one robot unit can be applied to a plurality of processes, and previously unavoidable time loss for hand change has been eliminated.

4. Positive effects of development of robot-assisted CVJ assembly line

NTN has adopted its newly developed robot-assisted CVJ assembly technology to all the CVJ assembly lines within its factory; consequently, full automation of CVJ assembly has been realized. Fig. 9 shows a view of the robot-assisted CVJ assembly line installed in NTN factory.

The effects of this development are elimination or mitigation of the burden of highly difficult operations and high-load operations associated with the transfer of heavy work pieces, each being the challenge with conventional assembly practice. They also provided improved work environments, as well as 60% labor saving compared with conventional assembly practices.

In addition, the intelligent part feeder checks the parts while they are loaded into the assembly robot, thereby misassembling the CVJ is prevented, positively helping improve the quality of NTN CVJ products.



Fig. 9 CVJ robot assembly line

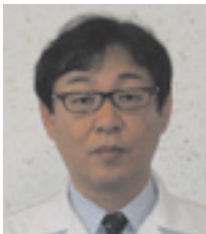
5. Conclusion

NTN believes that robot-assisted assembly lines will continue to be further sophisticated, diversifying into various configurations to meet contemporary needs.

While performance of industrial robots has been increasingly enhanced, NTN thinks that robot users need to deepen their knowledge about robot technology and improve their skills in utilizing robots.

Thus, NTN will remain committed to the development of robot technology that can be applied to not only CVJ assembly processes but also all the production processes for NTN products, and wishes to establish a production system that is safe and poses the least burden to human workers and helps improve work environments.

Photo of authors



Shigeki MATSUSHITA
Production Engineering
R&D Center



Genji NAGURA
Production Engineering
R&D Center

Market Trends for Wind Turbine and Bearing Technologies



Nobuyuki NINOYU*
Souichi YAGI**
Tsuyoshi NIWA***

Wind power generation, which contributes to the prevention of global warming, is being actively introduced to the worldwide market as a clean energy source. Bearings are increasing in size accordingly with the growth in the size of wind power generation equipment. Evaluation tests of bearings that simulate actual performance are important for selecting suitable bearings, but they are becoming difficult with equipment that is very large, so conducting structural analysis, including for shafts and bearing housings, for example, is necessary. This article introduces some of these analysis techniques.

1. Introduction

The total electricity generation capacity of wind power generation plants worldwide reached 122 GW as of the end of 2008 business year, and according to a report, this value means a 30% increase over the BY2007 level.

Fig. 1 graphically plots the trends in the total wind power electricity generation capacities of the world and major participating nations in the BY2004–2008 period. During this period, three major nations—USA, Germany and China—accounted for approximately 50% of the total installed capacity. In particular, the total installed capacity significantly increased in USA and China in the same period. 50% of the increase in newly installed capacity in the world in BY2008 is accounted for by USA and China.

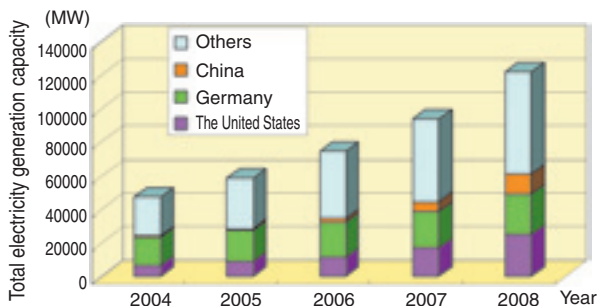


Fig. 1 Cumulative global wind power development

Being a clean energy source that does not emit CO₂, wind power generation plants are widely appreciated around the world, and their installed capacity has been increasing by more than 20% every year¹⁾.

As the market for wind power generation plants has been steadily expanding, more advanced wind turbine technologies have been increasingly developed. The current development efforts are focused on scale-up and offshore production of wind turbines. This report describes the current market trend for wind turbines and typical examples of the newest bearing technologies for wind turbines.

2. Market trend

2.1 Scale-up

In 1985, the rated output of a typical wind turbine with rotor diameter 15 m stood at 50 kW. About twenty years later, mass-production began with a larger wind turbine that boasts a rotor diameter of 126 m and is rated at 5,000 kW (5 MW).

In the engineering aspect, the contributing factors that have helped realize scale-up of wind turbines are improved mechanical strength for rotor blades by introduction of carbon fiber monolithic impregnated structure, advancement in mechanical strength design and analysis technique for the structures of tower and nacelle, and progress in design and production techniques for producing larger wind turbine bearings.

*Application Engineering Dept. Industrial Sales headquarters

**Industrial Sales headquarters

***Product Design Dept. Industrial Sales headquarters

Research works for super-large wind turbine designs are in progress in particular for offshore wind turbine power generators that are rated at 10 MW to 20 MW.

2.2 Offshore site production

Few sites are available on land where the wind profile is appropriate for wind power generation. For this reason, offshore wind farms site production has been increasing, especially in Europe. Fig. 2 shows an example of typical offshore wind farm in Europe.



Fig. 2 Under construction of offshore wind turbine

2.2.1 Offshore wind power generation programs in Europe

In Europe, there is a vast spread of continental shelves down to a depth of 40 m, and wind farms are often constructed on seabed foundation. In particular in the north Europe, there are large scale offshore wind farm projects²⁾. Fig. 3 maps the currently present offshore wind farm projects in the north Europe scheduled in the timeframe up to the year 2020.

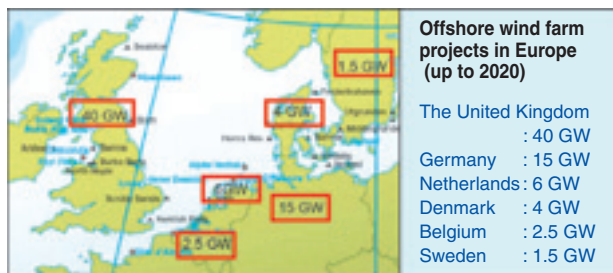


Fig. 3 Plan of offshore wind farms in north Europe

2.2.2 Offshore wind power generation programs in Japan

In Japan, application of seabed foundation for wind farms is difficult owing to topographical limitations. Therefore, joint industry-university teams have been developing floating platform wind power generation plants. Note that floating platform plants can be categorized into an anchor-secured type (floating platform structure is secured with the anchoring point

at seabed) and a sailing type (floating platform structure can freely move on the ocean surface). Research into a sailing type platform is attracting attentions as this platform type appears to be promising because offshore areas in Japan are often much deeper and Japan's long-established shipbuilding technologies can be applied to these sailing type structures.

3. Applicable bearing technologies

3.1 Efforts for analysis techniques for large bearings

3.1.1 Main-shaft bearing

To cope with the scale-up of wind turbines, the sizes must be larger for the bearings that support the main shaft, speed-up gearing and generator. In particular, the larger main-shaft bearings that support the larger rotors often measure 2,000 mm OD or greater, and their types include self-aligning roller bearing, double row tapered roller bearing, and cylindrical roller bearing.

To be able to determine the final specifications for a main-shaft bearing, an intended bearing needs to be tested by running on a test rig that can simulate the intended wind turbine so that the bearing in question can stably perform for an extended period. However, a simulation test of the bearing in question on an actual wind turbine requires a large test facility, higher cost and longer preparation period before actual test, and, therefore, cannot be readily executed. To address this issue, NTN has been performing not only simulation tests on an actual wind turbine but also finite element method-based structural analysis for the bearings and auxiliaries including the bearing housing and bearing bed so that a more reliable bearing design is achieved.

Figs. 4 and 5 show a result of the analysis with a main-shaft model. By an external force, the bearing as well as the bearing housing and shaft get deformed.

A larger wind turbine develops greater deformation owing to the greater external load it receives, and greater this deformation on the wind turbine more adversely affects the bearing clearance. Therefore, it is necessary to take into account this deformation for

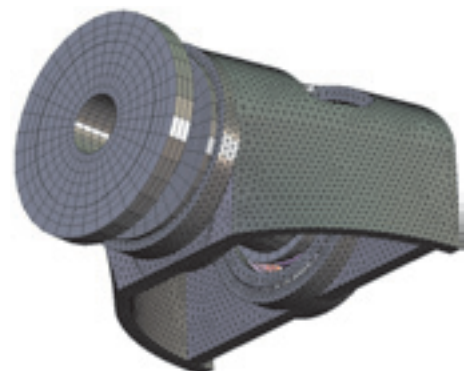


Fig. 4 Main shaft model

correct analysis of the main-shaft system. NTN performs design reviews after taking into account the effect of deformation on the entire wind turbine structure, and then finalizes the bearing specification optimized for the wind turbine in question. Fig. 5 shows an example of the structure for a bearing that supports the main shaft in nacelle, wherein the bearing structure comprises a double row tapered roller bearing in the blade side and a cylindrical roller bearing in the speed-up gearing side. Fig. 6 provides structural diagrams of the bearings used in this analysis model.

The diagrams in Fig. 7 show the results of the analysis of the effect of deformation on the bearing housing and other structural members. In Fig. 7, the load distribution pattern over the rolling elements is shown for each of two assumptions—where deformation is taken into account and where it is not taken into account.

In FEM analysis procedures, an “elastic body” element is used for the deformation analysis. If the element is assumed to be a “rigid body”, then calculations are possible without taking into account deformation.

The diagrams in Fig. 7 show that when deformation on a bearing housing and bearing are taken into account, the load zone expands and, consequently, load peak is mitigated, meaning the overall load imposed over the rolling elements is reduced. Compared with the “solid body” scenario, the bearing

life resulting from the “elastic body” scenario is apparently longer—the life of tapered roller bearing is approximately 20% longer and that of cylindrical roller bearing is 10% longer.

It is true that deformation helped increase bearing life in the example above. However, deformation in

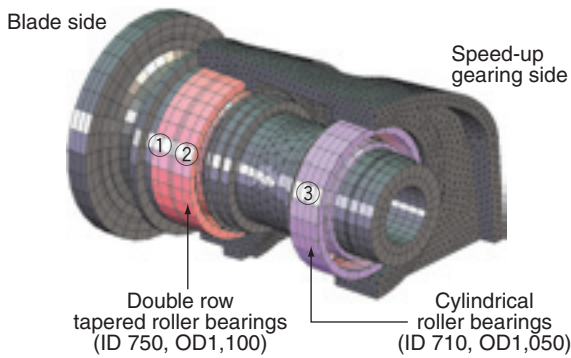


Fig. 5 Analysis example of main shaft model

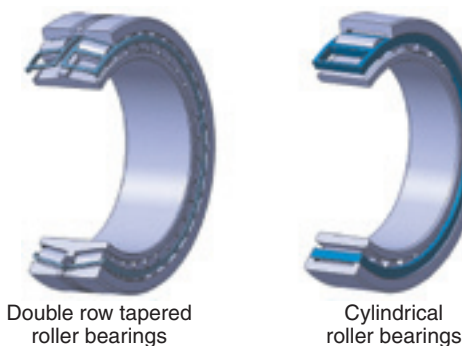


Fig. 6 Bearing structures for analysis

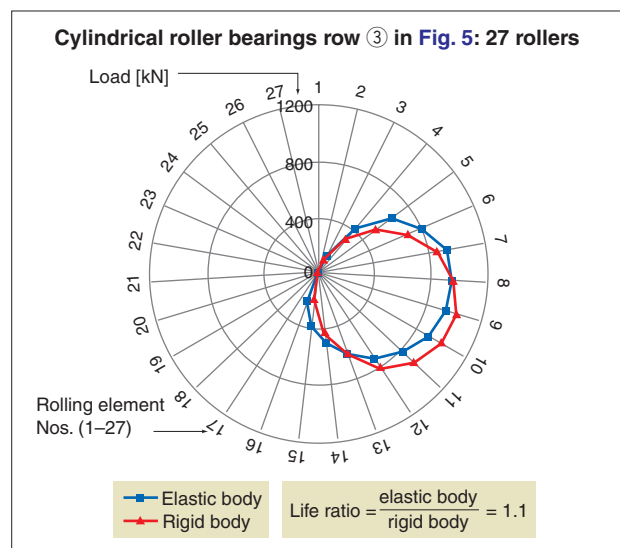
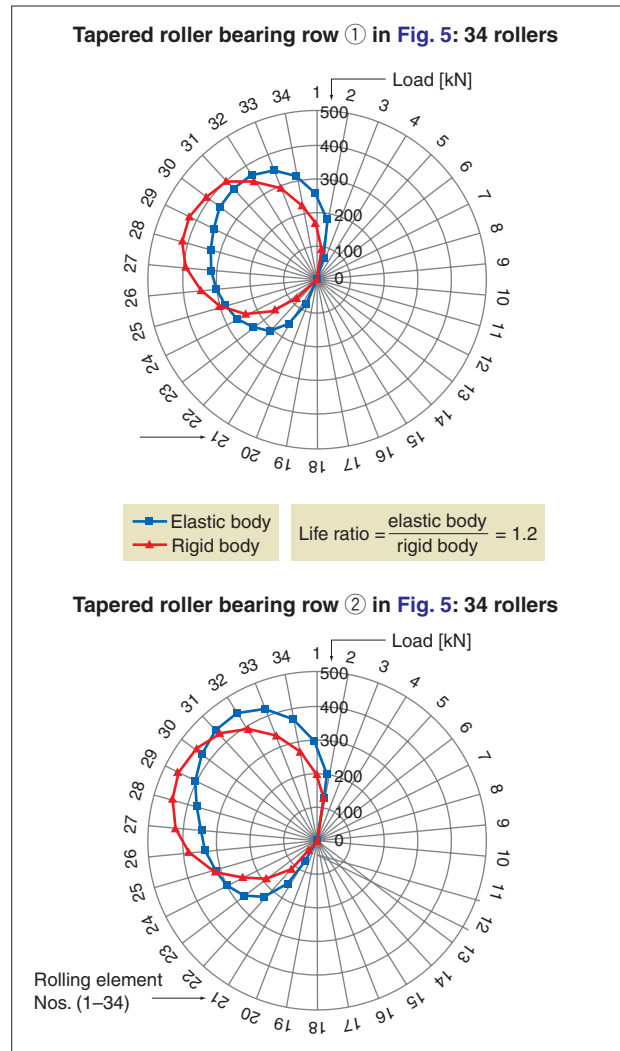


Fig. 7 Load distribution of each rolling elements

other scenarios can lead to reduced bearing life. Therefore, NTN is executing deformation analysis for the entire wind turbine system in order to design an optimal bearing for the main shaft on wind turbine.

3.1.2 Planet bearing for speed-up gearing

Figs. 8, 9 and 10 provide information obtained from structural analysis with bearings incorporated into speed-up gears in larger 2-2.5 MW class wind turbines. Note that through this analysis, the specification for relevant planet bearing has been developed while taking into account the magnitude of possible deformation on the carrier, pinion shaft and planetary gearing.

Fig. 9 shows an analysis example of the deformation mode with planetary gearing wherein gear load and centrifugal force are imposed onto the planetary gearing.

In the main mode, the force resulting from two tangential loads F_t shown in Fig. 7 acts on the bearing as a radial load. Consequently, the outer ring is deformed by two radial loads F_r , thereby the load zone expands.

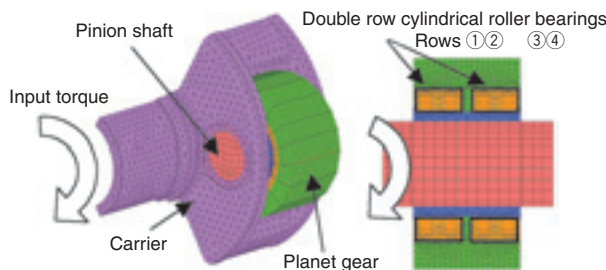


Fig. 8 Planet gear

Fig. 10 schematically illustrates the calculation result. If the deformation on the carrier and planetary gear resulting from the input torque is taken into account, the load acting on the rolling elements in rows ① through ④ on the two double row cylindrical roller bearings is mitigated, compared with a case where deformation is not taken into account. Compared with a case where deformation is not taken into account, the calculated bearing life with deformation being taken into account more closely matches the actual life obtained from the bearings installed to an actual wind turbine. In our test, the life of the two double row cylindrical roller bearings with deformation taken into account was approximately 50% longer compared with a case where deformation was not taken into account.

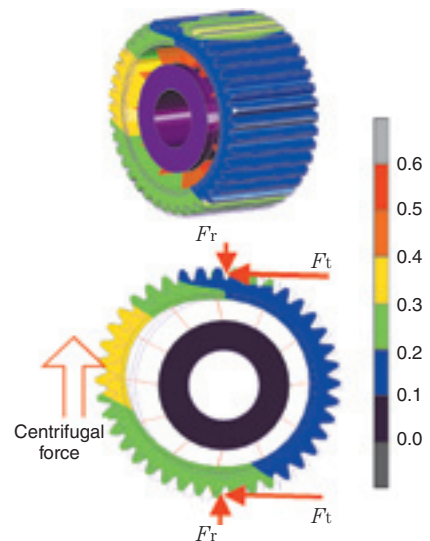


Fig. 9 Analysis example of planet gear

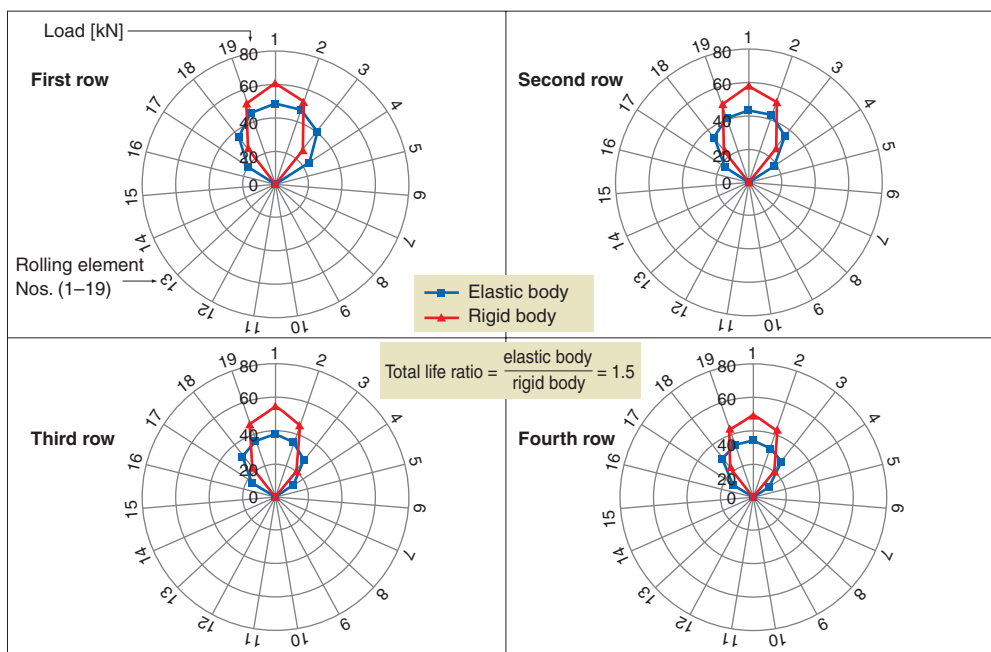


Fig. 10 Load distribution of each low

3.1.3 Thermal analysis

When assessing the performance of bearings incorporated into larger wind turbines, thermal deformation needs to be taken into account. Fig. 11 shows an example of a bearing model that was subjected to our thermal analysis. In the analysis work, the temperature distribution over the entire model was determined based on the heat release performance of the bearing as a heat source. Through analysis for a combination of heat and structure, it will be possible to develop bearing specifications that better reflect operating conditions of bearings installed on actual wind turbines. Note that in the thermal analysis work, the thermal characteristics including the heat transfer coefficient and heat release coefficient are affected by various factors including surface properties of the bearings, the weather, the ambient temperature, the humidity and the wind velocity. Therefore, we have attempted to improve precision of thermal analysis by feeding back data obtained from field tests. This effort is later described.

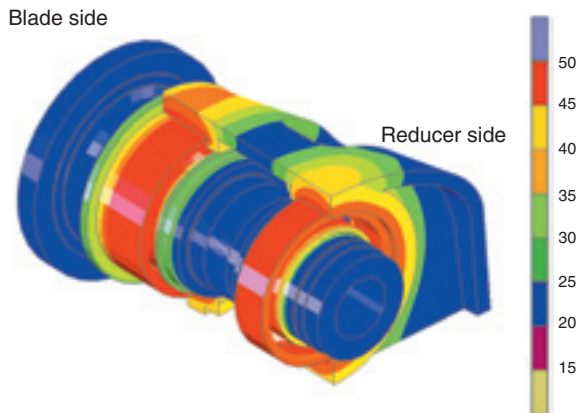


Fig. 11 Example of heat transfer analysis

3.2 Simulation on actual wind turbines

NTN owns and operates a unique test facility that is capable of simulating performance of super large bearings for the main shaft of a 2–2.5 MW class wind turbine while subjecting the bearing to a load that will occur on an actual wind turbine. Utilizing this facility, NTN has been performing tests on the bearings simultaneously with FEM analysis to improve precision of FEM analysis, so that the bearing development period is shortened.

Fig. 12 shows an example of results of the FEM analysis with a bearing model (double row tapered roller bearing: 2,000 mm pitch diameter with roller set) for 2–2.5 MW class wind turbine, wherein a moment load of 1700 kN-m was applied to the inner ring.

Table 1 summarizes the information about a comparison between analytical results of FEM and

measured value on a particular point (point A in Fig. 12) where the inclination of the inner ring is greatest.

In the test result data in Table 1, the difference between the pre-run analytical value and measured value is 5%, which qualifies as a fairly good match. In contrast, the difference between a post-run analytical value and a measured value is as great as 25%. A result of a post-run analysis is provided below. For this analysis, the heat transfer coefficient was determined based on the temperature rise on the inner and outer rings, and the coefficient was applied to the thermal analysis about the increase in bearing preload and change in bearing rigidity resulting from operation of the bearing.

The bearing housing in Fig. 13 houses a double row tapered roller bearing. This analysis model was continuously run thereby resulting in a temperature

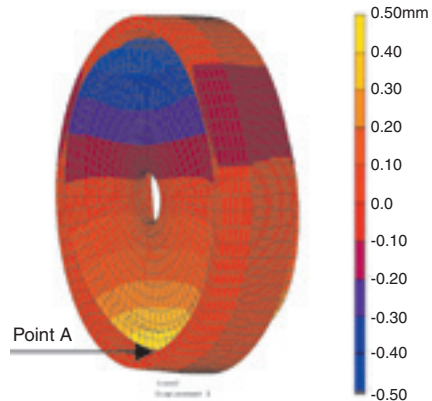


Fig. 12 Example of FEM analysis

Table 1 Test result

	Displacement on point A (mm)	
	Pre-run	Post-run
Analytical value	0.403	0.326
Measured value	0.424	0.259
Difference	5%	25%

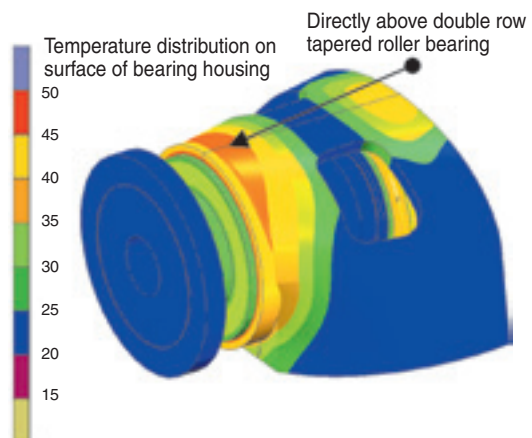


Fig. 13 Analysis model

distribution on the bearing and bearing box to be analyzed.

Incidentally, for an estimation of temperature distribution on the bearing through thermal analysis, tuning (a technique that approximates analytical results to measured values obtained by experiment) was employed. More specifically, with this technique, temperatures measured on various test points on the bearing of an actual wind turbine are incorporated into analytical results to adjust the heat transfer coefficient thereby increasing the reliability of the temperature distribution analysis.

The example of bearing temperature distribution inside a bearing housing in Fig. 14 reflects measured values for ambient temperature, nacelle inside temperature, and temperature on the outer circumference surface of the outer ring. Table 2 summarizes information about the comparison between analytical result of thermal analysis and measured values.

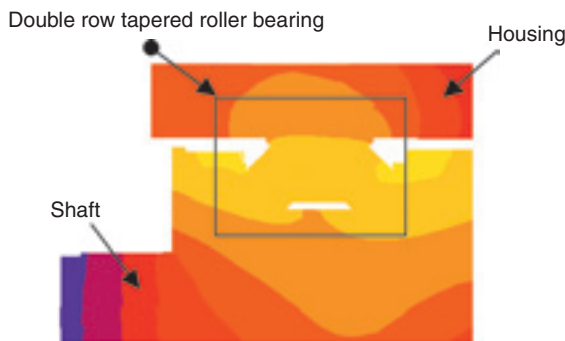


Fig. 14 Example of thermal analysis

Table 2 Bearing temperature distribution

	Temperature difference across inner ring and outer ring (°C)	Temperature on outer circumference surface of outer ring (°C)
Analytical value	2.2	50.5
Measured value	Not measured	50.0
Difference	—	1% (Post-tuning difference)

Based on the estimated analytical value of temperature difference across the inner ring and outer ring, as given in Table 2, the decrease in bearing clearance on the running bearing was estimated, and then, adequate initial bearing clearance has been accordingly determined. As a result, the difference between analytical value and measured value has decreased to 1%.

Considering the findings obtained from these analytical results, NTN has developed an optimal bearing design that has been installed in an actual wind turbine and is reliably running.

4. Conclusion

Wind power generation as a clean energy source has been increasing its output. The quantity of installed offshore wind turbine plants will further increase. At the same time, wind turbines will increasingly feature greater output and larger size, while they are required to withstand severer natural elements more reliably.

In this context, the bearing designs adopted for wind turbines need not only to satisfy conventional standards but also to be optimized for intended wind turbines through wind turbine-specific detailed analysis technique and review of analysis result.

Wishing to contribute to development of wind power generation which is a new energy source possibly helping prevent global warming, NTN will further develop and stably supply highly reliable and durable bearing products.

References

- 1) BTM Consult ApS International Wind Energy Development World Market Update 2008
- 2) SCOTTISH Development International: Offshore Wind Power Generation in Scotland and the UK

Photo of authors



Nobuyuki NINOYU

Application Engineering Dept.
Industrial Sales headquarters



Souichi YAGI

Industrial Sales
headquarters



Tsuyoshi NIWA

Product Design Dept.
Industrial Sales headquarters

Eco-friendly Product Development at SNR Roulements



Siegfried RUHLAND*
Ludovic SAUNIER*
Cynthia TSEN*
Bernard LIATARD**
Gérald MIRABEL***

The reduction of CO₂ emissions is being promoted in Europe, and every automobile company is considering various measures to achieve this goal. "Mass reduction" and "torque reduction" are effective ways to decrease CO₂ emissions, and automobile and parts makers are challenging the limits every day, including with existing products. SNR products that contribute to "mass reduction" and "torque reduction" are introduced in this article.

1. Preface

CO₂ emissions control has been posing a challenge to any manufacturer in attempting to address environmental issues including global warming. To be able to contribute to CO₂ emissions reduction, the automotive industry has been committed to design and produce lighter, lower-torque automotive parts to help improve the fuel efficiency of cars they manufacture. In this article, SNR will present its technologies for lighter weight and lower torque in their automotive hub bearings transmission bearings and suspension bearings.

2. Efforts for lighter bearing designs

This section describes the efforts of SNR for its automotive hub bearing (hereinafter H/B) products and water pump bearing products.

2.1 Automotive hub bearings

Based on a novel concept, SNR has developed unique H/B designs that can be applied to flanged 2nd generation and 3rd generation hub bearings for supporting brake disks and wheel rims. Through optimized shape design for H/B, the newly developed H/B products boast 15% weight reduction while keeping excellent strength and durability.

2.1.1 Design activities for automotive hub bearings

Under the loading conditions (rotational bending force, hub bolt tightening torque, etc.) possibly acting on bearings installed in actual cars, we have analyzed the stresses occurring on H/B. **Fig. 1** shows an analysis model used. As can be understood from this diagram, we have learned that the maximum stress occurs on both the flange tightening area and the chamfer area at the base of flange. Therefore, when developing the new bearing design, we have shifted a portion of the mass of the hub from a low stress region to a high stress region to mitigate stress concentration on the hub while not altering the design of critical areas including the raceway surface, disk and wheel receiving area.

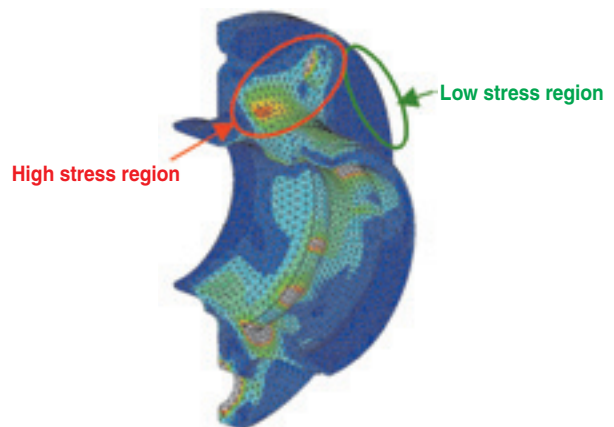


Fig. 1 Stress analysis on the hub bearing

Fig. 2 shows shapes of a conventional design and the new optimized design. The new hub design features a unique flange shape, each of its bolt-down segments being reinforced with two ribs. With this design, the mass of outer ring has been reduced by 20% and that of entire H/B by 15%. This weight reduction will mean a maximum weight reduction of 1,300 g per automobile axle.

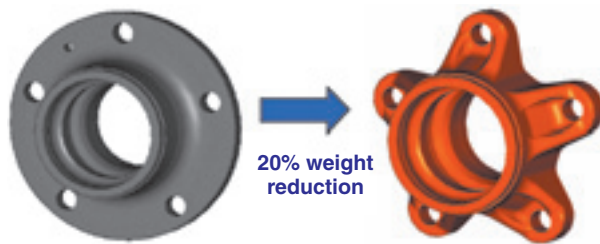


Fig. 2 Conventional design (left) and new optimized design (right)

2.1.2 Performance of new optimized design

As described above, the new optimized design boasts a much reduced weight, while its rigidity is equivalent to that of conventional designs. Furthermore, because the bolt-down segments are reinforced with ribs, the stress occurring at the flange base of the new design is 35% smaller as shown in **Fig. 3**.

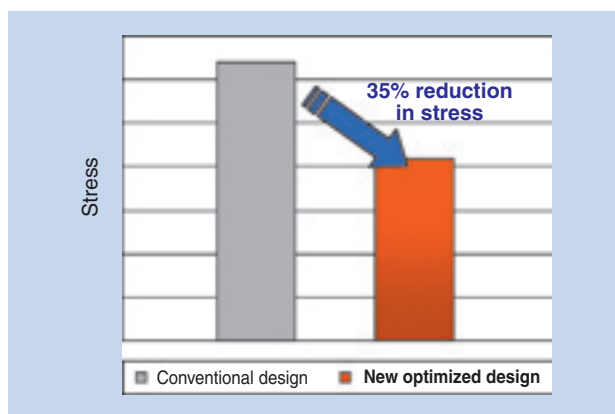


Fig. 3 Stress analysis results

2.2 Water pump bearing for automobile

Fig. 4 shows an appearance of a conventional water pump for cooling an automotive engine, and **Fig. 5** schematically illustrates the structure of the water pump. Many present-day water pumps used for cooling modern automotive engines incorporate integral shaft bearings that have a raceway surface on their shafts with their inner ring deleted.

With a conventional structure in **Fig. 5**, the belt tension poses an offset load onto the bearing and causes the contact pressure to be greater. This problem in turn poses a challenge in providing longer life for the bearing. At the same time, resultant misalignment of the bearing relative to the shaft can cause water to pass the seal and enter the bearing. Consequently, the grease can leak out of the bearing, leading to poor lubrication of the bearing. The bearing can then develop abnormal noise and/or exhibit excessively short life.

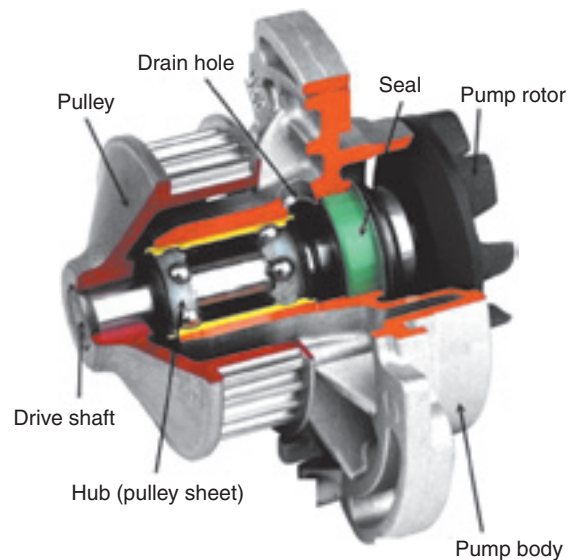


Fig. 4 View of Water pump

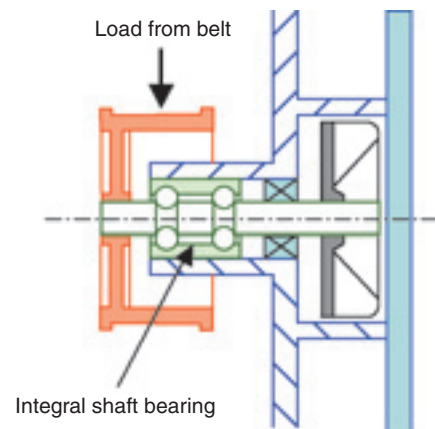


Fig. 5 Water pump structure

2.2.1 Structure of new bearing

In order to achieve lower running noise, lighter weight and longer bearing life, we have developed a novel external bearing that has a shaft integrated with a flange. Fig. 6 shows a view of this novel external bearing, and Fig. 7 schematically illustrates the structure of this bearing. This structure ensures that the tension from the drive belt acts on the center of bearing, helping prevent misalignment of the bearing relative to the shaft. Compared with conventional designs, the contact pressure between the balls and raceway surface on this bearing is lower, leading to improved bearing durability. In addition, because our new bearing is free from bearing-shaft misalignment which will develop moment load, the balls will roll at the bottom of groove, resulting in lower running noise occurrence.



Fig. 6 View of external bearing

Through improvement in our production technology, we have integrated the bearing and flange with the shaft, thereby we have successfully achieved an increase in load carrying capacity of bearing, increase in pump capacity, longer bearing life, lower noise emission and lighter weight. Fig. 8 summarizes changes in appearance and weight of water pump bearing over several years.

2.2.2 Determination of contact pressure occurring between balls and raceway surface

So that a water pump on an automobile remains operative without any need for repair until the automobile reaches the end of its useful service life, the life of water pump bearing needs to satisfy 3×10^5

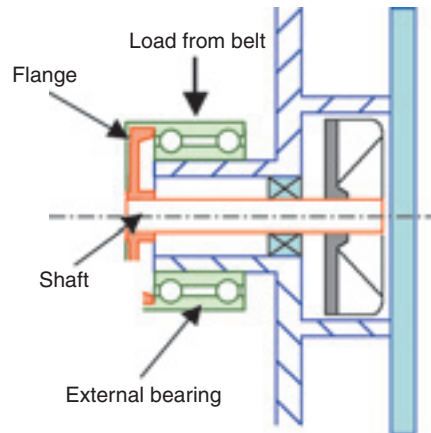


Fig. 7 Structure of external bearing

Greater pump capacity	→	Drive belt for auxiliaries is directly engaged with the outer ring; this arrangement helps realize a space-saving pump design. Use of larger balls helps reduce contact pressure, mitigating adverse effect of press-fitting operation.
Longer life	→	
Weight reduction	→	

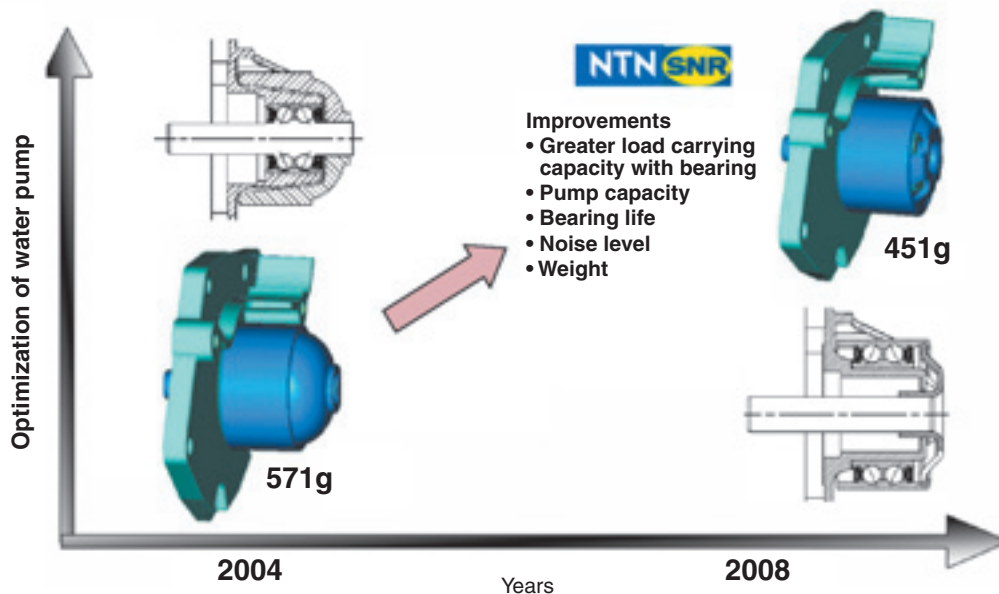


Fig. 8 Process of water pump bearing

km of automobile's total travel distance. In order for a given water pump bearing design to satisfy this life requirement, its internal design needs to be finalized so that the contact pressure at any portion in it does not exceed fatigue limit of that portion. To this end, it is also important to optimize tightening allowance of the seal, amount of prefilled grease, and location of prefilled grease.

We have studied various parameters including bearing life, temperature, parts tolerances, minimum and maximum clearances, and tightening allowance, executed functional test, and various tests with the pump lifetime tester shown in **Fig. 9**, thereby we have established the design standard that satisfies the bearing life requirement.

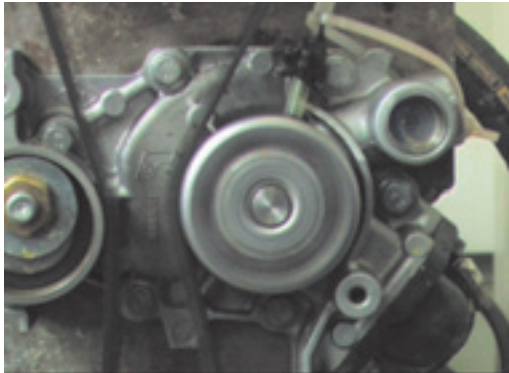


Fig. 9 View of pump lifetime test

3. Efforts for bearing products of lower torque

This section describes our efforts for low torque designs with automotive transmission bearings, hub bearings and suspension bearings.

3.1 Automotive transmission bearings

Various improvement activities have been performed by people involved in automotive technologies to help improve operability of automotive transmissions and reduce CO₂ emissions from automobiles. To promote various automotive transmission systems, SNR has been committed to lighter weight, higher efficiency (lower torque) transmission bearing designs.

Approx. 50% of torque loss occurring on a given automotive transmission results from stirring-induced resistance with lubricating oil. Therefore, an appropriate choice of lubricating oil is one of important considerations in achieving lower torque on an automotive transmission, and a currently more favored combination is a use of minimum amount of low viscosity lubricating oil. Incidentally, efficiency of an

automotive transmission is greatly affected by torque loss occurring from an inactive idler gear: therefore, bearing torque poses a critical factor in the torque loss on the transmission.

The efforts SNR has so far made with its transmission bearings in order to reduce CO₂ emissions are as follows:

- (1) The inner and outer rings and rolling elements of our bearings made of the standard steel material 100Cr6 are now subjected to a special heat treatment process. Consequently, these components boast longer life even under severe lubricating conditions.
- (2) Development of unique self-lubricating bearings for automotive gearboxes (**Fig. 10** shows examples of self-lubricating bearing lubricated with solid lubricant).
- (3) Decreased torque by superseding sliding bearings for idler gear with rolling bearings such as caged needle roller bearing.
- (4) Optimized bearing design through analysis for load and torque on transmission bearing by using newly developed engineering computation software (a simulation model is shown in **Fig. 11**).
- (5) Reduced frictional torque through improved internal design for bearings.



Fig. 10 Autonomous bearings using solid lubricant

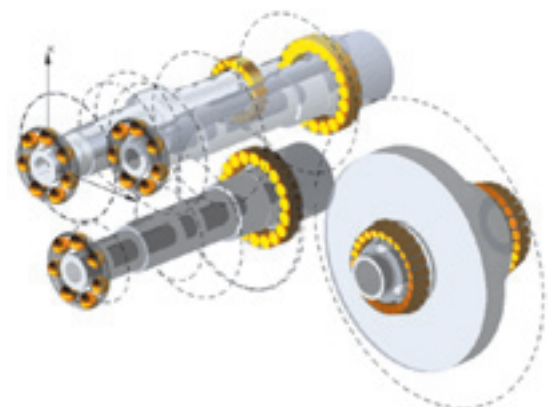


Fig. 11 Transmission simulation

3.2 Low torque ball bearings

To reduce friction-induced torque loss on an automotive transmission, use of a ball bearing rather than a tapered roller bearing is advantageous. However, since load carrying capacity of a ball bearing is smaller compared with a tapered roller bearing, the size of ball bearing tends to be larger so that the bearing can satisfy targeted life. Incidentally, the ordinary fracture mode of transmission bearing is surface damage starting from a dent mark on the raceway owing to lubricant contaminated with foreign matter, rather than fatigue failure of bearing material. Therefore, to prevent ingress of foreign matter into a bearing to ensure longer bearing life, a bearing having filter seals shown in Fig. 12 is used. Filter seals need to be optimally designed so that they not only provide good filtering performance but also allow lubricating oil to be introduced into the bearing to lubricate and cool down the bearing.

Many bearings with filter seals feature an increased bearing width dimension to accommodate an additional elastomer filter seal; however, this configuration leads to increased frictional torque on bearing. A novel design developed by SNR, as shown in Fig. 13 has a clipped double polyamide cage that has filtering function. The advantages of this design are as follows:

- (1) Compact and light-weight design is possible.
- (2) Labyrinth clearance between the cage and raceway can be controlled at higher precision.
- (3) Provision of two oil inlets helps increase lubricating oil flow into the bearing.
- (4) Reduced cost

The result of comparison between our newly developed double seal design and a conventional seal design is described below.

Fig. 14 illustrates results of measurement of oil flow through a bearing under oil bath lubrication environment. The data mapped along the vertical axis represent filtering effect and oil flow that passes a filter and contribute to lubrication. Compared with a conventional filter seal, our newly developed double filter seals boast better lubrication efficiency as more oil flows through the bearing though the filtering effect is roughly same.

Fig. 15 illustrates a result of comparing running torque of our newly developed bearing with double filter seals to that of conventional bearing. Torque occurring inside the bearing including rolling resistance is virtually the same with both bearing types; notwithstanding, the total torque on our new bearing design has been reduced by 65% because the torques occurring on the seals has been greatly reduced. Also, heat buildup in our bearing is mitigated; consequently,

our bearing boasts improved seizure resistance. Furthermore, filtering function of our bearing is virtually equivalent to that of conventional bearing design, and the width of our bearing can be smaller. Our bearing design can be applied to produce compact, light-weight transmission bearing products.

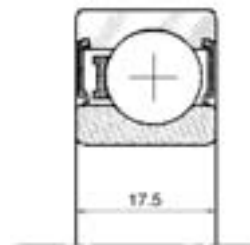


Fig. 12 Bearing with filter seals

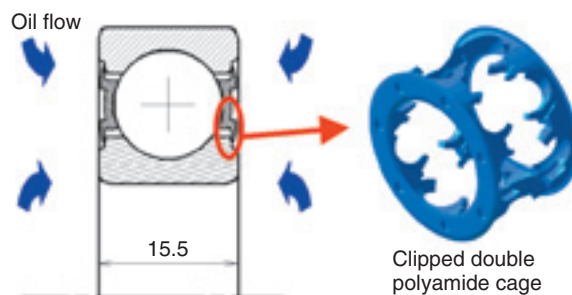


Fig. 13 Bearing with double filter seals into a clipped double polyamid cage

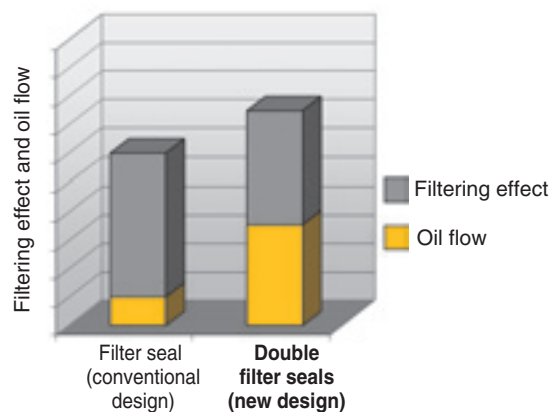


Fig. 14 Efficiency against pollution

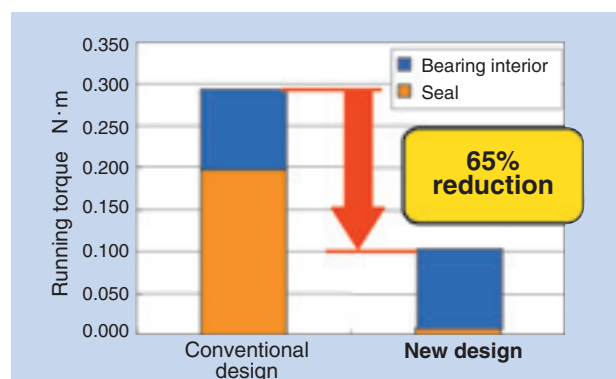


Fig. 15 Torque test results

3.3 Low torque tapered roller bearings

Tapered roller bearings are often used as transmission bearings because they can carry a greater combined axial and radial load compared with other bearing types of similar size. However, reduction in frictional torque occurring on this bearing type poses a challenge.

The SNR tapered roller bearings for automotive transmissions boasts decreased frictional torque through adoption of NTN's design and production technologies for low torque tapered roller bearings. The advantages of these SNR products can be defined as follows:

- (1) Special heat treatment process helps improve fatigue strength and resistance against dent mark that can result from foreign matter in lubricant.
- (2) Adoption of polyamide cage in which shear friction with oil is lower, compared with that in standard steel sheet cages
- (3) Improved design for bearing interior in order to improve load carrying capacity and rigidity and mitigate misalignment and frictional torque (optimized number and size of rollers, and special crowning on raceway surface and rolling surface)
- (4) Optimization of contact locations between inner ring flange surface, rollers, and raceway surface
- (5) Reduction in surface roughness of inner ring flange surface and roller end faces to reduce frictional torque on roller end faces

Fig. 16 graphically plots information about comparisons of SNR's tapered roller bearing for transmission and a competitor's tapered roller bearing, wherein the running speeds data of these bearings are plotted along the horizontal axis. As can be understood

from this diagram, the bearing products of SNR boast 25 to 50% reduction in torque loss, compared with competitor's products.

25% reduction in torque loss with transmission bearings means 2 g/km reduction in CO₂ emissions per vehicle. In addition, use of low torque tapered roller bearings helps improve seizure resistance as well as quality of shift-change operation.

3.4 Automotive hub bearings

About 50% of frictional torque occurring on a wheel bearing results from sliding friction on contact surface of seal(s). Therefore, the use of hub bearings featuring reduced sliding resistance is effective in reducing the CO₂ emissions from the vehicle that incorporates low friction wheel bearings. However, reduced frictional resistance on a given seal often means jeopardized sealing performance of that seal. Therefore, there has been a challenge of meeting conflicting needs for reduced frictional resistance and improved sealing performance.

SNR has developed a unique tribological effect-capable seal that boasts approx. 11% reduction in sliding resistance and 22% improvement in sealing performance, by improving lubrication quality on the sliding surface of seal lip. As SNR has applied the above-mentioned development concept to its currently present seal products, cost reduction and reduced development lead time have been achieved.

3.4.1 Advantages of tribological effect-capable seal products

On our newly developed tribological effect-capable seals, the lip sliding surface of the slinger is uniquely shaped so that oil film is readily formed on it.

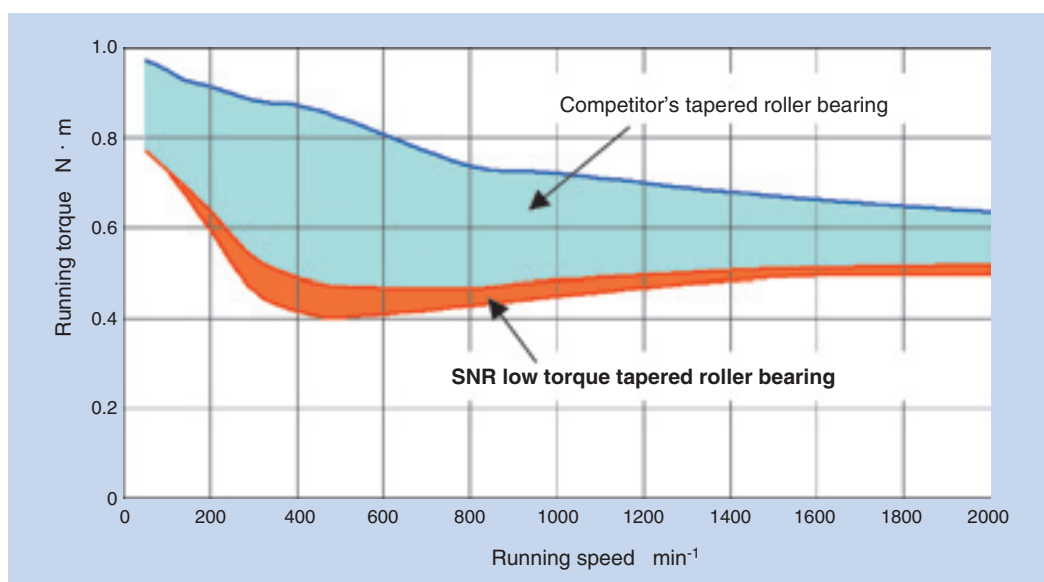


Fig. 16 Torque measurements with rotations

Consequently, lower torque and mitigation of heat buildup have been achieved. Fig. 17 illustrates a cross-sectional plan of our seal, and a view of the contact area of the slinger. Micro-pores present in this contact area help form an oil film between the seal lip and slinger, and the oil film reduces friction on the seal lip. Furthermore, these micro-pores prevent wear caused by ingress and trapping of foreign matters.

3.4.2 Performance of tribological effect-capable seal

Figs. 18 and 19 show running torque and test results of a muddy water bearing life test with conventional seal and our newly developed tribological effect-capable seal. Owing to reduced resistance on seal, the running torque has decreased by 11%, and the muddy water bearing life has increased by 22%.

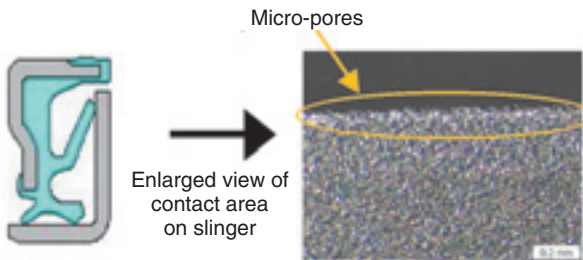


Fig. 17 Seal shape on the slinger

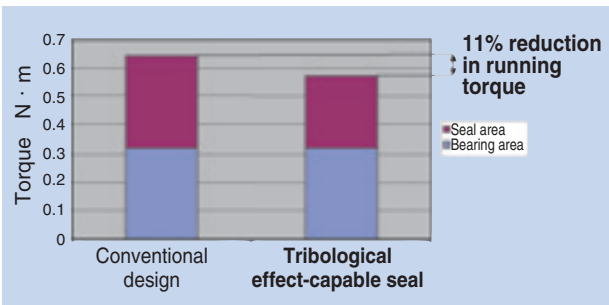


Fig. 18 Comparison of rotational friction between development seal and current one

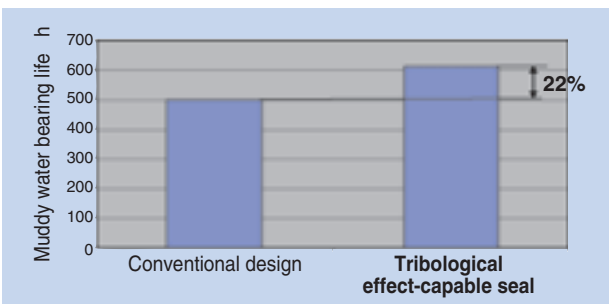


Fig. 19 Comparison of muddy water resistance between development seal and current one

3.5 Automotive suspension bearings

To be able to operate without problems under severe operating conditions (environments such as muddy water), a sealed strut bearing needs to feature improved reliability and sealing performance. In challenging this issue, SNR has developed a unique low torque sealed strut bearing complete with a floating seal in order to satisfy requirements for both an improvement in running torque and sealing performance (Fig. 21).

3.5.1 Features of sealed strut bearings

Muddy water resistance of a bearing is governed by lip performance of its seal. Therefore, it is important to develop a seal that is capable of satisfying both better sealing performance and stabler running torque performance. To address this challenge, we have recently developed a novel low torque sealed strut bearing complete with a floating seal. Fig. 20 shows a conventional design, and Fig. 21 illustrates our new design. For comparison purpose, Fig. 22 shows a structure of a different design, that is, an overmolded lip seal.

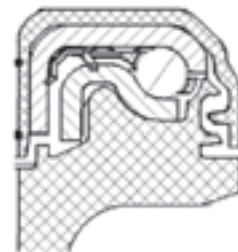


Fig. 20 Usual design

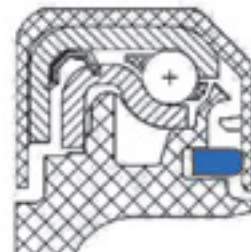


Fig. 21 SNR design: floating seal

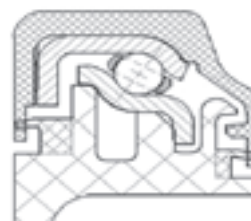


Fig. 22 Competitor design: overmolded lip seal

3.5.2 Test results

Fig. 23 illustrates the contribution of a seal onto the running torque of a strut bearing. Compared with a conventional design, the running torque on our newly developed floating seal (SNR design in **Fig. 21**) is 18% greater; compared with an overmolded lip seal, the running torque on our new seal design is 50% smaller.

Fig. 24 provides results of muddy water test. Compared with the conventional design, our newly developed floating seal (SNR design in **Fig. 21**) boasts greatly improved sealing performance that helps positively reduce water ingress into the bearing. Though excellent in initial sealing performance, the overmolded lip seal experiences wear of the overmolded lip: the SNR's newly developed design boasts 38% smaller water ingress.

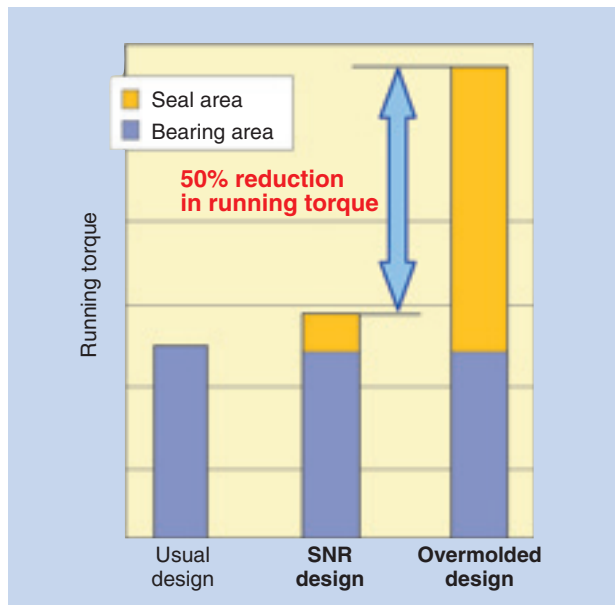


Fig. 23 Torque test results

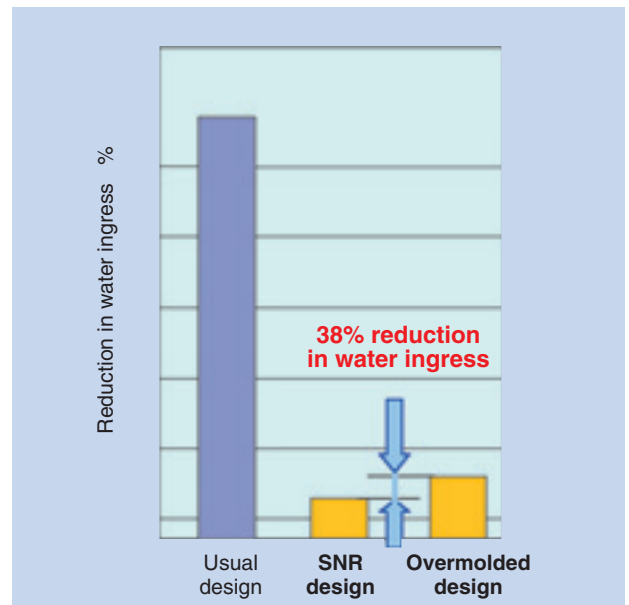


Fig. 24 Muddy water test results

Photo of authors



Siegfried RUHLAND

SNR Product Innovation
& Mechatronic



Ludovic SAUNIER

SNR Product Innovation
& Mechatronic



Cynthia TSEN

SNR Product Innovation
& Mechatronic



Bernard LIATARD

SNR Automotive
Transmission Engineering

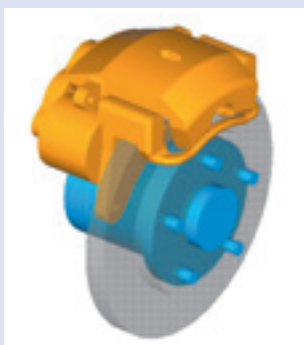


Gérald MIRABEL

SNR Automotive
Equipment Engineering

Actuator for Electromechanical Brakes

Tatsuya YAMASAKI*
Masaaki EGUCHI*
Yusuke MAKINO**



Electromechanical brakes (EMB) have some advantages, such as vehicle safety improvement and simple system. In electric vehicles and hybrid electric vehicles, which have received much attention in recent years, applying EMB and controlling them in coordination with regenerative braking is expected to improve fuel economy. On the other hand, it is desirable that the brakes be compact and lightweight, because they are installed under the springs of the vehicles. NTN has developed a small actuator for EMBs with our original linear motion device.

1. Introduction

The brake system plays a critical role in the safe operation of any automobile. Recently, car manufacturers have been improving the safety of their cars through improvements in ABS, ESC and brake assist systems that have resulted from improvements in hydraulic control technologies^{1), 2)}.

Incidentally, while concerns about the global environment have been mounting an increasing number of electric motor-driven cars such as Hybrid Electric Vehicles (HEV), which boast better fuel economy, and Electric Vehicles (EV), which do not use any fossil fuels, have been marketed and will see ever increasing demand.

On HEV's and EV's a regenerative braking system recovers energy during the deceleration process by allowing an electric motor to function as a generator. To be able to recover energy more efficiently, it is necessary to further improve control over mechanical and regenerative braking systems. In addition, on an HEV or EV, the negative pressure occurring on the engine is insufficient or cannot be used; therefore, if a conventional braking system is used a separate negative pressure generating system will be needed.

To sum up, it is difficult with conventional braking systems to readily solve difficult issues, such as brakes with more sophisticated functions and improved eco-

friendliness. There has been a mounting need in the market for an electrically actuated electromechanical braking system, as a means for solving these issues. However, conventional electromechanical braking systems, which use a ballscrew or ball-ramp for a linear motion device, require a reducer mechanism to obtain a greater reduction ratio; thus, a compact actuator design for this purpose has been difficult to realize.

By using its propriety linear motion mechanism, NTN has developed a compact actuator for electromechanical brakes³⁾. In this paper, we provide information about our actuator for an electromagnetic brake, whose performance has been improved by optimization of its internal design.

2. Structure of actuator for electromagnetic brake

2.1 Linear motion device

(planet roller screw mechanism)

The constitution and operating principle of our linear motion device are hereunder described. As shown in **Fig. 1**, our linear motion device comprises of a sun roller, planet rollers, outer ring, carrier, support pins, springs, and bearings. The planet rollers are circumferentially arranged at equal intervals between the sun roller that functions as an input means and the axially sliding outer ring that functions as an output

*Automotive Module Product Development Dept. New Product Development R&D Center

**Mechatronics Research Dept. New Product Development R&D Center

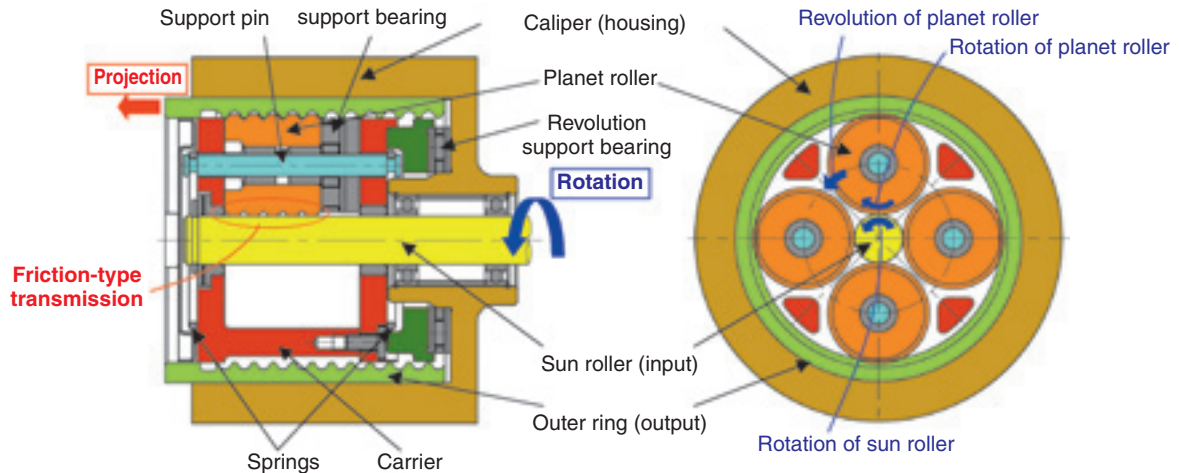


Fig. 1 Schematic of linear motion device

means. Torque on the sun roller is transmitted to the planet rollers through friction. The outer circumference of each planet roller has an external thread or circumferential groove that engages with an internal thread on the bore surface of the outer ring; wherein the pitch of the internal thread on the bore surface of the outer ring is the same as that of the external thread or circumferential groove on each planet roller but the lead of internal thread on the outer ring is reversed to that of the external thread or circumferential groove on each planet roller. The carrier that supports the planet rollers is supported by the caliper (housing) such that it can rotate, but does not slide in the axial direction. With this construction, when the sun roller rotates the planet rollers revolve while rotating, thereby the rotary motion of the sun roller is finally translated into the axial slide motion of the outer ring.

Next, let us describe a means for providing a normal load that is necessary to permit a friction-type transmission of torque from the sun roller to the planet rollers. In a report from a previous issue of the *NTN Technical Review*, the necessary normal load was provided by positioning the planetary rollers between the sun roller and outer ring by a shrink-fitting technique³⁾. With our new development, the planetary rollers are forced into contact with the sun roller by means of a spring force being applied by the springs connected to both ends of the support pin. At the same time, the contact areas between the planetary rollers and the outer ring are each designed to form a ramp having a particular flank angle; consequently, when an axial load acts on the outer ring as shown in Fig. 2, the ramp-type contact surface exerts a load that forces the corresponding planet roller toward the sun roller.

This structure helps mitigate the effect of a dimensional change owing to a worn torque transmission surface to the normal load; thereby, a

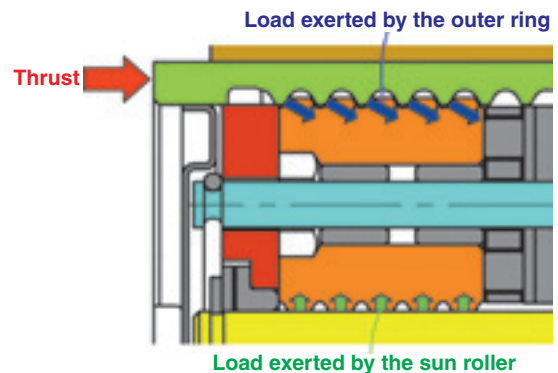


Fig. 2 Load acting on planet roller

stable load acts along a normal line. In addition, through optimization of the flank angle between the planet roller and the outer ring, reliable torque transmission is achieved without causing excessive slippage between the sun roller and the planet rollers even when a very high load is acting on the sun roller and the planet rollers.

2.2 Electromagnetic brake unit

Fig. 3 schematically illustrates our electromagnetic brake unit designed for the front wheels of a 1500 cc-class vehicle. To configure this brake unit, we have incorporated our linear motion device, described in Sec. 2.1, into the caliper together with an electric motor such that the entire axial length of the brake unit is shorter. The linear motion device and the driving motor are arranged in parallel, where the motor transmits driving power to the linear motion device through a gear train. Main specifications of this new EMB unit are summarized in Table 1. Note that the driving motor for this actuator has been designed by NTN Fig. 4 illustrates the structure of this motor, and Table 2 summarizes major specifications of this motor.

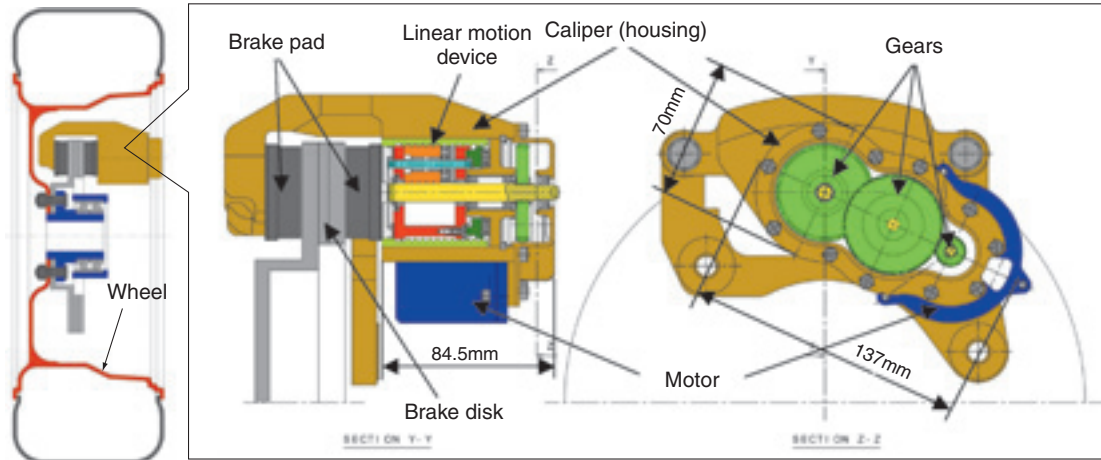


Fig. 3 Schematic of EMB unit

Table 1 Specifications of EMB unit

Characteristic	Specification	Remarks
Max. thrust force	30kN	Equivalent to that of front wheels for 1,500 cc-class vehicle
Load retaining function.	None	This setting may be changed to "Yes" by appropriately altering the specifications for threading for planet rollers and outer ring.
Size (excluding pad clamp)	137mm×70mm×84.5mm	—
Mass (excluding pads)	5.6kg	—
Lubrication system	Grease lubrication	—

3. Performance

3.1 Efficiency

Fig. 5 illustrates the interrelation between motor torque, thrust force and efficiency. Note that the calculated values in Fig. 5 have been determined by applying the efficiency calculation method presented in a previous issue of NTN Technical Review³⁾. The experimental values fairly match the calculated values. Thus, our EMB unit performs as designed.

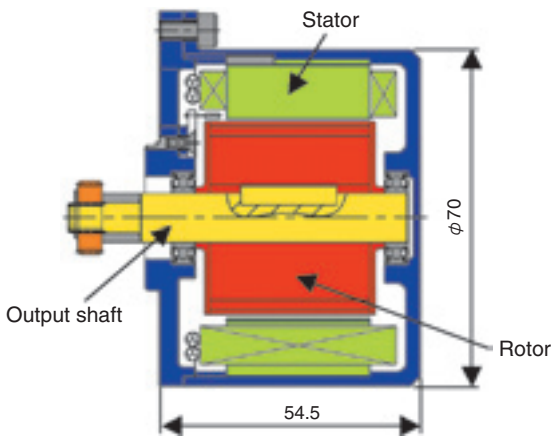


Fig. 4 Structure of motor

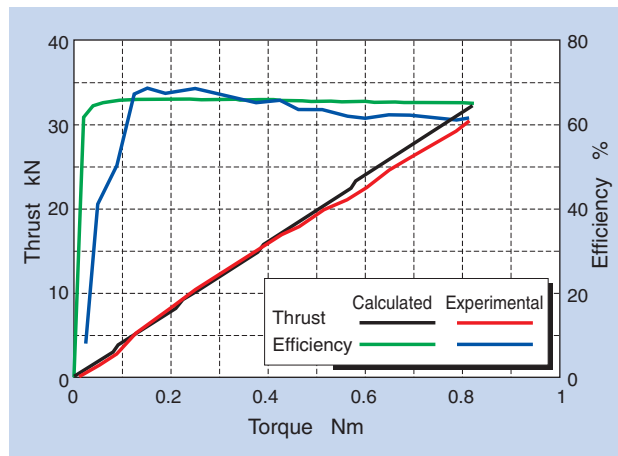


Fig. 5 Efficiency of EMB unit (developed)

Table 2 Specifications of motor

Characteristic	Specification
Type	DC brushless
Size	φ70×54.5
Voltage applied	12V
Max. running speed	5000min ⁻¹ (w/load)
Max. torque	0.8Nm

3.2 Thrust variation rate

By adopting the caliper shape shown in Fig. 3 and by using a pad and disk used on an actual brake system, the variation rate of thrust was assessed. Fig. 6 shows the results of the assessment obtained by applying a constant voltage (12 V) to the EMB unit placed in an ambient temperature of 20°C. Table 3 summarizes the response times and thrust variation rates defined by expressions (1) through (4).

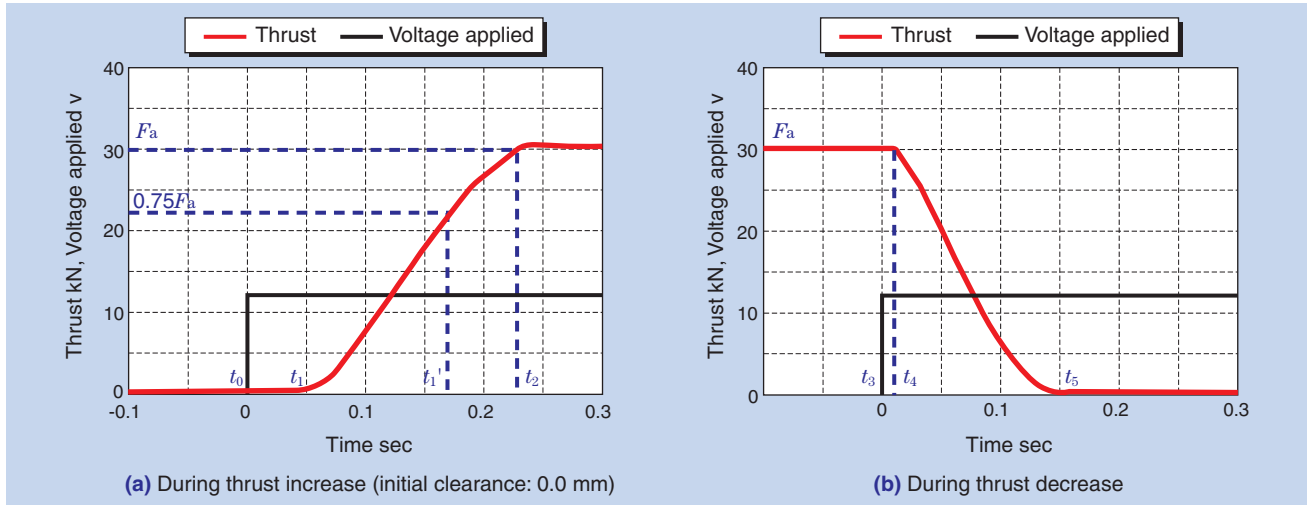


Fig. 6 Thrust variation rate of EMB unit (developed)

Table 3 Response time and thrust variation rate

Characteristic	Time	Thrust variation rate
During thrust increase	0.172 s (= Δt_{INC})	170 kN/s (= V_{INC})
During thrust decrease	0.146 s (= Δt_{DEC})	221 kN/s (= V_{DEC})

$$\Delta t_{INC} = t_1 - t_0 \dots\dots\dots (1)$$

$$\Delta t_{DEC} = t_5 - t_3 \dots\dots\dots (2)$$

$$V_{INC} = \frac{0.75 \cdot F_a}{t_1' - t_1} \dots\dots\dots (3)$$

$$V_{DEC} = \frac{F_a}{t_5 - t_4} \dots\dots\dots (4)$$

- F_a : Max. thrust force = 30 kN
- t_0 : Actuation start point (during thrust increase)
- t_1' : Thrust increase start point
- t_1 : 75% maximum thrust reached point (during thrust increase)
- t_2 : Maximum thrust reached point
- t_3 : Actuation start point (during thrust decrease)
- t_4 : Thrust decrease start point
- t_5 : Brake release end point
- V_{DEC} : Thrust variation rate (thrust decrease rate)
- V_{INC} : Thrust variation rate (thrust increase rate)
- Δt_{DEC} : Time (during thrust decrease)
- Δt_{INC} : Time (during thrust increase)

3.3 Durability

Table 4 summarizes the characteristics tested in the durability test that has been performed in accordance with JASO C 448-89 that specifies the bench test method for the disk brake caliper assembly of a passenger car. Our new design has satisfied the durability requirements for all the characteristics summarized in Table 4.

Table 4 Durability test

Characteristics tested	Test parameters
Torque durability	Braking torque Equivalent to 0.6G Number of braking cycles 20×10^4
High thrust durability	Magnitude of thrust 30 kN Number of thrust applications 1×10^4
Normal temperature actuation durability	Temperature 4~35°C Magnitude of thrust 15 kN Number of thrust applications 50×10^4
High temperature actuation durability	Temperature 120°C Magnitude of thrust 15 kN Number of thrust applications 7×10^4
Vibration durability	Vibration acceleration $\pm 20G$ (vertical direction) Vibration frequency 60 Hz Number of vibration applications 500×10^4

4. Conclusion

This paper has presented our unique actuator, which incorporates NTN's propriety linear motion device for a compact electromagnetic brake.

As electric motor-driven cars such as HEV and EV become more commonly used, there will be an increasing need for electromechanical brake systems. NTN will further improve durability and response speed of the actuator so that it can be reliably used on electromagnetic brakes.

References

- 1) Tomohiko Adachi: Trends in Electronic Stability Control (ESC) Systems, Journal of the Society of Automotive Engineers of Japan, Vol. 60, No.12 (2006) 28-33 (Japanese)
- 2) Bo Cheng, Tetsuo Taniguchi, Tadashi Hatano, Toshiya Hirose: Effects of Brake Assistance Systems in Emergency Situations, Proceedings of the Society of Automotive Engineers of Japan Annual Congress No. 20065894 (2006) (Japanese)
- 3) T. Yamasaki, M. Eguchi and M. Makino: Development of an Electromechanical Brake, NTN Technical Review No. 75 (2007) 53-61

Photo of authors



Tatsuya YAMASAKI
Automotive Module Product
Development Dept.
New Product Development
R&D Center



Masaaki EGUCHI
Automotive Module Product
Development Dept.
New Product Development
R&D Center



Yusuke MAKINO
Mechatronics Research Dept.
New Product Development
R&D Center

Electric Ball Screw Actuators for Automobiles



Yoshinori IKEDA*
Hirakazu YOSHIDA*

In the automotive market, many new hybrid cars and low -fuel -consumption and low -emission engines have been developed to reduce CO₂ and to produce cleaner exhaust. At the same time, many projects are advancing to achieve more car amenities and safer driving using quicker and more reliable electric motor drives. NTN had already developed a new electric ball screw for use in automatic manual transmission and engine control. Building on this, we have developed an electric ball screw actuator with modularized peripheral parts. This article introduces the structure and the features of this ball screw actuator unit.

1. Introduction

Control-by-wire technologies for automobiles are becoming more commonly adopted with one typical example being the by-wire throttle control system. Recently though, certain cars have adopted brake-by-wire technology. Control-by-wire technologies have been ever evolving in an effort to achieve better comfort and safety in operating vehicles.

Recently, NTN has developed a high-response, high-thrust, electrically driven ballscrew actuator for automobiles (hereinafter referred to as “actuator”) that can be adopted for control-by-wire systems.

This paper hereunder describes the structure and features of this actuator.

2. Structure of the actuator

Fig. 1 shows the structure of our actuator.

The ballscrew is coupled with an electric motor via an involute spline formed at one end of the ballscrew shaft to transmit torque from the motor.

At the other end of the ballscrew shaft, a double row angular ball bearing is situated securely in an aluminum case. The ballscrew and actuator are synchronized by means of an interlocking arm. Across both ends of the actuating shaft, linear ball bearings and oil seals are arranged symmetrically.

The linear ball bearings support the actuating shaft while developing only minimum friction so that the actuating shaft can slide in the axial direction. The oil seals situated around the linear ball bearings prevent ingress of foreign material into the aluminum case. An actuating wire is connected to the coupling member at the end of the actuating shaft.

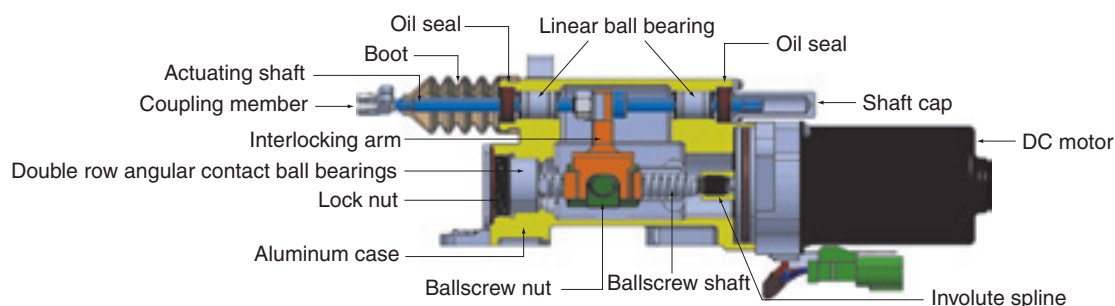


Fig. 1 Structure of actuator

*Automotive Sales Headquarters Automotive Engineering Dept.

3. Advantages of our actuator

Fig. 2 shows our actuator, and **Fig. 3** shows the ballscrew for our actuator.

The actuator has undergone various tests simulating various environmental conditions including water, snow, mud, gravel, and dust along with vibration and impact testing. Through these tests, the actuator has been progressively improved and now boasts a higher degree of reliability. The actuator boasts the following advantages:

- (1) **Highly efficient ballscrew and lower friction moving parts help achieve a higher degree of response and greater thrust force.**
- (2) **Sufficient corrosion resistance, and dust-proof & water-proof performance**

These advantages are described below:

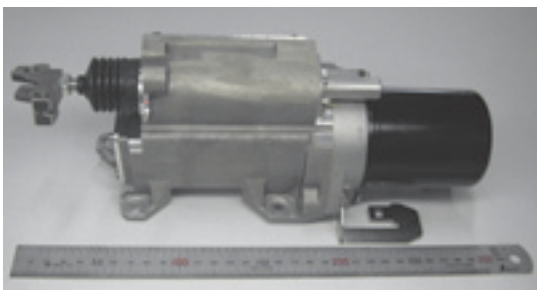


Fig. 2 Ballscrew actuator

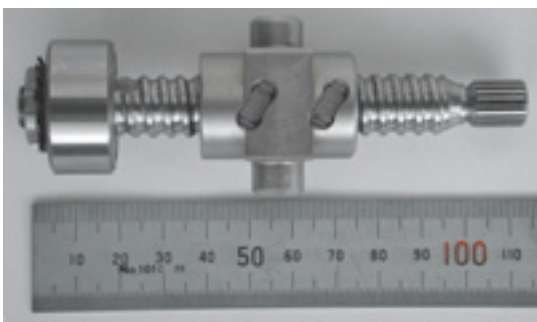


Fig. 3 Ballscrew for actuator

3.1 Higher efficiency and lower friction

We have set up the specifications for our actuator so that the conversion efficiency of motion of the ballscrew adopted, from both forward and reverse rotation directions, is 90% or greater. The actuating shaft can be readily moved by hand thanks to its low-friction design.

Table 1 provides the specifications for the ballscrew. **Fig. 4** graphically plots the theoretical efficiency of the ballscrew. At a lead angle of $4^{\circ}47'$, the efficiency with a benchmark sliding screw is as low

as 32%; in contrast, the efficiency of the ballscrew adopted in our actuator is very high, standing at 92%.

Fig. 5 shows the linear ball bearings that support both ends of the actuating shaft. The actuating shaft is supported by the linear ball bearings in rolling contact, thereby the resultant lower friction helps the actuating shaft to move smoothly.

Table 1 Spec. of ballscrew

Shaft diameter	Lead	Lead angle
14.5mm	4mm	$4^{\circ}47'$

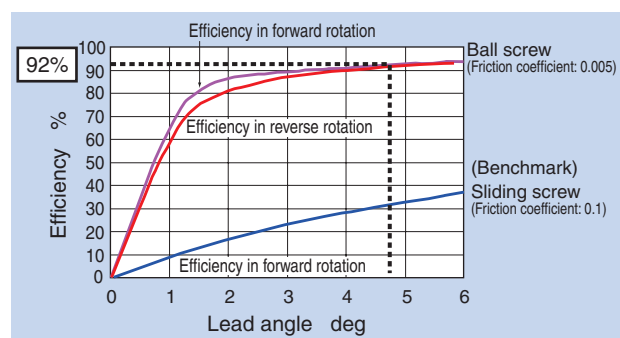


Fig. 4 Efficiency of ballscrew

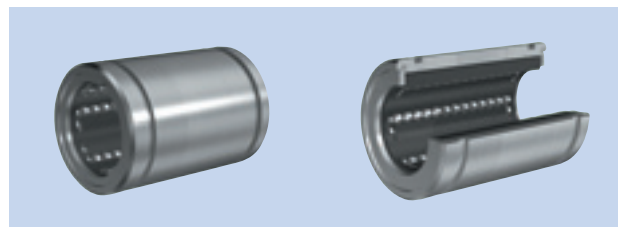


Fig. 5 Linear ball bearing

3.2 Corrosion resistance, dust-proof & water-proof performance

Any automotive actuator needs to perform as designed for a prolonged period under various environmental conditions. Our actuator, in particular, has an actuating shaft that is exposed outside the case; therefore, both ends of the shaft are provided with reciprocating motion-capable oil seals to prevent ingress of foreign material.

For enhanced corrosion resistance, the actuating shaft is provided with special plating. Furthermore, the actuating shaft is equipped with a boot and shaft cap so that the shaft is not directly exposed to the ambient air (**Fig. 6**).

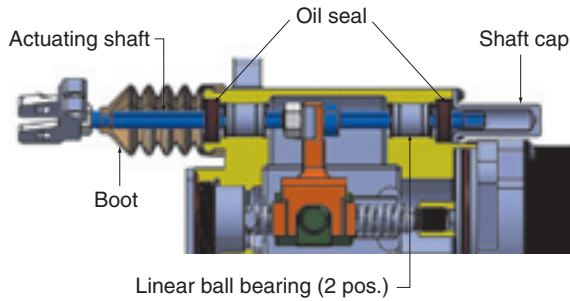


Fig. 6 Structure of sealing of shaft

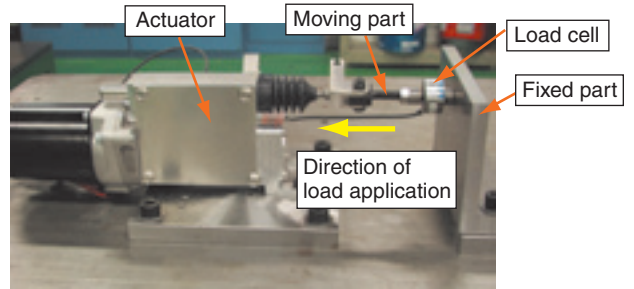


Fig. 7 Appearance of thrust force test

4. Evaluation test

In an effort to develop a highly reliable electromechanical actuator, we have performed various tests to verify that our actuator has sufficient performance and reliability. The major characteristics tested are described below:

4.1 Thrust force test

The load torque on a ballscrew can be determined with the following expression:

$$T = \frac{P \cdot L}{2 \pi \cdot \eta} \dots\dots\dots(1)$$

where,

- T : Load torque (N-m)
- P : Axial load (N)
- L : Lead of ballscrew (m)
- η : Efficiency 0.92

Using the result from expression (1), the thrust force can be determined with expression (2) below:

$$P = \frac{T \cdot 2 \pi \cdot \eta}{L} \dots\dots\dots(2)$$

For the thrust force test, a load cell was inserted between the coupling member and a fixed part as shown in Fig. 7 to measure the load.

The result of the thrust force measurement is plotted in Fig. 8. We have verified that the theoretical calculated value of 1,200 N is achieved with our ballscrew. The thrust force available from a sliding screw whose size is similar to that of our ballscrew is approximately 1/3 that of our ballscrew.

4.2 Durability test in severe environment

We have subjected the actuator samples to a durability test under severe environmental conditions with a high-temperature ambience while applying a predetermined load to each actuator sample. So that a constant load is applied to an operating actuator, we

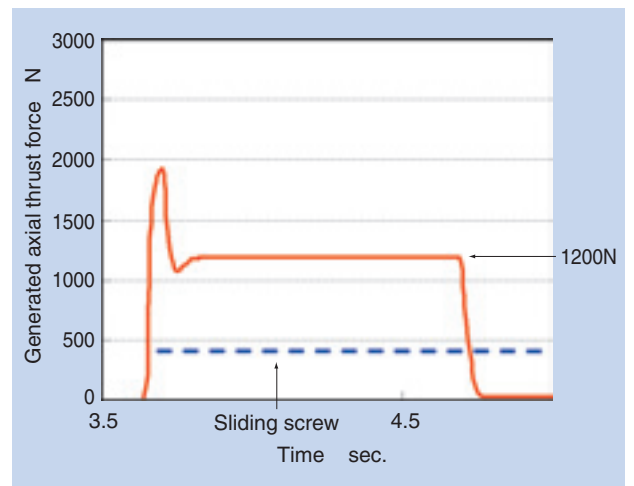


Fig. 8 Thrust force measurement

have fabricated a special durability tester that uses an additional ballscrew responsible for applying a constant load to an actuator sample. Fig. 9 shows a view of this tester. We performed a durability test for a number of loading cycles that is equivalent to the life of a car while applying the maximum expected working load to each actuator sample and, after completion of the durability test, we performed an actuator response test.

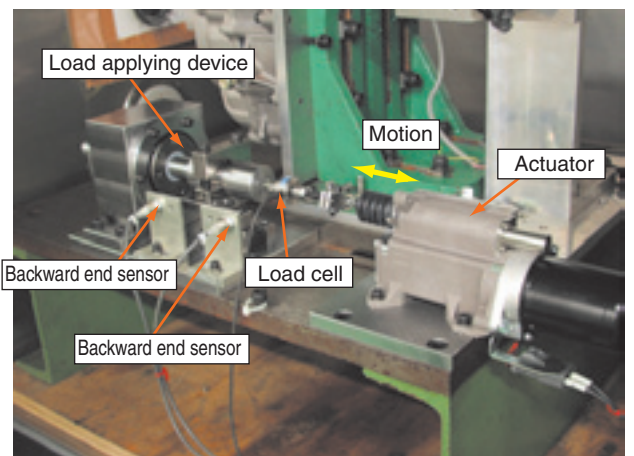


Fig. 9 Appearance of durability test

Fig. 10 shows results of the response test obtained from actuator samples before and after the durability test. Our actuator having undergone a severe durability test still boasts a higher level of response compared with the pre-test level and its post-test response shows no deterioration.

From these findings we have determined that even after having undergone a durability test under severe environmental conditions the performance of our actuator is as good as the pre-tested level.

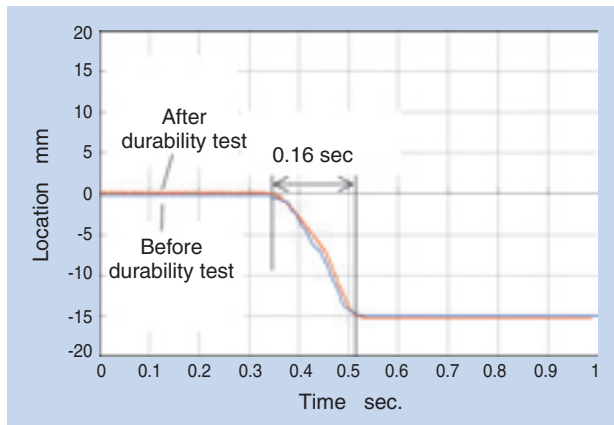


Fig. 10 Example of operating time measurement

4.3 Combined cyclic corrosion test

Our actuator was placed in the combined cyclic corrosion tester and each sample was subjected to repeated environmental cycles. Each cycle consisted of a salt water spray, high-temperature drying, and a high-temperature high-humidity condition to verify corrosion resistance of our actuator under severe environmental conditions.

Fig. 11 shows the appearance of our actuator having undergone the combined cyclic corrosion test. The interior of our actuator having undergone the severe test does not show any problems such as rust or water ingress; the characteristics of the post-test actuator do not show any signs of problem.

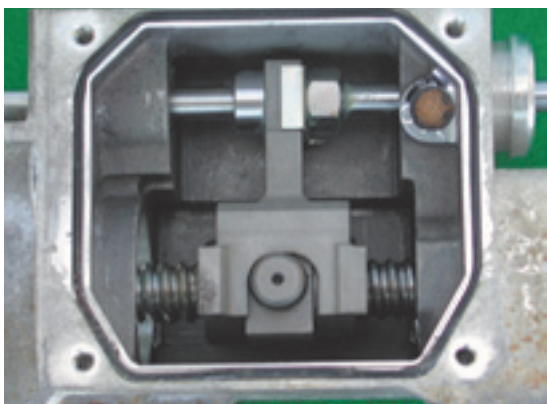


Fig. 11 Internal condition after cyclic corrosion test

5. Conclusion

We have presented information about our unique, automotive electromechanical ballscrew-driven actuator that adopts various mechanical element-related technologies for realizing higher response and greater thrust force.

With electromechanical moving parts increasingly being used in recent automobile designs, more automobile designers have been considering use of ballscrew-driven mechanisms that can be actuated with smaller electric motors. Thus, our ballscrew actuator products will find a greater market share.

To be able to further improve the lighter-weight and enhanced functionality designs for its automotive electromechanical ballscrew actuator products, NTN is committed to improvements in not only elementary parts such as the ballscrew but also auxiliary components such as sensors and electric motors. Through these efforts, NTN will help expand the scope of applications of its ballscrew actuator products.

References

- 1) K. Tateishi and K. Kazuno: Ball-screw for Automated Manual Transmissions, NTN Technical Review No. 73 (2005) 72-75
- 2) K. Kazuno: Ball-screw Unit for Variable Valve Event and Lift Systems, NTN Technical Review No. 75 (2007) 72-77

Photos of authors



Yoshinori IKEDA

Automotive Sales Headquarters
Automotive Engineering Dept.



Hirakazu YOSHIDA

Automotive Sales Headquarters
Automotive Engineering Dept.

Plastic Bearings for Electric Pumps for Next Generation Battery Cells



Norio ITOH*
Takuya ISHII*

In order to reduce CO₂ emissions, devices with next generation battery cells are being introduced or are already on the market. Fuel cell co-generation systems, electric evehicles and hybrid vehicles have electric pumps to circulate cooling water in the cooling systems for the cells and motors. BEAREE AS5704 bearings, which have excellent self-lubricity, chemical resistance and high flexibility in design, are used in these electric pumps. This article introduces the characteristics and applications of BEAREE AS5704 bearings.

1. Preface

To help reduce CO₂ emissions, unconventional apparatuses that do not burn fossil fuels have been increasingly marketed recently, and the need for apparatuses incorporating next generation battery cells has been mounting. The most common applications introducing these novel apparatuses include fuel-cell cogeneration systems in the industrial and home electric appliances fields and electric vehicles and hybrid electric vehicles in the automotive engineering field. Each of the cooling systems that mitigate heat buildup in these apparatuses has a built-in electromechanical pump that circulates cooling water. This article provides information about resin sliding bearings suitable for electromechanical pumps and the typical applications of such bearings are included.

2. Electromechanical pumps for various systems

2.1 Fuel-cell cogeneration system¹⁾

By the electrochemical reaction between hydrogen and oxygen, a fuel-cell generates electricity. The oxygen it uses is derived from air, while the hydrogen it uses is obtained by reforming the air with a reformer: the so-obtained oxygen and hydrogen are introduced

into a fuel-cell stack that generates electricity by electrochemical reaction. Electrochemical reaction taking place in a fuel-cell stack is an exothermic reaction; therefore, the cooling system (which circulates cooling water) that regulates the temperature inside the cell stack to a constant level is driven by an electromechanical pump. The typical requirements for this electromechanical pump are high efficiency and compact size. In order to satisfy these requirements, the electromechanical pump adopted is often a magnet drive-type centrifugal pump.

2.2 Cooling systems on electric vehicles (EV) and hybrid electric vehicles (HEV)

On conventional automobiles driven by internal combustion engines (ICE), a centrifugal pump is used to circulate radiator coolant to cool down the ICE, wherein rotary motion on the engine is input to the pump shaft via a drive belt.

Incidentally, any EV does not have an ICE, and an ICE on HEV is shut down in idling stop mode: therefore, an electromechanical pump is needed to actuate a cooling system for battery cells and/or electric motor. The electromechanical pump used for this purpose is often a magnet drive-type centrifugal pump.

*Engineering Dept. NTN Engineering Plastics Corporation

3. Construction of electromechanical pump

Generally, pumps transport fluids such as water, liquid fuels, lubricating oils, organic solvents, and acidic and alkali liquids. Three major pump operation types are available: centrifugal, volumetric rotary and volumetric reciprocating types, wherein their rotary shafts are supported by bearings. When the fluid transported by a pump is water, or acidic or alkali liquid, an ordinary metal bearing can develop a corrosion problem: to address this issue, carbon sliding bearings and resin sliding bearings may be used²⁾. Resin sliding bearings boast better self-lubricating performance and chemical resistance. In particular, injection-molded components of sliding bearing boast greater freedom of design for factors including shape.

3.1 Magnet drive-type centrifugal pump

Fig. 1 shows a structure of a typical magnet drive-type centrifugal pump. With this structure, the magnets installed onto the motor shaft rotate to cause their magnetic force to rotate the impeller integrated with the magnets in the casing, thereby causing the pump to transport the fluid.

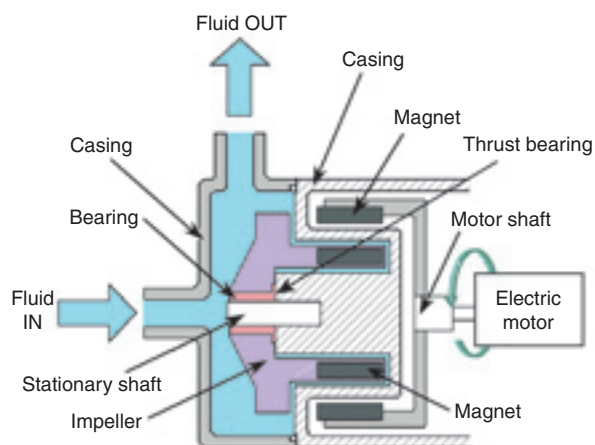


Fig. 1 Structure of magnet drive centrifugal pump

3.2 Resin sliding bearing

Conventional magnet drive type centrifugal pumps often use carbon sliding bearings. A carbon sliding bearing can be molded together with an impeller; however, because this bearing component is obtained only by machining a molded blank, the form factor flexibility of this work piece is limited. Therefore, this bearing type requires improvement in its resistance to impact-induced cracking and reduction of costs. Through an injection molding process, geometrical features can be readily formed on a resin-made sliding bearing, and the examples of such features include

lubricating slots on the bore surface and end face of the bearing and a retaining feature (D-shaped cutout, projection, etc.) on the outer circumference of the bearing to help securely engage the bearing with the impeller (see Fig. 2).

Without undergoing any machining process, a resin-made sliding bearing can be formed together with an integrated impeller.

When a resin sliding bearing runs, a radial load and an axial load act on it, thereby causing sliding contact between the bearing bore and stationary shaft and between the bearing end face and thrust force carrying face. The material used for this resin sliding bearing is NTN BEAREE AS5704.

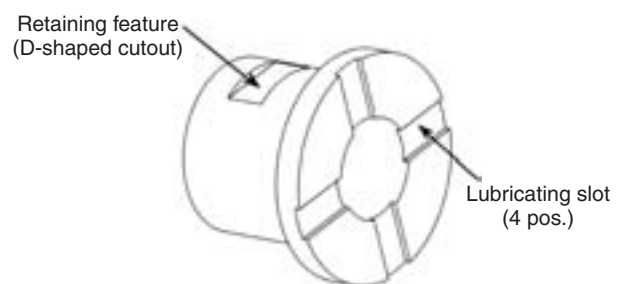


Fig. 2 Bearing

4. BEAREE AS5704 resin bearing

4.1 Features

The BEAREE AS5704 resin sliding bearing consists of PPS (polyphenylene sulfide) blended with a special filler.

<Advantages>

- (1) Compared with a general-purpose PPS resin sliding bearing, wear of our bearing in water is 20% or lower.
- (2) Low wear or abrasion on a mating material such as stainless steel
- (3) BEAREE AS5704 bearing boasts greater freedom of design in shape due to injection molding.
- (4) Can be used even in anti-freeze liquid, or acidic or alkaline liquid

4.2 Basic physical characteristics

Table 1 summarizes the basic physical characteristics of BEAREE AS5704 material.

Table 1 Basic characteristics of BEAREE AS5704

Characteristics	Test method	Unit of measurement	Characteristic value
Specific gravity	ASTM D792	—	1.64
Tensile strength	ASTM D638	MPa	54
Elongation		%	0.7
Bending strength	ASTM D790	MPa	103
Bending elastic modulus		GPa	10
Linear expansion coefficient	TMA method	1/°C	MD : 2.0×10^{-5} CD : 4.5×10^{-5}
Rockwell hardness	ASTM D785	R scale	112
Izod impact strength	ASTM D256 (Notch type)	J/m	27

*The values given above are representative values.

4.3 Comparison of various bearings (resin materials)

Examples of materials of typical resin sliding bearings used in liquid include phenol resins and PTFE (polytetrafluoroethylene) resins. To compare wear resistance characteristics of these materials with those of BEAREE AS5704 and carbon material, we have performed an underwater wear test. **Table 2** summarizes the test conditions applied, and **Fig. 3** shows specific wear^(NOTE) of various bearing materials.

BEAREE AS5704 boasts superior wear resistance and has lower friction compared with the carbon material.

(NOTE) “Specific wear” means a wear volume per unit sliding distance or per unit load calculated from wear before and after the test. Smaller specific wear means smaller wear.

Table 2 Wear test condition

Characteristics	Content
Test equipment	Underwater ring on disk type
Bearing pressure	0.4 MPa
Sliding velocity	25 m/min (Hv200, 0.4 μmRa)
Mating material	SUS304
Environment	Water (normal temperature, no temperature control)
Test time	50h

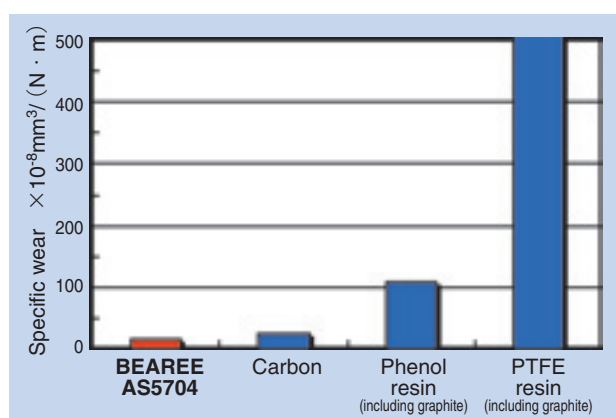


Fig. 3 Specific wear of various bearings

Table 3 provides a comparison of performance of sliding bearings made of these materials. Using PPS resin as a base material, the BEAREE AS5704 bearing excels in chemical resistance and dimensional stability after having absorbed water.

Table 3 Comparison of features various bearings

Bearing type	BEAREE AS5704	Carbon	Phenol resin (including graphite)	PTFE resin (including graphite)
Process used	Injection molding	Machining	Injection compression molding	Machining
Wear resistance (underwater)	◎	○	△	×
Chemical resistance	◎	◎	△	◎
Dimensional stability of material having absorbed water	○	×	△	○
Resistance to cracking due to impact	○	×	×	○
Resistance to deformation due to impact	○	○	○	×
Degree of Freedom of design	◎	×	○	×
Price	◎	×	○	×

◎ : Excellent ○ : Good △ : Acceptable × : Not acceptable

4.4 Comparison to PPS resin bearing

Under the test conditions summarized in **Table 2**, comparison test for friction wear characteristics has been performed for BEAREE AS5704 and three PPS-resin based bearing materials (PPS + fiber glass, PPS + carbon fiber, and PPS + PTFE). **Fig. 4** shows the time-dependent variation in dynamic friction coefficients of these materials, and **Fig. 5** provides the specific wear of these materials.

BEAREE AS5704 boasts the lowest dynamic friction coefficient, and the value of this coefficient remains stable. Furthermore, the specific wear of BEAREE AS5704 is less than 20% of the PPS resin blended with carbon fiber coefficient. The wear depth on the mating material (SUS 304) that underwent the test has been measured. As a result, the wear depth on the mating material tested with the PPS resin blended with carbon fiber was approximately 5 μm. In contrast, the mating material tested with BEAREE AS5704 did not develop any wear (**Figs. 6 and 7**).

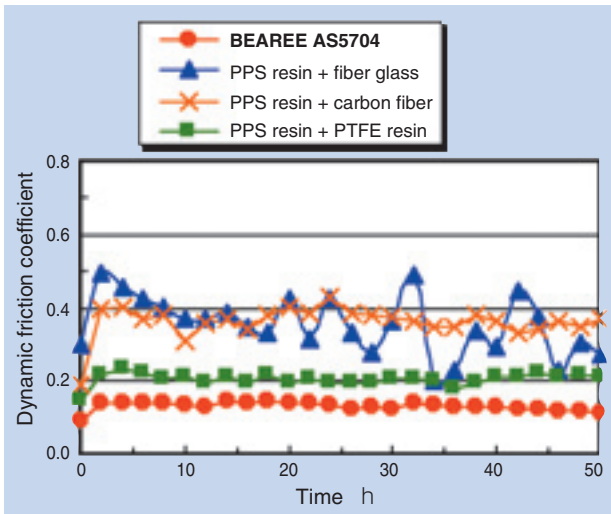


Fig. 4 Coefficient of dynamic friction of PPS bearings

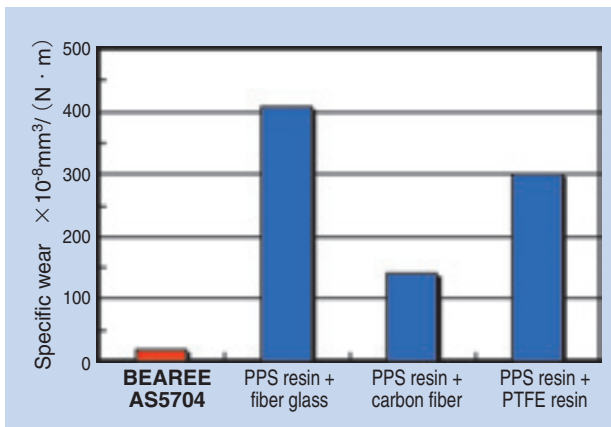


Fig. 5 Specific wear of PPS bearings

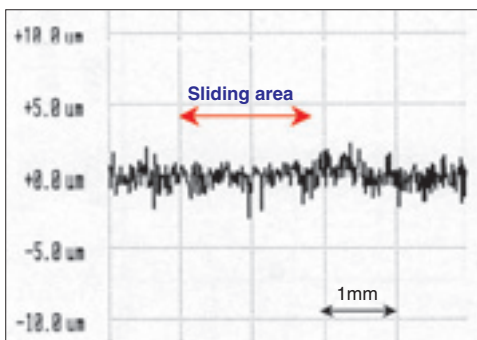


Fig. 6 Surface roughness of mating material after test

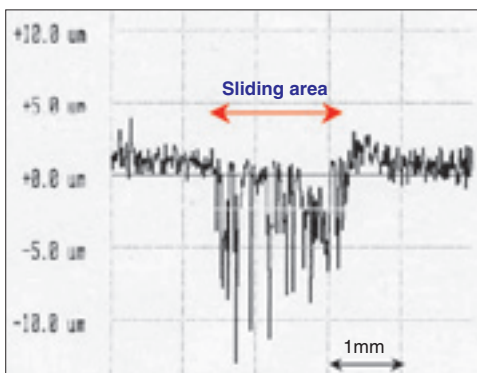


Fig. 7 Surface roughness of mating material after test

4.5 Limiting PV value of BEAREE AS5704

Two sets of velocity conditions summarized in Table 4 were tested. Under each set of conditions, the bearing pressure was increased by 1 MPa per hour. The limiting bearing pressure was recorded as the pressure at which the wear exceeded 20 μm or the sliding surface melted. Table 5 summarizes limiting PV values calculated from the test velocity and limiting bearing pressure.

Table 4 Limit PV test condition

Characteristics	Content
Test equipment	Underwater high-speed ring on disk type
Sliding velocity	100, 300 m/min
Mating material	SUS304 (Hv200, 0.4 μmRa)
Environment	Antifreeze (normal temperature, no temperature control)

Table 5 Limiting PV value

Sliding velocity (V)	Limiting bearing pressure (P)	Limiting PV value
100m/min	7 MPa	700 MPa · m/min
300m/min	3 MPa	900 MPa · m/min

4.6 Wear curve of BEAREE AS5704

Under the test conditions summarized in Table 6, the time-dependent wear on BEAREE AS 5704 specimen were measured; then the wear curve in Fig. 8 was plotted. This plot shows an initial wear phase beginning at the start of test and ending at 50 operating hours. After that point, the wear curve exhibits steady wear state and shows virtually no increase in the wear.

Table 6 Wear test condition

Characteristics	Content
Test equipment	Underwater high-speed ring on disk type
Bearing pressure	1.15 MPa
Sliding velocity	170 m/min
Mating material	SUS304 (Hv200, 0.4 μmRa)
Environment	Antifreeze (normal temperature, no temperature control)
Test time	500h

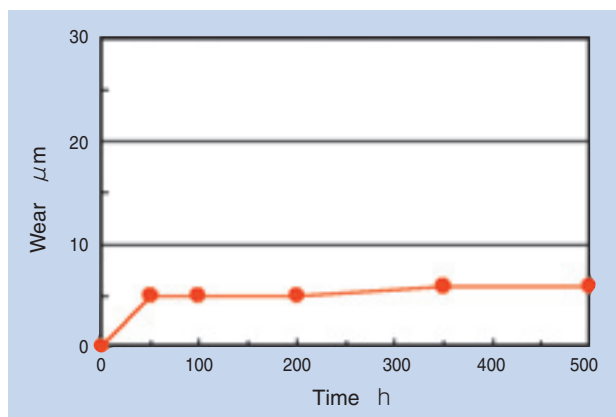


Fig. 8 Wear curve

5. Considerations about use of resin sliding bearings

When setting up the clearance between a resin sliding bearing and a mating shaft, it is necessary to consider the linear expansion coefficient of the resin material. Generally, linear expansion coefficients of resin materials are greater than those of metal materials. For example, in a case where the material of an impeller integrated with a bearing is a metal, or there is a temperature gradient across the bearing and the impeller, resulting in heat generation at the sliding area, the bearing expands toward its bore side. In this case, incorrect bearing clearance design can lead to elimination of bearing clearance to the mating shaft, and this in turn can lead to abnormally severe wear on the bearing and mating shaft³⁾.

6. Special materials for difficult applications

Electromechanical pumps have been used in various industrial fields and environments. In addition to BEAREE AS5704, NTN offers the BEAREE FL3700 and FL3642 lines of products made from PTFE resin as base material for difficult applications (Table 7).

Table 7 Bearings under special condition

Bearing	Base material	Advantages
BEAREE FL3700	PTFE resin	Chemical resistance
BEAREE FL3642	PTFE resin	Non-black color: may be used in contact with food or drinking water.

Because its base material and filler are highly resistant to chemicals, FL3700 remains impervious to virtually all chemicals, and therefore is used in chemical pumps.

For food machinery applications, the bearing resin material must not be black in color. Therefore, FL3642, which is pale yellow, is adopted⁴⁾.

7. Afterword

EVs and EHVVs will be more commonly used in the future. Consequently, demand for electromechanical pumps used on these vehicles will further expand. These electromechanical pumps need to be more efficient, have longer service life and feature much more compact size. Therefore, performance of resin sliding bearings for these pumps need to be further improved. To address these challenges, we are going to continue our research and development efforts for our resin sliding bearings so that we can further improve the sliding mechanism with our bearing products to improve their functionality. We believe that demands for resin sliding bearings will further increase in applications that require low friction and low wear characteristics. We hope this report may help deliver useful information to people involved in this engineering field.

References

- 1) O. Tajima: Development Status of Proton Exchange Membrane Fuel Cells (PEFC) 2, Denki (2004) 35 (Japanese)
- 2) T. Hayashi: Machine Parts and Elements, Japan Plastics Vol. 57, No. 4 (2006) 50 (Japanese)
- 3) NTN Corporation Editing Team: Understanding Bearings (2007) 154
- 4) Oki and T. Ishii: Tribological Properties of PTFE Composite Materials in Water, Monthly Tribology Vol. 13, No. 12 (1999) 48 (Japanese)

Photos of authors



Norio ITOH

Engineering dept.
NTN Engineering Plastics Co.,Ltd



Takuya ISHII

Engineering dept.
NTN Engineering Plastics Co.,Ltd

Low-torque Roller Lifter Unit



Masashi NISHIMURA*

The demand for improved fuel consumption and exhaust emissions control in cars has increased on a global basis in recent years. Automobile companies are working to develop gasoline direct-injection engines as one means to achieve new fuel efficiency targets. Other demands include increasing the fuel pressure and reducing the friction in the fuel compression process in the high-pressure fuel pumps used for direct-injection engines. NTN has developed a low-torque roller lifter unit that responds to these demands. This report introduces the features of this NTN low-torque roller lifter unit.

1. Introduction

EU has decided to enact in 2012 its CO₂ emissions regulation according to average CO₂ emission per passenger car of 130 g/km or lower, which means 20% reduction relative to the present emissions level. Also, USA has established targets for improved fuel economy which include average 40% improvement in fuel economy by fiscal year 2020 in terms of the amount of gasoline consumed by passenger cars or compact trucks¹⁾. Thus, NTN believes that the need for more fuel-efficient cars will increase and more stringent emissions standards will be introduced.

In Japan, a new fuel economy standard (see **Table 1**) has been legislated whose deadline is set at fiscal year 2015: accordingly, the fuel economy of passenger cars in Japan in FY2015 will be 23.5%

Table 1 2015 year fuel-efficient target
(Improvement rate compare with 2004)²⁾

Car type	Actual value for FY2004	Estimated value for FY2015	Improvement in fuel economy over FY2004 level
Passenger car	13.6(km/ℓ)	16.8(km/ℓ)	23.5%
Compact bus	8.3(km/ℓ)	8.9(km/ℓ)	7.2%
Compact truck	13.5(km/ℓ)	15.2(km/ℓ)	12.6%

better compared with the FY2004 level²⁾.

To address this situation, automakers have been committed to development of hybrid electric vehicles and electric vehicles; as well as fuel economy improvement through techniques including variable valve system and idling stop. Direct-injection gasoline engine also appears to be a particularly promising means.

Direct-injection engines are characterized by the fact that air alone is drawn into cylinders and compressed. Fuel is compressed by a fuel pump is directly injected into the cylinders where the fuel is fired. In contrast with conventional engines that draw air-fuel mixture generated in an intake pipe into the cylinders (port injection), direct-injection engines are said to develop better fuel economy owing to operation of the following reasons^{3), 4)}.

- (1) Improved anti-knock properties to allow for a higher compression ratio (greater engine power).
- (2) Accurate control of the air/fuel ratio
- (3) Reduced pumping loss at a lower load range

*Needle Roller Bearing Engineering Dept. Automotive Sales Headquarters

2. Peripheral structure around direct-injection engine and typical applications of roller lifter unit

Fig. 1 shows an appearance of a roller lifter unit while Fig. 2 illustrates a structure around a fuel pump on a direct injection engine. Fig. 3 provides a view of typical application of a roller lifter unit.

In combination with a cam, a roller lifter unit situated in a fuel pump drive on a direct injection engine transmits rotary motion of the engine shaft to a reciprocating plunger.

Previously, most commonly used roller lifter units had a sliding surface in contact with a cam. Now, certain automakers are adopting rolling type roller lifter units in order to reduce friction loss from contact with a cam and to allow a cam to be able to run at a higher speed.

Usually, on a direct injection engine, the fuel is injected with a pressure of 4 to 13 MPa. On certain direct injection engines, the injection pressure is as

high as 20 MPa⁵⁾ in order to improve combustion efficiency. It appears that much higher injection pressure will be increasingly adopted.

A higher fuel injection pressure means a greater load exerted onto the lifter. A conventional lifter, in particular, whose contact surface to the cam is a sliding surface can experience deterioration in fuel economy owing to greater friction with the cam.

At the same time, to be able to adopt higher fuel pressure, it will be necessary to increase a number of cam-operated compression cycles (increased cam cyclic rate and increased number of high points on cam) as well as a cam lift. To cope with these changes, the outer circumference length of cam needs to be longer if the base circle dimension of cam remains unchanged. Consequently, the bearing used in this type of application needs to be capable of higher running speeds.



Fig. 1 Appearance of roller lifter unit

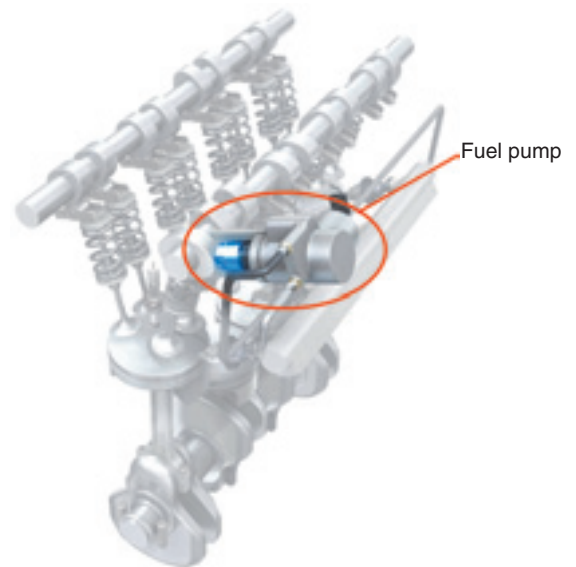


Fig. 2 Direct injection engine, fuel pump

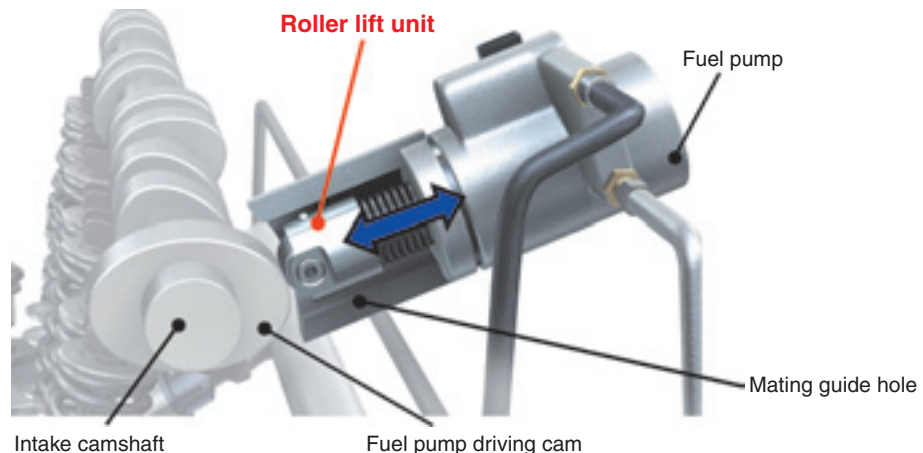


Fig. 3 Application of roller lifter unit

3. Structure and advantages of NTN Low Torque Roller Lift Unit

As mentioned above, more common roller lifter units previously used have sliding contact surface that is in contact with a cam: certain automakers are using roller lifter units incorporating rolling bearings in order to mitigate friction loss. The rolling bearings used for this purpose are full complement roller bearings because of their excellent load bearing performance and longer life*1. However, full complement roller bearings can pose problems such as heat buildup and increased running torque. Intermittent loading by the cam as well as inclination occurring from the gap between the roller lifter unit and mating guide hole will lead to skew on the rollers. This skew will cause the bearing to develop lateral runout, which triggers the above-mentioned problems.

In order to mitigate lateral runout on the bearing for roller lifter unit, NTN has adopted a caged roller bearing to inhibit skew occurrence on the rollers, reduce running torque on the bearing, and improve high-speed durability of the roller lifter unit. Also, NTN has adopted FA treatment which is NTN's propriety heat treatment technique to improve bearing life, thereby NTN has achieved a calculated bearing life that is equivalent to or better than that of full

complement roller type bearing.

Furthermore, NTN has optimized wall thicknesses of various areas of the casing of its roller lifter unit so that the casing features lighter weight while maintaining necessary mechanical strength. Thus, NTN has reduced the inertial force occurring on its roller lifter unit in reciprocating motion so that its roller lifter unit can more accurately follow the motion of cam running at higher speed.

Fig. 4 shows the specification for NTN low-torque roller lifter unit.

4. Evaluation by performance

Higher fuel temperature means a greater load applied to the lifter. In particular, on conventional lifters whose contact surface to the cam is a sliding surface. The friction on the contact surface will be greater and can cause deterioration in fuel economy. Furthermore, to help achieve higher fuel pressure, the lifter needs to be more durable at higher speed.

In order to evaluate the performance of our roller lifter unit, NTN measured torques and temperature increases on the bearing. The section below presents some portion of information about our tests for evaluating our roller lifter unit.

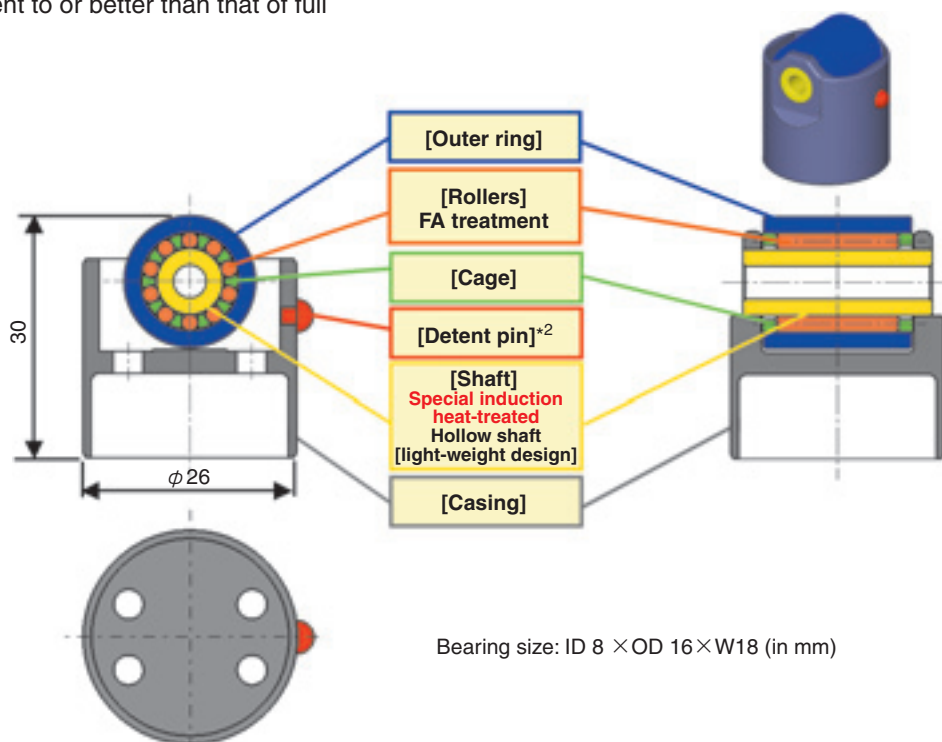


Fig. 4 Specification of NTN low-torque roller lifter unit

*1: "Full complement roller bearing" means a roller bearing type not having a cage. Though this bearing type boasts greater load rating because of a greater number of rollers for a given bearing size, but can develop problems such as skew proneness of rollers because the rollers are not guided by a cage.

*2: The detent pin slides in the groove formed in the mating guide hole to prevent the roller lifter from rotating in the circumferential direction on the casing.

4.1 Torque measuring operation

NTN measured torques on bearings in lifter units to determine the reduction of friction loss using NTN low torque caged roller lifter compared to conventional sliding type lifters and full complement roller type lifter units.

4.1.1 Torque measuring conditions

Table 2 summarizes the conditions for our torque measuring test and Fig. 5 schematically illustrates the test rig used.

Table 2 Rotational torque measurement conditions

Test equipment	Torque tester (outer ring rotation tester complete with a torque meter)
Samples being tested	<ul style="list-style-type: none"> Rolling bearing (caged type) Size: ID 8×OD 16×W18 (in mm) Rolling bearing (full complement roller type) Size: ID 7.67×OD 16×W16 (in mm) Sliding type lifter Size: D 30×H 25 (in mm)*3
Loading conditions	500 N, 1,000 N (Measurement was performed with starting torque set at 500 N.)
Bearing speed*4	1000min ⁻¹ , 3000min ⁻¹ , 6000min ⁻¹ , 9000min ⁻¹ The starting torque at start-up phase, where acceleration from 0 to 3,000 min ⁻¹ takes place, was measured (with outer ring rotated*5).
Lubrication	Lubricating oil: engine oil with dynamic viscosity of 0W-20 Lubricating temperature: ordinary temperature Lubricating system: splash lubrication (oil level: centerline of drive roll)

*3 Because the contact surface of sliding type lifter in contact with the cam is a flat face of cylindrical tappet, the diameter and height of the tappet are given here.

*4 Means running speed of outer ring of rolling bearings (caged type, full complement roller type). Measurement on sliding type lifter was taken while allowing the drive roll to run at a running speed equivalent to that for measuring bearing speed of rolling bearing.

*5 A test method where the drive roll is brought into contact with the outer circumference of outer ring to allow the outer ring to turn in response to the rotary motion of the drive roll. (The outer ring is allowed to rotate on the roller lifter unit installed on an actual automotive fuel pump.)

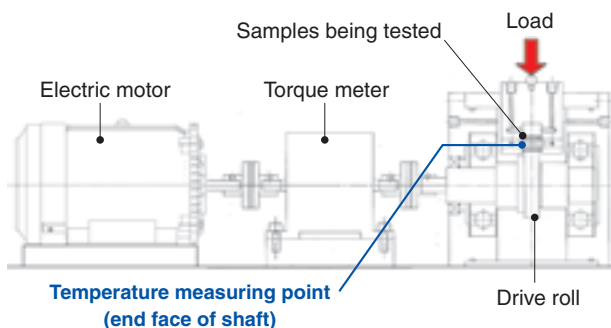


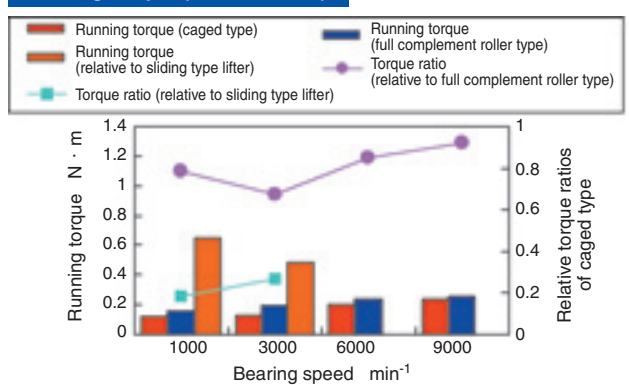
Fig. 5 Diagrammatic illustration of test machine

4.1.2 Result of torque measurement

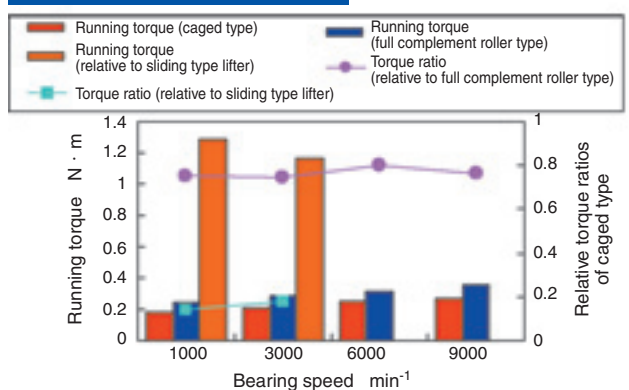
Fig. 6 Graphically plots the resultant torque measurements.

From Fig. 6, our findings are apparent; in comparison with a sliding type lifter, NTN's standard torque roller lifter unit (caged type) boasts an 85% reduction in starting torque and 73 to 86% reduction in running torque. Also, in comparison with a full complement roller type, NTN's standard torque roller lifter unit exhibits 8 to 29% torque reductions in various measuring conditions.

Running torque (at load 500 N)



Running torque (at load 1000 N)



Running torque

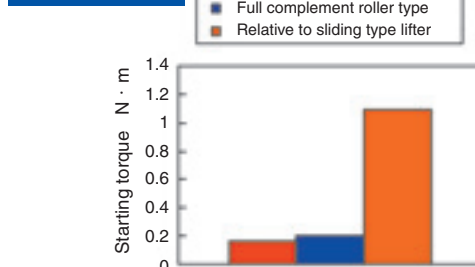


Fig. 6 Result of rotational torque measurement

4.2 Temperature-rise test

Temperature rise tests for bearings on roller lifter units have been performed to verify the excellent high speed durability of NTN's caged low torque unit compared to complement roller type lifter units.

4.2.1 Temperature-rise test conditions

Table 3 summarizes the test conditions adopted.

Table 3 Temperature-rise test condition

Tester	Outer ring rotation tester (See Fig. 5.)
Samples being tested	<ul style="list-style-type: none"> Rolling bearing (caged type) Size: ID 8×OD 16×W18 (in mm) Rolling bearing (full complement roller type) Size: ID 7.67×OD 16×W16 (in mm)
Loading conditions	<i>P/C</i> =0.22 *Relative to rolling bearing (caged type)
Bearing speed	Eight incremental steps: 4,500, 9,000, 13,500, 18,000, 22,500, 27,000, 31,500 and 36,000 min ⁻¹ (with outer ring rotated)
Lubrication	Lubricating oil: engine oil with dynamic viscosity of 0W-20 Lubricating temperature: ordinary temperature, lubricating oil flow rate: 150 ml/min Lubricating system: circulating lubrication

4.2.2 Results of temperature-rise test

Fig. 7 graphically plots comparison of temperature rise on the samples tested and Fig. 8 shows a view of seizure on a rolling bearing (full complement roller type) having undergone the test.

The full complement roller type has developed seizure as a result of lateral runout of its bearing at 18,000min⁻¹. In contrast, the NTN's standard low torque roller lifter unit (caged type) has not developed seizure up to 36,000 min⁻¹. Thus, we have verified that the high speed durability, in terms of maximum allowable running speed, of the caged type is more than twice as much as that of the full complement roller type.

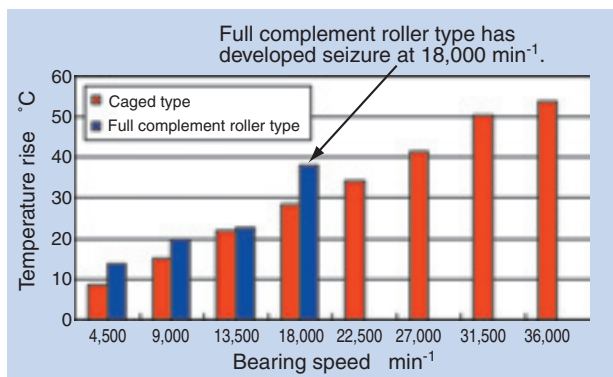


Fig. 7 Comparison of temperature-rise (Full complement roller type)



Fig. 8 Appearance of test sample (Full complement roller type)

4.3 Bearing life test

The bearing of the NTN's low torque roller lifter unit is a caged type. Accordingly, the number of rollers in this type is unavoidably smaller compared with the full complement roller type causing its load bearing capacity to be lower and expected service life is to be shorter. In order to address a problem of shorter bearing life on the NTN's low torque roller lifter unit, NTN is subjecting the rollers to our unique FA treatment and the shaft to special induction heating treatment as previously described in Sec. 3. NTN has performed a life test on the bearing section in question in order to verify the effectiveness of these life extending measures.

4.3.1 Test conditions for bearing life test

Table 4 summarizes the test conditions applied for the life test.

Table 4 Life test conditions

Test equipment	Outer ring rotation tester (See Fig. 5.)
Samples being tested	<ul style="list-style-type: none"> Rolling bearing (caged type) Size: ID 8×OD 16×W18 (in mm)
Loading conditions	<i>P/C</i> =0.22
Bearing speed	28000min ⁻¹ (with outer ring rotated)
Lubrication	Lubricating oil: engine oil with dynamic viscosity of 0W-20 Lubricating temperature: ordinary temperature, lubricating oil flow rate: 150 ml/min Lubricating system: circulating lubrication
Calculated life per JIS	97h (Information) Calculated life for full complement roller type is 203 hours.

4.3.2 Result of bearing life test

Fig. 9 shows graphical plotting of the result of our bearing life test.

NTN has subjected the rollers to FA treatment and the shaft to a unique induction heat treatment process. The results have verified that the standard rating life of our bearing stands at 1,370 hours, which is 14 times as long as a life value calculated according to a JIS method (97 hours).

When assuming that the average engine speed is $3,000 \text{ min}^{-1}$ (equivalent to average running speed of $7,500 \text{ min}^{-1}$ at the bearing of roller lifter unit^{*6}), the average load acting on the bearing is $1,000 \text{ N}$ ^{*7}, and the above-mentioned life value calculated per a JIS standard is multiplied by 14, then the resultant bearing life for our roller lifter unit stands at 5×10^4 hours and this life coincides with a life of 27 years^{*8}. Assuming that the useful life of an average passenger car is 15 years, the NTN's bearing well satisfies this useful life requirement.

*6 Assumptions: This speed is equivalent to cam running speed of $1,500 \text{ min}^{-1}$, and the cam outside circumference length is five times as long as the bearing outside circumference length.

*7 Assumptions: The fuel pressure is set at 13 MPa, and the pump plunger diameter measures 10 mm.

*8 Assumption: The average daily use time for an average passenger car is 5 hours.

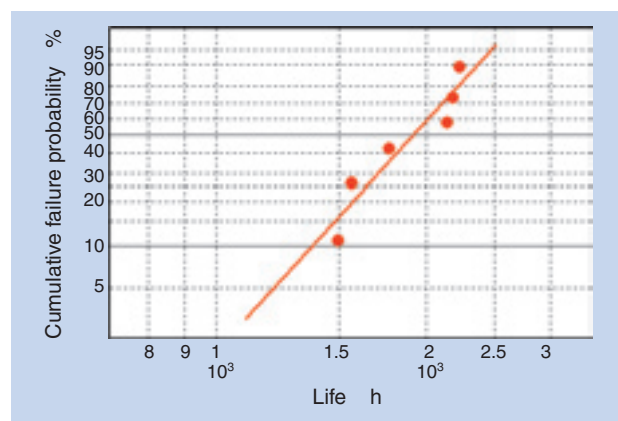


Fig. 9 Life test result

Photo of author



Masashi NISHIMURA

Needle Roller Bearing
Engineering Dept.
Automotive Sales Headquarters

5. Conclusion

This paper has presented information about NTN's low torque roller lifter unit and associated technology.

The size of market will further expand for direct injection engines as one of potential measures for improving fuel economy for automobiles. To address this trend, NTN will further market its low torque roller lifter products as well as enhance their functionality.

References

- 1) Website of Japan Automobile Manufacturers Association, Inc. (JAMA)
- 2) Website of Ministry of Land, Infrastructure, Transport and Tourism
- 3) H. Ando: Technical Prospects of Gasoline Direct Injection Engines, Engine Technology Review Vol. 1, No. 1 April 2009, 18-23
- 4) T. Sena and Y. Katsuragi, Introduction to Engine Science, first edition, Grand Prix Publishing, (1997) 173–183 (Japanese)
- 5) Direct Injection, Car Mechanism Encyclopedia Engine Volume, August 2009 special issue 111–115 (Japanese)

Hub Bearings for Automobiles that Conserve Resources

Isao HIRAI*



Automotive parts are being expected to respond to environmental issues such as global warming and to effectively use natural resources. This article introduces our hub bearings for automobiles that conserve resources in order to meet these demands. They are designed to be lighter than conventional products and to reduce the amounts of materials used in order to improve the yield from the materials during processing.

1. Preface

One of the leading environmental issues today is global warming. To help in the prevention of global warming it is necessary to reduce the emissions of green house gases - in particular, CO₂. Therefore, in the auto industry around the world there is an ever increasing need for light-weight, low friction designs that will lead to lower energy consumption on cars during travel as well as a reduction in the amount of materials consumed during car manufacturing.

Believing that coexistence with the global environment is its most urgent challenge, NTN has long been committed to efforts for designing lighter, lower-friction car components. We have developed a unique hub bearing, which is one of the underbody car components. In this paper we are going to present information about this novel "resource-saving automotive hub bearing design" that features a reduction in the amount of materials consumed in production while boasting functions and characteristics equivalent to or better than those of conventional hub bearing products.

2. Structure and features

In developing our "resource-saving automotive hub bearing design", we have adopted the Gen3 hub bearing for non-driven wheels (rear wheels on front drive vehicles) as a model case. In this development work we have attempted to meet the following targets:

- **Compatibility with conventional designs in terms of mounting dimensions**
- **10% or more weight reduction compared with conventional designs**
- **At least 20% reduction in the materials used for the hub and outer rings whose masses account for a large portion of the bearing product**
- **Functions including rolling fatigue life, mechanical strength and rigidity of our novel hub bearing design are equivalent to or better than those of conventional designs, even though our hub bearing design does not adopt special materials and/or heat treatment technique.**
- **Production cost equivalent to that of conventional designs**

To fulfill these targets, we have improved forging techniques in the manufacturing aspect, and fully utilized structural analysis techniques including FEM in the design aspect. We have optimized the bearing shape so that the amount of material scrapped in the forging process and the amount of material removed in the machining process are minimized, while still

*Axle Unit Engineering Dept. Automotive Sales Headquarters

maintaining functionality of the hub bearing. Thus, we have achieved a light weight hub bearing product as well as a reduction in the amount of materials consumed in production.

2.1 Hub flange

Fig. 1 shows a typical example of the structure of a Gen3 hub bearing for a non-driven wheel. The hub ring as a rotary body has a hub flange that functions as a mount for installing the wheel and brake disk. The most commonly used hub flanges are disk type hub flanges such as a one shown in **Fig. 2**. Light-weight hub flange products are available; examples of which include a hub flange having lightening holes as shown in **Fig. 3** and a cross shaped hub flange (non-common shape) shown in **Fig. 4**.

A hub ring is prepared by obtaining a work blank from a round steel bar and then subjecting the blank to forging, turning, heat treatment and grinding processes. The ratio of the mass of the steel blank work loaded into the forging process to the mass of the finished hub ring is known as “material yield”.

The lightening holes shown in **Fig. 3** are formed by punching during the forging process. Despite its lightening effect, this technique leads to deteriorated material yield. When a cross shaped hub flange is manufactured, a work blank is first forged into a shape

somewhat larger than the flange design, and then the work piece is punched to the final flange shape, and this technique also leads to deteriorated material yield.

In order to achieve not only improved material yield but also a lighter hub ring, we have developed a hub bearing shape shown in **Fig. 5**. In finalizing this shape, we have adopted an FEM analysis technique to optimize the mechanical strength and forgeability of the hub flange. More specifically, concaves of a larger radius are included in the outer circumference of the hub flange so that the convexes on the outer circumference are readily formed during the forging process and the number of portions which can later develop intermittent cutting during the turning process (which means deteriorated workability).

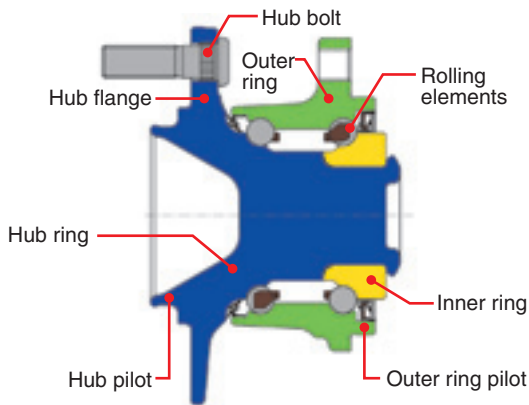


Fig. 1 Structure of Gen3 hub bearing for non-driven wheel

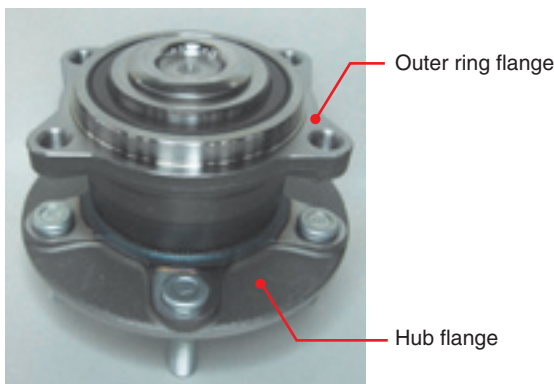


Fig. 2 Round shaped hub flange

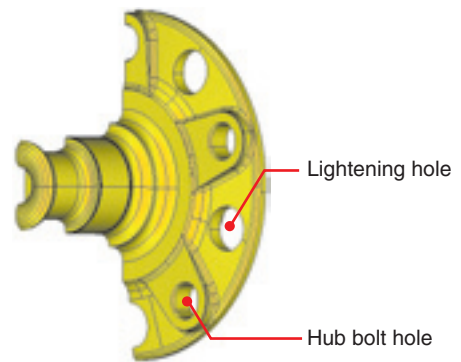


Fig. 3 Lighter holes in hub flange

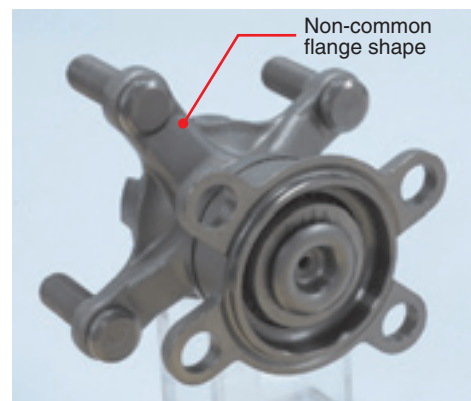


Fig. 4 Cross shaped hub flange

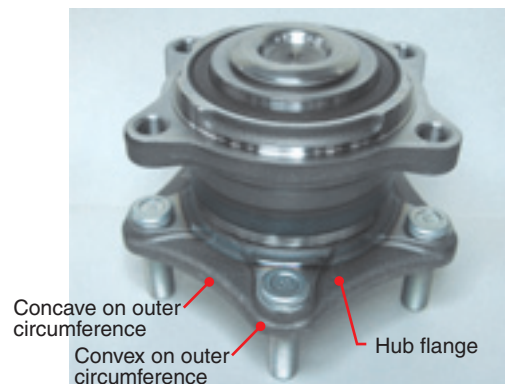


Fig. 5 Shape of developed hub bearing

2.2 Hub pilot

The hub ring is provided with a hub pilot that serves as a guide for the wheel and brake disk installation on the hub. Previously, the outer circumference of the hub was machined to generate a hub pilot in the form of a cylindrical-sectioned belt as shown in Fig. 6, and the mass removed by the machining process was scrapped as chips.

In the case of our newly developed hub bearing, to achieve lightening as well as reduce the portion removed by machining, the previous pilot (cylindrical-sectioned belt) has been superseded with an intermittent hub pilot shown in Fig. 7 that consists of a plurality of teeth formed by forging.

An intermittent pilot shape can contribute to lightening as well as improved material yield owing to a reduction in surface being machined. However, this feature necessitates intermittent cutting, which leads to shorter tool life. At the same time, because this pilot shape involves an increased number of edges on the work piece, a chamfering process is needed to remove burrs.

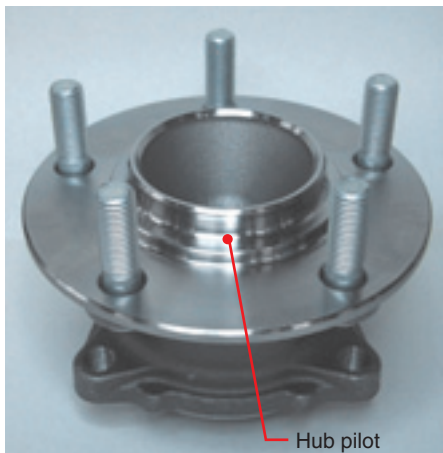


Fig. 6 Example of conventional shaped hub pilot

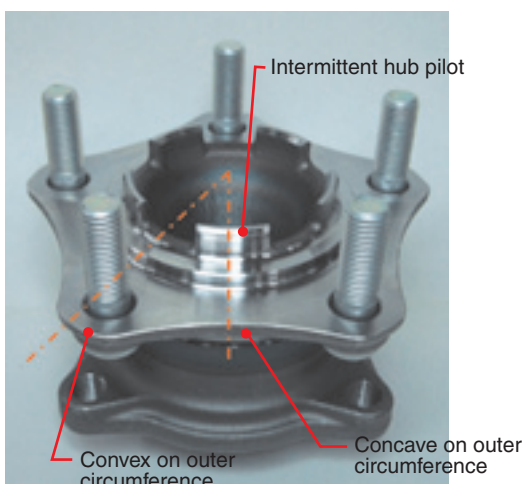


Fig. 7 Discontinuous shaped hub pilot

To address this problem, ramps are formed during the forging process at both ends on each pilot tooth along the circumferential direction as shown in Fig. 8. This arrangement helps not only mitigate the impact that occurs when the cutting tool comes into contact with the pilot teeth but also inhibits the occurrence of burrs, thereby extending the life of the cutting tool and decreasing the number of machining steps. Furthermore, as can be understood from Fig. 7, the pilot is situated in a location whose phase is the same as that of a concave on the outer circumference of our hub flange; consequently, the difference in cross-sectional area between a convex and a concave on the outer circumference of our hub flange is minimized and forgeability of the hub flange is improved.

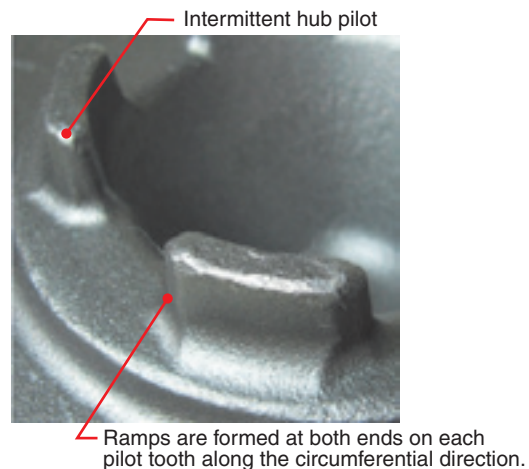


Fig. 8 Measure for intermittent cutting of hub pilot

2.3 Outer ring pilot

When a hub bearing is installed to the car body (suspension), the outer ring of the hub bearing offers a mounting point to the car body. The outer ring has a ring pilot that serves as a guide.

We have again chosen an intermittent configuration for the outer ring pilot on our hub bearing in order to reduce the area being machined and realize a lighter outer ring design. However, unlike the hub pilot, the inner bore of the outer ring pilot is fitted with a seal that prevents ingress of water and dust into the hub bearing. Therefore, as can be understood from the views given in Fig. 9, the inner edge of the outer ring pilot is continuous while the outer edge features a discontinuous form.

Incidentally, we have adopted a continuous machined surface around the flange of outer ring pilot in order to improve accuracy for installing the hub bearing and prevent corrosion of the flange surface due to the ingress of muddy water. Like in the case of the hub pilot, areas subject to intermittent cutting on

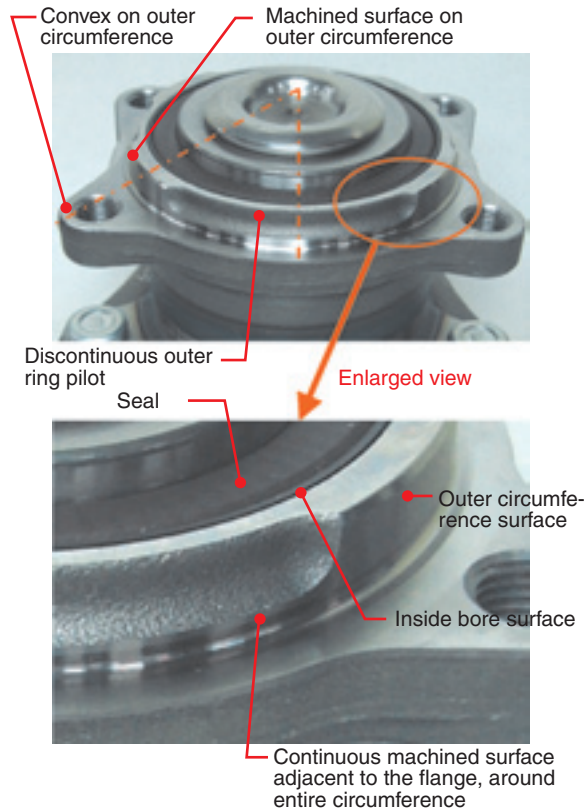


Fig. 9 Shape of outer ring pilot

the outer ring pilot have outward inclined ramps formed by forging in order to help extend the useful life of the cutting tool used.

As can be understood from Fig. 9, the portions being machined on the outer circumference of the outer ring pilot are situated in the same phases as those of the convexes on the outer circumference on the hub flange. This arrangement is intended to promote ease of installation of the hub bearing to the car body and improve mechanical strength and rigidity of the installation. Because projection of the outer ring flange is small, we can give priority to this objective rather than improvement in its forgeability as described in Sec. 2.2.

2.4 Lightening and reduced material consumption

As a result of the reduction in material consumption and improved material yield, our new design has achieved the following improvements over conventional designs: approximately 10% weight reduction of the hub bearing, approximately 20% reduction in material consumption with the hub ring and outer ring, and approximately 30% reduction in the total amount of material scrapped as a result of machining for the hub ring and outer ring.

3. Evaluation test

We first performed the theoretical review by FEM analysis technique of our novel “resource-saving automotive hub bearing design” that reflects the previously mentioned lightening technique and material consumption reduction technique. Then, we have subjected the prototype to a bench test looking at five characteristics, whereby we can verify that our new design is equivalent to the conventional design in terms of functionality:

- (1) Bearing rolling fatigue life: life (durability) test for bearing subjected to turning load on the car
- (2) Fatigue strength of hub flange: fatigue strength test
- (3) Rigidity of hub bearing: rigidity measurement
- (4) Mechanical strength of hub bearing: static strength test
- (5) Rotational balance of non-common shape flange: unbalance measurement

3.1 Bearing life (durability) test for bearing subjected to turning load on the car

The findings from the bearing life test are given in Table 1. The measured rolling fatigue life of our new design is more than six times as long as the targeted rating life. Thus, it has been proven that our new bearing design has sufficient durability.

Table 1 Results of durability test with curving moment

Subject of evaluation	Result
Conventional design	At least six times as long as rating life

3.2 Fatigue strength test

As summarized in Table 2, the samples have been run for a number of revolutions in excess of a target number. Though having undergone a test whose run time was longer than that of a conventional hub flange design, our newly developed hub flange has not developed any fractures, thereby we have determined that our new design has sufficiently high fatigue strength.

Table 2 Results of fatigue strength test

Subject of evaluation	Result
New design	Number of revolutions at least 1.9 times as many as the targeted value No fracture on flange
Conventional design	Number of revolutions at least 1.7 times as many as the targeted value No fracture on flange

3.3 Rigidity measurement

Table 3 summarizes the results of the rigidity measurement. The rigidity of our newly developed hub flange is virtually equivalent to that of a conventional design.

Table 3 Measurement of stiffness with curving moment

Subject of evaluation	Rigidity of tilted hub flange kN/°
New design	21
Conventional design	22

3.4 Static strength test

The mechanical strength required for our bearing in the static strength test is that the bearing does not develop a fracture when subjected to a lateral G load of 2.0 in the vehicle turning mode (side collision situation where the wheel has hit a curb). As can be understood from the information given in **Table 4**, our new bearing design satisfies the load requirement and has mechanical strength equivalent to that of conventional bearing designs.

Table 4 Result of static strength test

Subject of evaluation	Lateral G in turning mode equivalent to fracture load
New design	2.4
Conventional design	2.4

3.5 Unbalance measurement

To be able to determine the magnitude of effects of a non-common hub flange shape on the rotational balance of the hub ring, the unbalance of the hub ring needs to be measured. The resultant unbalance of this design is better than G16 per JIS B 0905 and this level well satisfies G40, which is the level recommended by the same JIS (Japanese Industrial Standard) for quality of balance with automotive wheels.

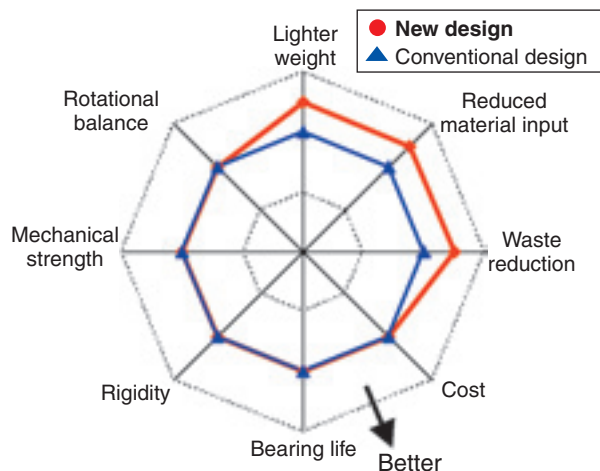


Fig. 10 Image for comparison

From these findings, we are sure that our novel “resource-saving automotive hub bearing design” has functions equivalent to those of conventional hub bearing designs. The chart in **Fig. 10** provides a comparison between our new hub bearing design and conventional design in terms of functionality and advantages in manufacture.

4. Afterword

To be able to contribute to the reduction of CO₂ emissions, NTN has designed a unique hub bearing product that boasts lighter weight through improved design as well as a reduction in materials consumed through an improved forging technique.

The applicable specification for individual NTN hub bearings can vary depending on the vehicle type and/or location of use. It is possible that all the considerations described in this document may not be applicable for the intended usage; notwithstanding, NTN will as necessary expand the scope of applicability of this product line. NTN is going to integrate its already proven “hub bearing with built-in high-sealing low-torque seal” technology with its novel “resource-saving automotive hub bearing” technology described above. Through these efforts, NTN will promote the reduction in weight and friction for hub bearings and thereby will further contribute to reductions in energy consumption by cars in travel as well as proceeding with development of novel eco-conscious technologies.

References

- 1) K. Shibata and T. Norimatsu: Technical Trends in Axle Bearings and the Development of Related Products, NTN Technical Review No. 75 (2007) 29-35

Photo of author



Isao HIRAI

Axle Unit Engineering Dept.
Automotive Sales Headquarters

V-series Hub Joint

Mitsuru UMEKIDA*
Yuuichi ASANO**



To improve fuel efficiency, reducing the weight of axle units is desirable. NTN has developed various hub-bearing and CV joint products to meet this requirement. This report introduces the V-series hub joint, which is an integrated hub-bearing and CV joint crafted using NTN's original press-cut fitting. This product achieves a lighter weight through integration of a hub-bearing and a CV joint

1. Preface

A typical environmental issue to be addressed today is global warming. Recently, emissions reduction of CO₂, the most abundant greenhouse gas, has been posing a challenge that needs to be addressed urgently. The car-manufacturing industry around the world has been committed to develop cars with better fuel efficiency in order to help reduce CO₂ emissions from their products. As a result of this, the global market for hybrid electric vehicles has been dramatically expanding.

In this paper, we will provide information about our V series hub joint products (hereinafter, may be simply referred to as V series H/J) that are modularized products each obtained by joining a hub bearing (hereinafter, may be referred to as H/B) with a constant velocity joint (hereinafter, may be referred to as CVJ) by a "press-cut fitting" technique that is NTN's propriety joining technique; consequently, the V series hub joints boast improved ease of assembly and productivity for our clients as well as a 12% weight reduction compared with conventional products.

2. Structure and advantages

Hub joints (hereinafter, may be referred to as H/J) are products each integrally comprising H/B and CVJ;

in particular, H/J products adopting press cut fitting technique are referred to as V series H/J products. NTN has developed two types of V series H/J products: "non-separable type" that boasts the lightest weight, and a "separable type" that features separable construction that allows a bearing user to be able to repair the purchased bearing product easily.

This report hereunder describes the information about the press cut fitting technique as well as the structural features of "non-separable type" and "separable type" of V series H/J products.

2.1 Previous fitting technique

A previous NTN fitting technique for H/B's with CVJ's is hereunder described. Fig. 1 illustrates the structure of NTN's previous serration fitting joint. Both the outer circumference of the outer ring stem of the CVJ and the inside bore surface of the H/B are serrated. Torque is transmitted via the serrated joint between both serrated members. Also, the CVJ is secured to the H/B with a hub nut tightened onto the threaded end of CVJ outer ring stem.

Torque transmission from CVJ to H/B takes place at the contact surfaces between tooth flanks of both serrated portions. However, because of the limitation of machining accuracy with both members (difference in tooth pitch between both serrated parts), it is difficult to realize a tight fit between both members.

*C.V.Joint Engineering Dept. Automotive Sales Headquarters

**Axle Unit Engineering Dept. Automotive Sales Headquarters

Consequently, variation in the gap between tooth flanks can occur as shown in Fig. 2, and excessive play can occur on the joint in the circumferential direction with the previous fitting technique.

There has been a method available for eliminating circumferential play between CVJ and H/B, that is, the provision of a helix angle on the serration of the CVJ. However, this method has its drawbacks. As non-uniformity in contact pressure occurs across the tip side and the root side of the serrated shafts, the entire tooth surface on the serrated shaft may fail to uniformly bear the load owing to the difference between the tooth pitch of the CVJ side serration and that of the H/B.

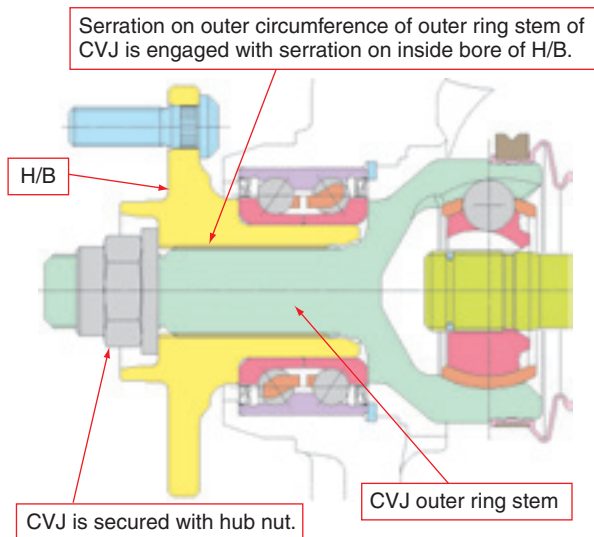


Fig. 1 Fitting by serration (previous method)

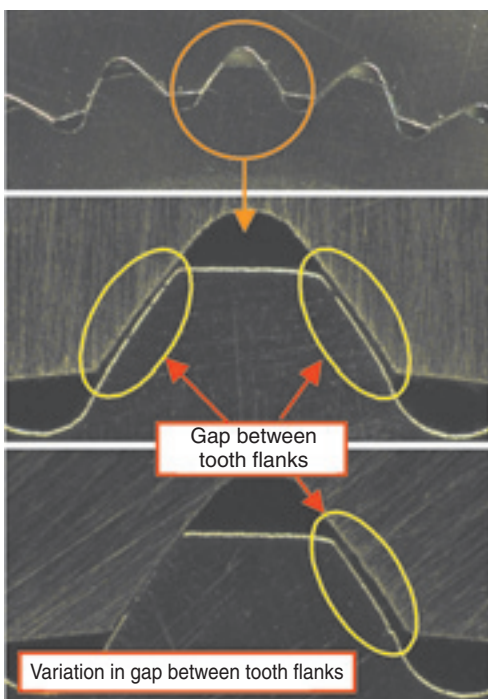


Fig. 2 Contact condition of teeth (previous method)

As explained above, the serrated joint of the previous method fails to evenly bear the torque and therefore, the design length of the mesh between both serrations has to be longer.

2.2 Joint formed by press cut fitting technique

With the previous fitting method, both the CVJ and H/B are serrated. In contrast, with our press cut fitting method the CVJ outer ring alone is provided with a special serration as shown in Fig. 3, while the inside bore of H/B remains cylindrical.

With our press cut fitting system, the CVJ outer ring stem is hardened through heat-treatment, while the inside bore surface of the H/B is not hardened so that there remains a difference in hardness between the CVJ outer ring stem and inside bore surface of the H/B. Consequently, when the CVJ outer ring stem is fitted into the H/B inside bore, the serration on the CVJ outer ring stem generates serrations on the inside bore surface of the H/B. NTN calls this unique fitting method “press cut fitting”.

During the press cut fitting process, the inside bore surface of the H/B is serrated as this surface is under elastic deformation. As a result, the ridges found on the CVJ outer ring stem fit into the grooves formed on the inside bore surface of the H/B while a tightening allowance is present between the ridges and grooves. Thus, a preload is exerted onto the resultant joint, and the CVJ outer ring stem is tightly fitted within the inside bore of the H/B as illustrated in Fig. 4.

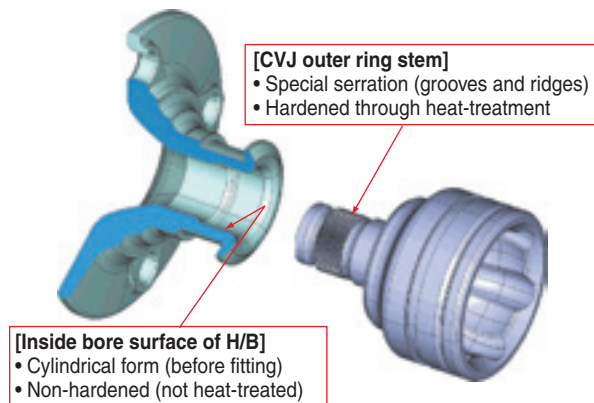


Fig. 3 Press cut fitting (before fitting)

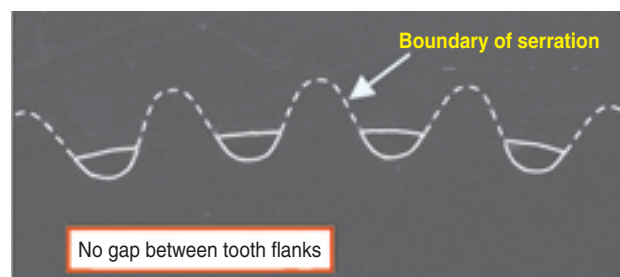


Fig. 4 Contact condition of teeth (Press cut fitting)

As a result of this unique fitting method, the torque input is uniformly borne by all the teeth and tooth flanks, and the allowable torque capacity of this joint is greater, thereby the necessary length of mesh between serrations can be much shorter compared with the previous fitting method.

2.3 Structure of V-series hub joint

As previously mentioned, the V-series H/J products subjected to press cut fitting method can be categorized into “non-separable type” and “separable type”. The structures of these product types are hereunder described.

2.3.1 Non-separable H/J

The “non-separable type” products boast lighter weight through integration of the H/B with the CVJ. **Fig. 5** shows a cross-sectional view of a V-series non-separable H/J product.

As previously mentioned, both members in a joint remain in full a contact state, and do not come apart while the hub joint is running because a preload remains applied to the joint. Nevertheless, to prevent accidental disengagement of the CVJ outer ring stem in a non-separable type from the H/B, the outer end of the CVJ outer ring stem is coined to secure the CVJ to the H/B.

The V-series H/J products boast lighter weight because the length of meshed serration is shorter compared with previous products and they do not have a hub nut.

With the previous fitting method (**Fig. 1**), when torque from the CVJ is input to the H/B and sudden slip develops on the contact surfaces between the oscillation-capable coined area of the H/B and the rear face of CVJ outer ring, a unique noise known as “stick-slip sound” can occur. Reduction in bearing pressure

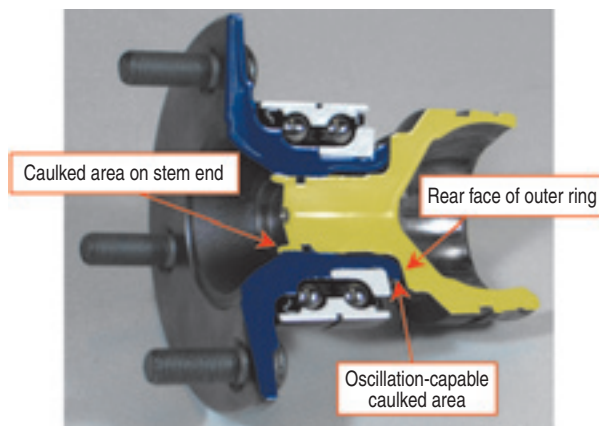


Fig. 5 V-series H/J (Non-separable type)

on the contact surfaces is effective in preventing occurrence of the stick-slip sound.

Unlike the previous structure, the joint formed by our press cutting fitting method is resistant against accidental disengagement, and is capable of controlling the axial pressing force during the press cutting fitting process; thereby, the bearing pressure on the contact surfaces between the CVJ and the H/B can be reduced. Thus, our press cut fitting method is useful in preventing the stick-slip sound.

[Structure and features of non-separable H/B]

Fig. 6 shows the structure and features of NTN non-separable H/B.

- ① Press cut fitting: No gap between contact surfaces of serration on H/B and that on CVJ
- ② Deletion of flange on H/B outer ring, that is, a flange for installing a knuckle: Adoption of a press-fitting technique for weight reduction
- ③ Deletion of hub pilot: Lighter weight (Area A on flange outer circumference shown in **Fig. 6** serves as a pilot)

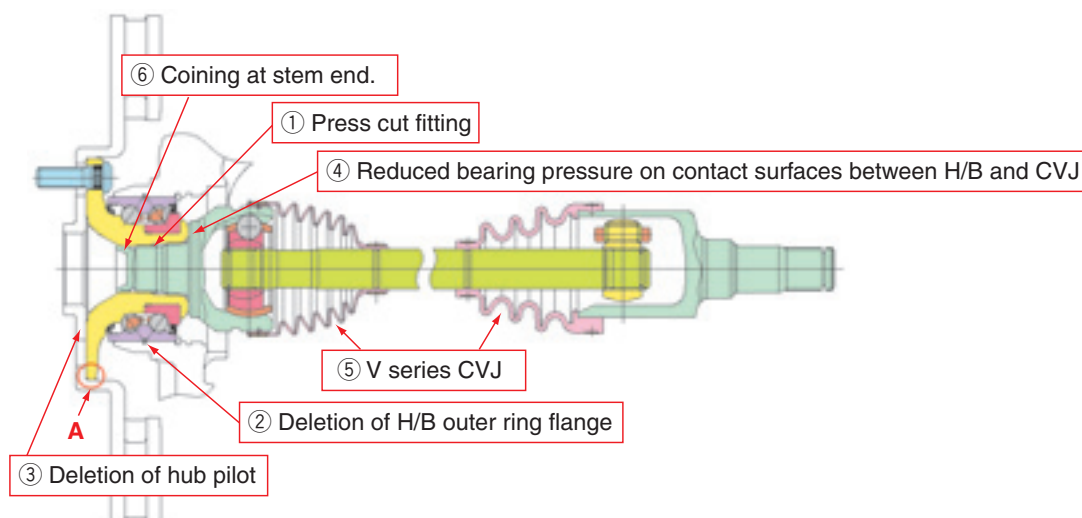


Fig. 6 Structure and characteristics of V-series H/J Non-separable type

- ④ Reduced bearing pressure on contact surfaces between H/B and CVJ: Structure to prevent stick-slip sound
- ⑤ V series CVJ
- ⑥ Coining at stem end

2.3.2 Separable H/J

A hub joint consists of a constant velocity joint integrated with a hub bearing. To help realize easy repair work for a marketed hub bearing, NTN has developed a “separable” hub joint design that is capable of disassembly and reassembly. **Figs. 7 and 8** show the structure of our separable hub joint.

To allow the H/B to be separated from the CVJ, the CVJ outer ring stem is secured by fastening a bolt, instead of coining at the stem end on the non-separable H/J. This bolt is also used to retract the CVJ outer ring stem into the inside bore of the H/B during the reassembly procedure for the separable H/J. To

allow the CVJ outer ring stem to be pulled in, the H/B has an inside wall and the CVJ outer ring stem has a threaded hole along its centerline to accept this bolt.

This unique structure allows the H/B to be separated from and reinstalled to the CVJ as necessary.

As mentioned previously, a joint formed by our press cut fitting technique is preloaded and as a result the H/B cannot be readily separated from the CVJ, unlike the joint obtained from the previous method described in Sec. 2.1; this drawback remains true when the H/B is reinstalled to the CVJ. The unique advantage of our newly developed “separable” hub joint is being able to disassemble and reassemble the joint, which the procedures for our “separable” design are briefly described below.

<Disassembly procedure>

Referring to **Fig. 9**, fit the stem push-out bolt into the threaded hole on the CVJ outer ring, and then mount the pulley extractor onto the H/B. Turn the stem push-out bolt to push out the CVJ outer ring stem. Then, the H/B can be separated from the CVJ.

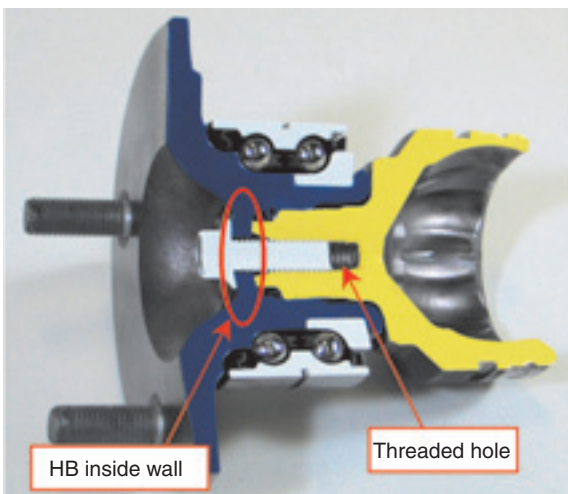


Fig. 7 V-series H/J (Separable type)

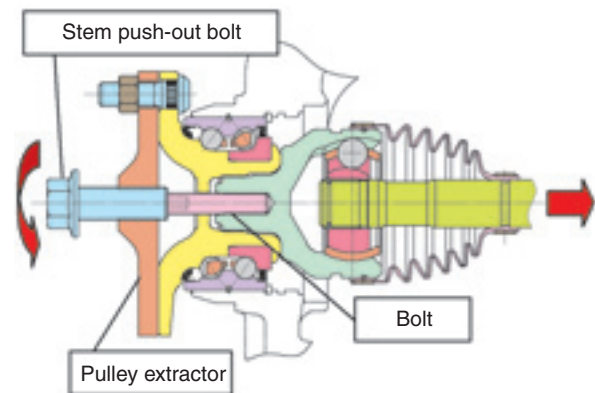


Fig. 9 Separate method of separable type

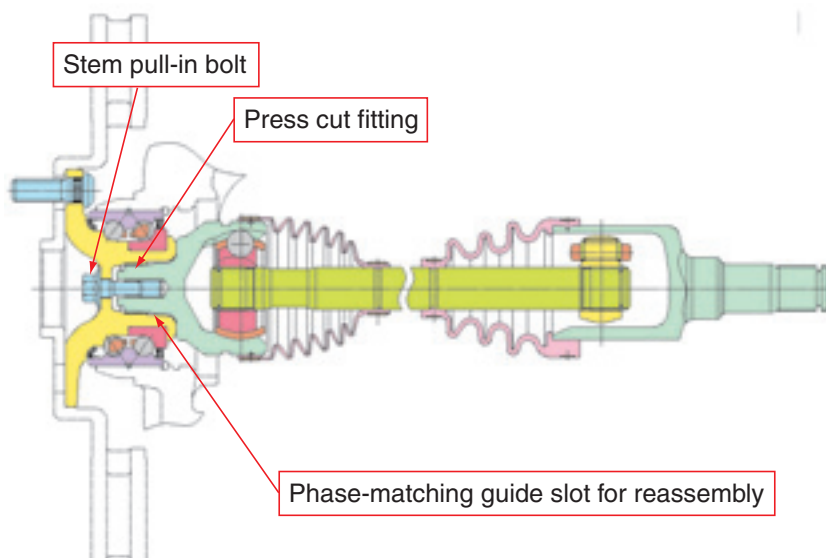


Fig. 8 Structure and characteristics of V-series H/J (Separable type)

<Reassembly procedure>

The joint formed by our press cut fitting technique is a tight-fitting joint that's being preloaded. If a H/B is separated from a CVJ, it will be impossible to readily reestablish circumferential phase-matching between the ridges on CVJ outer ring stem and the grooves on the H/B. To address this drawback, the entrance to inside bore of the H/B in our "separable" design has a phase-matching guide slot that is geometrically situated in a circle greater than the one defined by the ridges of the serration on the CVJ outer ring stem.

For reassembly, the CVJ outer ring stem is guided along the guide slot on the H/B, and the stem pull-in bolt is tightened to a recommended tightening torque.

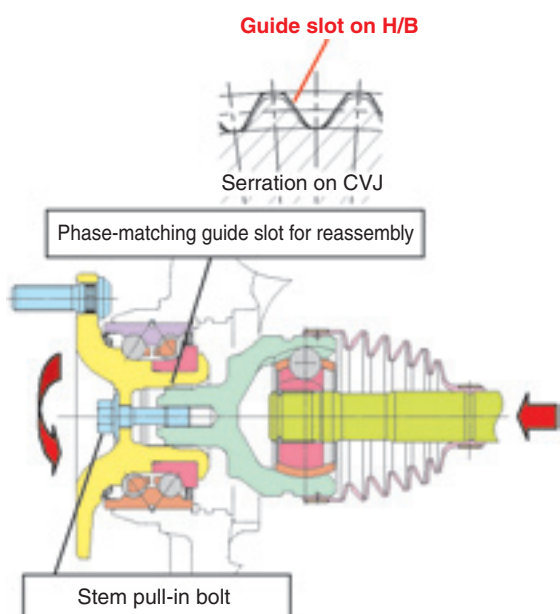


Fig. 10 Re-assemble method of separable type

3. Function assessment test

The functions required of a joint formed by press cut fitting technique are sufficient static torsional strength, torsional fatigue strength against torque transmitted from the CVJ to the H/B, and durability of the joint against a bending moment that occurs when the CVJ is operating at a greater angle.

In the assessment test, we used a CVJ whose press cut fitting joint that has sufficiently great static torsional strength and tested the CVJ samples under the test conditions that led to a fracture of the press cut fitting joint.

(1) Static torsional strength test (with non-separable type)

Fig. 11 graphically plots the test result from the static torsional strength test with non-separable

specimens.

The non-separable product has sufficiently high torsional strength as the specimens of non-separable design satisfy the strength target while the press-fit allowance (difference between the outside diameter of serration on CVJ outer ring stem and the inside diameter of H/B) remains in the standard range.

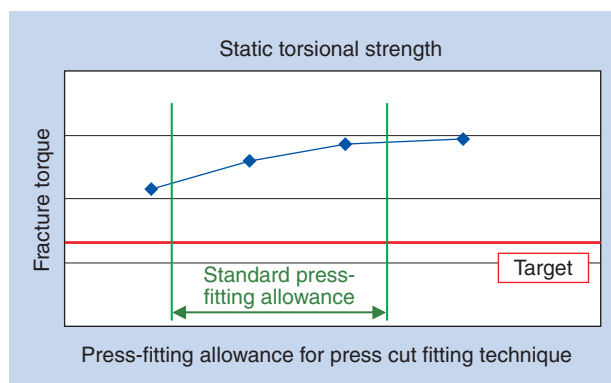


Fig. 11 Static torsional strength test

(2) Bi-directional torsional fatigue strength test (with non-separable type)

Fig. 12 graphically plots the test result from the bi-directional torsional strength test with non-separable specimens.

Assessment has been performed with two types of CVJ samples whose operating angles are 0 degree and 43 degrees respectively. Both sample types have withstood a targeted number of load applications and have exhibited sufficient durability.

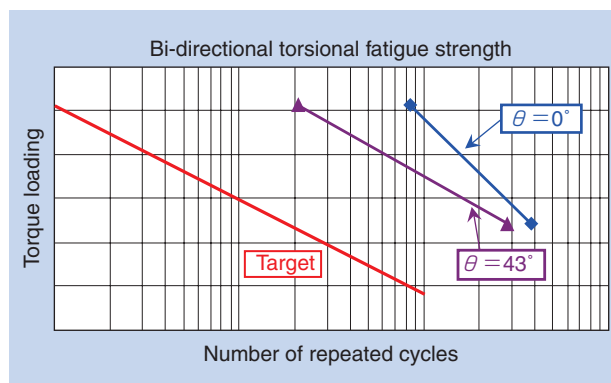


Fig. 12 Bi-directional torsional fatigue strength test

(3) Static torsional strength test (separable type)

Fig. 13 shows the test result from the static torsional test with separable specimens.

Static torsional strength has been assessed with samples having undergone disassembly/reassembly cycles. The samples having undergone disassembly/assembly cycles do not show any evidence of deterioration in mechanical strength, and boast sufficient mechanical strength.

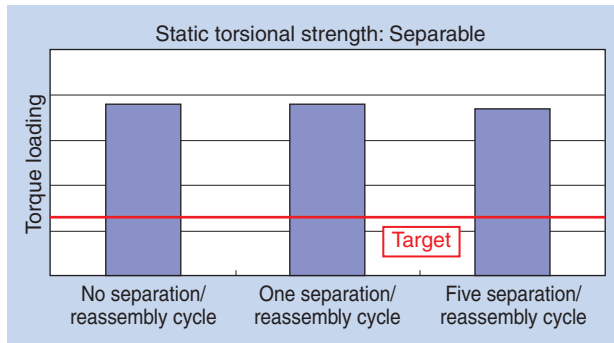


Fig. 13 Static torsional strength test (Separable type)

4. Afterword

NTN has successfully developed the V series hub joint products that feature lighter weights by integrating a hub bearing with a constant velocity joint through NTN's propriety press cut fitting technique. The V series hub joints are categorized into two types: "non-separable" type boasting a light-weight design and a "separable" type featuring easy repair work. This paper has presented information about the structures and advantages of both types. By fully utilizing the technology described above, we will continue to remain committed to the development of novel corner module products for hybrid electric vehicles and electric vehicles.

Photo of authors



Mitsuru UMEKIDA

Axle Unit Engineering Dept.
Automotive Sales Headquarters

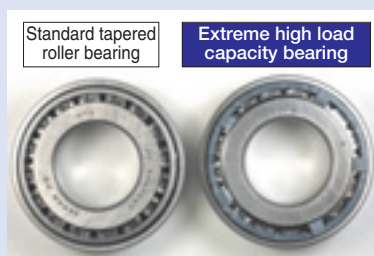


Yuuichi ASANO

C.V. Joint Engineering Dept.
Automotive Sales Headquarters

Extremely High Load Capacity Tapered Roller Bearings

Takashi UENO*
Tomoki MATSUSHITA*



NTN developed a tapered roller bearing with extremely high load capacity to improve the fuel efficiency of cars. This new bearing has improved capacity from increasing the number and length of the rollers. This bearing is used for transmissions and differential gears. This article introduces the design and performance of this product that we have developed.

1. Foreword

People around the world have been increasingly concerned with prevention of global warming and improvement in air quality. In this context, the level of allowable vehicle emissions has been increasingly more stringent, and a Japanese target value for improvement in fuel economy for cars has been established—average 23.5% improvement in fuel economy by the end of fiscal year 2015 relative to the fiscal year 2004 level¹⁾. While automakers have been more deeply committed to efforts for improved fuel economy, engineering people specializing in automotive transmission and differential gearing have been attempting to use less viscous oil and more compact, lighter weight designs aimed at reduced friction of automotive transmissions and differentials. To help contribute to this trend, the bearing industry has been challenged with a life and rigidity requirement for compact, light-weight bearings. To address these challenges, NTN has developed and marketed a line of extreme high load capacity tapered roller bearing products²⁾, which result in lighter, more compact bearings at the same bearing life or a longer bearing life bearing size.

These new products feature longer rollers: the length of rollers has been maximized by further incorporating new engineering improvements into the cage and inner ring of the NTN's already developed high load capacity tapered roller bearings. As a result of this new

development, the NTN extreme high load capacity tapered roller bearing products boast much decreased bearing pressure with a bearing under load; longer bearing life under severe lubricating conditions or contaminated lubricating conditions; and higher rigidity. This paper describes the structure and advantages of this newly developed bearing product.

2. Structure of NTN extreme high load capacity tapered roller bearing

Previous NTN high load capacity tapered roller bearings are characterized by a smaller clearance between the cage and outer ring as well as a greater cage pitch circle diameter—these features are intended to ensure presence of spaces sufficient for the width of cage bars and reduced distances between rollers. Consequently, the number of rollers in any NTN high load capacity tapered roller bearing is virtually equivalent to that of a similarly sized full complement roller bearing.

In addition to these structural features of the previous high load capacity bearing products, our newly developed extreme high load capacity tapered roller bearings (the example in the right in Fig. 1) have a resin cage and maximized-length rollers, and are available in two structural types: (1) bearing without inner ring small side rib, and (2) bearing with inner ring small side rib.

*Automotive Engineering Dept. Automotive Sales Headquarters

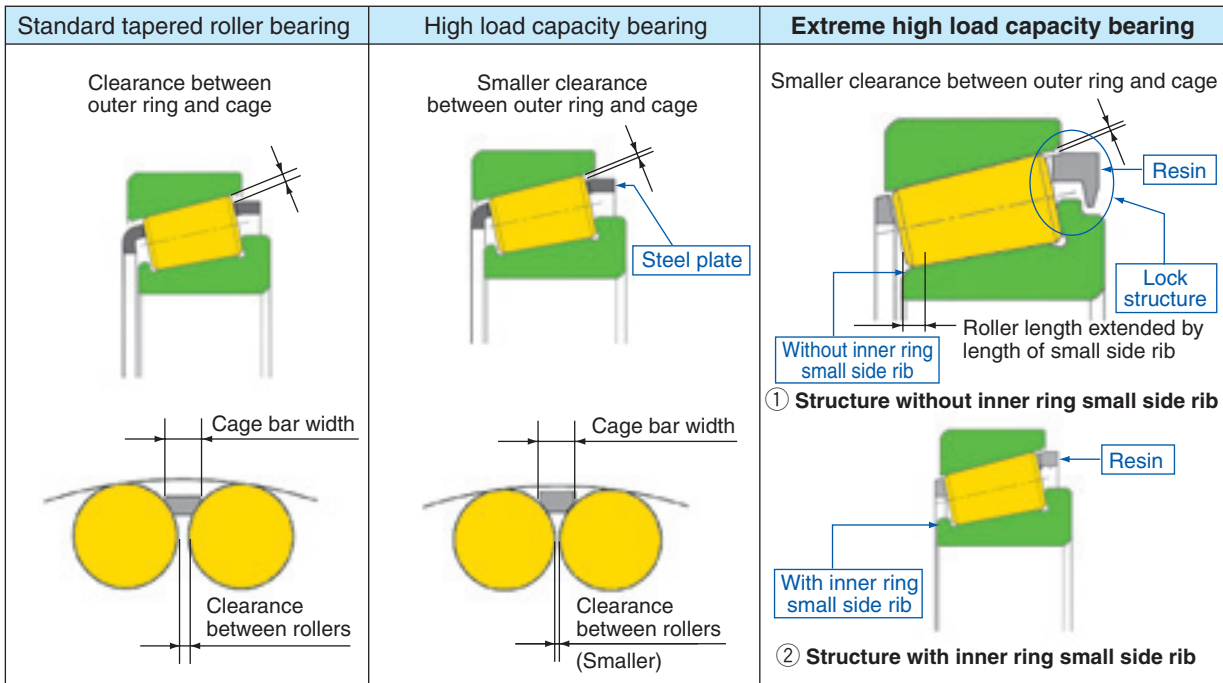


Fig. 1 Structure of extreme high capacity tapered roller bearing

2.1 Bearings without inner ring small side rib

Fig. 2 schematically shows the structure of a bearing without an inner ring small side rib, and Fig. 3 illustrates a 3D model of this bearing.

A bearing design without an inner ring small side rib is intended to be used in space constrained applications where the additional geometry required for the rib would make the overall bearing too large. The features of this bearing structure are as summarized below:

- (1) Cage: The small side rib has a minimum width just sufficient for satisfying the mechanical strength required of it.
- (2) Roller length: The length of rollers may be increased to the maximum width of inner and outer ring raceways provided that the maximum

allowable cage protrusion is not exceeded.

- (3) Lock structure using teeth on cage: So that an inner ring/rollers/cage ASSY can remain non-separable, a lock structure is provided which consists of teeth on the large diameter side on cage, wherein these teeth are engaged with the grooves formed on the outer circumference of inner ring large side rib.

2.2 Bearings with inner ring small side rib

Fig. 4 shows one example of a bearing structure with an inner ring small side rib.

There may be cases where the dimension of inner ring width can be increased even though the allowable dimension of protrusion of cage is limited. Then, the bearing with inner ring small side rib may be adopted, and its features are described below.

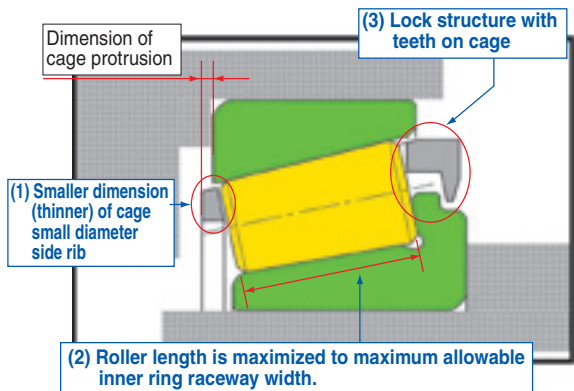


Fig. 2 Structure of extreme high capacity tapered roller bearing without inner ring small side rib

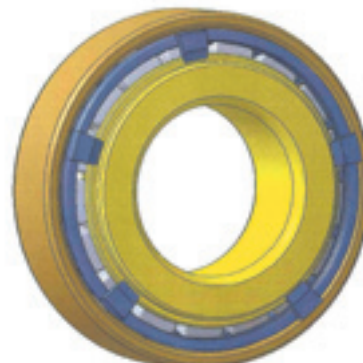


Fig. 3 3D model of Extreme High Capacity tapered roller bearing

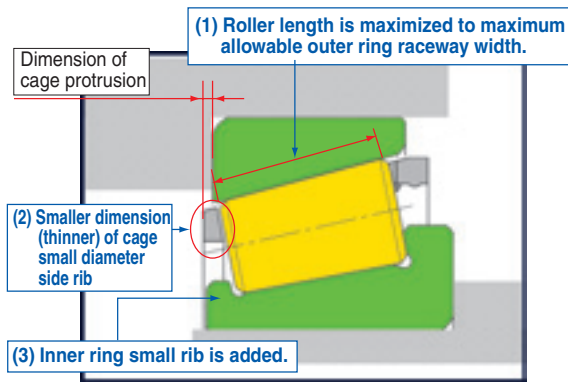


Fig. 4 Structure of extreme high capacity tapered roller bearing with inner ring small side rib

- (1) **Cage:** The cage is designed with the minimum rib width necessary to satisfy the mechanical strength required of the cage small diameter rib under the intended bearing operation conditions.
- (2) **Roller length:** The length of rollers are maximized while leaving sufficient room for the small rib and having a cage small end protrusion which is acceptable.

3. Features of NTN extreme high load capacity tapered roller bearings

Thanks to increase in quantity and length of rollers, the NTN extreme high load capacity tapered roller bearings boast functions improved over the NTN standard tapered roller bearing products, and the examples of improvement in functions are as described below:

(1) Greater load rating

- Basic dynamic load rating: 16% increase at maximum (64% increase at maximum in calculated life)
- Basic static load rating: 21% increase at maximum (21% increase at maximum in safety factor)

(2) Greater rigidity

- Bearing rigidity: 14% improvement at maximum (14% reduction at maximum in elastic displacement)

(3) Longer bearing life

- Useful life under clean oil lubrication condition is extended.

The use of an increased number of longer rollers helps reduce the maximum bearing stress, leading to an increased oil film thickness and alleviation of stress that occurs in a metal-to-metal contact mode. Consequently, occurrence of surface initiated flaking,

which can occur from metal-to-metal contact under a condition where formation of oil film is difficult, has been prevented and bearing life has been extended.

- Useful life under contaminated lubrication condition is extended.

The use of an increased number of longer rollers helps reduce the maximum bearing stress, limiting the size of dent mark caused by trapped foreign matter. The stress occurring on the raised material around a dent mark is also reduced thereby resulting in longer life under contaminated lubrication conditions.

4. Performance of NTN extreme high load capacity tapered roller bearings

The NTN extreme high load capacity tapered roller bearing differs from other NTN tapered roller bearings in having an increased number of longer rollers and a lock structure on the large side diameter of the cage. To study the effects of these special features on the bearing, we have performed a function assessment test comparing the standard tapered roller bearing and extreme high load capacity tapered roller bearing (without inner ring small side rib) shown in [Table 1](#).

(1) Result of pumping performance test

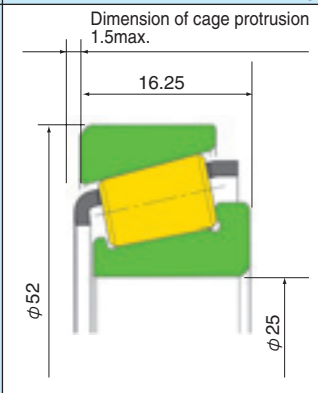
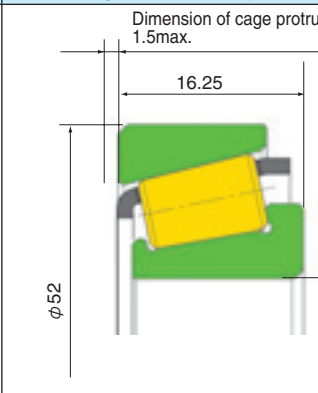
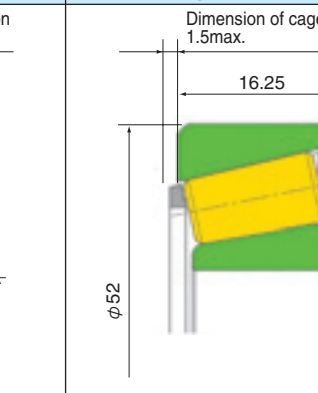
The NTN extreme high load capacity tapered roller bearing features a unique lock structure on the larger diameter side of cage as well as increased number of rollers and roller length. [Fig. 5](#) provides visual comparison between both bearing types in terms of the space volume. It is apparent that the clearance between rollers is smaller on the NTN extreme high load capacity tapered roller bearing owing to increase in the number of rollers and as a result, the space volume in the bearing is smaller.

We have compared the flow rates of lubricating oil flowing through both bearing types in running mode. [Fig. 6](#) schematically illustrates concept of the pumping performance test. When a bearing is run with the interior of bearing and housing filled with lubricating oil, a pumping function takes place on the bearing, thereby the lubricating oil flows from the large diameter side of the bearing. [Fig. 7](#) graphically plots the measured amounts of lubricating oil pumped through the bearings after operating for a fixed duration. Though having a smaller space volume within its interior, the NTN extreme high load capacity tapered roller bearing offers a flow rate comparable to that of the standard roller bearing sample.

(2) Roller settling performance comparison test

When an NTN extreme high load capacity tapered roller bearing without inner ring small rib is used, the

Table 1 Comparison of bearing internal design

	Standard tapered roller bearing	High load capacity bearing	Extreme high load capacity bearing
Schematic view			
Bearing size	$\phi 25 \times \phi 52 \times 16.25$		
Load rating (comparison with standard tapered roller bearing)	Basic dynamic load rating $C_r = 31.5\text{kN}$	Basic dynamic load rating $C_r = 34.0\text{kN}$ (8% increase)	Basic dynamic load rating $C_r = 36.5\text{kN}$ (16% increase)
	Basic static load rating $C_{0r} = 34.0\text{kN}$	Basic static load rating $C_{0r} = 37.0\text{kN}$ (9% increase)	Basic static load rating $C_{0r} = 41.0\text{kN}$ (21% increase)
Number of rollers	16 rollers	17 rollers	17 rollers
Length of rollers	10.5mm	10.5mm	11.8mm
Cage material	Steel plate	Steel plate	Resin

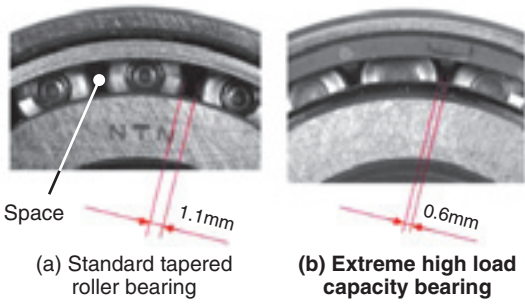


Fig. 5 Space volume of bearing inside

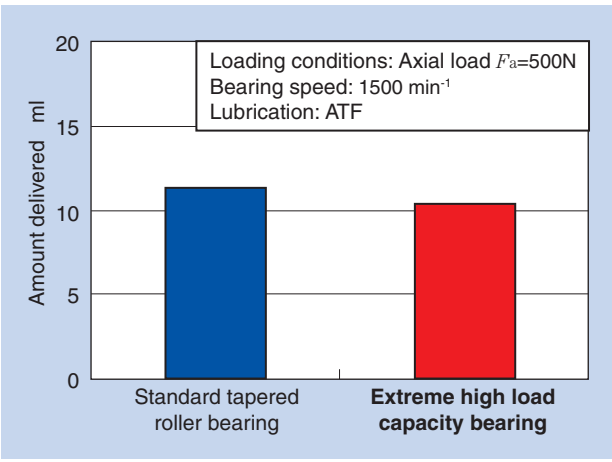


Fig. 7 Test result of oil flow

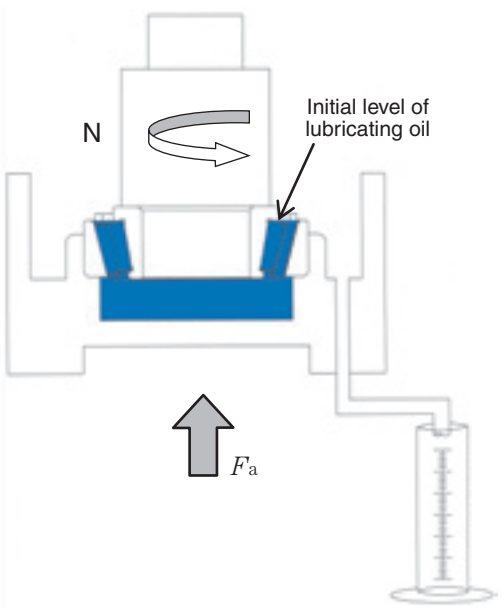


Fig. 6 Evaluation of oil flow through bearing inside

roller settling performance in the bearing may differ from that of other tapered roller bearings because of absence of inner ring small side rib that otherwise limits the location of rollers.

Let us describe roller settling performance. When an inner ring assembly is fitted into an outer ring from above, a clearance will occur on the inner ring large side rib since the length of rollers is usually smaller than the inner ring raceway width (see Fig. 8). Because the rollers in a running bearing rotate while being guided by the inner ring large side rib surface, the bearing needs to be subjected to a seating operation in order to allow the rollers to shift to normal

locations where they remain in contact with the inner ring large side rib surface (considered fully seated). The lower the number of bearing revolutions needed for the bearing to be fully seated means easier preload setting for the bearing.

Fig. 9 schematically illustrates the test method used for investigating roller seating performance on the NTN extreme high load capacity tapered roller bearing, and Fig. 10 graphically plots the test results for roller seating performance. The test result in Fig. 10 shows that the rollers in the NTN extreme high load capacity tapered roller bearing fulfill settlement in about five revolutions while the rollers in the standard tapered roller bearing reaches settlement in about 13

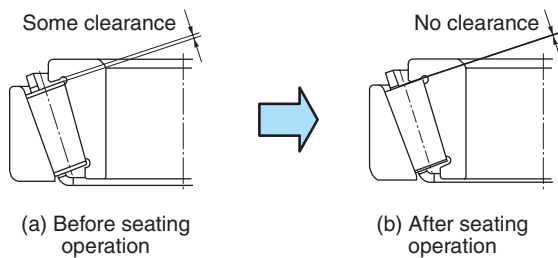
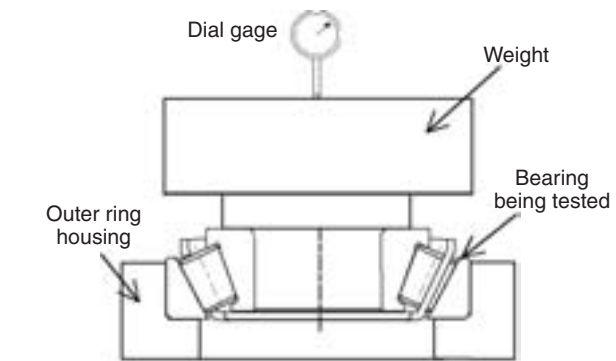


Fig. 8 TClearance change between inner raceway width and roller



Loading conditions: Axial load $F_a=302$ N
Measuring method: Dimension of inner ring displacement resulting from revolutions of bearing is measured.

Fig. 9 Testing method of roller settling

revolutions. The reason the NTN extreme high load capacity tapered roller bearing achieves good roller settlement performance can be explained as follows:

Fig. 11 provides schematic diagrams for situations where the rollers in both NTN extreme high load capacity tapered roller bearing and standard tapered roller bearing are in settled state.

On the NTN standard tapered roller bearing, the dimension of roller displacement is limited by the end face of inner ring small side rib. In this state, the cage remains in contact with the roller large diameter side end faces of rollers: consequently, as soon as break-in operation begins, working forces occur between associated components and generate a thrust that forces each roller toward the inner ring large side rib; thereby while this thrust continues to lift up the cage, the rollers shift toward the inner ring large side rib.

In contrast, on the NTN extreme capacity tapered roller bearing, the dimension of roller displacement is limited by the end face of cage pocket small diameter side. As soon as break-in operation begins, the rollers shift toward the inner ring large side rib by a distance equivalent to the distance between the rollers and cage pockets, causing them to come into contact with the cage pocket large side end faces; then like in a movement on the standard tapered roller bearing, the

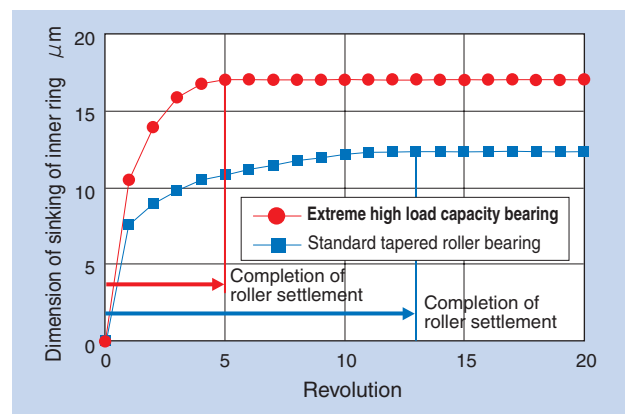


Fig. 10 Test results of roller settling

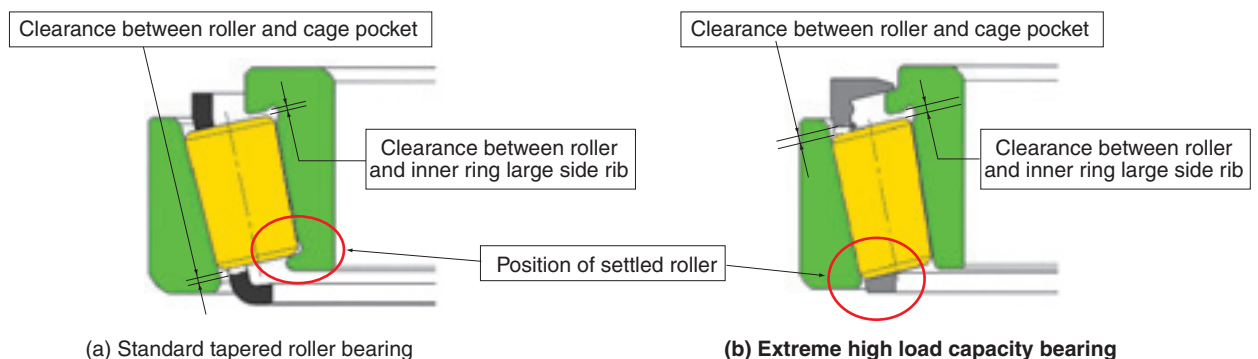


Fig. 11 Clearance to determine roller seating characteristics

rollers shift to the inner ring large side rib end face while lifting up the cage.

As described above, the dimension of roller displacement in the extreme high load capacity tapered roller bearing is greater owing to the structure of this bearing: at the earlier stage of break-in operation, the rollers alone, independent of the cage, shift toward inner ring large side rib; thereby the shift per revolution of the bearing is greater and the rollers will settle in a shorter time.

5. Compact, light-weight design technique for NTN extreme high load capacity tapered roller Bearing

Demands will continue to grow for improved fuel economy and riding comfort with automobiles, as well as higher engine power and greater number of transmission speeds. To help satisfy these demands, automotive bearings have to be capable of withstanding greater loads with no changes to the envelope dimensions, or feature compact size and lighter weight with a given load bearing capacity. In this paper, **Table 2** below summarizes technical data for studies into compact size, lighter weight design for a same set of a given load bearing capacity and a given shaft diameter. Because a compact size, lighter weight design helps a tapered roller bearing to achieve lower running torque, this paper includes the facts about the bearing torque reduction with the NTN extreme high

load capacity tapered roller bearing: **Table 3** summarizes the parameters adopted for calculating the running torque of bearing samples.

The high load capacity tapered roller bearing boasts 16.2% reduction in bearing weight and 2% reduction in running torque.

Adoption of the NTN extreme high load capacity design helps achieve 25.3% reduction in bearing weight and 7.5% reduction in running torque. Thus this tapered roller bearing technology contributes to the goal of reduced size (more compact), lighter weight, and reduced torque.

Table 3 Calculation condition of rotating torque

Radial load F_r	5000N
Axial load F_a	5000N
Bearing speed	5000min ⁻¹
Lubrication	ATF
Lubricating oil temperature	90°C

Table 2 Study of down sizing under same load capacity

	Standard tapered roller bearing	High load capacity bearing	Extreme high load capacity bearing
Load rating	Basic dynamic load rating $C_{1r}=31.5kN$		Basic static load rating $C_{0r}=34.0kN$
Bearing size	$\phi 25 \times \phi 52 \times 16.25$	$\phi 25 \times \phi 49.3 \times 15.4$	$\phi 25 \times \phi 49 \times 15$
Bearing mass (reduction in comparison with standard tapered roller bearing)	0.154kg	0.129kg (16.2% reduction)	0.115kg (25.3% reduction)
Calculation result for running torque※ (reduction in comparison with standard tapered roller bearing)	0.293Nm	0.287Nm (2.0% reduction)	0.271Nm (7.5% reduction)
Schematic view			

※Does not include stirring resistance on lubricating oil.

6. About special cage structure

By adoption of toothed lock structure on the large diameter side and narrower rib on the small diameter side on the cage of the NTN extreme high load capacity tapered roller bearing, the length of rollers can be maximized. The shape of this cage is very unique, and the cage cannot be shaped with steel plate: therefore, it is made of a resin. Information about the resin used for this purpose and mechanical study about the special cage structure are hereunder discussed.

(1) Resin material

Lubricating oil in a transmission and/or differential sometimes contains phosphorus or sulfur content as extreme pressure additive which are known to be detrimental to some resin materials. Therefore, the resin material for the cage needs to be resistant against oils containing these additives.

When considering ease of assembly into bearing and durability in bearing, each needed for a material of tapered roller bearing cage, the resin material of the cage also needs to have excellent physical properties including mechanical strength, toughness and heat resistance. Beginning with these considerations, NTN has performed a necessary research and has successfully developed a PPS (polyphenylene sulfide) resin cage that features physical properties needed for the cage on the NTN extreme high load capacity tapered roller bearing.

Fig. 12 graphically plots the results of oil resistance test with various resin cage materials. The PPS resin does not exhibit deterioration in tensile breaking strength even after undergoing immersion for 2,000 hours: it is apparent that this resin material has

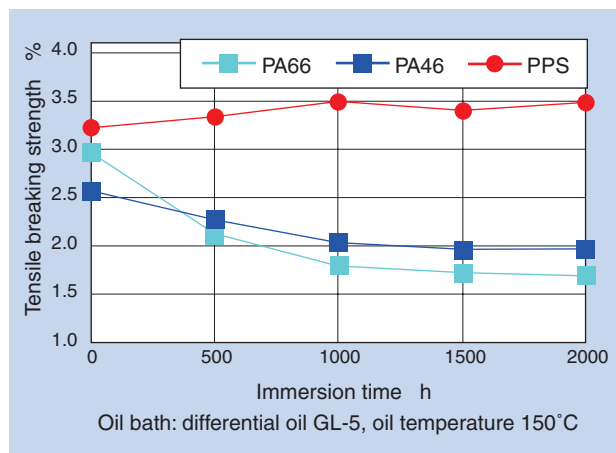


Fig. 12 Test result of oil resistance

sufficiently high oil resistance performance.

If our extreme high load capacity tapered roller bearing is used in a lubricating oil that does not contain a lot of phosphorus or sulfur content, it is possible to adopt PA46 (polyamide 46) or PA66 (polyamide 66) each often used as a resin material for a bearing cage.

(2) Dynamic analysis of extreme high load capacity cage

We have attempted to determine the mechanical strength needed for the cage small diameter side rib that is a unique feature of the cage for the NTN extreme high load capacity tapered roller bearing, and have found a minimum necessary rib width. To be able to determine the stress occurring on the cage in the running bearing, we have used an NTN-developed 3D dynamic analysis tool for tapered roller bearings³⁾.

Fig. 13 shows one typical example of model for dynamic analysis of tapered roller bearing. This diagram shows that the largest stress occurs at the small diameter side rib among various areas on the cage. In designing the small diameter side rib on the cage, we have determined the size of rib that has necessary mechanical strength by reflecting the findings obtained from the dynamic analysis.

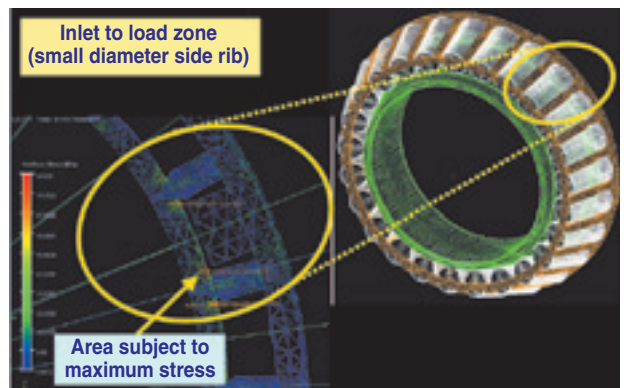


Fig. 13 Model of dynamic analyzed bearing

7. Conclusion

As the challenge to prevent global warming and improve air quality continues, people committed to automotive technologies have been more strenuously involved in improving fuel economy. Thus, demand for smaller, lower torque, longer-life automotive bearings will continue to increase.

This paper has presented information about the “NTN extreme high load capacity tapered roller bearing” that boasts compact size, lighter weight and higher rigidity by reflecting novel bearing design techniques—“maximized roller length” and “adoption of newly developed resin cage”—in the NTN high load capacity tapered roller bearing that has been already running on actual automobiles.

By remaining committed to development of bearing technologies and products, NTN will further cope with increasingly demanding operating conditions and diversifying structures where NTN bearing products will be used.

References

- 1) Website of Ministry of Land, Infrastructure, Transport and Tourism
http://www.mlit.go.jp/kisha/kisha07/09/090702_.htm
- 2) T. Tsujimoto and J. Mochizuki: High Capacity Tapered Roller Bearings, NTN Technical Review No. 73 (2005) 30-39
- 3) K. Harada and T. Sakaguchi: Dynamic Analysis of a High-Load Capacity Tapered Roller Bearing, NTN Technical Review No. 73 (2005) 20-29

Photo of authors



Takashi UENO

Automotive Engineering Dept.
Automotive Sales Headquarters



Tomoki MATSUSHITA

Automotive Engineering Dept.
Automotive Sales Headquarters

New ULTAGE Series EA and EM Types of Spherical Roller Bearings

Yukihisa TSUMORI*



For spherical roller bearings that are used in industrial machinery, including construction equipment and iron and steel facilities, we have achieved the world's best load capacity and possible rotation speed through major revisions to the internal design. We began sales of these bearings as the new ULTAGE series of models in March 2009, allowing us to contribute further to creating a society that is more harmonious with the environment.

1. Introduction

In contribution to realization of the ecology-oriented society, novel technologies have been developed in every technical field for industrial machinery.

The bearings used on rotary mechanisms in industrial machines need to satisfy requirements for improvements in "bearing life", "load capacity", "high-speed performance", and "handling quality". NTN has been marketing the "ULTAGE*" Series bearing products that boast the world's best performance to meet these requirements. The "ULTAGE" Series line of bearing products already includes product series for precision angular ball bearings and cylindrical roller bearings intended for use on machine tool main spindles.

Recently, NTN has added new standard product series to the ULTAGE Series: they are new self-aligning roller bearings, EA Type (pressed steel cage) and EM Type (machined copper alloy cage) each boasting higher load capacity and longer life.

**"ULTAGE" (a name created from the combination of "ultimate," signifying refinement, and "stage," signifying NTN's intention that this series of products be employed in diverse applications) is the general name for NTN's new generation of bearings that are noted for their industry-leading performance.

2. Structure of new self-aligning roller bearings in ULTAGE Series

Fig. 1 shows the structure of the NTN conventional Type B self-aligning roller bearing. The structure of this roller bearing is unique in that the bearing has asymmetric rollers, and its inner ring center rib bears the thrust induced by the running bearing. Due to being guided by the inner ring center rib, the running rollers are maintained in stable attitude. This structure is appropriate for larger bearings and high-speed bearings.

At the same time, recent needs for self-aligning roller bearings, other than high-speed capability, are longer life and greater rigidity. To cope with these needs, bearing manufacturers have been developing bearing products with improved cage shape and more amply sized rollers.

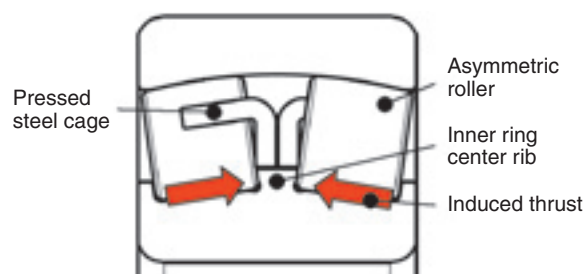


Fig. 1 Spherical roller bearings (type B)

*Product Design Dept. Industrial Sales headquarters

Table 1 Comparison of spherical roller bearing type

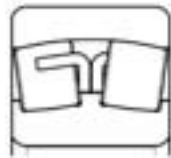
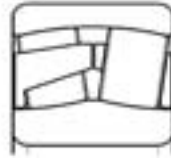
Type	Type B	Type C	Type E
Cross-sectional plan			
Rollers	Asymmetric roller	Symmetrical rollers	Symmetrical rollers
Cage	Pressed steel	Pressed steel	Resin molding
Center rib	Yes	None (w/guide ring)	None

Table 1 provides information about comparison of several self-aligning roller bearing types. In order to cope with the above-mentioned needs for higher load capacity bearing products, NTN has been series-producing unique self-aligning roller bearings with the inner ring center rib deleted. They are the Type C self-aligning roller bearings having a guide ring and the Type E self-aligning roller bearings whose rollers are stabilized in terms of attitude with the resin cage. NTN will include these types in the ULTAGE Series bearing products.

Fig. 2 shows the structure and features of the newly developed ULTAGE Series Type EA bearing. Both Types EA and EM employ symmetric rollers, wherein the diameter and length of the rollers have been maximized so that the bearings can withstand a much

greater load.

In addition, by adoption of novel cage featuring higher rigidity and simplified form, it has become possible to delete the inner ring center rib and incorporate a maximum number of rollers of maximized length.

As shown in **Fig. 3**, the pressed steel cage in the Type EA bearing guides the rollers with its both end faces. In addition, four tabs (protrusions) situated in the cage pocket shown in **Fig. 4** help stabilize the attitude of rollers while the bearing is running and generate smooth lubricating oil flow in the bearing (**Fig. 5**). Furthermore, the entire surface of pressed steel cage is subjected to a special surface treatment to improve wear resistance of the cage.

Fig. 6 shows the structure and features of the Type

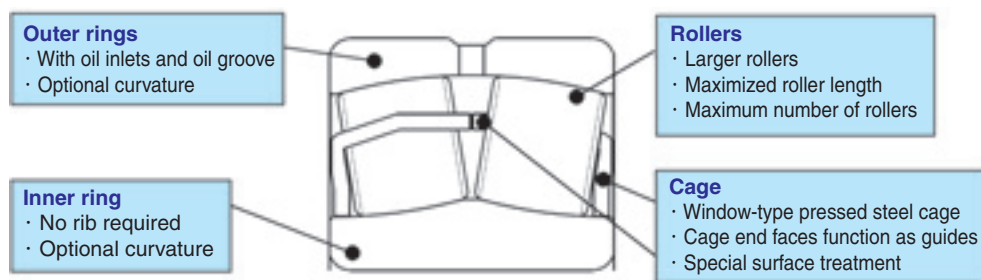


Fig. 2 Ultage series type EA spherical roller bearings

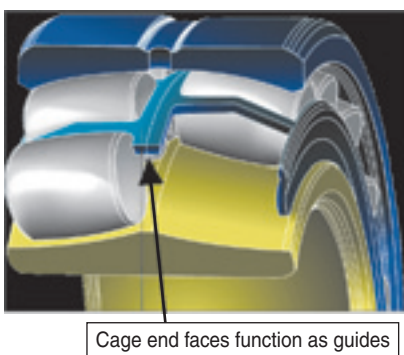


Fig. 3 Cage guide type of EA spherical roller bearings

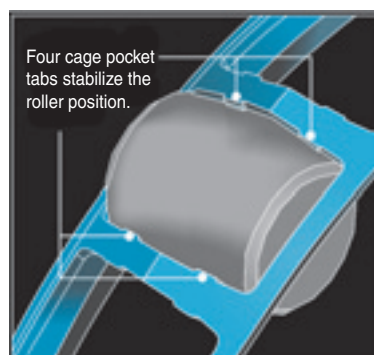


Fig. 4 Design of cage pocket tabs

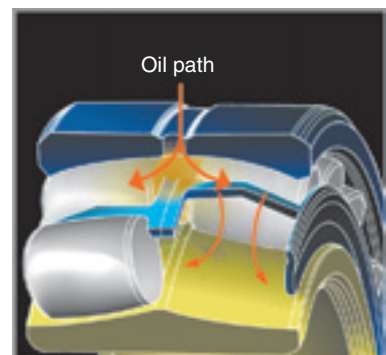


Fig. 5 View of oil path

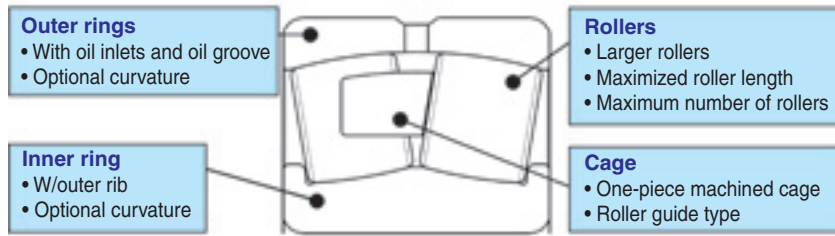


Fig. 6 Ultage series type EM spherical roller bearings

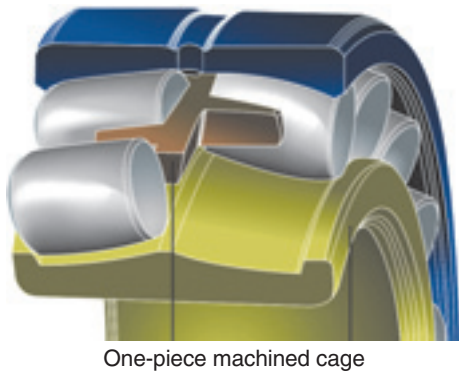


Fig. 7 Cage type of EM spherical roller bearings

EM bearing and Fig. 7 illustrates the machined high tensile brass cage. This cage adopts roller guide type in order to stabilize the attitude of rollers while the bearing is running. The right half and left half of the cage constitute a non-separable body and the inner ring has the outer rib in order to prevent loss of rollers. The Type EM bearing is particularly advantageous in applications subject to severe vibrations and impacts.

The dimensions in a Type EM bearing are same as those of an equivalently sized Type EA bearing.

3. Advantages of ULTAGE Series self-aligning roller bearings

3.1 Load capacity

Maximized roller diameter and maximized number of rollers help the Types EA and EM bearings achieve the world's highest load capacity.

- (1) Basic dynamic load rating: Comparison with competitors' products is summarized in Fig. 8.
- (2) Basic static load rating: Comparison with competitors' products is summarized in Fig. 9.

3.2 Allowable speed

Employing a high-rigidity, pressed steel cage type, the Types EA and EM bearings boast the world's highest allowable speed as compared with the competitors' catalogue values given in Fig. 10.

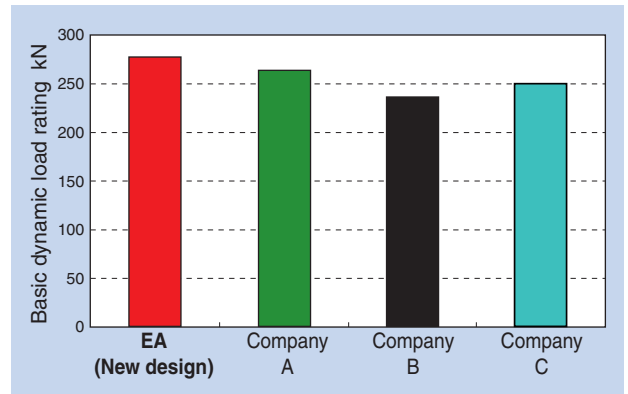


Fig. 8 Catalogue comparison of basic dynamic load rating (C_r)
22216($\phi 80 \times \phi 140 \times 33$)

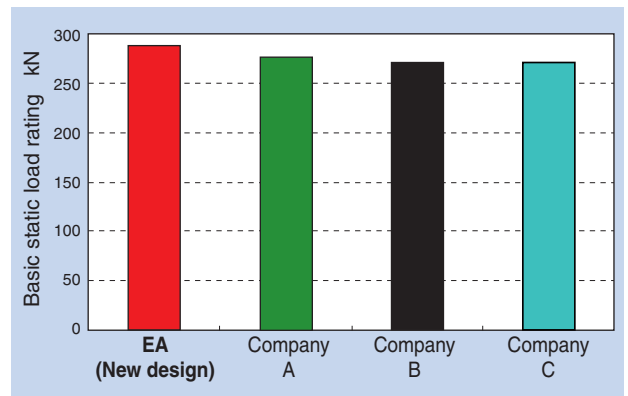


Fig. 9 Catalogue comparison of basic static load rating (C_{or})
22216($\phi 80 \times \phi 140 \times 33$)

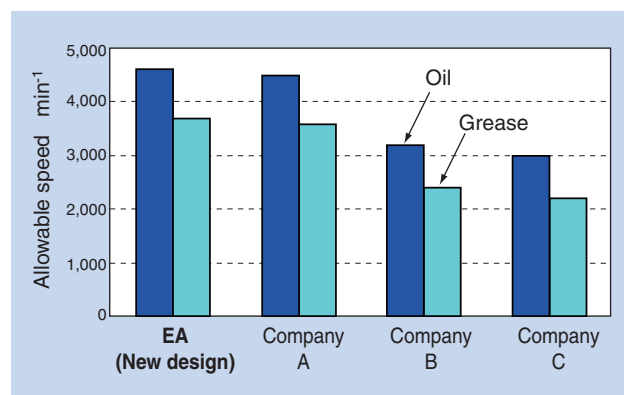


Fig. 10 Catalogue comparison of allowable speed
22216($\phi 80 \times \phi 140 \times 33$)

Fig. 11 graphically plots test results for bearing temperature rise under circulation lubrication condition. It is apparent that the temperature rise on the Types EA and EM bearings is limited compared with the competitors' bearings, while the running torque is low.

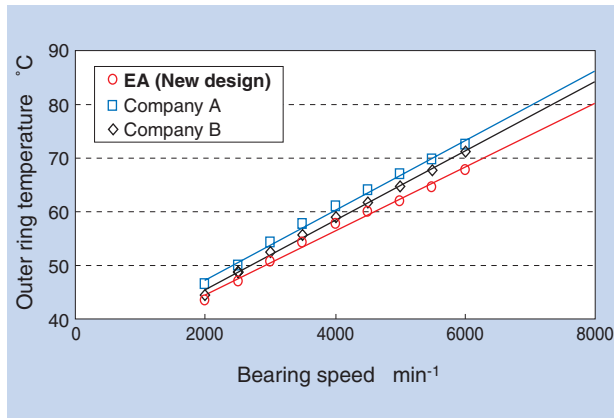


Fig. 11 Test results of temperature rise 22216($\phi 80 \times \phi 140 \times 33$)

3.3 Operating temperature range

Thanks to adoption of a special heat-treatment technique, the maximum allowable operating temperature is set as high as 200°C.

3.4 Compact and lightweight design

By developing the Types EA and EM bearings, NTN has achieved the following improvements over the previous designs: 65% increase at maximum in basic dynamic load rating, 35% increase at maximum in static load rating, and 20% increase at maximum in allowable bearing speed.

A higher load capacity design technique helps achieve a line of compact and lightweight bearing products. **Table 2** summarizes an NTN's attempt to realize such an improved bearing product. By applying this design technique, the size of conventional bearing No. 22220B (dia. 100×dia. 180×46 in mm) can be reduced to that of a product of the new series—22218EA (dia. 90×dia. 160×40 in mm): this size

Table 2 Example, compact and lightweight

Model No.	Load rating (kN)		Boundary dimensions (mm)	Bearing volume (cm ³)	Mass (kg)
	C_r	C_{or}			
22220B (Conventional design)	315	415	$\phi 100 \times \phi 180 \times 46$	810	4.95
22218EA (New design)	385	398	$\phi 90 \times \phi 160 \times 40$	600	3.28
				△25%	△34%

reduction means an approximately 30% reduction in both bearing volume and mass. NTN believes that this achievement will positively help machine designers design lighter, much compact industrial machines.

3.5 Improved handling quality

Introduction of a simple-shaped window type pressed steel cage helps simplify assembly, disassembly, and greasing works.

(1) Easy grease application to roller surfaces (**Fig. 12**)



Fig. 12 Grease application

(2) Projection of rollers from the cage is small, and rollers smoothly return to their normal state. Thus, the disassembly/reassembly procedure for the bearing is simple (**Fig. 13**).



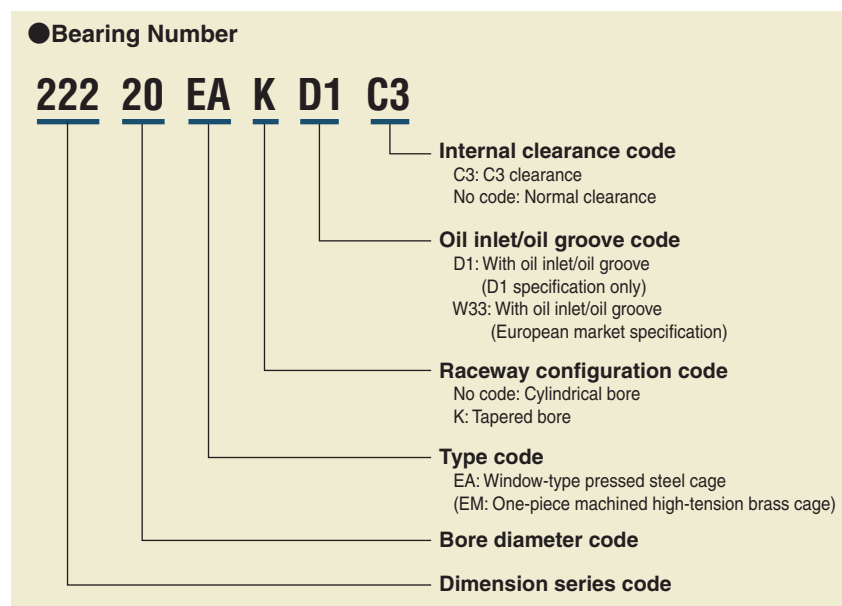
Fig. 3 Assembly / disassembly

4. Inclusion into standard ULTAGE Series products

The ULTAGE Series Types EA and EM self-aligning roller bearing products are now available in all the series range with outside diameter 420 mm or smaller.

NTN is going to modify the conventional types (B, C, and E) to the new ULTAGE standards. For details, the readers are encouraged to contact the NTN.

For the bearing number system for the new ULTAGE Series products, see an example of bearing number shown below:



5. Conclusion

NTN has developed an improved functionality version of its standard self-aligning roller bearing products, and added these improved products to its ULTAGE Series—that is NTN's next generation bearing product series.

Industrial machinery technologies have been increasingly innovated to help realize the ecology-oriented society. NTN believes that the new bearing products in the ULTAGE Series that boast greater load capacity and higher speed positively satisfy demanding market needs for lighter weight, smaller size and longer life.

NTN will remain committed to development of bearing products of a next generation, through further improvement, realization of advanced functionality and lower cost in order to cope with diversifying market needs.

Photo of author



Yukihiisa TSUMORI

Product Design Dept.
Industrial Sales
headquarters

Compact Free-type Torque Diode

Shoji ITOMI*



NTN developed a free-type torque diode that rotates the output shaft by turning the input shaft, but does not rotate the input shaft by turning the output shaft. Recently, NTN has developed a small and light free-type torque diode that we call a “compact free-type torque diode.” This report introduces the structure and function of this product.

1. Preface

Free type torque diodes (TDF) are often used as an automatic switching mechanism to switch over between electromechanical mode and manual mode on rotary equipment and as a safety-protection mechanism for electric motors. To be able to expand the scope of applications of this product line, NTN has developed the “Compact Free Type Torque Diode” that can be used on compact precision equipment.

2. Dimensions and features

Figs. 1 and **2** provide information for comparison in size between the NTN newly developed product and conventional product.

The size of the newly developed product is 1/3 as small as that of the conventional product.

The features of the newly developed compact free type torque diode product can be summarized as follows:

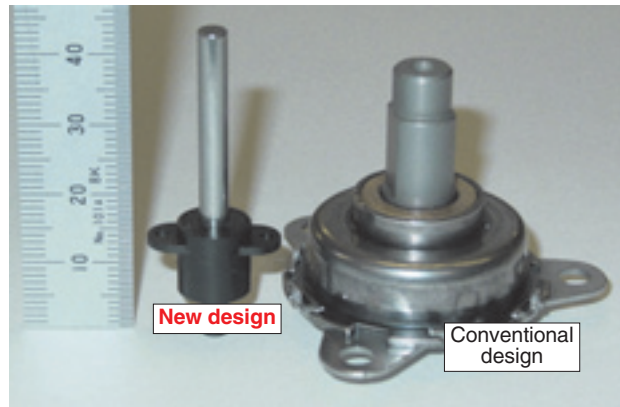


Fig. 1 Comparison of size of developed product and current product

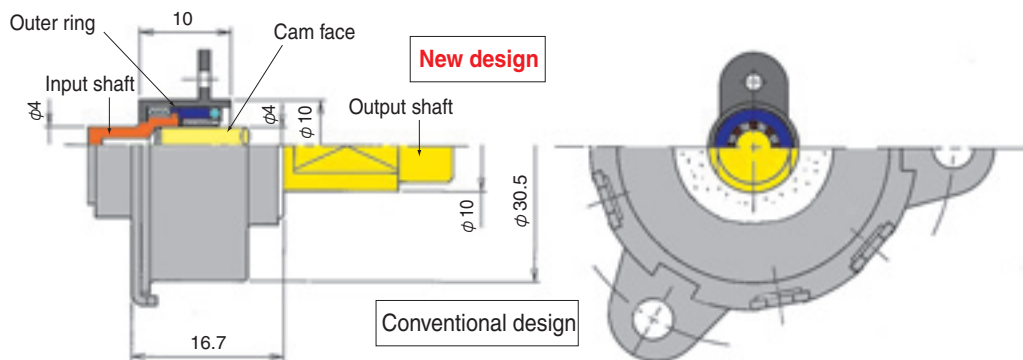


Fig. 2 Comparison of size of developed product and current product

*Application Engineering Dept. Industrial Sales headquarters

[Features]

- (1) A portion of the output shaft also serves as a cam face: consequently, the size of output shaft has been greatly reduced to OD 10 mm × 10 mm (1/3 reduction, compared to the conventional product).
 - (2) Now, the housing and input shaft are made of resin: consequently, the newly developed product weighs mere 28 g (2/5 reduction compared to the conventional product).
 - (3) The area of sliding surfaces has been reduced to decrease the running torque* (resultant torque is 5 mN-m or smaller; 1/25 reduction compared to the conventional product).
- (*The running torque mentioned here is a torque on the product in unloaded state.)
- (4) Now, the housing is made of a resin; thereby the shape of mount area of the housing can be designed with greater freedom.

clutch can be categorized into two clear-cut types according to the behavior of the clutch in response to reverse input situation: “locked rotation type” that prevents torque transmission to the input shaft, and “free-rotation” type whose output shaft turns freely and does not transmits torque to the input shaft.

Now, **Table 1** summarizes the relation of transmission of rotational torque from the input shaft to the output shaft on a free type torque diode.

Figs. 3 and **4** illustrate the structure and operating principle of the newly developed compact free type torque diode.

The outer ring is coupled to the input ring, remaining capable of transmitting the rotational torque from the input shaft; and the inner bore surface of outer ring has a cam face. The cage retains the rollers and balls, wherein the balls are forced to the outer ring end face and bearing cover side face by spring force.

3. Operating principle of free type torque diode

“Torque diode” can be defined as a reverse input blocking mechanical clutch that transmits rotational torque from the input shaft to the output shaft but does not transmit rotational torque from the output shaft to the input shaft. The reverse input blocking mechanical

Table 1 Relation of input and output shaft rotation of Free type Torque Diode

Input shaft		Output shaft
Rotation		Rotation (When the input shaft is turned, the output shaft rotates too.)
Does not rotate.		Rotation (When the output shaft is turned, the output shaft alone rotates.)

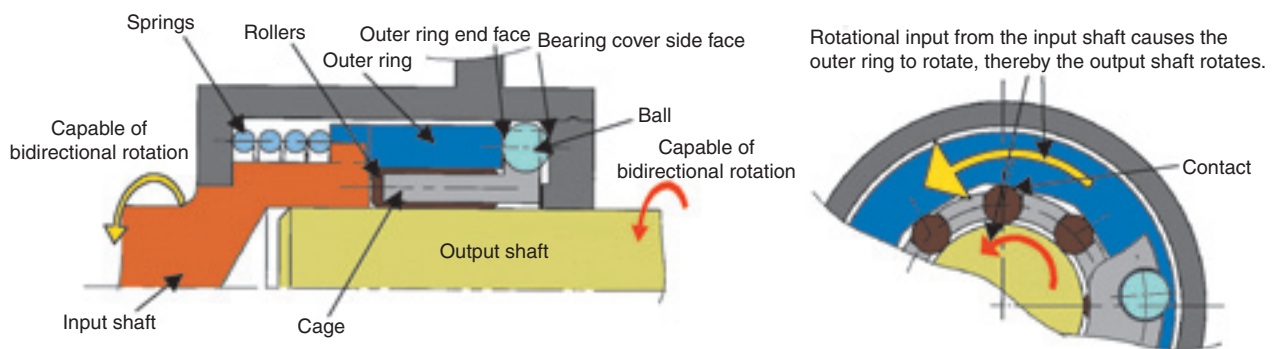


Fig. 3 Case of input shaft rotating

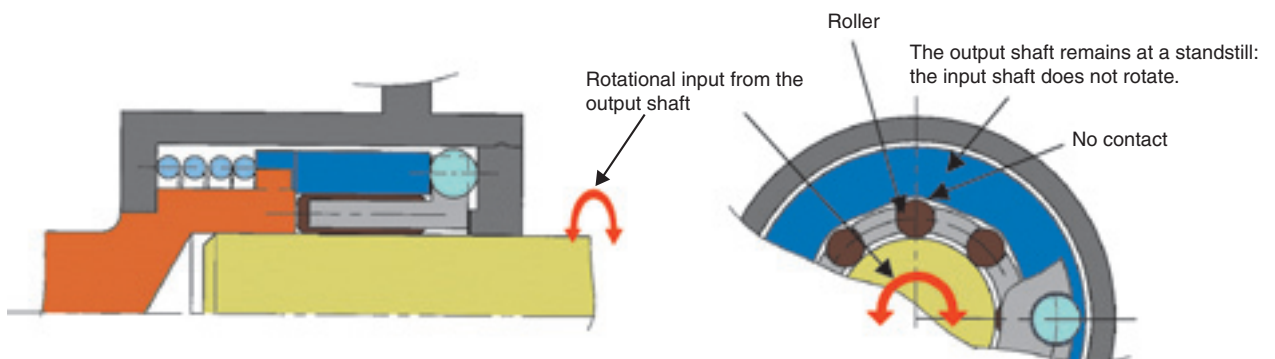


Fig. 4 Case of output shaft rotating (Input shaft not rotating)

Variation in the torque transmission path is described below between a case where the torque is input from the input shaft and another case where the torque is input from the output shaft.

3.1 Case where rotational torque is input from the input shaft

When the input shaft turns, the outer ring coupled with the input shaft rotates; and the cage rotates in a direction same as that of the outer ring at a speed about 1/2 as fast as that of the outer ring. The balls retained by the cage roll on the outer ring end face and bearing cover side face; the rollers shift to the outer ring end face owing to difference in rotational speed between the outer ring and cage, and then locked between the outer ring cam face and output shaft; and the output shaft rotates together with the outer ring (Fig. 3).

3.2 Case where rotational torque is input from the output shaft

When rotational torque is input from the output shaft, the rollers are held in location where they do not come into contact with the outer ring cam face; thereby, the rollers are not engaged with the outer ring cam face; consequently, even when the output shaft rotates, the input shaft does not rotate (Fig. 4).

NOTE) After having stopped rotation, the input shaft is turned slightly in the reverse direction: consequently, the rollers come off the cam face and take a relation shown in Fig. 4; and then rotation of the output shaft is not transmitted to the input shaft any more.

4. Endurance test

By using the forward-reverse rotation test machine illustrated in Fig. 5 and applying the endurance test conditions summarized in Table 2, durability of the newly developed Compact Free Type Torque Diode has been investigated by turning the input shaft in forward and reverse directions to turn the output shaft.

Table 3 summarizes the tests result obtained. There is not much difference found in the running torque, state of internal structure. And backlash between, before, and after operation for 11×10^4 cycles with the newly developed Compact Free Type Torque Diode; this new product has proved its good durability.

Table 2 Test condition of endurance test

Running speed	100min ⁻¹
Test equipment	Forward and reverse rotation test machine (see Fig. 5)
Operating pattern	One operating cycle consists of one forward rotation (1 sec.), one standstill (0.5 sec.), one reverse rotation (1 sec.) and one standstill (0.5 sec.).
Torque loading	50mN·cm (Loading is governed with a bidirectional torque limiter.)
Temperature	Room temperature
Output shaft Dia.	φ 4 mm needle pin is used (hardness number: HRC60 or greater).

Table 3 Test results

Running time	110,000 cycles (61 hours)
Rotational torque with no load applied	Remains at 3 mN·cm, no change between before and after test operation.
State inside the product	Very minor wear on contact surfaces No apparent variation in the amount of residual grease
Backlash	No variation between before and after test operation

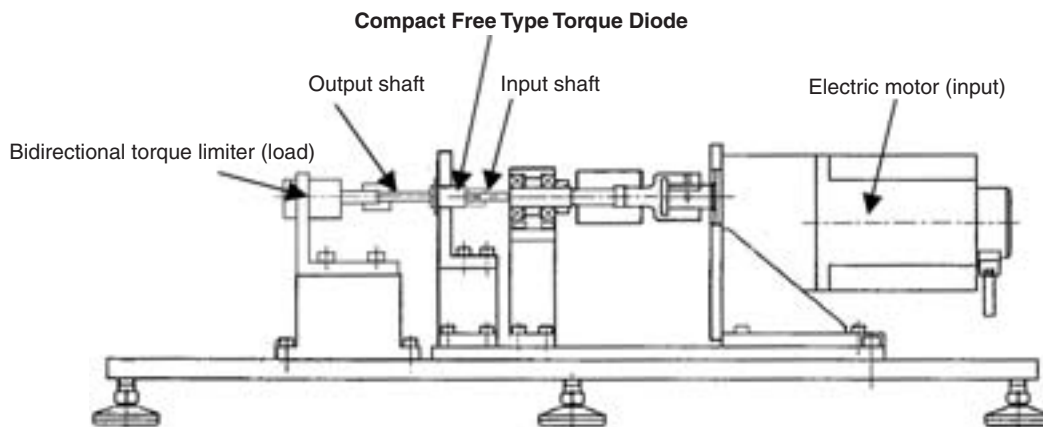


Fig. 5 Forward and reverse rotation test machine

5. Intended application

The product will be conveniently used for switching over between motor-driven mode and manual mode for lens zooming functions on still cameras and video cameras.

6. Conclusion

Previously, switch-over between electromechanical mode and manual mode for rotary mechanism has been achieved by switching over between paths for transmitting rotational motion by actuating an electro-mechanical component such as an electromagnetic clutch or a manually operated component such as a hand lever. Use of a free type torque diode helps realize automatic switch-over between these modes without using an electrical switch.

The newly developed NTN Compact Free Type Torque Diode helps realize automatic switch-over between electromechanical mode and manual mode for small-sized mechanisms. NTN will not only remain committed to efforts for cost reduction and function improvement, but also propose other applications to be able to support activities to develop low energy-consumption equipment.

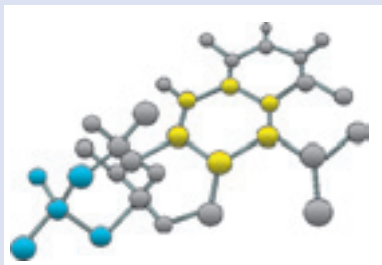
Photo of author



Shoji ITOMI

Application Engineering Dept.
Industrial Sales
headquarters

Characteristics and Applications of DLC films



Kouya OOHIRA*

From the view point of environmental and energy issues, vigorous efforts have been put into research and development activities for tribological coating films in order to reduce friction and wear of sliding surfaces. In particular, diamond-like carbon (DLC) coatings have superior low-friction and anti-wear properties compared to other coating films, and they are attracting a great

amount of attention from tribology researchers and engineers. The friction and wear properties of DLC films, however, depend on their use conditions as well as their production processes, and therefore it is necessary to choose appropriate DLC films according to their use conditions and engineering purposes. This article introduces various properties of DLC films.

1. Introduction

NTN Group strives to reduce its environmental footprint and thus remains committed to continued mitigation of environmental impacts caused by its corporate activities through improving energy efficiency and utilization of resources in its production activities. As an example, bearing engineers have been proposing reduced use of rare materials, such as Mo, included in bearing lubricant, as well as reduction in the amount and viscosity of the lubricating oil used which, result in lower bearing torque. However, these attempts can result in deteriorated lubrication of the bearing components, and conventional techniques may fail to sufficiently lubricate the bearing components involved.

Surface modification appears to be a promising technique that can dramatically improve the tribological characteristics of bearing components. Bearing engineers have been considering the adoption of various hard films in order to alleviate friction and wear on sliding surfaces within bearings. In particular, Diamond-Like Carbon (DLC) film boasts higher hardness, excellent wear resistance, and lower friction coefficient and has been applied to automotive parts, dies, and tools.

There are various reports available about applications of DLC films: examples state that when

sliding in nitrogen gas or a vacuum, a-C:H (hydrogenated amorphous carbon), which is a hydrogen-rich DLC, exhibits an extremely low friction coefficient of 0.001^{1), 2)}; another report says that ta-C (tetrahedral amorphous carbon), which is a hydrogen-free DLC, exhibits low friction when lubricated with oil in an automotive gasoline engine³⁾. A variety of DLC films are available, and their sliding properties can vary significantly depending on coating method and/or conditions and the operating environment. Therefore, the optimal DLC film design must be selected based on the expected operating conditions. The following article describes various properties of DLC films and examples of their application to molding dies.

2. Features of DLC films

2.1 What is DLC film?

A DLC film can be defined as an amorphous film (**Fig. 3**) consisting of an irregular mixture of diamond atoms that form sp^3 bonds (diamond structure shown in **Fig. 1**) and diamond atoms that form sp^2 bonds (graphite structure shown in **Fig. 2**). To provide a concept diagram that helps to better explain DLC films, Frrai and Robertson⁴⁾ have proposed a ternary phase diagram such as given in **Fig. 4**. In this diagram, the corner at the top represents diamond, the lower left corner graphite, and the lower right corner hydrogen.

*Elemental Technological R&D Center

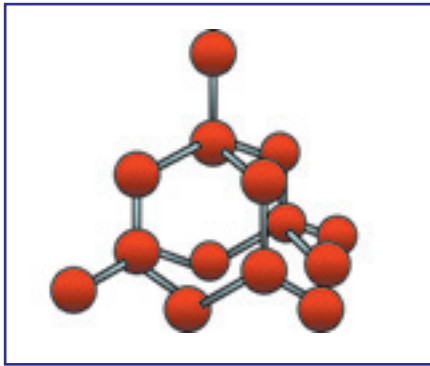


Fig. 1 Structure of diamond

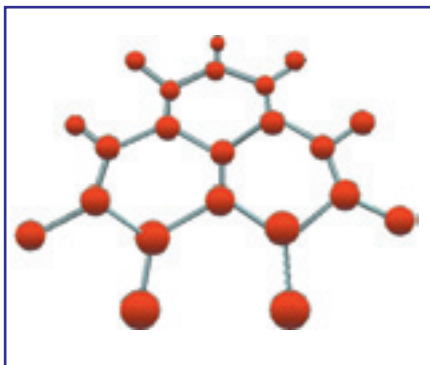


Fig. 2 Structure of graphite

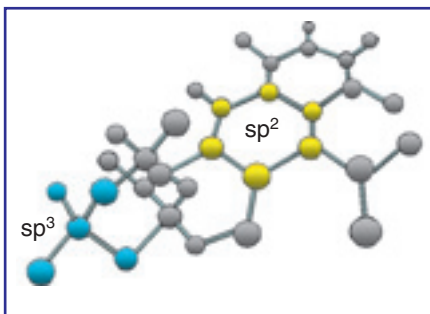


Fig. 3 Structure of DLC films

- ta-C : Tetrahedral amorphous carbon
- a-C : Amorphous carbon
- a-C:H : Hydrogenated amorphous carbon
- ta-C:H : Hydrogenated ta-C

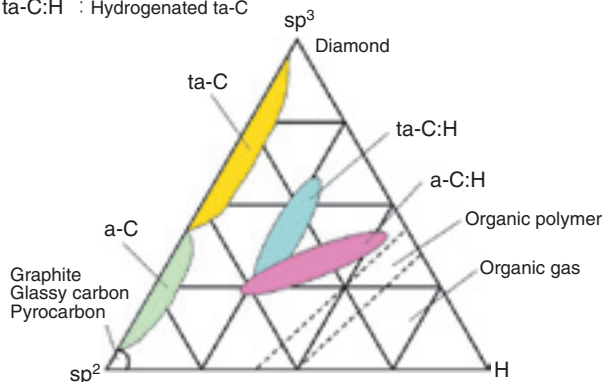


Fig. 4 Classification of amorphous carbon

Table 1 summarizes the general physical properties of carbon materials including graphite, diamond, and DLC films. Data for Young’s modulus, hardness number, and the electrical characteristics of DLC film are similar to those of diamond, and the thermal conductivity of DLC film is similar to that of graphite. The variation in physical property values of DLC films exist due to variation in proportion of sp^3 bonds to sp^2 bonds and hydrogen content^{5, 6, 7}.

Table 1 Comparison of characteristics of carbon material

	Graphite	Diamond	DLC
Specific gravity	2.25	3.52	1.0~3.0
Specific electric resistance ($\Omega \cdot \text{cm}$)	10^{-3}	$10^{12} \sim 10^{16}$	$10^9 \sim 14$
Thermal conductivity (W/cm/K)	0.4~2.1	1000~2000	0.2~30
Lattice constant (nm)	a=0.2456 c=0.6708 (interlayer)	a=0.3567
Young’s modulus (GPa)	...	1000~2000	100~800
Hardness number (Hv)	...	10000~12000	1000~8000
Oxidation start temperature	400~450	600	300~500

2.2 Coating methods for forming DLC films

DLC films can be created from solid carbon or hydrocarbon gases such as methane, acetylene and benzene and are usually formed in a vacuum chamber. Depending on the carbon source used, the DLC film falls within one of the following two categories:

(1) PVD: Physical Vapor Deposition

A process that uses solid carbon as a starting material, wherein solid carbon is evaporated and then the resultant carbon vapor is allowed to deposit on a substrate to form the DLC film.

(2) CVD: Chemical Vapor Deposition

A process that uses hydrocarbon gas as a starting material, wherein the gas is decomposed in a vacuum chamber and then the resultant carbon vapor is allowed to deposit on a substrate to form the DLC film.

By using solid carbon as an evaporation source, the PVD process can produce a DLC film solely composed of carbon. In contrast, since the CVD process uses hydrocarbon gas as a starting material, the resultant DLC film unavoidably contains hydrogen atoms of approximately 15 to 50 atm%. Either the PVD or CVD processes can be applied in various methods. **Fig. 5** summarizes typical coating processes applied to form DLC films.

Table 2 lists several general physical characteristics of DLC films formed by various coating processes. It has been known that characteristics of synthesized DLC films can vary greatly depending on starting materials, atomic elements added, and coating conditions^{5, 6, 7}.

The UBMS (Unbalanced Magnetron Sputtering) process listed in **Table 2** is one type of sputtering process, and is characterized by an unbalanced magnetic field that is employed to expand a plasma layer in the vicinity of the substrate. Because the plasma density near the substrate is increased, the ion assist effect (ions are allowed to collide the substrate) is enhanced; consequently, the film characteristics including density and adhesion are improved⁸.

The AIP (Arc Ion Plating) process uses a solid carbon cathode and the chamber inner wall as an anode in order to trigger an arc discharge and allow carbon on the target surface to evaporate. The

resultant carbon vapor is ionized and is allowed to deposit on the sample surface to which a negative bias voltage is applied. As a result, a DLC film with a higher degree of adhesion is formed⁵.

In a plasma CVD process, hydrocarbon gas (such as methane, acetylene, benzene, etc.) is decomposed in a vacuum chamber to generate hydrocarbon ions that are accelerated and allowed to collide into a substrate to which negative voltage is applied resulting in the DLC film. Because of using gas as a starting material, the CVD process features better “coverage” and is suitable for forming a DLC film on samples with complex geometry. Also, with this process, a DLC film of uniform thickness can be formed without the need to reorient the sample.

2.3 Comparison of DLC films with various other hard coatings

2.3.1 Characteristics in general

Table 3 summarizes the characteristics of DLC films and other hard coatings. DLC films boast particularly high hardness and excel in anti-seizure quality. However, DLC films have an unavoidable drawback that is, poor adhesion to a substrate. Poor adhesion occurs because stresses within a DLC film are high, and carbon atoms, which are chemically stable, do not readily coagulate with a dissimilar material. Therefore, improved DLC film adhesion poses an engineering challenge.

2.3.2 Friction wear resistance

Using the NTN Savin type wear test rig, NTN has evaluated the sliding characteristics of DLC films (formed with UBMS process) and of various other nitride coatings.

This test rig is designed to maintain sliding contact between the flat test piece and a driven rotating cylinder which is crowned. **Fig. 6** illustrates the configuration of the NTN Savin test rig, and **Table 4** summarizes the test conditions applied. The test rig uses a crowned cylinder so that uneven contact does not occur between the test piece and cylinder, thus achieving a much more accurate assessment of the film’s wear resistance. **Fig. 7** summarizes the test results, where the specific wear has been calculated based on the width of wear marks found on the test piece and the friction coefficients that have been determined based on friction values measured with the load cell.

The specific wear of DLC film is 1/6 or less compared with that of TiN, which was the best of the nitride films tested. In addition, the friction coefficient of DLC film is about 0.2 while the friction coefficients of other hard films fall in a range of 0.4 to 0.8, indicating the DLC film features excellent friction characteristics.

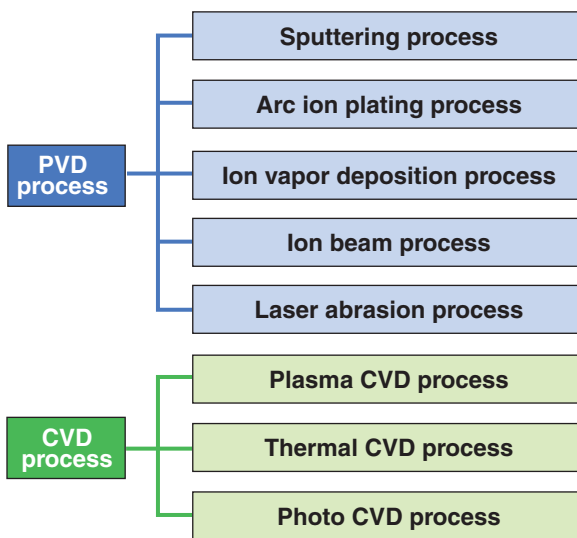


Fig. 5 Classification of coating methods

Table 2 Characteristics of various DLC films

	PVD process		CVD process
	UBMS process	AIP process	Plasma CVD process
Coating material	Solid carbon	Solid carbon	Hydrocarbon gas
Coating temperature (°C)	<250	<300	<200
Hardness number (Hv)	2000~5000	5000~8000	1000~2000
Surface roughness	○	△	◎
Coverage	△	△	◎
Adhesion	◎	○	○
Wear resistance	◎	○	△
Cost	△	△	○

Table 3 Characteristics of DLC films and other hard coatings

Film type	Color	Hardness number (Hv)	Corrosion resistance	Oxidation resistance	Seizure resistance	Adhesion	Applications
DLC	Gray to black	1000~8000	○	○	◎	△	Cutting tools, dies, functional films
TiN	Gold	2000~2400	○	○	○	◎	Cutting tools, dies, jewelry
ZrN	White gold	2000~2200	○	△	△	○	Jewelry
CrN	Silver white	2000~2200	◎	○	◎	◎	Machine parts/components, dies
TiC	Silver white	3200~3800	△	△	○	○	Cutting tools, dies
TiCN	Purple to gray	3000~3500	△	△	○	○	Cutting tools, dies
TiAlN	Purple to black	2300~2500	○	◎	○	○	Cutting tools, dies, jewelry

Thus, the DLC film appears to be a promising means for creating a highly wear-resistant surface treatment used on machine parts/components, dies, and tools.

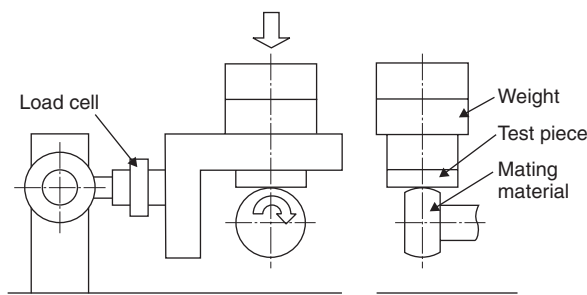


Fig. 6 Wear test rig

Table 4 Test conditions

Test piece	Hardened SUS440C stainless steel, OD 48 mm, thickness 7mm, surface roughness 0.005 mmRa
Mating material	Quenched and tempered SUJ2 steel, curvature R60 mm, hardness Hv784, surface roughness 0.01 mmRa
Load	50 N (max. contact pressure 0.5 GPa)
Speed	0.05 m/s
Time	3 min (sliding distance 9 m)
Environment	Under blowing of dry air, temperature 0~20%RH

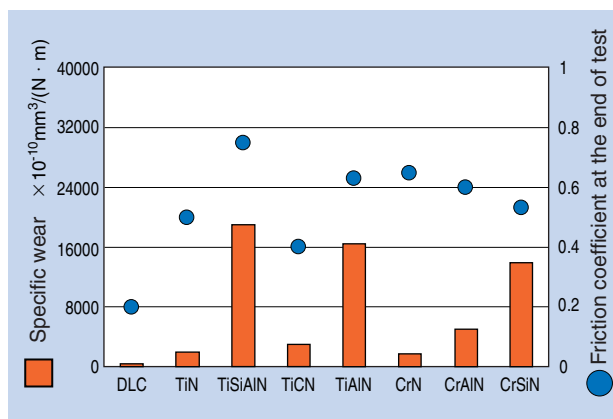


Fig. 7 Wear property and coefficient of friction of each specimen

3. Coating method-dependent variation in characteristics of DLC films

3.1 Sliding wear characteristics

Fig. 8 plots the NTN Savin type wear test results of three DLC film samples, wherein the DLC films of these samples were prepared by UBMS process, AIP process, and plasma CVD process previously described in Sec. 2.2. **Table 5** summarizes the coating methods, hardness numbers and thicknesses of these samples. The test conditions are the same as those specified in Sec. 2.3.2 except in that the test duration was changed to 30 minutes.

It is apparent that among three DLC film types, the UBMS process boasts best wear resistance and the AIP process features the lowest friction coefficient.

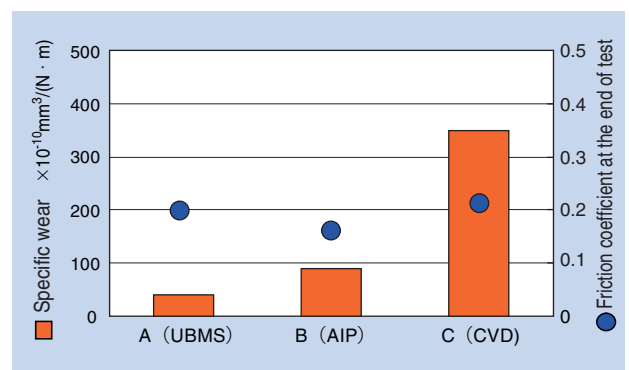


Fig. 8 Wear property and coefficient of friction of each specimen

Table 5 Coating method, hardness, thickness of DLC films

Test piece	Coating method	Hardness, Gpa	Thickness, μm
A	UBMS	26	1.2
B	AIP	53	1.0
C	CVD	15	2.0

3.2 Power of adhesion to substrate

NTN performed an adhesion evaluation test per the Rockwell indentation test method to determine adhesion of the DLC films which were tested in Sec. 3.1 to substrates. The Rockwell indentation test forces a cylindrical diamond indenter into each DLC film sample under a particular load (1,470 N) to form an indentation mark on the film. The quality of adhesion of the DLC film to a substrate has been evaluated based on the evidence of cracking or flaking of the film around the indentation mark. **Figs. 9** through **11** show the resulting test samples.

In this evaluation, DLC film (A) has not developed cracking or flaking: DLC film (B) has developed radial cracks, though not flaking: DLC film (C) has exhibited severe flaking around the indentation.

Generally, DLC films are prone to peeling because their hardness is very high and internal stress exists: therefore realization of reliable adhesion to a substrate poses an engineering challenge. Techniques for improving film-to-substrate adhesion include:

- (1) Higher substrate hardness (created by nitriding, shot peening, etc.)
- (2) Surface pre-treatment (by chemical etching, abrasive blasting, etc.)
- (3) Adoption of an intermediate layer that is highly affinitive to both the substrate and DLC film

Through adoption of techniques best suited for the intended operating conditions, a DLC film will positively adhere to a substrate.

As described above, DLC films can have diverse characteristics depending on coating method and conditions adopted. The optimal coating method and conditions for forming a DLC film need to be selected according to the intended application and performance requirements.

4. Applications to dies-DLC film application to dies for sintered metal moldings

In molding/forming work for sintered copper alloy parts, tungsten carbide dies are usually used because of their excellent wear resistance. However, in this type of work, excessive wear is occasionally observed on the dies even though the tungsten carbide material boasts significantly higher hardness compared with the copper alloy material. As a result, dies of much longer life have been increasingly needed. To address this challenge, NTN has attempted to adopt DLC films that provide much greater wear resistance.

Using the NTN Savin type wear test rig, NTN has evaluated wear resistance of non-coated tungsten carbide test pieces and tungsten carbide test pieces coated with a DLC film. The DLC film used was formed using the UBMS method. **Table 6** summarizes the test conditions applied; **Figs. 12** and **13** show wear marks found on the sliding surfaces; and **Figs. 14** and **15** plot the resultant profile measurements on the worn surfaces of the test pieces.

The tungsten carbide-only test piece has exhibited a noticeable wear mark on its sliding surface even though it has undergone sliding contact with a sintered copper alloy member (a relatively soft material). The maximum depth of wear has reached 0.8 mm. In contrast, the test piece consisting of tungsten carbide

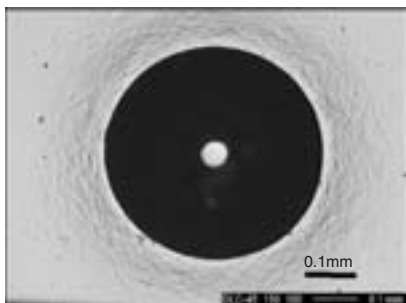


Fig. 9 Indentation of DLC film(A)

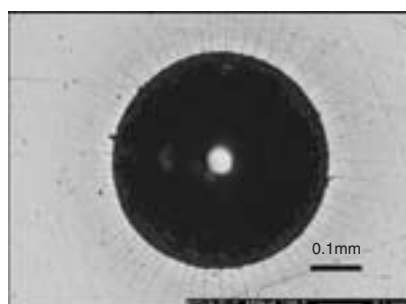


Fig. 10 Indentation of DLC film(B)

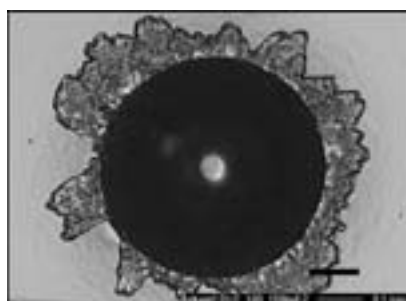


Fig. 11 Indentation of DLC film(C)

Table 6 Test conditions

Test piece	Tungsten carbide (WC-Co), OD 48 mm, thickness 7 mm, surface roughness 0.005 mmRa
Mating material	Sintered copper alloy (Cu58%, Fe40%), surface roughness 0.3 mmRa
Load	50 N
Speed	0.1 m/s
Time	30 min (sliding distance 180 m)
Environment	Under blowing of dry air, temperature 0–20%RH

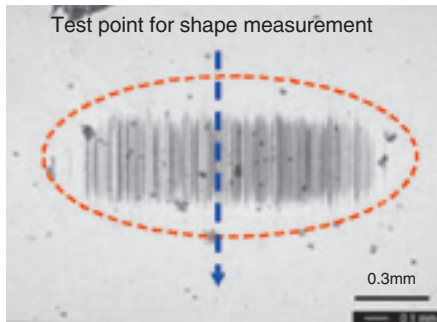


Fig. 12 Wear of sliding part (WC)

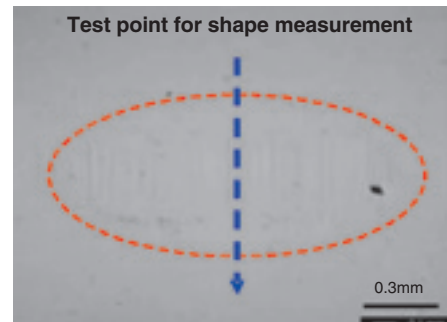


Fig. 13 Wear of sliding part (WC + DLC film)

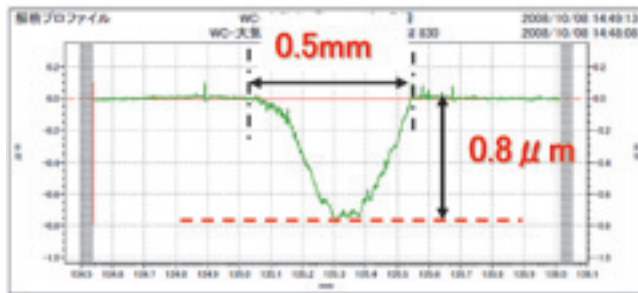


Fig. 14 Surface profile of wear (WC)

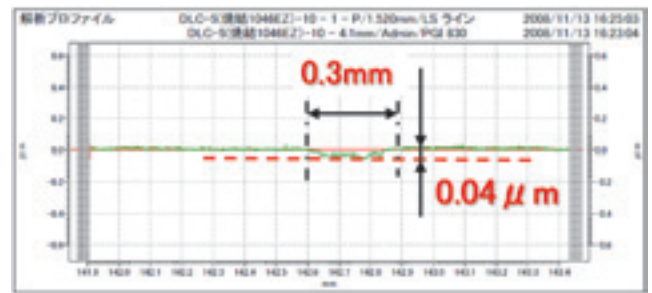


Fig. 15 Surface profile of wear (WC + DLC films)

coated with DLC film exhibited a wear depth of 0.04 μm which is 1/20 that of the uncoated test piece. The DLC film has helped dramatically reduce wear on the tungsten carbide test piece.

The reason tungsten carbide (WC-Co) wears as a result of sliding against the softer sintered copper alloy may be because the copper atoms diffuse into the cobalt particles at the contact interface. The cobalt particles act as a binder in the tungsten carbide structure. As a result of this diffusion, the Cu concentration between the WC and Co particles increases, thereby deteriorating the mechanical strength of the tungsten carbide structure. By coating the surface of a tungsten carbide die with a DLC film, which does not readily react with copper atoms while maintaining wear resistance, wear on the die is much reduced. In addition, based on endurance test results with a die used commercially for sintered copper alloy, it has been verified that the life of the die coated with the DLC film is much longer compared with a non-coated die of a same geometry.

5. Conclusion

As described above, the DLC film treatment is a technique that is effective in extending life of dies and tools. Boasting a higher degree of wear resistance and lower friction, the DLC coating provides a promising technology that helps address environmental and energy issues. NTN will attempt to further develop this technology and expand the scope of its applications.

References

- 1) A. Erdemir et al., SAE Paper, 2000-01-0518
- 2) J. Andersson et al., Wear, 254 (2003), 1070-1075
- 3) M. Kano et al.: Proceedings of The Third Asia International Conference on Tribology, October 2006, Kanazawa, 399
- 4) A.C. Ferrari, J. Robertson, Phys. Rev., B61, 14095 (2000)
- 5) M. Ikenaga (ed.), Film Technologies for Advanced Functionality, Nikkan Kogyo Shimbun (2007) (Japanese)
- 6) N. Otake, Surfaces, Vol. 45, No. 9, 22-35 (2007) (Japanese)
- 7) M. Ikenaga and H. Suzuki, Principles of Super Hard Films Made through Dry Processing and their Industrial Applications, Nikkan Kogyo Shimbun (2000) (Japanese)
- 8) N. Otake: Application and Technology of DLC Films "Evolving Industrial Applications and Future Technologies of Diamond-Like Carbon," CMC Publishing Co., Ltd. (2007) (Japanese)

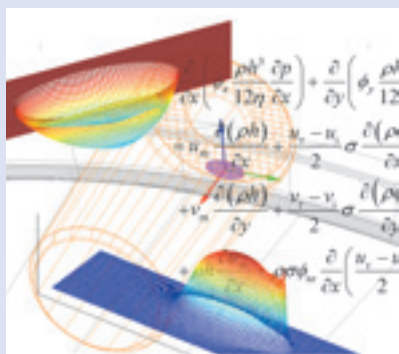
Photo of author



Kouya OOHIRA

Elemental Technological
R&D Center

Optimized Radius of Roller Large End Face in Tapered Roller Bearings



Hiroki FUJIWARA*
Takashi TSUJIMOTO**
Kazuto YAMAUCHI***

Tapered roller bearings can support heavy combined radial and thrust loads, and are widely used for automobiles, railcars and industrial machines. The bearings have an inner ring rib into which the large ends of rollers are thrust, and the contacts are accompanied with rolling-sliding motions. The large ends of rollers and the rib surfaces are spherical and conical in shape, respectively. The typical lubrication regime of the

contact is elastohydrodynamic lubrication (EHL). However, some surface damage may occur if the oil film formation is insufficient due to low-rotational and/or heavy-load operations. The film thickness should be thick enough to prevent damage in a given operating condition. In this paper, an EHL numerical model is developed in consideration of both asperity contact and roller skewing. A parameter study shows that to form thicker oil films the optimum radius of the large end face of a roller is about 85% that of the rib face conical surface.

1. Preface

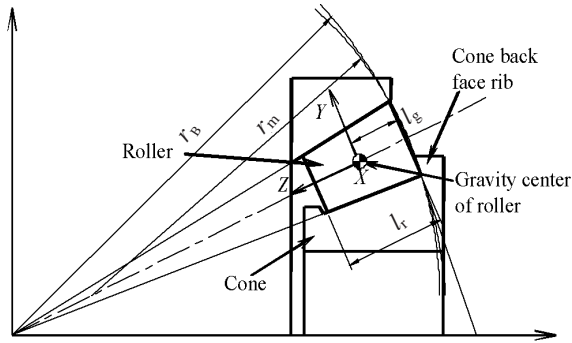
A basic tapered roller bearing consists of a complement of tapered rollers that are arranged between inner and outer rings having conical raceways. The inner and outer ring of a tapered roller bearing is commonly referred to as a cone and a cup respectively. Because tapered roller bearings can support both a relatively high radial load and a single-directional axial load, they are widely used in drive systems in automobiles and railway cars, steel mill machines, and other industrial applications. The apex of the inner and outer ring raceways and the roller contact surfaces of a tapered roller bearing converge on the bearing centerline. The rollers develop pure rolling motion without sliding on the conical raceway surfaces. However, when a radial load acts on the bearing, an axial component force occurs on the rollers due to a disparity in angles between the inner and outer ring raceways. As a typical means for bearing this force, a cone flange is provided. As a result, the large end face of each roller is guided while being forced to the cone flange. Though each roller undergoes pure rolling motion on the raceway surface, there remains rolling-sliding contact between the roller

large end face and the cone flange.

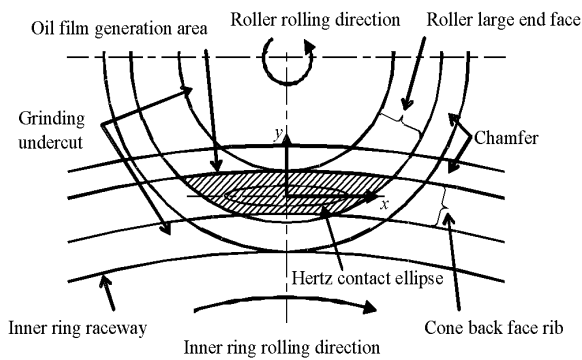
Fig. 1 (a) shows a cross-sectional view of a tapered roller bearing. The cone flange face usually consists of a part of a conical surface perpendicular to the bearing axis, while the roller large end face comprises a part of spherical surface. This condition results in roller end-flange face point contact resulting in the highest pressures. The cone flange face may possess a concave surface matches the contour of the roller large end face. In this situation, the pressure between these two faces will be smallest. However, even small rotations of the roller on the y -axis (see **Fig. 1 (a)**) in this condition can cause the edge of the roller large end face to come into contact with the cone flange face, possibly damaging the roller or the cone flange face. To avoid this problem, the radius of curvature on the roller large end face is designed to be somewhat smaller than that of cone flange face. Note that rotational motion on the y -axis is referred to as “skewing” while rotational motion on the x -axis is called “tilting”.

At the roller end-flange contact a sufficiently thick oil film may not be readily formed when the bearing runs at lower speeds or is insufficiently lubricated. Consequently, frictional torque on the bearing will

*Elemental Technological R&D Center **Automotive Sales Headquarters Automotive Engineering Dept. ***Graduate School of Engineering Osaka University



(a) Radial cross-section and legend



(b) Mode of contact between roller large end face and cone guide flange, and associated coordinates system

Fig. 1 Tapered roller bearing

increase and under higher loads sliding will occur at the contact surfaces. This will increase the possibility of surface damage or seizure at these areas. Note that the situation where mating components have insufficient lubrication is known as “starvation”.

So far, the mode of contact between the roller large end face and the cone flange face has been reviewed through experimental methods and theoretical analysis. The experimental methods include the following examples. Yamada performed a series of experiments to study the effects of surface roughness on oil film formation at lower speeds. This resulted in achieving lower torque at these contact surfaces through reduction in surface roughness of the roller end face and flange face¹⁾. Okamoto, et al. attempted to reduce the distance from the roller large end-flange face contact point to the cone raceway. The intent was to reduce the slip ratio of these components in order to improve their anti-seizure properties²⁾.

There are many examples of applying EHL (Elastohydrodynamic Lubrication) analysis. Jiang, et al. performed thermal EHL analysis with non-Newtonian fluids and discussed the relationship between the shape of the contact area and the oil film thickness³⁾. Nishida, et al. performed EHL analysis under a mixed lubrication condition⁵⁾ by introducing the Patir-Cheng

mean flow model⁴⁾.

Incidentally, a tapered roller has a tendency to skew even if factors such as misalignment are not present, as pointed out by Harada et al.⁶⁾. However, so far, there have been few examples of EHL analysis that consider roller skewing. Furthermore, there have been no examples of experiments to optimize the radius of the roller large end face. We recently performed EHL analysis considering roller skewing. Based on the results obtained from this work, we now propose an optimal radius for the roller large end face in order to form a reliable lubricating oil film. This optimal radius will be verified through a series of experiments.

2. Analysis of elastohydrodynamic lubrication (EHL) between roller end and flange faces

2.1 Isothermal EHL analysis

EHL analysis was conducted for the contact area between the roller large end and cone flange face of tapered roller bearings. The velocity, bearing load, and lubricating oil viscosity used for this analysis were selected in order to minimize heat generation at the contact area. Therefore, the temperature condition for this analysis was assumed to be isothermal.

Specifically, the following assumptions were made:

- Adequate lubrication exists.
- Heat generation in the lubricating oil due to shearing is ignored.

Equations involving the following variables are solved simultaneously:

- Reynolds' equation
- Elastic deformation derived from semi-infinite elastic contact theory
- High-pressure viscosity properties of the lubricating oil
- Balance between force and moment

As shown in Fig. 1 (b), in the entire region of contact, both roller end face and flange face have a velocity distribution in the x and y directions. Therefore, the Reynolds' equation needs to incorporate considerations about stretch terms (3rd and 4th terms in the right-hand side in expression (1)). Consequently, the Reynolds' equation will be expressed as:

$$\frac{\partial}{\partial x} \left(\frac{\rho h^3}{12 \eta} \frac{\partial p}{\partial x} \right) + \frac{\partial}{\partial y} \left(\frac{\rho h^3}{12 \eta} \frac{\partial p}{\partial y} \right) = u_m \frac{\partial(\rho h)}{\partial x} + v_m \frac{\partial(\rho h)}{\partial y} + \rho h \frac{\partial u_m}{\partial x} + \rho h \frac{\partial v_m}{\partial y} \dots \quad (1)$$

where, h stands for clearance, η viscosity of lubricating oil, p pressure, ρ density of lubricating oil, u_m and v_m x -direction component and y -direction

component of the mean velocity at the contact area between roller large end face and flange face, respectively.

To investigate the high-pressure viscosity property of the lubricating oil, Houpert converted the formula given by Rolelands into the SI system⁷⁾. This formula incorporates considerations for temperature change. However, because our study was intended to determine the isothermal viscosity of the lubricating oil, we have ignored the terms associated with temperature and have adopted the following expression:

$$\eta = \eta_0 \exp \left\{ \left[\ln \eta_0 + 9.67 \right] \left[-1 + (1 + 5.1 \times 10^{-9} p)^2 \right] \right\} \dots (2)$$

where, η_0 stands for atmospheric viscosity and is expressed as:

$$z = \frac{\alpha_0}{5.1 \times 10^{-9} (\ln \eta_0 + 9.67)} \dots \dots \dots (3)$$

where, α_0 represents the viscosity-pressure coefficient, and is given by the following Wu-Klaus-Duda formula⁸⁾:

$$\alpha_0 = (0.1657 + 0.2332 \log_{10} v) m \times 10^{-8} \dots \dots \dots (4)$$

where, v means the kinematic viscosity (mm²/s), and m viscosity slope constant appearing in Walther-ASTM formula⁹⁾.

2.2 Effects of surface roughness

We adopted the mean flow model of Patir-Cheng⁴⁾ to be able to determine the effects of surface roughness, and introduced the mixed fluid lubrication theory¹⁰⁾ of Greenwood-Tripp. Incidentally, with these two models, surface roughness is handled in a probabilistic manner. In other words, the above-mentioned methods have a low probability of calculating results for pressure and film thickness distribution that agree with results obtained from those of a fixed contact area.

In our study, we only considered isotropic roughness in the Patir-Cheng's mean flow model⁴⁾. When assuming that the pressure flow factor is defined as:

$$\phi_x = \phi_y = 1 - 0.90 \exp \left(-0.56 \frac{h}{\sigma} \right) \dots \dots \dots (5)$$

and that the roller large end face is a smooth surface; and when adopting the shear flow factor¹¹⁾ that results from these assumptions and is defined as:

$$\begin{aligned} \phi_s &= A_1 \left(\frac{h}{\sigma} \right)^{\alpha_1} \exp \left\{ -\alpha_2 \left(\frac{h}{\sigma} \right) + \alpha_3 \left(\frac{h}{\sigma} \right)^2 \right\} \quad \text{when } \frac{h}{\sigma} \leq 5 \\ \phi_s &= A_2 \exp \left(-0.25 \frac{h}{\sigma} \right) \quad \text{when } \frac{h}{\sigma} > 5 \end{aligned} \dots \dots \dots (6)$$

provided that, when $\frac{h}{\sigma} > 5$

$$\begin{aligned} A_1 &= 1.899 \\ \alpha_1 &= 0.98 \\ \alpha_2 &= 0.92 \\ \alpha_3 &= 0.05 \\ A_2 &= 1.126 \end{aligned}$$

then, the Reynolds formula (1) will be modified as follows:

$$\begin{aligned} &\frac{\partial}{\partial x} \left(\phi_x \frac{\rho h^3}{12 \eta} \frac{\partial p}{\partial x} \right) + \frac{\partial}{\partial y} \left(\phi_y \frac{\rho h^3}{12 \eta} \frac{\partial p}{\partial y} \right) \\ &= u_m \frac{\partial(\rho h)}{\partial x} + \frac{u_r - u_i}{2} \sigma \frac{\partial(\rho \phi_{sx})}{\partial x} \\ &\quad + v_m \frac{\partial(\rho h)}{\partial y} + \frac{v_r - v_i}{2} \sigma \frac{\partial(\rho \phi_{sy})}{\partial y} \dots \dots \dots (7) \\ &\quad + \rho h \frac{\partial u_m}{\partial x} + \rho \sigma \phi_{sx} \frac{\partial}{\partial x} \left(\frac{u_r - u_i}{2} \right) \\ &\quad + \rho h \frac{\partial v_m}{\partial y} + \rho \sigma \phi_{sy} \frac{\partial}{\partial y} \left(\frac{u_r - u_i}{2} \right) \end{aligned}$$

If surface asperities of mating components come into contact then the resultant contact pressure can be, based on Greenwood-Tripp theory¹⁰⁾, expressed as:

$$p_a = k_c E' F_{2.5} \left(\frac{h_c}{\sigma} \right) \dots \dots \dots (8)$$

$$F_{2.5} \left(\frac{h_c}{\sigma} \right) = \int_{\frac{h_c}{\sigma}}^{\infty} \left(t - \frac{h_c}{\sigma} \right)^{\frac{5}{2}} f^{*s}(t) dt \dots \dots \dots (9)$$

$$k_c = \left(\frac{8\sqrt{2}}{15} \right) \pi (N\beta\sigma)^2 \sqrt{\frac{\sigma}{\beta}} \dots \dots \dots (10)$$

For function $F_{2.5} \left(\frac{h_c}{\sigma} \right)$, Patir-Cheng offers the following approximation¹²⁾:

$$F_{2.5} \left(\frac{h_c}{\sigma} \right) = \begin{cases} 4.4086 \times 10^{-5} \left(4 - \frac{h_c}{\sigma} \right)^{6.804} & \text{when } \frac{h_c}{\sigma} < 4 \\ 0 & \text{when } \frac{h_c}{\sigma} > 4 \end{cases} \dots \dots \dots (11)$$

where, h_c stands for the oil film thickness at the midpoint. For values of N , β and σ , available research so far has attempted to define them in the form of $N\beta\sigma$ and σ/β . Greenwood-Tripp have assumed that $N\beta\sigma = 0.03$ to 0.05 ¹⁰⁾. We also assume $N\beta\sigma = 0.05$. Incidentally, Patir-Cheng assumes that $\sigma/\beta = 100$ ¹²⁾; however, through our experience, we believe that $\sigma/\beta = 20$ is a reasonable assumption.

Bearing engineers believe through experience that the boundary friction coefficient μ_a related with contact surface between roller large end face and flange face falls in a range of 0.12 to 0.15. For this study, we have assumed $\mu_a = 0.12$.

2.3 Boundary conditions

In ordinary EHL analysis works, researchers choose an evaluation region whose size is several times larger than the area of projected Hertzian contact surfaces so that the projected pressure at the outer fringes in this region is zero. By contrast, when studying roller large end-flange contact, the region of generated oil film (hatched area in Fig. 1(b)) is not sufficiently large relative to the size of Hertzian contact surfaces. Therefore, we have introduced the boundary conditions defined below.

The contact pressure occurs only in the region where the roller large end face contacts the flat surface of the cone flange face. The contact pressure in other regions is assumed to be zero.

2.4 Assumptions about motions

We developed the following assumptions about the motions of the rollers, inner and outer rings:

- Angular velocities of the rollers and inner and outer rings occur due to the mechanical relationship between them.
- Centrifugal force and gravitational force can be ignored.
- Interface between the rolling surfaces of the roller and raceways and between the rollers and the cage do not affect roller skewing.
- The rollers do not tilt.
- Skewing occurs due to the oil film pressure distribution between the roller large end face and cone flange face, traction, and metal-to-metal friction between surface roughness asperities.

3. Skewing on rollers in EHL mode

Generally, under an EHL (Elastohydrodynamic Lubrication) condition, the pressure on the oil film gradually increases at the fluid inlet side, and suddenly drops at the outlet of the Hertzian contact area. Consequently, the pressure gradient along the oil film is asymmetric relative to the center of contact. Because of this, a moment is created between the contacting objects. This moment will cause the rollers to skew as shown in illustrated in Fig. 2. While slip of approximately 20% is occurring between the roller large end face and cone flange, a moment of force deriving from traction is also occurring. Furthermore, if metal-to-metal contact is present, the resultant frictional force also contributes to the occurrence of a moment. Each roller turns such that balance is achieved among the pressure on the oil film, the tractional force from the oil film, the frictional force from metal-to-metal contact, and the outer force (force acting on the cone flange). The moments taking part in

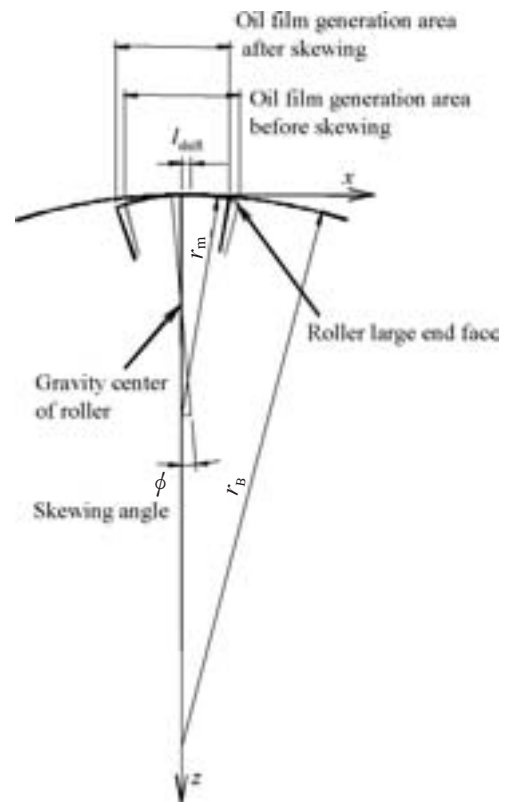


Fig. 2 Skewing of roller

this rotational motion of rollers are described below, wherein the center of rotation is assumed to be at the center of gravity of the roller.

When referring to the coordinates system given in Fig. 1, the moment of force M_h deriving from pressure on the oil film p can be calculated by the expression below:

$$M_h = \iint xp dx dy \dots\dots\dots (12)$$

wherein, the origin is defined as the intersection point of the x -axis and y -axis in Fig. 1 (b).

The magnitude of the moment caused by the tractional force can be determined in the following manner: from the experiment by Ono et al.¹³⁾, the maximum tractional coefficient $\mu_{t,max}$ is determined as follows:

$$\mu_{t,max} = \frac{0.09}{25} \times \alpha_0 p \quad \text{when } \alpha_0 p \leq 25$$

$$\mu_{t,max} = \frac{0.09}{25} \quad \text{when } \alpha_0 p > 25 \quad \dots\dots (13)$$

where, α_0 stands for the viscosity-pressure coefficient. Since the maximum projected skewing angle is as small as approximately 0.05 degrees, the slip ratio s can be calculated with the following expression, ignoring minor variation by skewing:

$$s(x, y) = \left| \frac{u_r - u_i}{(u_r + u_i)/2} \right| \dots\dots\dots (14)$$

where, u_r and u_i represent the velocity at the roller large end face and the velocity at the cone flange face respectively. If the slip ratio leading to the maximum tractional coefficient is taken as s_{max} , then the tractional coefficient μ_t can be determined, by adopting the circular-model of Lee-Hamrock¹⁴⁾, with the following expression:

$$\mu_t = \frac{s / s_{max}}{\sqrt{1 + (s / s_{max})^2}} \mu_{t, max} \dots\dots\dots (15)$$

Therefore, the tractional force F_t is defined as:

$$F_t = \mu_t \iint p dx dy \dots\dots\dots (16)$$

Then, when assuming that the distance between the ontact point to the center of gravity of the roller is l_g , the tractional moment M_t can be expressed as:

$$M_t = l_g F_t \dots\dots\dots (17)$$

The frictional force resulting from metal-to-metal contact can be investigated using the Greenwood-Tripp theory¹⁰⁾. When assuming the boundary frictional coefficient as μ_a and the apparent contact area as A_0 , then the frictional force F_a on the asperity contact surface can be expressed as:

$$F_a = \mu_a A_0 p_a \dots\dots\dots (18)$$

The moment M_a deriving from F_a is:

$$M_a = l_g F_a \dots\dots\dots (19)$$

When a roller begins skewing, the contact point between the roller large end face and cone flange shifts, and the vector of the contact force no longer intersects the center of the roller. As a result, the flange generates moment M_r , that helps reduce skewing. When the distance in the x -direction between the roller flange contact point and center of the roller (i.e. the distance the contact point shifts), is taken as l_{shift} , M_r can be defined as follows:

$$M_r = l_{shift} P \dots\dots\dots (20)$$

where, P is load on rib. Then, the geometrical relationship between l_{shift} and the skewing angle ϕ can be expressed as:

$$l_{shift} = \frac{r_B (r_m - l_g) \sin \phi}{r_B - r_m} \dots\dots\dots (21)$$

where, r_m , r_B and l_g are lengths shown in Figs. 1 and 2.

Finally, skewing angle ϕ can be determined by solving the expression below:

$$M_h + M_t + M_a + M_r = 0 \dots\dots\dots (22)$$

4. Calculation results

4.1 One detailed example of calculations

Calculations were performed under the analysis conditions summarized in Table 1, and the results are shown in Fig. 3. The R ratio of roller large end face given in Table 1 can be defined as r_m/r_B , using the associated codes in Fig. 1. The analysis conditions in Table 1 correspond to a situation where lubricating oil

Table 1 Analysis condition

Cup tapered angle	deg.	57.62
Roller tapered angle	deg.	8.5
R ratio of roller large end face		0.8
Roller length	mm	13.52
Young's modulus	GPa	208
Poisson ratio		0.3
Oil kinematic viscosity at 40°C	mm ² /s	32.2
Oil kinematic viscosity at 100°C	mm ² /s	5.45
Oil density	kg/m ³	850
Viscosity - pressure coefficient	Pa ⁻¹	1.93~10 ⁻⁸
Rotating speed	min ⁻¹	2000
Rib load	N	200
Oil temperature	°C	40
Root mean square roughness of roller large end face	µm	0.025
Root mean square roughness of cone back face rib	µm	0.1

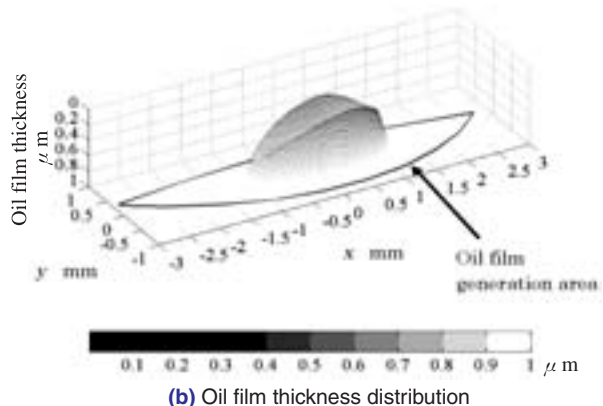
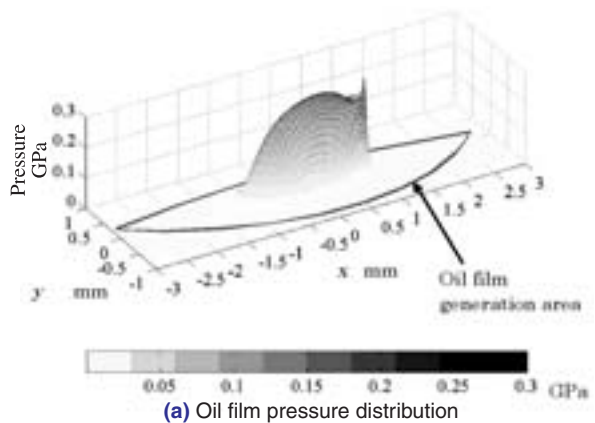


Fig. 3 Result of EHL analysis between roller large end face and cone flange face

of viscosity grade ISO VG32 is kept at 40°C, pure axial load of 9.8 kN is applied to the tapered roller bearing 30306D, and the inner ring is allowed to run at 2,000 min⁻¹.

Fig. 3 (a) provides an oil film pressure distribution diagram. **Fig. 3 (b)** shows an oil film thickness distribution diagram. The x and y -axis in these diagrams are the same as those in **Fig. 1 (b)**, and the region enclosed with solid lines is the zone where lubricating oil film formation can occur. The two faces generally shift in the positive direction along the x -axis. As shown in **Fig. 3 (a)**, a pressure spike indicative of EHL occurs at the location near the exit of the fluid flow. A skewing angle of -0.019° of the roller is present, an angle at which oil film tends to occur due to a wedge film effect. The point of maximum oil film pressure has shifted by 0.2 mm in the positive direction along the x -axis due to skewing. As a result, the inlet oil flow area is greater than if the roller was not skewed. As shown in **Fig. 3 (b)**, the deformed region constitutes an oval having its long axis in the x -direction, which is the major flow direction of the lubricating oil. There is a horseshoe-shaped neck at the oil flow outlet. Unlike a one-way oil flow situation, the oil film profile is not symmetric along the x -axis at $y = 0$.

4.2 Experimental verification of skewing angle

Harada et al. measured the skewing angle on a running 32310 tapered roller bearing⁶⁾. The resultant report states that a skewing angle was calculated using the roller large end face/cone flange face contact program. This program simulates an isoviscosity-rigid body region but there was a discrepancy in magnitude. Harada et al. think this is because in the experimental study, a high viscosity-elastic body region was used in contrast to the calculation-based study, which assumed an isoviscosity-rigid body region.

We compared the experimental result of Harada et al. with the calculation results obtained from our method described in this paper. The results are graphically plotted in **Fig. 4**. In this chart, “Exp.” are

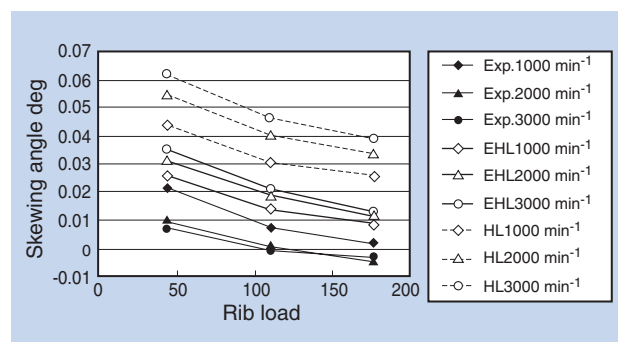


Fig. 4 Comparison between experimental and calculated of skewing angle

experimental results of Harada et al., “EHL” stands for calculation results obtained from our EHL analysis technique previously described in this paper, and “HL” indicates a results of fluid lubrication analysis on roller large end flange performed by Harada et al. assuming an isoviscosity-rigid body region. Compared with values associated with “HL”, the values obtained from “EHL” are more similar to the experimental results. This is because with “HL” results, the force as an integral of pressure is significantly shifted toward the fluid inlet path since elastic deformation is not considered. In contrast, with “EHL” results, the oil film pressure is approximately the same as the Hertz pressure; thereby, the force (i.e. integral of pressure) acts on a point situated near the contact center.

The calculated effects of the rotational speed qualitatively differ from the experimental results. In the calculated results, a greater rotating speed leads to a greater magnitude of the skewing angle for both “EHL” and “HL”. However, at lower rotational speeds (e.g. 1,000 min⁻¹), the experimental skewing angle closely matches that obtained from EHL analysis. From these findings, we believe that at low rotational speeds, where starvation seems not to be present, the results of our EHL analysis technique well represents the experimentally determined lubrication state. Furthermore, we reason that the experimentally obtained skewing angle is smaller than that obtained from the EHL technique because experimentally at high pressure, the pressure at the inlet oil flow path drops due to starvation causing the moment derived from the oil film pressure to drops.

4.3 Effects of surface roughness

Behavior of fluid flow is primarily governed by the pressure gradient across and velocity between two faces. Roughness asperities within the pressure gradient will result in localized pressure variation. In addition, fluid in the troughs of a rough surface will move along with the surface: affecting the oil flow rate caused by relative motion between the faces, resulting in a substantial decrease of the oil film thickness. Consequently, the expected flow will vary. By adopting a pressure flow rate coefficient and a shear flow rate coefficient in the Patir-Cheng mean flow model⁴⁾, we can quantitatively determine the effects of 2D (two-dimensional) surface roughness.

The “pressure flow rate coefficient” can be defined as the ratio of the mean pressure flow on a rough surface to that on smooth surface. The “shear flow rate coefficient” is similar but with additional flow caused by a shift of the rough surface. Both the pressure flow rate coefficient and the flow rate are affected by directional parameters associated with roughness. For

convenience of discussion, we will deal with isotropic surface roughness.

Taking the values in **Table 1** to define surface roughness, we have determined changes in the oil film thickness caused by the presence/absence of roughness. **Fig. 5** plots the resultant change of the oil film thickness.

Using the same conditions, the samples including factors for surface roughness have exhibited somewhat larger minimum oil film thickness.

In the roller large end-flange contact mode, the cone flange has higher surface roughness and surface velocity. As a result, it seems that the additional oil flow caused by the shifting of the surface roughness of the rib is greater than the inward oil flow restricted by the surface roughness of the roller large end face. Also, the amount of oil flowing into the contact area is higher, leading to a thicker oil film.

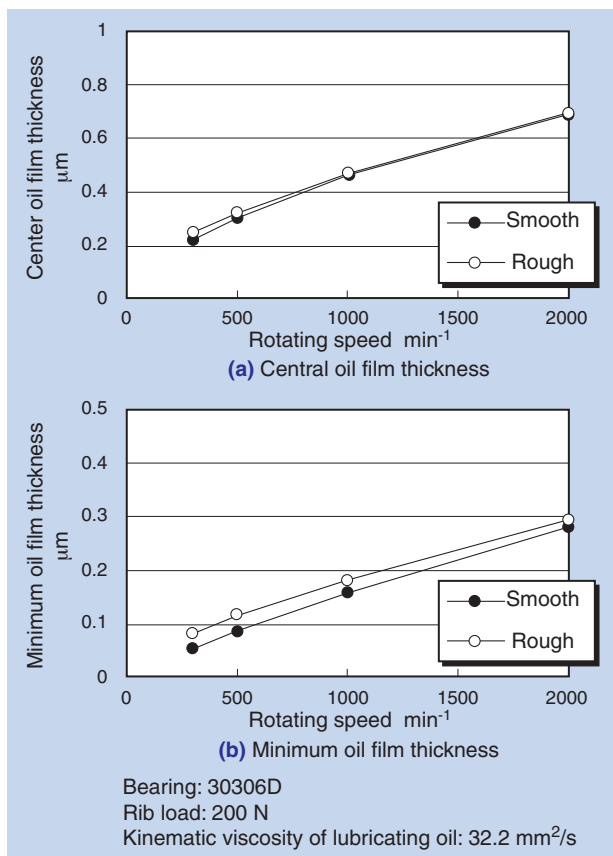


Fig. 5 Effect of surface roughness on oil film thickness

5. Optimal end face R ratio resulting from oil film forming capability

So far, proposed factors triggering seizure of contacting objects include critical oil film thickness, temperature and frictional loss. Note that regardless of the underlying cause, metal-to-metal contact must be avoided to prevent seizure. Therefore, a maximum possible oil film is preferred. In order to maximize the oil film thickness in a bearing, we have attempted to optimize the roller end face R ratio. Because the optimal roller end face R ratio appears to be governed by bearing operating conditions, we have calculated the oil film thickness using velocity, viscosity and load as parameters.

Fig. 6 includes examples of plotting the relationship between roller large end face R ratio and oil film thickness, with several sets of operating parameters. These charts show the following trends:

- (1) Regardless of the combination of operating parameters, there is a particular R ratio that leads to a maximum oil film thickness. However, the oil film thickness can suddenly decrease when the R ratio is increased above the optimum value (though R ratios smaller than the optimum value do not lead to as drastic a decrease).
- (2) The R ratio that leads to a minimal oil film thickness appears to be least affected by rotating speed and viscosity (except for cases with a high viscosity lubricating oil).

Now, let us discuss the relationships we have learned so far concerning velocity, viscosity and optimal R ratio with our tapered roller bearings.

5.1 Effects of velocity

As shown in **Fig. 6 (a)**, at a rotational speed of 500 min⁻¹, the minimum oil film thickness is largest when the R ratio is 93%; with a higher rotating speed, the optimal R ratio is somewhat smaller, standing at 88% at 4,000 min⁻¹. However, at the lower rotational speed range where the oil film thickness is smaller, the variation in minimum oil film thickness near the optimal R ratio is smaller. Therefore, we think it is not necessary to seriously consider the effects of rotating speed for optimal R ratio at low rotational speeds.

5.2 Effects of viscosity

In **Fig. 6 (b)**, the minimum oil film thickness is largest when the R ratio is 78% and the kinematic viscosity is 335 mm²/s. Because the magnitude of the oil film thickness is large in this case, the viscosity of the lubricating oil is not an important factor when pertaining to oil film formation and R ratio. On the other hand, at lower viscosities where the oil film thickness is small, the

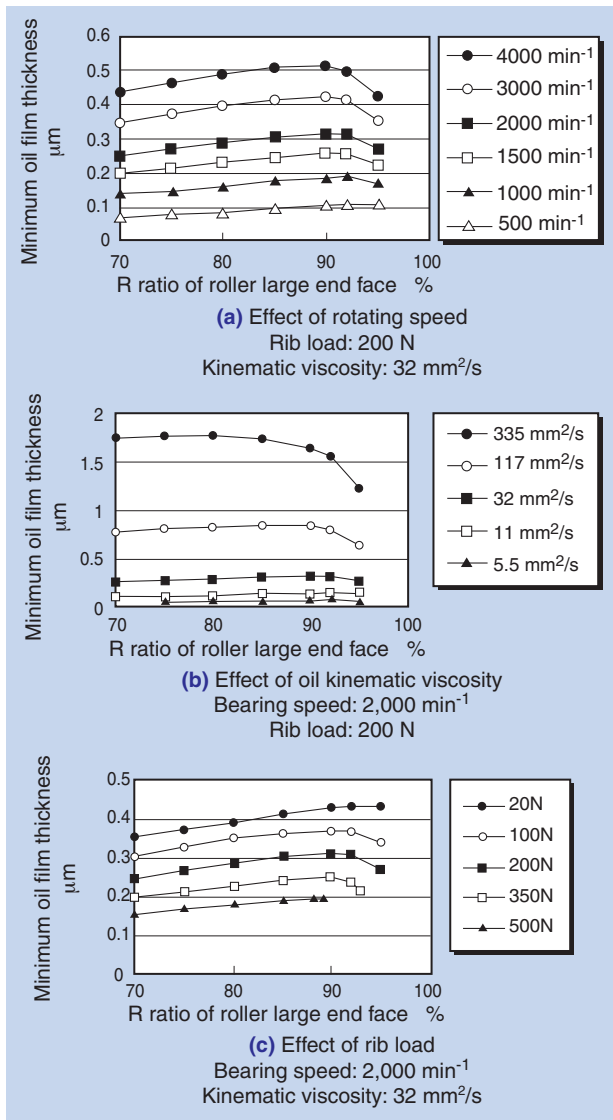


Fig. 6 Relationship between R ratio of roller large end face and minimum oil film thickness

effect of the viscosity of the lubricating oil on the optimal R ratio is small.

5.3 Effects of load

From Fig. 6 (c), it is apparent that increasing the load causes the optimal R ratio to be smaller. Furthermore, under higher loads, the minimum oil film thickness resulting from an R ratio greater than optimal will be smaller. Therefore, when the oil film thickness is smaller and the rib load is higher, the R ratio needs to be smaller.

In summary, based on our results of the optimal R ratio and oil film formation, it is not necessary to give particular considerations to the effects of velocity and/or viscosity, assuming the operating conditions in our study. It is reasonable to set the R ratio to approximately 85% for a high load situation and to approximately 95% for a low load situation. At the same time, it is desirably

to design the R ratio smaller than the optimal value since the oil film thickness decreases dramatically when the R ratio exceeds the optimal value, but much less so when the R ratio is less than the optimum value.

5.4 Experimental verification

We produced tapered roller bearing samples with varying roller end face R ratios—97%, 91.7% and 80%. We analyzed the temperature rise of the outer ring with increasing outer ring rotational speeds. Fig. 7 shows a plot of the measured bearing temperatures. Typically, flange faces are super-finished. However, the flange faces in these samples were ground so that the effects of lubrication would be more apparent. Excessive heat buildup occurred in the samples with 97% R ratios running at 2,000 min⁻¹ and 91.7% R ratios running at 3,000 min⁻¹. It was determined that these samples were generating an excessive amount of heat, too high for recommended operation. In contrast, samples with 80% R ratios proved to be able to run at 5,000 min⁻¹ without excessive heat generation. In the previous sections, we demonstrated through analysis that oil film thickness is optimized by selecting an R ratio of 85% or smaller. Through experimental verification, we proved the appropriateness of our analytical results.

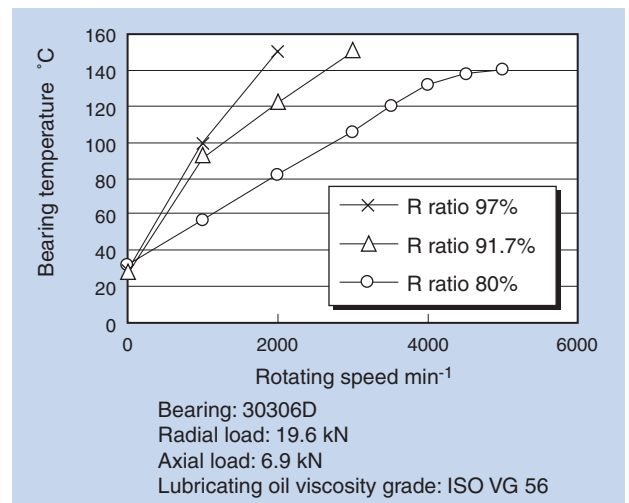


Fig. 7 Results of measured bearing temperature: Effects of R ratio of the roller large end face

6. Conclusion

Studying roller large end-flange face contact on tapered roller bearings, we performed isothermal EHL analysis while considering roller skewing. We discovered the following characteristics about lubrication at the roller large end-flange face:

- Assuming isotropic surface roughness, the magnitude of oil film thickness will be greater when surface roughness is taken into account.
- If an EHL condition is assumed, the calculated value of the roller skewing angle is smaller than that obtained without considering deformation of the contacting elements; it more closely matches the actual measured value.

In addition, we discovered the following design guidelines for end face R ratios to maximize the lubricant oil film thickness:

- The optimal end face R ratio that helps maximize the lubricating oil film thickness can vary depending on the rotational speed, lubricating oil viscosity and load conditions. Basically, it should be approximately 85% for high load situation. However, once the end face R ratio exceeds the optimal value, the oil film thickness suddenly decreases. Therefore, the design end face R ratio should be smaller than the optimal value.
- Tapered roller bearings can experience operational problems when the oil film thickness is very low. If the low oil film thickness is due to low speed or low oil viscosity, then the optimal end face R ratio has little affect.

From these studies it is desirable to design the roller with an end face R ratio of approximately 85% at most. This will allow the tapered roller bearing to operate properly under heavy loads.

In preparing this technical paper, the authors have revised Transactions of the Japan Society of Mechanical Engineers (Trans. Jpn. Soc. Mech. Eng.), Book C, Vol. 75 (2009), pp. 2319-2326.

References

- 1) T. Yamada, Torque Control and Operational Improvement of Tapered Roller Bearings, SAE Technical Paper Series, (1986), 860726.
- 2) Y. Okamoto and T. Tsujimoto: ECO-Top Tapered Roller Bearings, NTN Technical Review No. 68 (2000) 34-38.
- 3) X. Jiang et al., Thermal Non-Newtonian EHL Analysis of Rib-Roller End Contact in Tapered Roller Bearings, Transactions of the ASME, Journal of Tribology, 117 (1995), 646-654.
- 4) N. Patir and H.S. Cheng, An Average Flow Model for Determining Effects of Three-Dimensional Roughness on Partial Hydrodynamic Lubrication, Transactions of the ASME, Journal of Lubrication Technology, 100 (1978), 12-17.
- 5) H. Nishida et. al., Analysis of mixed lubrications between the Large End Faces of Tapered Roller Bearings and Ribs, Proceedings of the Fall 2001 Tribology Conference in Utsunomiya, (2001), 277-278. (Japanese)
- 6) K. Harada and T. Sakaguchi, Rolling Element Skew in Dynamic Analysis for Tapered roller Bearings, Proceedings of The Third Asia International Conference on Tribology, (2006), 647-548.
- 7) L. Houpert, New Results of Traction Force Calculations in Elastohydrodynamic Contacts, Trans. ASME, J. Tribol., 107-2 (1985), 241-248.
- 8) C.S. Wu, E.E. Klaus and J.L. Duda, Development of a Method for the Prediction of Pressure-Viscosity Coefficients of Lubricating Oils Based on Free-Volume Theory, Trans. ASME, J. Tribol., 111-1 (1989), 121-128.
- 9) ASTM, Annual Book of ASTM Standards, Section 5, Vol.05.01 Petroleum Products, Lubricants, and Fossil Fuels, (1987), 197.
- 10) J.A. Greenwood and J.H. Tripp, The Contact of Two Nominally Flat Rough Surfaces, Proceedings of IMechE, 185 (1970-71), 625-633.
- 11) N. Patir and H.S. Cheng, Application of Average Flow Model to Lubrication Between Rough Sliding Surfaces, Trans. ASME, J. Lub. Tech., 101 (1979), 220-230.
- 12) N. Patir and H.S. Cheng, Effect of Surface Roughness Orientation on the Central Film Thickness in E.H.D. Contacts, Proc. of 5TH Leeds-Lyon Symp. on Tribol., (1978), 15-21.
- 13) N. Ohno et al.: Effect of Bulk Modulus of Solidified Oils under High Pressure on Tractional Behavior, Journal of Japanese Society of Tribologists, Vol. 38 (1993), 927-934 (Japanese)
- 14) R.T. Lee and B.J. Hamrock, A Circular Non-Newtonian Fluid Model: Part I - Used in Elasto-hydrodynamic Lubrication, Transactions of the ASME, Journal of Tribology, 112 (1990), 486-496.

Photo of authors



Hiroki FUJIWARA

Elemental Technological
R&D Center



Takashi TSUJIMOTO

Automotive Sales Headquarters
Automotive Engineering Dept.



Kazut0 YAMAUCHI

Graduate School of Engineering
Osaka University

Essential Elements for Ecology

Large bearings for gearboxes
OD: 980 mm

Bearings for reducers
OD: 400 mm

Extra large bearings for main shafts
OD: 1,580 mm

Insulated bearings for generator
OD: 380 mm

Creating quality and protecting the environment

NTN[®]
www.ntn.co.jp

NTN bearings support green energy generation

Advances in and the Future of Analysis Techniques for Constant Velocity Joints



Kei Kimata Former Director

Participants

Kei Kimata	Former Director
Masakazu Hirata	(Intellectual Property Strategy Department)
Yoshinori Terasaka	(C.V.Joint Engineering Dept.)
Hisaaki Kura	(C.V.Joint Engineering Dept.)
Shin Tomogami	(C.V.Joint Engineering Dept.)
Kisao Yamazaki	(C.V.Joint Engineering Dept.)
Teruaki Fujio	(C.V.Joint Engineering Dept.)
Masashi Funahashi	(C.V.Joint Engineering Dept.)
Kazuhiko Yoshida	(New Product Development R&D Center)

Hirata: Former Director Kimata received a doctoral degree in engineering from Nagoya University in December 2008 with a thesis entitled “Research related to analysis methods for ball-type constant-velocity joints.” Before Dr. Kimata retired from our company in 1998, he had, for example, been the chief of our bearing technology research laboratory and the president of NTN Engineering Plastics Corporation. He also served as a corporate director. Since retiring, he has continued his research, which culminated with his dissertation at the age of 72. Today, Dr. Kimata, who is one of our great predecessors, joins us in a discussion about the “Advances in and the future of analysis techniques for constant velocity joints” with some of our young engineers.



Masakazu Hirata

Tomogami: The three young engineers here today helped Dr. Kimata with the numerical analysis used in the completion of his thesis. As they advanced this numerical analysis, they were able to study his theories, so this was a valuable experience for them. We are very grateful for this.

Currently, we are also working on applying this analysis to the development of constant-velocity joints (hereafter, “CVJ”) in order to accelerate development. MSC. Adams* (hereafter, “Adams”), which is a commercially-available general-purpose software application for dynamic mechanism analysis, is being used as one means for analysis. I would like to ask Dr. Kimata for his opinions regarding the differences between his own “ball-type constant-velocity joint analysis method” and Adams.

(*Registered trademark of MSC. Software)

Differences between the “ball-type constant-velocity joints analysis method” and Adams

Kimata: The main contents of my thesis are related to the static analysis and dynamic analysis of ball-type CVJs. As equations of motion for dynamic analysis, I used Euler’s equations of motion. Adams is general-purpose software for the dynamic analysis of mechanisms, and it is supposed to use Lagrange’s equations of motion, so I think that their fundamentals for dynamic analysis are the same.

I believe that in order to correctly interpret data from numerical analysis, it is necessary to have knowledge about analytical theory. Even when using Adams, I think that analytical theory related to CVJs is useful when interpreting the results.

Static analysis is very useful in understanding the fundamental characteristics of CVJ. I think that it is also useful in understanding the results of dynamic analysis.



From the left, Yoshida, Tomogami, Terasaka, Fujio, Funahashi, Yamazaki and Kura

About the application of analysis technology

Tomogami: In other words, regarding the results that come from analysis using Adams, it is important to have the sense to always verify whether or not they are valid in consideration of analytical theory. In our development—particularly in the development of parts for automobiles—I believe the main approach has been a method that involves the creation of prototypes, their evaluation and the consideration of the results, or, in other words, trial and error. I wonder, however, how our young colleagues feel about this way of proceeding.

Yamazaki: Through analysis it is possible to evaluate the performance of a product without creating a prototype, so I think this has the effect of reducing development time and cutting costs. On the other hand, since there is uncertainty as to whether the results are accurate and whether phenomena have been suitably simulated, I think it is necessary to proceed by using both analysis and experimentation skillfully.

Fujio: In the process of development, we conduct analysis, of course. In particular, when we are designing a new CVJ, for example, to investigate how the internal contact load differs in comparison with an existing product, we analyze using Adams. Analysis is convenient because it allows conditions to be changed easily. Adams is also useful because it allows the visualization of the internal force vectors from calculation results.

I believe that even though development should be advanced with analysis in the lead, at present we still cannot say that we are able to accurately simulate every phenomenon, so in the future I want to investigate new methods.

Funahashi: I think that analysis using Adams is valuable during the initial investigation of new structures. However, the fact is that there are many cases where numerical analysis is difficult when plastic deformation and destruction occur. The pursuit of both mechanism analysis and finite element analysis is necessary. Particularly in miniaturization, the ratio of plastic deformation volume increases making analysis complex. I want to apply the power of youth to resolving this.

Terasaka: That is a reassuring statement (laughs).

Improving analysis technologies for the future

Kimata: For the improvement of analysis technologies, efforts in elastic-plastic analysis are necessary. Are efforts in the engineering division advancing?

Fujio: I think that, for CVJ development in particular, analysis must be undertaken related to the failure of CVJs caused by plastic deformation where inner and outer rims contact balls. I want to accelerate development by applying dynamic finite element analysis in the analysis of these parts.

Hirata: At the Elemental Technology Research & Development Center, as one fundamental technology, we are also striving to develop coupled analysis that combines the dynamic analysis of mechanisms comprised of multiple parts and deformation analysis of those comprising parts.

Kimata: Being able to process mechanism analysis based on dynamics and elastic-plastic finite element analysis in one program would be good. However, at this point realizing this is going to be very difficult. High-speed computers with great processing capacity are necessary for dynamic analysis.

Seeking the strength conditions with dynamic analysis and using these as input conditions to conduct elastic-plastic analyses with a finite elements approach and then applying this procedure repeatedly might be the only way.

Funahashi: I also feel this way. I think that at present conducting analyses at each small step is probably the most suitable.

Yoshida: In CVJ testing, there is a semi-torsional test in which it is twisted and fractured in low-speed fixed-revolution conditions. In order to clarify this destruction mechanism, we are working on dynamic elastic-plastic finite element analysis. This model is at a level that allows the semi-torsional fracture mechanism to be simulated qualitatively. Currently we are striving to improve this model to allow quantitative simulation.

Kimata: I hope that you will continue your efforts for CVJ elastic-plastic analysis as a manufacturer that specializes in CVJs.

How to advance efficient development

Tomogami: If we want to further increase the speed of development, I believe that we must apply the latest technologies for analysis. Could our young engineers who are advancing our development work receive some advice from you, Dr. Kimata?

Kura: We also discussed this earlier, but when interpreting data, I wonder if the way to advance to the next step will differ depending on the approach to the interpretation of data from dynamic analysis and experimentation.

Kimata: Well, accurately evaluating the data is necessary. In addition, I think that grasping the mechanisms that produce that data is important. A graph of the results of dynamic analysis is complicated, but the results of static analysis are transformed by the impact of the friction generated by rotational movement. Looking at the data from that analysis and the dynamic analysis together can sometimes make it easier to understand. By considering and investigating how the friction worked, I have had the experience of being able to easily interpret a dynamic analysis graph that had appeared complicated at first glance.

In analysis, it is easier to understand if we start by thinking about a model that has been simplified as much as possible. In some senses, I think that in analysis, while considering the necessary conditions, the crucial point is how much it can be simplified.

The future of constant-velocity joints

Tomogami: Now I would like to change the topic and discuss future technologies for constant-velocity joints. As you all know, environmental considerations have become an extremely important theme even for automobiles. As parts for the driving force of automobiles, CVJs are said to be mature products. In order to meet the needs of customers, however, we are still working on issues that include making them lighter and more compact and further increasing their torque transfer performance.

Terasaka: Make them lighter, make them smaller, and make them thinner. In every case, we must consider rigidity and deformation, but I think that it is difficult to investigate thoroughly enough to be able to identify the limits. Do you have any suggestions for how to approach this?

Kimata: I think that in design it is important that you focus on reducing the concentration of stress. I think the approach of increasing the number of balls, which NTN is advancing, is also one solution (E Series CVJs).

By making the balls smaller in size and bearing the force with numerous balls, the stress at the point of load can be decreased. By reducing the concentration of stress, the possibility of using materials other than steel also arises. Incidentally, have you been able to utilize resin materials in constant-velocity joints yet?

Yoshida: In propeller shaft assemblies, by using CFRP shafts, weight has been reduced and the use of two joints has been made possible where three joints had been used before.

Yamazaki: In the case of drive shafts, since the axial diameter is fine and the input torque is great compared to propeller shafts, contact surface pressure and shear stress are higher. At present, we have not yet utilized resin materials in high-strength parts such as drive shafts, but we are investigating the possibility of application.

Hirata: Among non-ferrous materials, ceramic also has a high modulus of elasticity and high strength, so we are considering its application in strong parts.

Tomogami: It is a light and appealing material, but pliability, processing characteristics and cost are issues at this time.

Kimata: For these reasons, I think that the age of steel continues...

Hirata: Considering the long-term, I believe that there probably is a need to work with new materials besides steel, and the current state is that we are advancing efforts from the standpoint of elemental technologies. Looking to the future, I am convinced that we must work with these new materials.

Kura: Have you ever investigated sliding type constant-velocity joints, for example, which are completely different from ball-type CVJs?

Kimata: I have investigated TJ-type CVJs, but it did not go well in the end. With two-way sliding, I think that it is probably difficult to achieve an oil film. Friction increases obviously. For bearing large loads, with the exception of parts like cages that must be made sliding, rolling or rolling-sliding is probably better. The reason for this is that the lubrication characteristics are better.

Hirata: In the application of sliding for CVJs, I have investigated surface modifications and greases, but, as you say, with rolling-sliding, the grease is replenished well, while with sliding only, the grease is expelled, reducing performance in my experience.

Kura: So we should think about new joints as we use rolling-sliding skillfully.

Kimata: It would be good if there was a sliding material with low friction and high load capacity, but...

To further increase performance

Tomogami: Please give us some advice about how to further improve the performance of CVJs.

Kimata: It might be obvious, but I think it is minimizing the coefficient of friction of the contact surface as much as possible. I think that inside CVJs, the coefficient of friction is not fixed, but rather depends on the relative movement (sliding or rolling-sliding) conditions of the contact parts. They change depending on the conditions of the contact surfaces and the grease.

For this reason, I think that surface modification is a good method.

Yamazaki: Recently, HL treatment of balls for CVJs that we have developed is an example of this. By combining HL treatment of balls for CVJs with grease that has been matched to this, we are able to achieve a great reduction in torque loss.

Encouragement for young engineers

Terasaka: We have enjoyed discussing a variety of topics, but we have come to the end of our time. During your many years of research and development work, including analysis related to constant-velocity joints, I expect that you have also run into a few walls. One of the things you said was to start by simplifying things to think about them. At times when you have a problem and think that things are difficult, are there any other kinds of things that form the basis for your thinking?

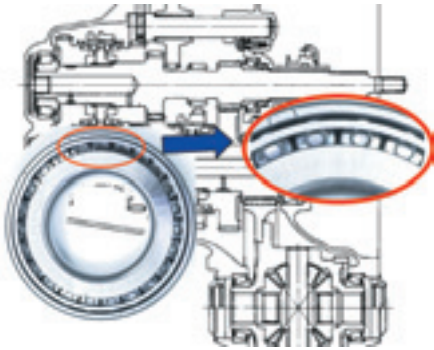
Kimata: I believe that it is returning to the fundamentals to think about the problem. By practicing returning to the fundamentals, I believe that you will gain a variety of cognitive abilities.

Terasaka: For example, when test results disagree with a theory that you have devised, what is a good way to proceed?

Kimata: You should probably check and confirm everything thoroughly. Was there a mistake in the test procedures? You have to return to the fundamentals and reconsider even when conducting analysis. The greatest danger is becoming overconfident and believing that there are no mistakes in what you have done. I have also had many failures, but the important thing has always been returning to the basics to think and reviewing to confirm that there are no contradictions in the theory.

Hirata: Today you have given us the opportunity to participate in this valuable and lengthy discussion. Thank you very much.

Everyone: Thank you very much.



**“2009 ‘CHO’ MONOZUKURI Innovative Components Awards”
Encouragement Award**

High Capacity Tapered Roller Bearing

Takashi UENO

1. Introduction

NTN “High Capacity Tapered Roller Bearing” won an Encouragement Award in “CHO MONOZUKURI Innovative Parts and Components Award 2009” sponsored by The Conference for the Promotion of MONOZUKURI and Nikkan Kogyo Shimbun Ltd., Japan’s leading business and industry newspaper publisher (and backed up by Ministry of Economy, Trade and Industry in Japan, and The Japan Chamber of Commerce and Industry).

With bearing size unchanged, this novel high capacity tapered roller bearing design boasts a 10% increase at maximum basic dynamic load rating (37% increase at maximum calculated bearing life), 15% increase at maximum basic static load rating (15% increase in safety factor) and 10% increase at maximum bearing rigidity (10% reduction at maximum elastic displacement). This novel tapered roller bearing also features lower contact pressure and has exhibited longer life even in a difficult lubricating environment where the bearing is lubricated with a low viscosity lubricating oil ¹⁾.

2. Structure of NTN high capacity tapered roller bearing

The NTN high capacity tapered roller bearing features a unique structure which include: a smaller clearance between the cage and outer ring combined with a larger pitch circle diameter with the cage, helps the cage to be situated nearer to the outer ring. Therefore, the roller-to-roller clearance has been reduced to maximize the number of rollers (a number same as that on a full complement roller bearing of a same size) while the cage bar width dimension remains same as that on the NTN standard tapered roller bearing (see **Figs. 1** and **2**).

3. Conclusion

Boasting longer life and higher rigidity, the NTN high capacity tapered roller bearings will help solve challenges occurring from needs for much improved fuel economy with automobiles. By additionally adopting NTN’s propriety FA heat treatment technique to help design unique tapered roller bearings of longer life and lower torque, the new NTN high capacity tapered roller

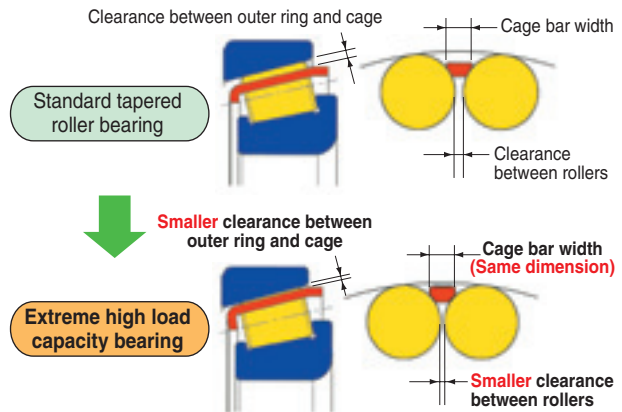
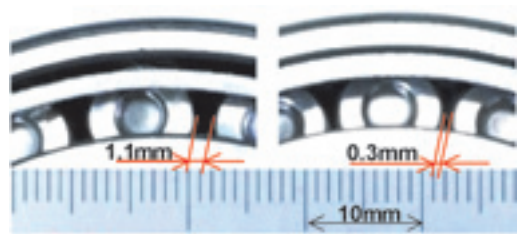


Fig. 1 Structure of high capacity tapered roller bearing



[Left: Standard tapered roller bearing Right: High capacity tapered roller bearing]

Fig. 2 Figure of high capacity tapered roller bearing

bearings will feature much reduced size, weight, and running torque. Thus, NTN is going to more positively market this line of bearings as products that will contribute to better fuel economy on automobiles.

References

- 1) T. Tsujimoto and J. Mochizuki: High Capacity Tapered Roller Bearings, NTN Technical Review No. 73 (2005) 20-29

Photo of author



Takashi UENO
Automotive Engineering Dept.
Automotive Sales Headquarters



**“2008 ‘CHO’ MONOZUKURI Innovative Components Awards”
Automotive Component Award**

**Constant Velocity Steering Joint (CSJ)
Development**

Kenta YAMAZAKI

1. Introduction

NTN “Constant Velocity Steering Joint (CSJ)” won an Automotive Component Award in “CHO MONOZUKURI Innovative Parts and Components Award 2008” sponsored by The Conference for the Promotion of MONOZUKURI and Nikkan Kogyo Shimbun Ltd., Japan’s leading business and industry newspaper publisher (and backed up by Ministry of Economy, Trade and Industry in Japan, and The Japan Chamber of Commerce and Industry).

The CSJ satisfies otherwise conflicting requirements for “smooth rotation” and “reduced play on steering wheel” through provision of a special preloading mechanism within the joint to eliminate backlash on the joint and optimization of internal design.

Compared with the double Cardan joint, which is a conventional constant velocity steering joint (hereinafter referred to as “D-CJ”), NTN CSJ are about half the weight and volume which can run at a constant speed in the operating range (0-48 C°) without developing backlash. Thus, the NTN CJS helps car steering system designers flexibly design the steering system layout.

2. Structure of constant velocity steering joint CSJ

The basic structure of CSJ¹⁾ comprises as a basis, the BJ, (ball type constant velocity joint) that is frequently used for driveshaft a plunger, and a spherical plate incorporated into the BJ (see Fig. 1). The spring force of the plunger causes the inner ring to shift rightward in this diagram; thereby the balls always remain in contact with the surfaces of ball grooves on the inner and outer rings; as a result, clearances between related parts are eliminated in order to inhibit rotational backlash.

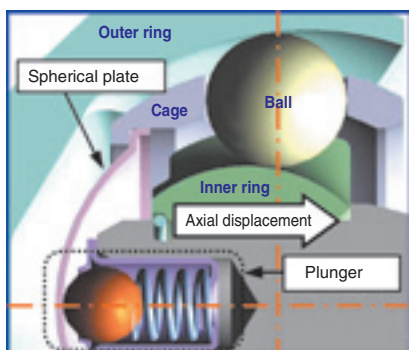


Fig. 1 Structure to reduce rotational play

3. Features of constant velocity steering joint CSJ

Results of comparison of performance of the NTN CSJ with conventional constant velocity steering joint (D-CJ) are summarized below²⁾:

1) Result of comparison in terms of rotational backlash

As shown in Fig. 2, compared with the D-CJ, the CSJ boast smaller hysteresis and higher rigidity.

2) Result of comparison in terms of rotational torque

Fig. 3 graphically plots the relation between rotational angle and rotational torque. There is no significant variation in the rotational torque of CSJ. In other words, the NTN CSJ has characteristics needed for an automotive steering joint.

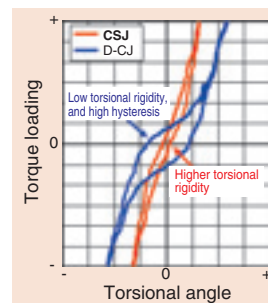


Fig. 2 Rotational bach lash

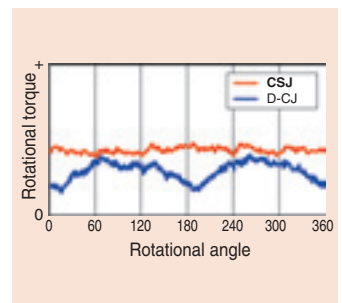


Fig. 3 Rotational torque

4. Conclusion

Being the world’s first ball type constant velocity steering joint product, the NTN CSJ boasts not only great functionality but also significant reduction in both weight and size—approximately 50% reduction compared with the NTN’s conventional D-CJ. This novel constant velocity steering joint will positively contribute to mitigation of environmental impacts possibly caused by automobiles.

References

- 1) K. Yamazaki: Constant Velocity Steering Joint (CSJ), NTN Technical Review No. 73 (2005) 84-87

Photo of author



Kenta YAMAZAKI

C.V. Joint Engineering Dept.
Automotive Sales Headquarters

Presentation of award-winning articles



**“2008 Resource Recycling Technology and Systems”
Encouragement Award**

**Development of a Briquetting Machine and the
Construction of a Recycling System
for Steelmaking Dust**

Shouzo GOTO* Ikuo YAMADA** Katsutoshi MURAMATSU***

Overview

In Japan, approximately 500,000 tons of steelmaking dust annually occurs in steelmaking electric furnace plants. This type of “waste” has been traditionally disposed of by landfill, dezincification or reuse.

Now, disposal by landfill poses problems—increasingly limited availability of landfill sites and mounting costs. Incidentally, costs for dezincification are high, including expenses needed for transportation. Therefore, it is necessary to reduce the amounts of steelmaking dust to be disposed of.

Various recycling techniques for steelmaking dust have been proposed. However, to be able to improve melting efficiency and cost-effectiveness, NTN has chosen DAIWA STEEL CORPORATION as a partner. Consequently, the team has successfully developed a unique steelmaking dust recycling method that realizes both mitigation in environmental impacts and reduction in costs.

In the newly developed recycling system, which is schematically illustrated in Fig. 1 below, carbon and water are added to steelmaking dust, and then the

mixture is pelletized. The resultant pellets are formed into cylindrical briquettes by pressure, without using glue, and then the resultant briquettes are loaded into an electric furnace together with steel scraps.

Because the carbon content included in the briquettes serves as a fuel/reducing agent, NTN’s new recycling system boasts higher degree of melting efficiency. In addition, the density of steel content in the briquettes obtained from the NTN’s novel steelmaking dust recycling system is high compared with the previous methods. thus, more iron content will be melted in the molten bath and recovered as an iron. Note that with previous steelmaking dust disposal methods, steelmaking dust either unmodified or pelletized was fed into an electric steelmaking furnace.

This new development has already resulted in improved economy, total elimination in amount of disposal by landfill and improved electricity use in the NTN Group. The resultant recycling ratio of steelmaking dust (increase in recovered iron material) has helped decrease the amount of steelmaking dust being subjected to dezincification. Thereby, NTN has been contributing to mitigation in environmental impacts resulting from its manufacturing activities.

While environmental conservation poses challenges to manufacturers, this novel steelmaking dust briquetting system has been positively contributing to realization of the recycling-oriented society.

Photo of author (Representative)



Shouzo GOTOH

Fomer Production Engineering,
R&D Center

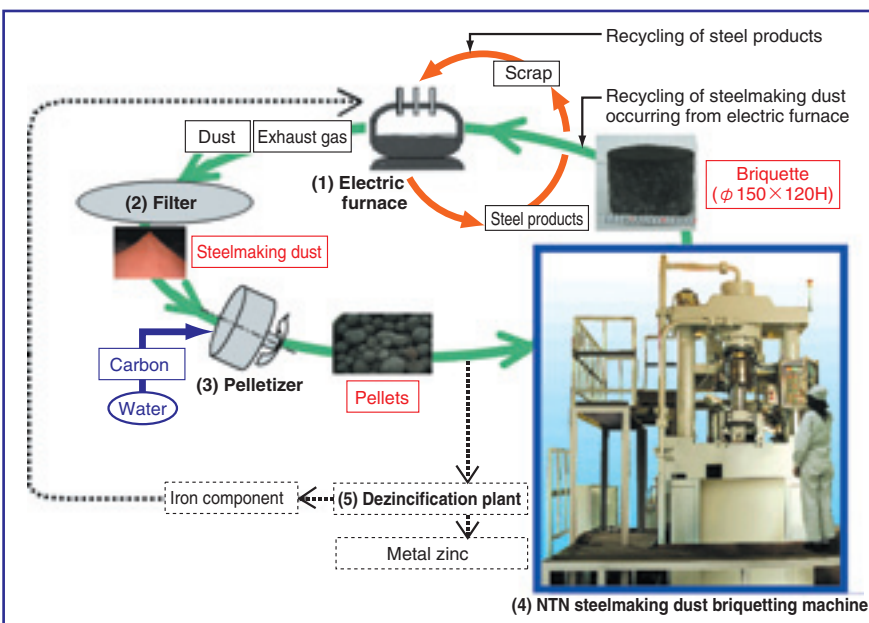


Fig. 1 Briquetting Machine and Recycling System for Steelmaking Dust

*Fomer Production Engineering R&D Center

**Production Engineering R&D Center

***Elemental Technological R&D Center

Essential Elements for Construction



Intelligent In-wheel Unit

Integration of electric motor, brake and sensor as well as size reduction in in-wheel unit contribute to optimal energy regeneration and **vehicle stability control**, and **improved driving performance**.



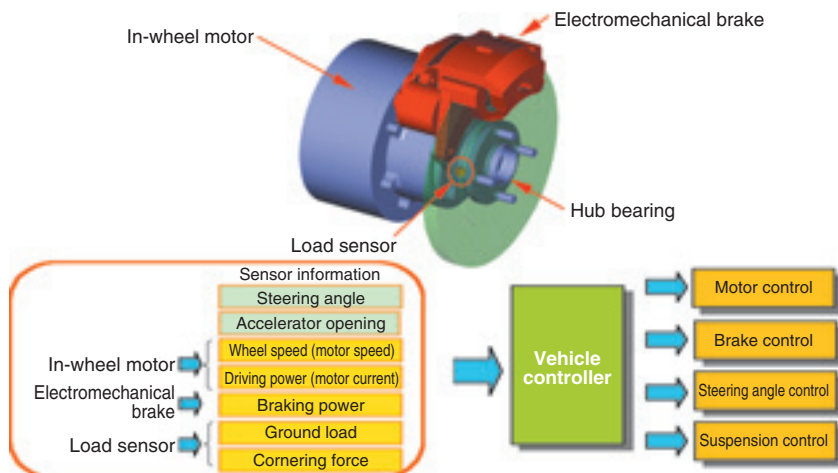
Features

- (1) Improvement in both fuel economy and driving safety
- (2) Much improved freedom in designing vehicle itself and automotive components
- (3) Car maneuverability can be tailored according to users' needs.

Applications

- Electric vehicles, fuel cell vehicles

Construction





Wide-Range High-Resolution Small Sensor Integrated Hub Bearing

Two sets of control signals are available to contribute to improvement in **precision and reliability in vehicle safety control.**



Features

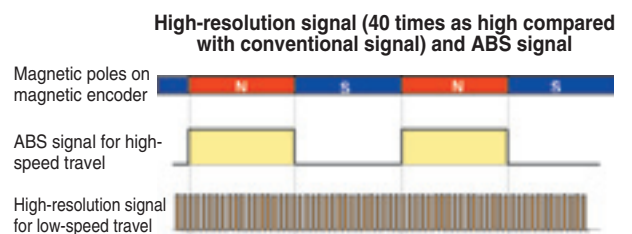
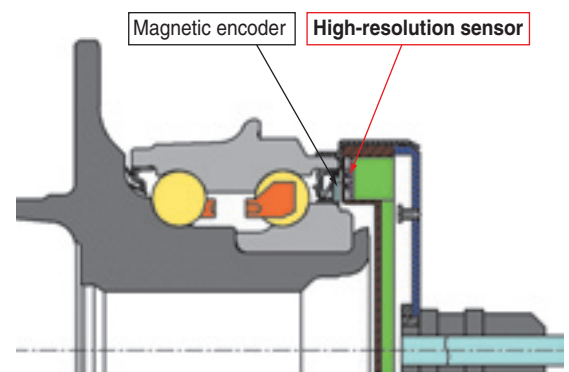
- (1) The built-in sensor covers the entire speed range from extremely low to high-speed regions: will contribute to mitigation of load in signal processing.
- (2) Running speed detection at higher resolution (40 times as accurate compared with a previous detection system): now, the motion of wheel is detected to accuracy in steps of mm.
- (3) Now, judgment on whether the wheel is running forward or reverse is possible: also, fall motion in hill launch mode is possible.
- (4) Use of a compact sensor contributes to size reduction of hub bearing product.

Applications

Wheel hub bearings for passenger cars

- Car attitude control
- Hill hold control

Construction



High Efficiency Fixed Type Constant Velocity Joint (EUJ-S)

Positively assists in **fuel efficiency of cars** thanks to 30% reduction in torque transmission loss!
Compact, light-weight constant velocity joint products capable of higher operating angle (50 degrees).

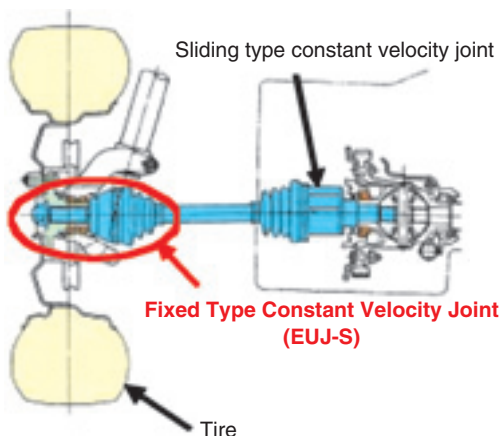


Features (comparison with conventional products)

- (1) Torque transmission loss: Reduced by approx. 30%
- (2) Strength/Durability: Same level
- (3) Max. working angle: Same level (50°)

Applications

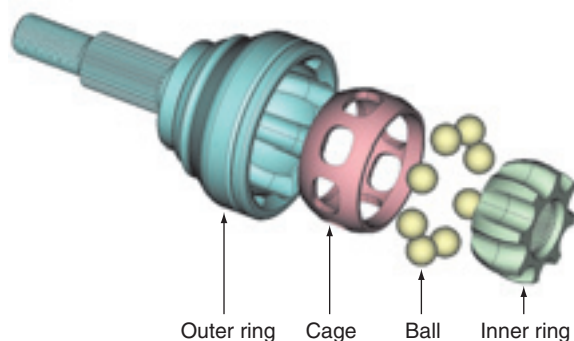
- Automotive drive shaft



Construction

- Advantages over conventional products (EUJ) -

- Design of internal structure has been optimized to reduce friction loss that results from contact between internal components in joint.
- Use of newly developed low- μ grease and adoption of surface modification technique for metal components help decrease friction loss.



High Efficiency and Low Heat Generation Ten Ball Constant Velocity Joint (HELJ) for Propeller Shafts

Realization of reduced torque loss, limited heat generation and light weight!
Contributes to **higher functionality** and **improved fuel economy!**

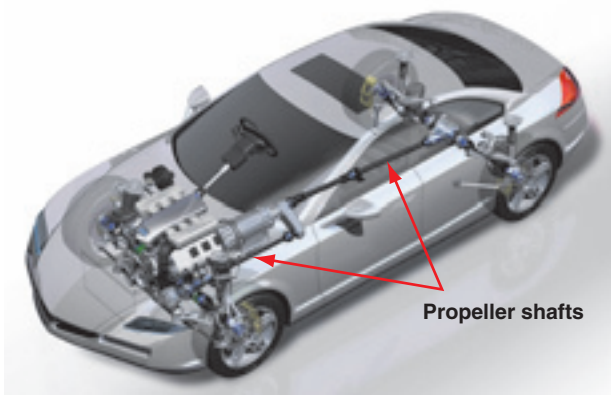


Features (comparison with conventional products)

- (1) High efficiency: Torque loss reduced by 50%
- (2) Low heat generation: Temperature rise reduced by 50%
- (3) Light weight: Mass reduced by 5%

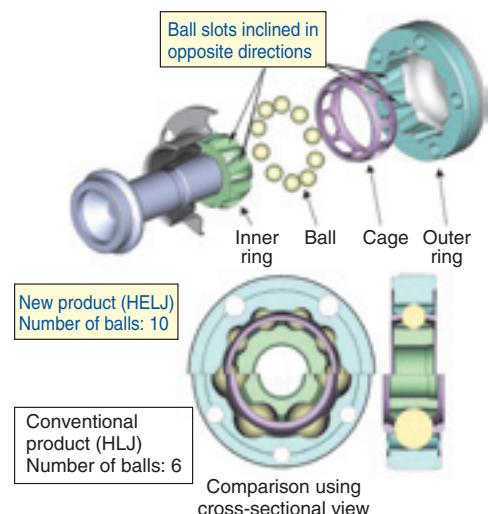
Applications

- Automotive drive shaft
(Propeller shafts on FR and 4WD vehicles)



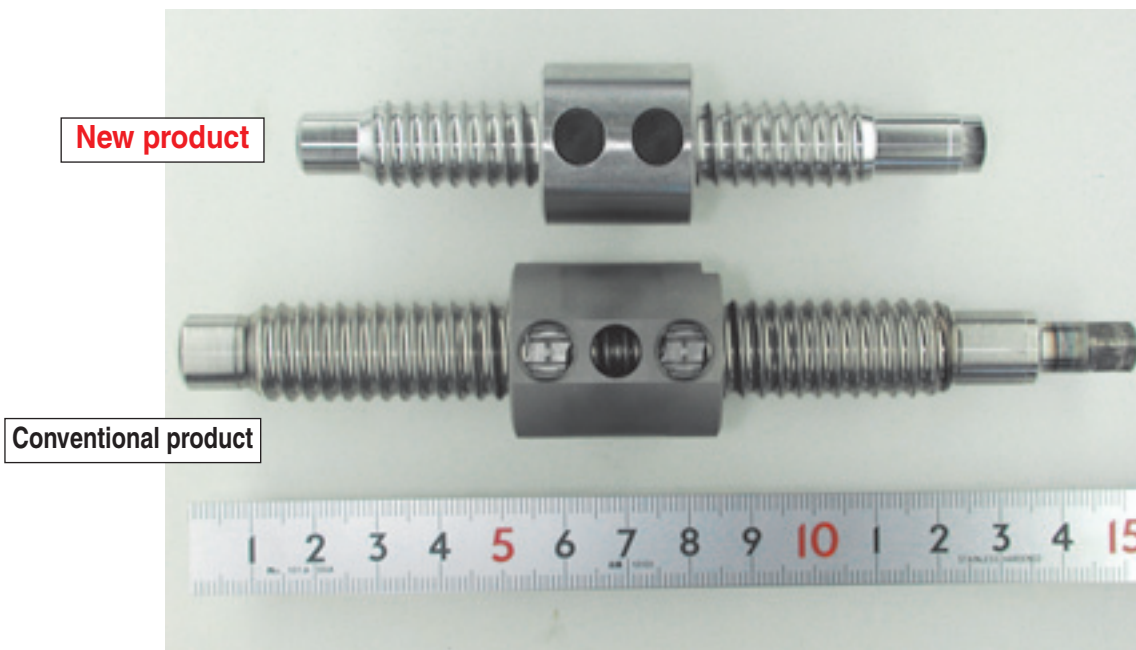
Construction

- Advantages over conventional products (HLJ) -
- Optimally angled ball slots helps reduce frictional resistance occurring on balls in axially shifting motion; consequently, heat generation on balls is mitigated.
- Smaller diameter balls are adopted: number of balls has been increased from six to ten: the size and weight of inner ring, outer ring and cage have been much reduced.



Long Life Ball Screw for Actuators

Longer life in spite of compact, light-weight design. **Contributes to realization of electromechanical design that contributes to better fuel efficiency.**

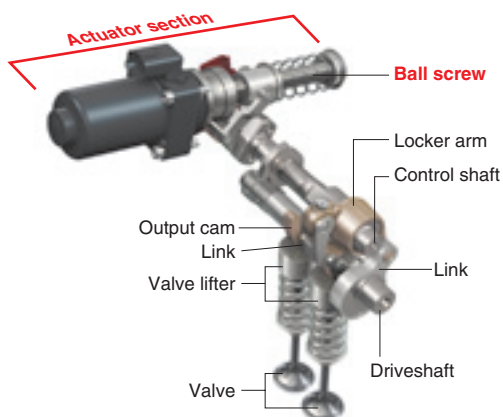


Features (comparison with conventional products)

- (1) Life: Improved by 6 times (compared to the same size product)
- (2) Size: Down sized axially by 7% (compared to products with similar life)
- (3) Mass: Reduced by 30% (compared to products with similar life)

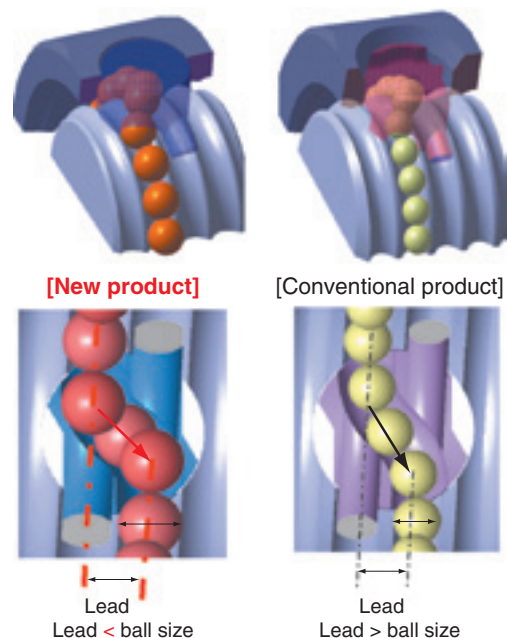
Applications

- Automotive continuous variable valve mechanism and electromechanical actuator



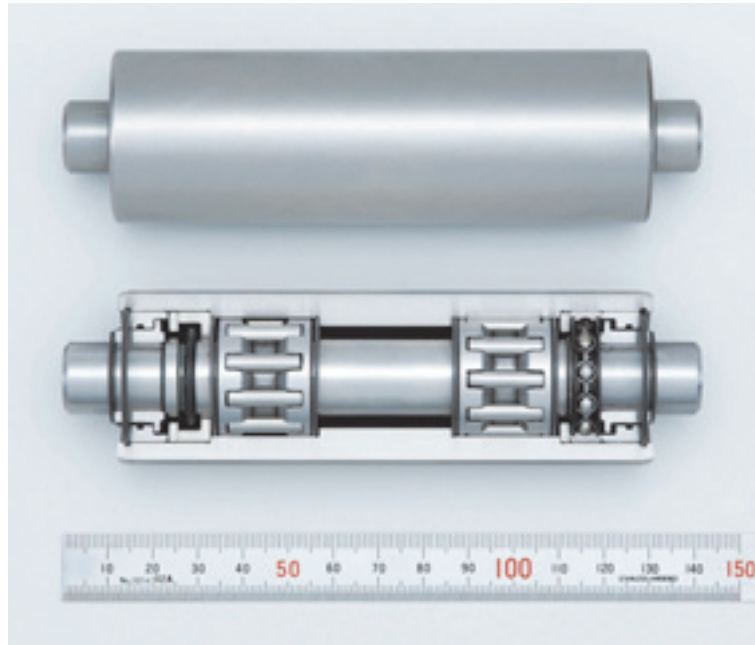
Construction

- Balls whose size is greater than that of lead
Maximized ball size helps increase load capacity of ball-screw.



Ultra Low Torque Back-up Roll Unit for Tension Levelers

Much reduced torque contributes to **improvement in productivity** and **alleviation in environmental impact!**



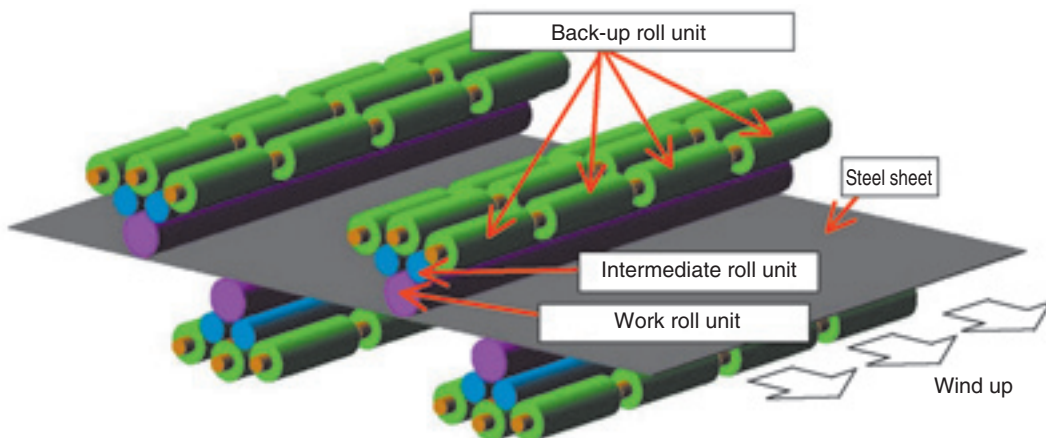
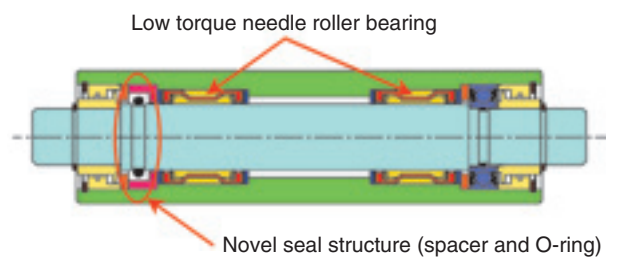
Features (comparison with conventional products)

- (1) Rotational torque: Reduced by 40%
- (2) Temperature rise: Reduced by 20%

Applications

- Steel sheet production equipment, Tension levelers

Construction



Two Way Sorting Feeder

Parts feeding mechanism derived from new concept contributes to **improvement in productivity!**



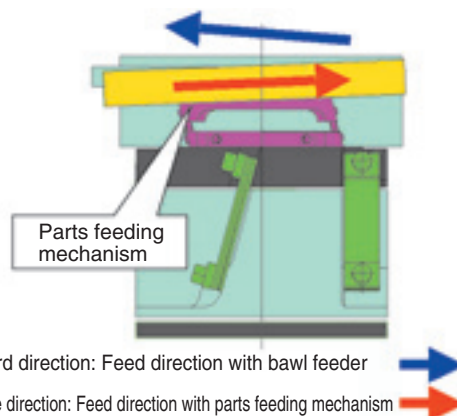
Features

- (1) Feeding in two opposing directions
A well conceived mounting system for a pair of leaf springs can realize parts feeding in two opposing directions.
- (2) Increasing speed/Decreasing speed
Speed can be varied for the attachment section that aligns and feeds parts.
- (3) Transfer of vibration to the sloped chute
Congestion of parts within the chute is prevented.

Applications

- Aligning and feeding of automotive parts, parts for electric equipment, and parts for medical equipment, etc.

Construction



Increasing speed/
Decreasing speed



Sloped chute

New-Type One-Way Clutch for Office Equipment (NCT)

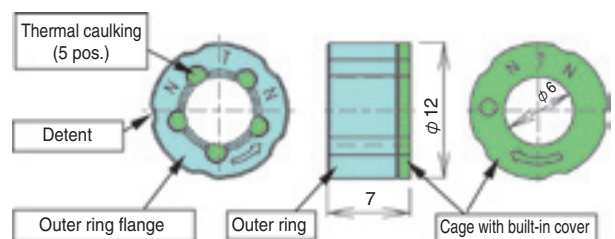
This one-way clutch **can be readily built** into a resin-built component, while maintaining **highly reliable** clutching function!



Features

- (1) Can be integrated with a resin-built component.
(Detents are situated on the outer circumference of outer ring.)
- (2) Improved handling ease
 - Cage cover is thermally caulked to the outer ring to form a single component (non-separable type).
 - Orientation for assembly can be identified by color-coding (lock direction is clearly indicated on the product).
 - Lock direction can be altered by simply reversing the orientation for installing the clutch.
- (3) Higher reliability and durability
 - Equivalent with the unit type (NCZ) one-way clutch
- (4) Capability for bearing radial load
 - The cage bore surface on the clutch bears radial load.

Construction



Applications

- Paper feeding section in printers and photocopiers

